THE USE OF HYDROLOGICAL INFORMATION TO IMPROVE FLOOD MANAGEMENT – INTEGRATED HYDROLOGICAL MODELLING OF THE ZAMBEZI RIVER BASIN

AGOSTINHO C F VILANCULOS
Student Number: 609V7301
Supervisor: Professor Denis Hughes
Co-Supervisor: Dr. Helonio Muiwane

A thesis submitted in fulfilment of the requirements for the degree of

DOCTOR OF PHILOSOPHY
in the
Faculty of Science
RHODES UNIVERSITY

February 2015

DEDICATION

This thesis is dedicated to the following special people:

firstly to my wife, Luisa Boene, for all her support and encouragement;

to my mother, Joaneta Deze Timbe, for her great initiative and enterprising mind (which made it possible for me to remain in school – she also taught me to be sincere, to respect humanity and to show gratitude to others);

to my daughter, Kissa, and my sons, Oldin, Akono and Yanick, – this is a challenge to all of you to reach greater heights, knowing you can always try to be better;

to my late father-in-law, Sebastião Gustavo Boene, for his encouragement;

to my late father, Chuquelane Faduco Vilanculos: I wish you had lived longer to see what you had put before you. May God rest your soul in eternal peace!

ACKNOWLEDGEMENTS

I am grateful to my supervisor, Prof. Denis Hughes of the Institute for Water Research (IWR) and my co-supervisor, Dr. Helonio Muiwane of the Universidade Eduardo Mondlane (who provided ideas and gave me the necessary skills from the beginning, throughout the whole project), and whose encouragement, and contribution (through constructive criticisms and patience of reading the whole document) were key to this study.

I would also like to thank DHI South Africa, Rhodes University and *Universidade Eduardo Mondlane* for developing numerous scripts that preceded this final thesis. The equations developed for the estimation of several of the procedures were packaged into a small and neat computer programs by these institutions. I extend my gratitude to the following: Prof. Denis Hughes, Eng. Mef Mehari and Dr. Kwabena Asante, for developing the routines that allowed the conversion of predicted streamflow from GeoSFM into acceptable formats for the MIKE BASIN software. A number of small programs were written for data exchange processing, cross-sections re-definitions and flood mapping delineation and this is greatly appreciated. A special word of thanks is due to the providers of the data used in the development and testing of the estimation methods in this thesis. These data specialists included: the National Directory of Water (DNA); ARA-Zambezi; *Hidroletrica de Cahora Bassa* (HCB) and ARA-Sul in Mozambique.

I also would like to express my gratitude to the numerous colleagues who helped shape this thesis through constructive comments and encouragement. Thanks are also due to Dr. Tendai Sawunyama (IWR Water Resources Pty Ltd) and Dr. Evison Kapangaziwiri (CISR) for their comments, spelling and grammar checking in this thesis. Thank you to Lisanne Frewin for proof reading the final document.

My sincere gratitude is also extended to the Carnegie Corporation of New York, through the Regional Initiative in Science and Education (RISE) Programme, and the Sub-Saharan African Water Resources Network (SSAWRN) for providing a bursary for my PhD research. I would like to thank all members of staff of the Institute for Water Research (IWR) and *Universidade Eduardo Mondlane (UEM)* for various fruitful and enlightening discussions that aided in developing my understanding and appreciation of various water related issues.

Lastly, I am extremely grateful for the collaboration with my research colleagues – Sithabile, Raphael, Madoka and Jane – thank you for your support and encouragement.

DECLARATION

I declare that this thesis is my own unaided work in fulfilment of the degree of Doctor of Philosophy in the Institute of Water Research, Faculty of Science, the University of Rhodes, Grahamstown. This thesis has not been submitted previously for any degree or examination at any other university.

I further declare that the work presented in the thesis:

> THE USE OF HYDROLOGICAL INFORMATION TO IMPROVE FLOOD MANAGEMENT – INTEGRATED HYDROLOGICAL MODELLING OF THE ZAMBEZI RIVER BASIN

is authentic and original unless clearly indicated otherwise and in such instances full reference to the source is acknowledged and I do not pretend to receive any credit for such acknowledged quotations, and that there is no copyright infringement in my work. I declare that no unethical research practices have been used and no material gained through dishonesty. I understand that plagiarism constitutes a serious offence and, should I contravene the Plagiarism Policy (notwithstanding signing this affidavit), I may be found guilty of a serious criminal offence (perjury) that would compel the University to inform all other tertiary institutions of the offence. The University would also be able to issue a corresponding certificate of reprehensible academic conduct to whoever may request such a certificate from the institution.

(Agostinho Vilanculos)

February 2014

ABSTRACT

The recent high profile flooding events – that have occurred in many parts of the world – have drawn attention to the need for new and improved methods for water resources assessment, water management and the modelling of large-scale flooding events. In the case of the Zambezi Basin, a review of the 2000 and 2001 floods identified the need for tools to enable hydrologists to assess and predict daily stream flow and identify the areas that are likely to be affected by flooding.

As a way to address the problem, a methodology was set up to derive catchment soil moisture statistics from Earth Observation (EO) data and to study the improvements brought about by an assimilation of this information into hydrological models for improving reservoir management in a data scarce environment. Rainfall data were obtained from the FEWSNet Web site and computed by the National Oceanic and Atmospheric Administration Climatic Prediction Center (NOAA/CPC). These datasets were processed and used to monitor rainfall variability and subsequently fed into a hydrological model to predict the daily flows for the Zambezi River Basin. The hydrological model used was the Geospatial Stream Flow Model (GeoSFM), developed by the United States Geological Survey (USGS). GeoSFM is a spatially semi-distributed physically-based hydrological model, parameterised using spatially distributed topographic data, soil characteristics and land cover data sets available globally from both Remote Sensing and *in situ* sources. The Satellite rainfall data were validated against data from twenty (20) rainfall gauges located on the Lower Zambezi. However, at several rain gauge stations (especially those with complex topography, which tended to experience high rainfall spatial variability), there was no direct correlation between the satellite estimates and the ground data as recorded in daily time steps. The model was calibrated for seven gauging stations. The calibrated model performed quite well at seven selected locations *(R^2=0.66 to 0.90, CE=0.51 to 0.88, RSR=0.35 to 0.69, PBIAS=−4.5 to 7.5)*. The observed data were obtained from the National Water Agencies of the riparian countries. After GeoSFM calibration, the model generated an integration of the flows into a reservoir and hydropower model to optimise the operation of Kariba and Cahora Bassa dams. The Kariba and Cahora Bassa dams were selected because this study considers these two dams as the major infrastructures for controlling and alleviating floods in the Zambezi River Basin. Other dams (such as the Kafue and Itezhi-Thezi) were recognised in terms of their importance but including them was beyond the scope of this study because of financial and time constraints. The licence of the reservoir model was limited to one year for the same reason. The reservoir model used was the MIKE BASIN, a professional engineering software package and quasi-steady-state

mass balance modelling tool for integrated river basin and management, developed by the Denmark Hydraulic Institute (DHI) in 2003. The model was parameterised by the geometry of the reservoir basin (*level, area, volume relationships*) and by the discharge-level (Q-h) relationship of the dam spillways. The integrated modelling system simulated the daily flow variation for all Zambezi River sub-basins between 1998 and 2008 and validated between 2009 and 2011. The resulting streamflows have been expressed in terms of hydrograph comparisons between simulated and observed flow values at the four gauging stations located downstream of Cahora Bassa dam. The integrated model performed well, between observed and forecast streamflows, at four selected gauging stations *(*R^2*=0.53 to 0.90, CE=0.50 to 0.80, RSR=0.49 to 0.69, PBIAS=−2.10 to 4.8)*.

From the results of integrated modelling, it was observed that both Kariba and Cahora Bassa are currently being operated based on the maximum rule curve and both remain focused on maximising hydropower production and ensuring dam safety rather than other potential influences by the Zambezi River (such as flood control downstream – where the communities are located – and environmental issues). In addition, the flood mapping analysis demonstrated that the Cahora Bassa dam plays an important part in flood mitigation downstream of the dams. In the absence of optimisation of flow releases from both the Kariba and Cahora Bassa dams, in additional to the contribution of any other tributaries located downstream of the dams, the impact of flooding can be severe. As such, this study has developed new approaches for flood monitoring downstream of the Zambezi Basin, through the application of an integrated modelling system. The modelling system consists of: predicting daily streamflow (using the calibrated GeoSFM), then feeding the predicted streamflow into MIKE BASIN (for checking the operating rules) and to optimise the releases. Therefore, before releases are made, the flood maps can be used as a decision-making tool to both assess the impact of each level of release downstream and to identify the communities likely to be affected by the flood – this ensures that the necessary warnings can be issued before flooding occurs.

Finally an integrated flood management tool was proposed – to host the results produced by the integrated system – which would then be accessible for assessment by the different users. These results were expressed in terms of water level (m). Four discharge-level (Q-h) relationships were developed for converting the simulated flow into water level at four selected sites downstream of Cahora Bassa dam – namely: Cahora Bassa dam site, Tete (E-320), Caia (E-291) and Marromeu (E-285). However, the uncertainties in these predictions suggested that improved monitoring systems may be achieved if data access at appropriate scale and quality was improved.

TABLE OF CONTENTS

LIST OF FIGURES

LIST OF TABLES

ABBREVIATIONS, ACRONYMS, AND DEFINITIONS

AET	Actual evapotranspiration
ADPC	Asian Disaster Preparedness Center
amsl	above mean sea level
a priori	Latin: = meaning ‘from the earlier’
APR	Allocation Pool Reservoir
ARA-Sul	*Administração Regional Aguas do Sul*
ARA-Zambeze	*Administração Regional de Aguas do Zambeze*
AVHRR	Advanced Very High Resolution Radiometer
CE	Coefficient of Efficiency
CPC	Climate Prediction Center
DCP	Department of Civil Protection
DEM	Digital Elevation Model
DEMs	Digital Elevation Models
DEPTH	Hydrologically Active Depth
DFO	Dartmouth Flood Observatory
DHI	Denmark Hydraulic Institute
DMMU	Disaster Management and Mitigation Unit Centre
DNA	*Direção Nacional de Aguas*
DP	Dynamic Programming
DS	Dead Storage
DSMW	Global Digital Soil Map of the World
DSS	Decision Support Systems
e.g.	Latin: *exempli gratia* = meaning ‘for example’
EMCWF	European Centre for Medium-Range Weather Forecasts
EM-DAT	Emergency Disaster Database
EO	Earth Observation
EROS	Earth Resources Observation System
ET	Evapo-Transpiration
et al.	Latin: *et alia* = meaning ‘and others’
FAO	(United Nations) Food and Agriculture Organization
FCL	Flood Control Level
FFEWS	Flood Forecasting and Early Warning System
GDAS	Global Data Assimilation System
GeoSFM	Geospatial Stream Flow Model
GIS	Geographic Information Systems
GLCC	Global Land Cover Characterisation
GRACE	Gravity Recovery and Climate Experiment
GRG	Generalized Reduced Gradient Code
HCB	*Hidroeléctrica de Cahora Bassa*
HYCOS	Hydrological Cycle Observing System
IA	Index of Agreement

IDW	Inverse Distance Weighting procedure
i.e.	Latin: *id est* = meaning ‘that is’
IEWS	Integrated Early Warning System
IFEWS	Integrated Flood Early Warning System
IGBP	International Geosphere Biosphere Program
INAM	*Instituto Nacional de Meteorologia*
in situ	Latin: meaning ‘in its original place’
IRS	Indian Remote Sensing Satellite
ITCZ	Inter-Tropical Convergence Zone
inter alia	Latin: meaning = ‘among other things’
IWRM	Integrated Water Resources Management
KC	Saturated Hydraulic Conductivity
Ks	Hydraulic Conductivity
LCWG	Land Cover Working Group
LEC	Local Emergency Centre
LIDAR	Light Detecting and Ranging
LIE	Linear Interpolation Estimator
LM	L-Moments
LP	Linear Programming
MAP	Mean Annual Precipitation
MLE	Maximum Likelihood Error
MLP	Maximum Likelihood Procedure
MM	Method of Moments
MODIS	Moderate Resolution Imaging Spectroradiometer
MOL	Minimum Operation Level
MOSCEM	Multi-objective Shuffled Complex Evolution Metropolis Algorithm
MRR	Minimum Release Requirement
NHS’s	National Hydrological Services
NLP	Nonlinear Programming
NOAA	National Oceanic and Atmospheric Administration
NRCS	Natural Resources Conservation Service
NSCE	Nash–Sutcliffe Coefficient of Efficiency
NWP	Numerical Weather Prediction
OAT	One-at-a-Time
OP	Operation Rules
PD	Power Demand
PET	Potential Evapotranspiration
PPA	Power Purchase Agreement
PWM	Probability Weighted Moments
QPF	Quantitative Precipitation Forecasting
RBOs	River Basin Organisations
RC	Rule Curve
RCN	Runoff Curve Number

RFE	Satellite Rainfall Estimates
RFWC	Regional Forecasting and Warning Centre
RMF	Regional Maximum Flood
RMSE	Root Mean Square Error
RRC	Reservoir Rule Curve
RMSE	Relative Root Mean Square Error
RS	Remote Sensing
SADC	Southern African Development Community
SADC HYCOS	Southern African Development Community Hydrological Cycle Observing System
SARCOF	Southern African Regional Climate Outlook Forum
SARFFGS	Southern African Region Flash Flood Guidance System
SCS	Soil Conservation Service
SCS CNs	Soil Conservation Service Curve Numbers
SDP	Stochastic Dynamic Programming
SoilWHC	Soil Moisture Holding Capacity
SRTM	Shuttle Radar Topographic Mission
stationarity	parameters (such as the mean and variance, if they are present) that do not change over time and do not follow any trends
STD	Standard Deviation
stochastic	simulation that operates with variables that can change with certain probability – means that particular factors (values) are variable or random
SWDFP	Severe Weather Forecasting Demonstration Project
TRMM	Tropical Rainfall Measuring Mission
UH	Unit Hydrograph
UNESCO	United Nations Educational, Scientific and Cultural Organization
USGS	United States Geological Survey
WHC	Water Holding Capacity
ZAMCOM	Zambezi River Basin Commission
ZDSS	Zambezi Decision Support System
ZRA	Zambezi River Authority

1. INTRODUCTION

1.1. Background

The complexity of the various current approaches to water resource management poses many challenges. Among the main challenges in water resource management are: how to balance supply and demand; how to provide water for food security and energy generation; how to mitigate the damage caused by floods and droughts; how to maintain environmental functions and also how to reach the best compromise solutions toward achieving integrated river basin management (Acreman, 2009; MRC, 2011). Water managers need to solve a range of interrelated water problems: balancing water quantity and quality; flooding; drought; maintenance of biodiversity and ecological functions; and the supply of water services to the local populations (Myšiak, 2010). However, the scope of water resources planning and management in most parts of the world has drastically changed in the last decade. This has been partly because hydro-meteorological data collection and analysis techniques were not keeping pace with actual water development and management needs (Kundzewicz, 2007). In Southern Africa, for instance, water availability is highly variable, both spatially and temporally, with low runoff coefficients (between 9% and 15%) prevalent across large parts of the region (FAO, 2003). As a result, it is probable that water availability and supply will play a crucial role in determining the development of localised regions. The Southern African Development Community (SADC, 2006) contends that *"…a majority of the region's approximately 200 million people lacks access to basic safe water, appropriate sanitation and often face food insecurity…"* and that a mismatch exists between resource availability and demand, with some of the greatest demand located in semi-arid areas, posing challenges for resource allocation.

Another complicating factor for water resource management in Southern Africa is the trans-boundary nature of the major river systems including: the Congo River Basin (catchment area of 3 800 000 km^2); the Zambezi River Basin (1 400 000 km^2); the Limpopo River Basin (480 000 km^2); the Orange-Senqu River Basin (721 000 km^2) and the Okavango River Basin (530 000 km^2) (SADC, 2002). This implies that approximately 70% of the region's water resources cross various national borders, making any decision and/or policy-making for the present (and the future) very challenging. Thus, the reliable quantification of hydrological variables – such as rainfall and streamflow – is a prerequisite for mutually beneficial, cooperative and sustainable water resource management, planning and development within river basins (Winsemius *et al.*, 2006). In addition, adequate and reliable resource quantification can improve the region's chances of attaining increased food security and enhancing the access to, and availability of, cheap energy through hydropower.

Water-induced disasters are also very prevalent in several of these major basins – with many lives and properties being destroyed annually (INGC, 2009). The focus of the present study is the Zambezi River Basin. The basin was selected as the study area because of its importance to the riparian countries in terms of both energy and food production. It supports a total population estimated at 38 million, spread across eight countries and, if current growth rates are maintained, the population is expected to double in 30 years (Tilmant *et al.,* 2010). This population growth in the Zambezi River Basin will, therefore, lead to increased growth in water demand for food and energy production – demands which may compete with flow requirements for environmentally sensitive areas. Based on 40 years of data (accumulated between 1960 to 2000), the basin is highly vulnerable to flood disasters (INGC, 2009). The highest recorded flood event in the basin during the past 15 years took place in 2001. Beilfuss *et al.* (2009) argued that if there had been a flood forecasting system for the Zambezi River Basin available in 2001, the loss of lives could have been significantly reduced.

However, studies done by Beilfuss (1997); Beilfuss & Davies (1998); Beilfuss (1999); Beilfuss (2005), Nyatsanza and Van der Zaag (2011) have demonstrated the impact of operating multi-propose reservoirs on the environmental flows in the Zambezi Basin. However, the development, operation, effectiveness and maintenance of these multi-purpose reservoir systems are dependent on funding availability, capacity of the human resources and effective channels of communication to relay emergency messages. While technically these systems can easily be designed, their development is hampered by the shortage of the requisite data to train the systems' controllers. To alleviate the problem of data paucity, hydrological simulation models have become standard tools for the generation of information and have been used extensively in the region. As a result, water resource decision-making has been heavily dependent on the modelling results. Many rainfall-runoff models, of varying complexity, have been developed worldwide and selecting the best model for a particular application within the region is not easy (Pitman, 1978).

Streamflow estimation at a point in a river is vital for a number of hydrologic applications, including flood forecasting. Using hydrologic modelling techniques therefore helps communities to prepare for, and respond to, flood events (Artan *et al.,* 2002; Asante *et al.*, 2008). The use of appropriate models for advance prediction of basin hydrologic conditions can mitigate flood damage, support contingency planning and provide warnings to people threatened by floods (Acreman, 2009; Reza, 2007). However, all predictions are subject to uncertainty as a result of both model-simplifying assumptions and errors in model variables and input parameters (Walker *et al.*, 2003; Gupta *et al.*, 2005). In many developed regions of the world, operational flood forecasting has traditionally been based upon a reliable, dense network of rain gauges or ground-based rainfall measuring radar stations that report in real-time. In the Southern African countries, the hydro-meteorological station networks are sparse and rainfall data are available only after a significant delay (Winsemius *et al.*, 2006; Asante *et al.*, 2008). Because of the limited spatial coverage of ground-based gauges, the unavailability of real-time rainfall data and constraints in technical and financial resources, operational flood forecasting has been difficult to implement – in spite of the range of water problems in the region and the acute need for reliable predictions to protect many water-based developments, lives and livelihoods. The availability of global coverage satellite data may offer an effective and economical means of calculating areal rainfall estimates in sparsely gauged areas (Artan *et al.*, 2007). The use of satellite rainfall estimates was found to be the most appropriate approach for predicting future levels of rainfall induced runoff – thereby forecasting likely flooding in the Zambezi Basin. This approach has been demonstrated in previous studies based on research in Africa (USGS, 2000a; Artan *et al.,* 2002; Winsemius *et al.*, 2006; Artan *et al.*, 2007; Asante *et al.*, 2008; Sawunyama and Hughes, 2009; Funk, 2009; Liechti *et al.*, 2011). However this study recognised that floods in the Lower Zambezi (in particular if the floods are more frequent and/or smaller) bring a number of positive impacts to the ecosystem (Beilfuss, 2005; 2009; Nyatsanza and Van der Zaag, 2011). Beilfuss (2005), for example, demonstrated that flood waters carry nutritious and fresh water for feeding (fish, birds and other wildlife) and improving the grassland growth for grazing (wildlife and cattle) down to the Indian Ocean coastal wetlands. Therefore the Zambezi Delta is a wetland of international conservation value, which supports a great diversity of wetland communities of African wildlife including: elephants, Cape buffalo and waterbuck. The delta also has an extensive coastal mangrove and estuaries which support a lucrative prawn fishery (Nyatsanza and Van der Zaag, 2011). Various studies (Beilfuss and Dos Santos, 2001; Beilfuss, 2005; Beilfuss *et al.*, 2009; Nyatsanza and Van der Zaag, 2011) have noted that even if the Cahora Bassa dam was operating at its full capacity (in coordination with the Kariba dam), there would be limited chances to feed the delta with regular flood flows (i.e. for inundation over the river banks), since the peak flood discharge in the Lower Zambezi has been reduced and regularised by upstream dams (mainly Kariba and Cahora Bassa) to meet the hydropower objectives. A similar study, conducted by Nyatsanza and Van der Zaag (2011) on reservoir operating policies for the environmental flows of large dams in the Zambezi River Basin, concluded that the rule curves for Kariba and Cahora Bassa, were not being strictly followed. Therefore, if the Cahora Bassa dam was being strictly operated by the rule curve, it would then be possible to release environmental flows to recover the hydrograph – by up to 50% (or even 100%) – in normal to wet years, without any large negative impact on hydropower production. However, fewer shortages are experienced when the Kariba dam also releases environmental flows. The flood releases in February and March, on the Zambezi, are possible, in normal to wet years, without significantly affecting the hydropower production (although this remains dependent on the magnitude of the environmental flow releases). In real terms, operational difficulties arise from the fact that the hydropower production objectives are, by nature, often contradictory. Managers of both the Kariba and Cahora Bassa reservoirs face multiple constraints: on one hand, they manage a common resource used by multiple partners (e.g. to maximise both hydropower production and water supply for irrigation); on the other hand, they are responsible for the protection of the urban developments (including rural village dwellings etc.) located in flood-prone areas (Beilfuss and Dos Santos, 2001).

This study attempts to address these constraints by making available, for both the operators and the decision makers, a dynamic simulation system of the Zambezi basin, using an integrated model (with routing techniques) that will be useful for assessing potential scenarios (calculated with different timings and water levels) and for predicting the impact of flooding events downstream of the Cahora Bassa dam.

As part of the overall Kariba and Cahora Bassa dams complex, the Zambezi River Basin has three large hydropower schemes; it has also remained the main challenge of this study – primarily because of the time and financial constraints that have hindered the integration of the Kafue hydropower systems into the modelling.

1.2. Motivation

This study has been motivated by two key issues. The first issue was defined by one of the objectives of Integrated Water Resources Management (IWRM) (coordinated water management), taking into account various operating constraints such as: flood control; environmental flow requirements; financial constraints and existing bilateral or multilateral agreements (such as the Power Purchase Agreement (PPA) with Eskom of South Africa) that impact on the Zambezi Basin (Tilmant *et al.*, 2010). Beilfuss *et al.* (2009) and Tilmant *et al.* (2010) reported that the coordination of water resources management aims at optimising the resources in line with the recommendations of the World Commission on Dams, dated 1st November 2000 (Munasinghe, 2004). The Commission recommended that more attention should be paid to the improvement of the operational effectiveness and the efficiency of existing reservoir systems for maximising the beneficial uses of these systems, together with minimising their adverse impacts. This recommendation, which called for more integrated operational strategies, brought forward a number of challenges, including: the increase in the number of alternative operational decisions; the consideration of conflicting objectives and the uncertainties associated with future hydrologic conditions (Madsen *et al.,* 2007). The second issue has been the need to set up, within the Zambezi Basin, a methodology to incorporate Earth Observation (EO) data into the hydrological models and thereby assess the improvements brought by this assimilation on reservoir management in a data scarce environment. Verdin (2000) and Funk *et al.* (2010) demonstrated the applicability of rainfall data obtained from the National Aeronautics and Space Administration's Tropical Rainfall Measuring Mission (TRMM) and from the infrared recorders of the National Oceanic and Atmospheric Administration (NOAA). These products, for detecting areas experiencing rainfall, were tested and verified, with a certain degree of confidence, and the information was fed into a hydrological model for flow prediction in Southern Africa (Artan *et al*., 2002; Funk *et al.,* 2010). While *in situ* river hydro-climatological gauges have served as the primary method for obtaining the data required for managing water resources, the serious shrinkage of monitoring networks, particularly in the developing countries (because of the inadequate funding for both data collection and the maintenance of hydro-meteorological stations (Asante *et al.*, 2008)), has necessitated re-thinking data acquisition techniques.

This study offered an opportunity to initiate the introduction of an integrated flood management for the Zambezi River Basin. The study has developed an integrated tool for flood management to alleviate flood-related destruction and losses, mainly for saving lives downstream of the Zambezi Basin. This tool is comprised of the USGS Geospatial Streamflow Model (GeoSFM) (Artan *et al*., 2007), integrated with the Denmark Hydraulic Institute (DHI) MIKE BASIN reservoir simulation model (DHI, 2010).The main reason for selecting the GeoSFM model was because it is a spatially semi-distributed, physically-based model, parameterised using spatially distributed topographic data, soil characteristics and land cover data sets which are available globally, from both remote sensing and *in situ* sources. The MIKE BASIN reservoir model was selected based on its ability to easily integrate information generated by the GeoSFM model. The combination of these models was expected to provide a robust solution by achieving a coordinated management approach for the areas between the Cahora Bassa dam and the areas downstream of the dam.

1.3. Research questions

This study directly explores several of the main issues associated with water resources management for making predictions in ungauged basins (Sivapalan *et al.*, 2003) and for the application of hydrological models to solve practical problems in a data-poor but socio-economically important river basin in Southern Africa. The study attempts to provide answers to the following set of questions:

i. Can satellite rainfall and globally available data source be successfully used as input into hydrological modelling for flooding forecasting in data scarce environment?

This question addresses the issue of using satellite data in filling the data gaps. It can generate guidelines for collecting, analysing and validation of satellite data before using as input to hydrological modelling.

ii. How can a rainfall runoff model be integrated with existing reservoir simulations for daily water resources operation systems?

The issue raised by this project was to investigate how the estimated streamflow could be used by the reservoir managers to both operate a dam and alleviate flooding downstream of the Zambezi Basin. To address this question the selected reservoir modelling needed to be compatible with the rainfall-runoff model and to produce reliable results.

iii. How can the impact of floods be minimised by the use of integrated hydrological models?

This question addresses the issue of using integrated models in an operational context offering methods to the hydrologist for the quantification of the downstream impact of floods. This study also presents methods for flood mapping according to the water level.

1.4. Research objectives

The objective of the study has been to contribute towards the development of methods and guidelines for improving water resource management systems in the Zambezi River Basin through the use of tools that incorporated both Geographic Information Systems (GIS) and Remote Sensing techniques. To achieve the main aim of the study, it has been necessary for relevant data being fed into the selected models to be accurately collected and thoroughly validated, and for the relationships that exist in the basin (for instance: between using water for power generation and reducing flood impacts downstream of Cahora Bassa dam) to be identified and discussed. In this study four specific objectives have been identified:

1. **Assessment and evaluation of satellite data: to determine the appropriateness of satellite products as input data in hydrological modelling for flood forecasting in the Zambezi Basin.** To assess the model applicability and performance (whether hydrologic or hydraulic modelling) data inputs were acquired. It was also considered necessary to define the spatial and temporal scales of the available data. Given that rainfall is the major driver of any hydrological model, remote sensing data sets, in conjunction with ground-based observations, were investigated and used as inputs to the hydrological model. The processing and preparation of the remote sensing data are becoming a valuable contribution towards rainfall data validation, particularly for the community of hydrologists in the data-poor Southern Africa region, leading to an

improvement in the ongoing collection, validation and use of satellite data and the application of both GIS and statistical methods.

2. **To assess and evaluate the performance of the selected hydrological model as flood forecasting tool in the Zambezi Basin**. This study provided an opportunity to explore the application of remotely sensed data as input to hydrological models for natural streamflow forecasting. The hydrologic simulations were then used as input into a reservoir simulation model to forecast downstream flooding conditions.
3. **To integrate and assess the performance of the selected hydrological model with reservoir simulations for the daily water resources operation system**. This study provided an opportunity to explore the procedures and guidelines for both the establishment of an integrated flood forecasting and management tool in the Zambezi Basin by integrating predicted flow from the hydrological model into reservoir simulation model and for balancing the conflicting water uses (power production, and flood control). Such an approach offered management agencies and practitioners working in the basin an operational (and forecast) tool that would help make integrated management of the basin a reality.
4. **To develop an integrated flood management tool for flood forecasting and management downstream of the Cahora Bassa dam**. Based on the results of the simulations, the study proposed an integrated flood management tool that may assist the dam operators to run a number of possible releases alternatives for flood management downstream of the Cahora Bassa dam before the actual releases would take place. It is expected that the analysis of the release alternatives would cover the range of conditions that may realistically be expected to occur within the basin.

1.5. Summary of the general methods

To accomplish the planned activities, a summarised research process for data collection, analysis and interpretation is explained in this section and shown in Figure 1.1. This study was conducted using a desk-top approach. A review of existing and applied models in the study area was conducted to judge their applicability, weaknesses and strengths towards selecting the two water resource modelling systems most useful for improving flood forecasting in the Zambezi Basin.

The model input data was quality-checked before being used for the modelling process. A simple comparison was done for CPC-RFE 2.0 and TRMM 3B42 satellite rainfall data and spatially averaged rain gauge-based data at the same pixel. Secondly, a simple regression (R^2), Relative Percentages of Bias (RPB), the Relative Root Mean Square Error (RRMSE), and the Index of Agreement (IA) were all used to compare the observed data with estimated satellite datasets.

The verification of the model was first done by comparing (r-squared) with the observed information and model generated streamflows. The Relative Root-Mean-Square Error (RMSE) in Moriasi *et al.* (2007) and Nash-Sutcliffe Coefficient Efficiency (NSCE) in Nash and Sutcliffe (1970) were used to evaluate the results produced by the model before and after the calibration process. To assess the relationship between the flows discharged at the Kariba and Cahora Bassa dams and the flooded areas downstream, a computer-based information system and a flood mapping procedure was established – primarily to support decision-making by water resources managers. The simulated flows from the rainfall-runoff model were used to drive a reservoir and hydropower model. To complement the application of flow simulation models towards visualising and clearly predicting the impact of flow on the local communities and the socio-economic infrastructure, flood mapping areas were delineated for the Lower Zambezi.

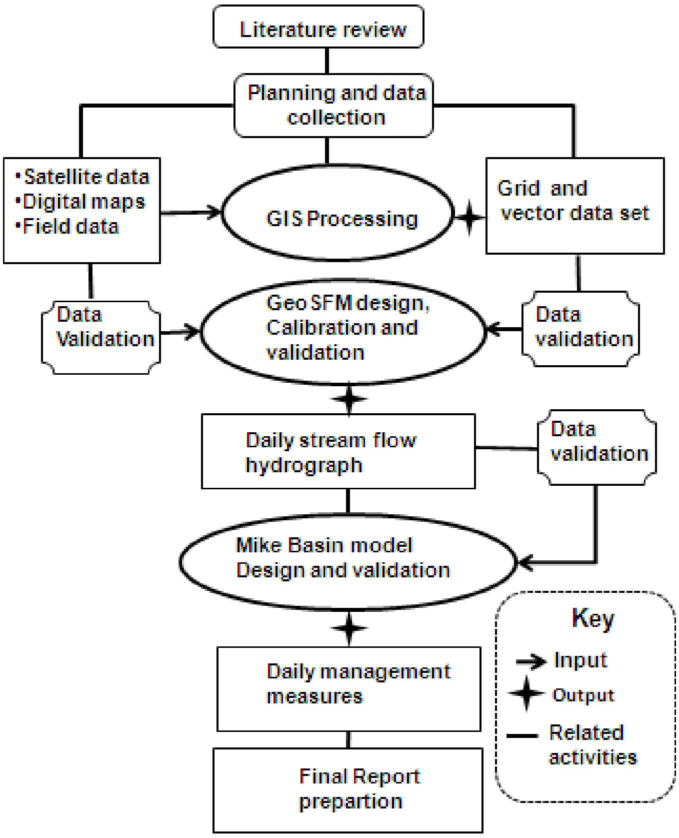

Figure 1.1: Summary of the applied research process

1.6. Expected outputs

Given the regional situation, this study could potentially provide a practical solution for water resource managers who are often called upon to make hydrological predictions in data-scarce areas for long-term, highly capitalised water resource monitoring projects. On one hand, progress has been made by USGS (2000) – through the use of Geographic Information Systems (GIS) combined with Remote Sensing Techniques – to provide input data for the Geo-spatial Streamflow Model, which was used to predict excess runoff. DHI have developed the MIKE BASIN reservoir simulation model which uses runoff as input, to provide options to the reservoirs managers on daily reservoirs operations. These developments led to the formulation of a standard hydrological integrated tool in the Zambezi River Basin, for use now and in the future. The scope of these models will also continue to rise as more uses for the model are discovered. Published results indicate that climate model results based on the daily time-step have been more reliable for flood prediction and flow monitoring than those at longer time scales (Artan *et al.*, 2002). Thus the GeoSFM and MIKE BASIN models could possibly be used for forecasting flood scenarios and quantifying their likely impact before they occur. Therefore, this study aims to contribute to supporting the decision-making in Integrated Water Resources Management, especially for the implementation of water system technologies in hydropower reservoir operation. The study is also expected to produce the following outputs:

- Knowledge of the variability of climatic and hydrological processes occurring at the various spatial and temporal scales in the basin;
- Knowledge of how well the multi-reservoir systems can be operated mainly through integrated water resource systems framework;
- Knowledge of flood risk impacts downstream of Cahora Bassa dam, for flooding of different extents.

1.7. Thesis structure

The thesis consists of a total of eight Chapters. The present chapter gives an introduction to the problem, motivation for undertaking the research in the Zambezi Basin, research questions, objectives of the study, expected outputs, summary of the applied research process and organization of the thesis. Chapter 2 contains a detailed review of the relevant literature on hydrological, water resource systems and forecasting modelling, concepts and example of similar studies which have been undertaken elsewhere in the world (as well as in the study area). Chapter 3 presents the description of the study area including the location, physiographic aspects, land cover, climate and issues related to water resources and flood management. It also provides a summary of the available data and the current operating approaches within the basin. Chapter 4 introduces the model development and describes the data and methods used in the study. In this chapter the actual data used are presented, including the algorithms which were developed for the model development process. Chapter 5 presents and discusses the results of satellite rainfall data validation, including the criteria for selecting remote sensing products for hydrological forecasting. Chapter 6 is a presentation of the results and discussion of the modelling calibration for the Zambezi Basin and the main findings of the study. Chapter 7 presents and discusses the application of the integrated modelling system for Lower Zambezi. Chapter 8 contains the conclusions and recommendations based on the findings of the study. In this last chapter conclusions related to the verification of the model, importance of flood area and key recommendations intended to improve model operation in the study area are outlined.

2. LITERATURE REVIEW AND THEORETICAL BACKGROUND

2.1. Introduction

This chapter provides a general discussion on flooding and an overview of the problems that have affected communities in the Lower Zambezi Basin in Mozambique. The relevant published literature, open source online information and national reports have been used to provide information on the major issues associated with flood events, the methods that have been applied for the estimation of flood peaks and the need for hydrological models. The general concepts of rainfall-runoff modelling in both gauged and ungauged basins, and reservoir modelling, are introduced. The chapter also reviews recent advances in hydrologic modelling and flood mapping, together with modelling of large-scale flooding events. The methods of estimating floods based on calculating flood peaks, flood hydrographs and flooding extent are described in the subsequent sections.

2.2. Flooding in the Zambezi River Basin

2.2.1. Background on flooding

There is consensus worldwide that hazards which occur as a result of hydrological extremes (such as flooding), are on the increase (IPCC, 2007; Samarasinghe *et al*., 2009; Uddin *et al*., 2013). This is evident from recent changes in the frequency and severity of floods and droughts and through analysing the outputs from the climate models used to predict increases in hydrological variability (IPCC, 2007; Todd *et al*., 2011). Extensive work on the assessment of flood risk has been carried out in many parts of the world – including Africa (Artan *et al*., 2002; 2004; Bambaige, 2007; Bilberry *et al.,* 2011; Uddin *et al*., 2013). In these studies, structural and non-structural methods have been developed and tested as contributing components of flood management systems (Beilfuss, 2001; Artan *et al*., 2001; Islam and Sado, 2002; Shrestha, *et al.,* 2008; Asante *et al.*, 2008). Complex assessments of the flood process chain that link the different processes leading to flood disasters have been carried out. These processes include the causes of extreme precipitation events, runoff generation and concentration in the catchment and flood routing through the river network (Mark *et al*., 1998; Bates and DerRoo, 2000; Horritt and Bates, 2001a; Spachinger *et al.*, 2008). There are many definitions of floods. The definitions below were selected because of their relevance to the present study. According to Malilay (1997), floods are: the inundation of areas that are not normally submerged; a stream that has broken its normal confines; water has accumulated because of the lack of drainage; or failure of flood control structures. Floods occur in rivers when the flow exceeds the capacity of the river channel, spreading water onto the adjacent floodplain. Floods often cause damage to homes and businesses if they are located within the natural flood plains of rivers (Malilay, 1997; Kugler *et al*., 2007; Shrestha, *et al.,* 2008; Harun, 2009). Therefore, according to Malilay (1997) and Fonseca (2012), to understand the source of water that results in flooding, it is necessary to look at the whole catchment area as a united system (Figure 2.1). The upstream rainfall can cause flooding of a downstream area. In cases of poor drainage of a flat area, the rain directly falling on it may cause floods also (ponding of rainwater).

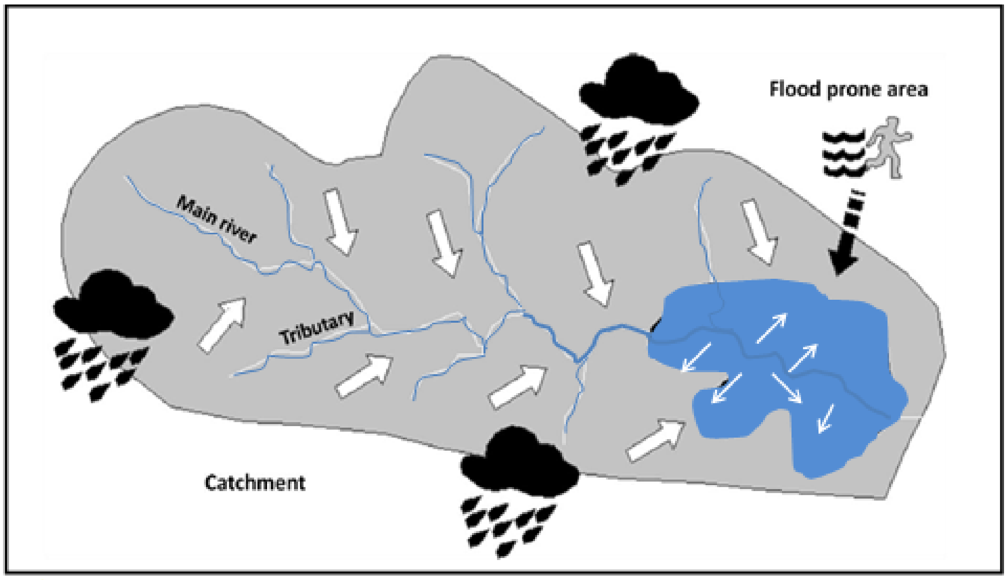

Figure 2.1: Schematisation of the catchment system in context of flood

Mozambique, for example, is one of the southern African countries most exposed to hydro-meteorological hazards (USAID, 2002; SARDC and IMERCSA, 2007) and specifically prone to flooding in the Central and Southern regions. Mozambique shares nine (9) of the fifteen (15) transboundary river basins of southern Africa, and is located downstream of eight (8) of them (Figure 2.2). During recent decades, Mozambique has repeatedly suffered tragic loss of life, massive economic damage, and severe environmental losses caused by catastrophic flooding (INGC, 2009; DNA, 2014). In the summers of 2000, 2001, 2005, 2006, and 2008, scenes of devastated cities, villages, and landscapes, caused by flooding around the six major river basins, resulted in economic costs estimated at one billion of U$D (Table 2.1). Coming just five years after the floods that caused havoc across Southern and Central Mozambique, and less than a decade since the dramatic floods along the lower and middle courses of the Limpopo, Zambezi and Licungo rivers, a major flood occurred in the summer of 2013. The government of Mozambique, and people in general, wondered why such events seemed to be happening more often, to be causing more damage than in the past, and how better to deal with the floodwaters (DNA, 2014). Floods are natural phenomena which occur from time to time everywhere that rivers exist. However, as natural floodplains and river courses in Mozambique have been heavily transformed by human intervention, especially since the colonial times of the 19th century (DNA. 2014), the natural environment can no longer buffer and absorb flooding that easily. Moreover, floodplains are used intensively as areas for settlement and for the production of food, wood, and water. These interventions in the natural system, as well as the dependency on the floodplains' productive, regulatory, and protection functions, make the human system additionally susceptible to the hazardous event of river flooding (INGC, 2009).

Therefore, a naturally-induced hazard is more likely to become a social disaster because of its frequency (Table 2.1, (DNA, 2014)). Further, Table 2.1 demonstrates that the Zambezi River is the most prone to flooding – flooding occurs at least once every 5 years – costing the Mozambican Government more than 300 million U$D in relief and reconstruction of socio-economic infra-structure, (DNA, 2014; INGC, 2009). A study by SMEC (2004), quantified that, in the Zambezi Basin during 2000/2001 flood, approximately 217 000 people were temporarily relocated and 115 lives were lost. It may be inferred that at least 50 000 houses, more than 100 schools and hospitals were inundated, more than 30% of the total area was inundated and more than 40% of the total population was affected during the same flood. Other sectors which suffered heavy damage included: health; education; water and sanitation; energy; telecommunications; railways; livestock; trade and tourism. The high risk areas of the Lower Zambezi are: the districts of Mutarara, Chemba, Caia, Mopeia and Marromeu (DNA, 2014).

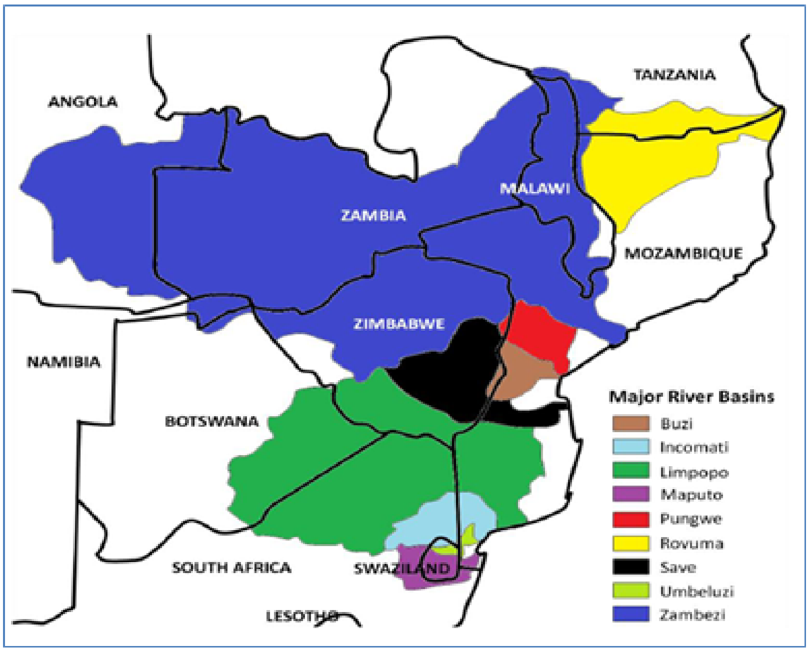

Figure 2.2: International river basins shared by Mozambique (Source: Fonseca, 2012)

Table 2.1: Major flood events in Mozambique within the last 15 years (2000 to 2014 inclusive)

Major floods events	Year of Occurrence	People affected	People dead	Houses affected	Houses destroyed	Cost (Million U$D)
Limpopo, Incomati, Umbeluzi, Pungwe, Zambezi and Lugela	2000	3 000 000	783	500 000	390 000	600
Zambezi and Pungwe	2001	400 000	200	155 000	147 000	25
Incomati, Limpopo and Buzi Rivers	2004	50 000	5	1 000	450	5
Zambezi River	2005	25 000	7	5 000	250	0,9
Zambezi and Buzi Rivers	2006	800 000	50	90 000	6 000	100
Zambezi, Pungwe, Buzi, Save, Licungo and Messalo Rivers	2008	50 000	140	75 000	15 000	75
Limpopo, Licungo and Zambezi	2013	154 000	117	350 000	70 000	550
Total	-	**4 479 000**	**1 204**	**1 176 000**	**628 700**	**1 355,9**

Sources: INGC and DNA database

2.2.2. Causes of flooding

Floods occur when high flows overtop normal confining banks and cover land that is usually dry (Sheila, 2000; Murwira, 2006; Moel *et al.,* 2009).There are a number of factors that can contribute to flood conditions and these can be meteorological or non-meteorological (AMS, 2000; INAM, 2002; WMO, 2011). In the case of the Zambezi Basin, flooding in Mozambique is because heavy monsoon rainfall, caused by the general global circulation patterns of the air-masses through the trade winds, converges in the Inter-Tropical Convergence Zone (ITCZ) and the high levels of tropical cyclone activity result in the frequent failure of existing infrastructures designed to prevent flooding (Beilfuss and Dos Santos, 2001; Asante *et al*., 2008). The ITCZ is a zone close to the equator where massive rain-bearing clouds form rain when the South East Trade Winds meet the North East Monsoon Winds (Tallaksen and Van Lanen, 2004; Brandon, 2011). Under convection, the air rises to the upper atmosphere where it is met by a compensating pole-ward flow (Hadley cell). Sinking and diverging air-masses from the Hadley cell form a permanent Subtropical High Pressure Belt at latitudes 20^{o} – 40^{o} South This belt is largely made up of anticyclones, which form as a result of high pressure. Westerly winds (westerlies) prevail in the mid-latitudes between 60^{o} – 80^{o} South. Pole-wards, beyond 60^{o}S, is the Polar Front, which is a mixture of cold polar air and warm tropical air. This mixture forms a meandering jet stream in the upper atmosphere. The ITCZ migrates north and then migrates South of the equator because of seasonal changes in global radiation (Tallaksen and Van Lanen, 2004). As the ITCZ shifts position, other circulation features (e.g. the jet stream and the sub-tropical high pressure belt) are also shifted and so cause heavy rainfall in the South East, where the Zambezi Basin is located. Figure 2.3 shows general global circulation patterns and an example of the trajectory of Cyclone Eline on February 21, 2000. As a consequence, flooding of extensive areas occurred in the six major river basins of Mozambique namely: the Zambezi, Pungue, Buzi, Save, Limpopo and Incomati Rivers.

The nature of flood events, the damage that they cause, as well as the approaches that can be adopted to prevent or reduce damage are often scale related. Small scale floods are typically caused by high intensity, short duration rainfalls (flash floods) and can be exacerbated by urban development that restricts infiltration and generates higher rates of surface runoff (Brakenridge, 1999; Kugler *et al.,* 2007; Shrestha, *et al.,* 2008; Harun, 2009). While larger scale floods are caused by larger weather systems, often covering whole river basins, they are typically easier to predict because they develop over longer periods of time. However, the very large volumes of runoff and streamflow mean that they are also difficult to manage (Khalequzzaman, 1994; Murwira, 2006; Alam and Rabbani, 2007).

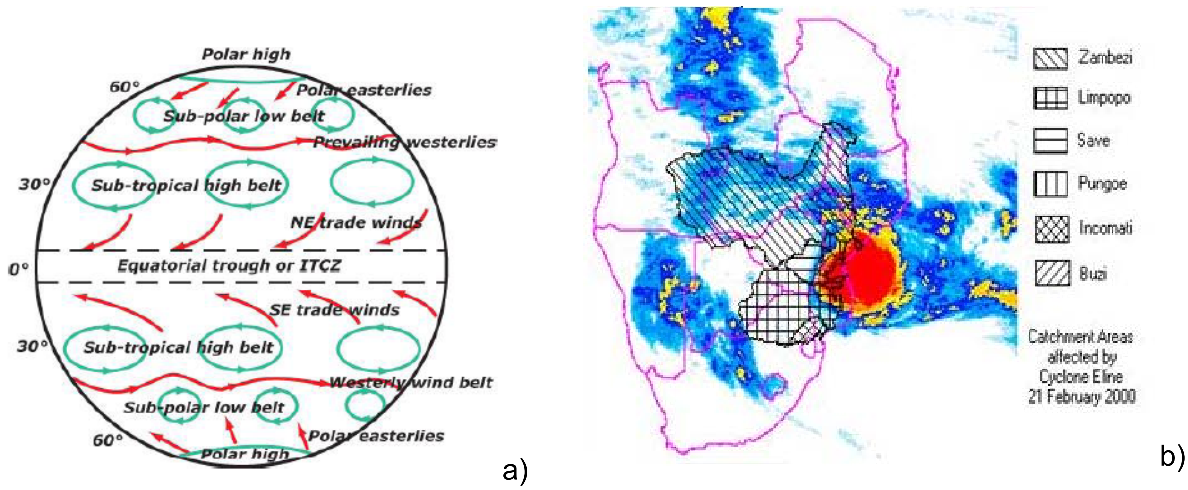

Figure 2.3: General global circulation patterns. (a) map of the satellite image, (b) trajectory of Cyclone Eline and basin areas affected – 21 February 2000 (Sources: RM and UNDP, 2000; Brandon, 2011)

2.2.3. Impacts of flooding

Many studies on flooding (Khalequzzaman, 1994; EMA, 2002; El-Raey and Beoro, 2003; Jinchi, 2005; Asante *et al*., 2007c), classify the impacts of flooding in two stages: firstly impact during the flooding event (negative impacts because they are destructive) and, secondly, the impact after the flooding event The latter impact can include positive factors which are ultimately productive for the environment and society.

Negative impacts: Floods are one of the most widespread and destructive natural disasters and while many of the effects can be attributed to the natural events themselves, others are also associated with poor land-use management (Khalequzzaman, 1994; Asante *et al.,* 2005).

Floods occur naturally along most river systems and in low-lying areas (Kundzewicz and Takeuch, 1999; Beilfuss and Dos Santos, 2001). Flooding occurring in densely populated urban areas has the capacity cause a large amount of damage to life and property (EWC *et al*., 2003; Chiesa *et al*., 2012). Flood damage consists of both primary and secondary effects (Murwira, 2006). Primary effects include: loss of human life and livestock; physical damage to property and infrastructure (such as bridges, roads and sewer systems). Primary effects also include the erosion of agricultural land and the destruction of crops (El-Raey and Beoro, 2003; Jinchi, 2005). Secondary effects occur after the floods have receded and can include breakdowns in the water supply and sanitation infrastructures or the contamination of water supplies – both these breakdowns can lead to unhygienic conditions and the spread of diseases (Murwira, 2006; Moel *et al*., 2009).

In developing countries, floods cause a large number of deaths, and billions of dollars' worth of property damage (Shrestha *et al.,* 2008; Uddin *et al*., 2013). According to Chiesa *et al.* (2012), flooding is a major cause of fatalities and infrastructure damage worldwide. In 2003, for example, major floods caused more than U$D 8 billion in damages and more than 4 000 deaths worldwide. In Southeast Asia, the Mekong River Basin has been extremely hard hit by floods in recent years (including 2000, 2001 and 2002) (Chiesa *et al*., 2012; EWC *et al*., 2003). In southern Africa, the INGC (2009) and SMEC (2004) studies in Mozambique, showed that the flooding experienced in 2000 was the worst flood in 50 years, directly affecting 2 million people and forcing them to leave their homes. Approximately 700 people died, and the damages were estimated to be U$S 600 million – losses which led to a decrease in the country's economic growth, down from 10% to 4% per annum (MICOA, 2006; Bambaige, 2007). Figure 2.4 shows an example of negative impacts after the 2000 flood in the Limpopo and Incomati basins. Shrestha *et al.* (2008) demonstrated that the increases in vulnerability to flood disasters in most of the developing countries are directly related to high levels of poverty and high rates of population growth.

In early 2008, La Niña-related heavy rain caused widespread flooding South Africa, Zimbabwe, Namibia, Botswana, Zambia, Malawi and Mozambique. In the Mozambique area of the Zambezi Basin, more than 6 000 people were displaced and more than 115 lost their lives because of the floods (INGC, 2009).

a) b)

Figure 2.4: Negative impacts of the 2000 flood, Incomati and Limpopo River Basins in Southern Africa. (a) railway line destroyed in the Incomati River basin; (b) electricity supply disruption in Xai-Xai in the Limpopo River basin

Positive impacts: Flooding may also bring many positive impacts (Beilfuss and Dos Santos, 2001; El-Raey and Beoro, 2003; Jinchi, 2005). These include: recharging of natural ecosystems; provision of abundant fresh water for agriculture, health and sanitation; and the deposition of nutrient-rich sediment on floodplains, thereby enhancing crop yields (Beilfuss and Dos Santos, 2001; El-Raey and Beoro, 2003; Jinchi, 2005). For example, after the 1999 flood in the Yellow River Basin, Jinchi (2005) concluded that the agricultural production of cotton in China increased by 15%. El-Raey (2003) showed the importance of the Nile River basin annual flooding to be the main source of water supply for agriculture activities in Egypt. Agriculture accounts for 70 percent of full-time employment in Africa, 33% of total GDP, and 40% of total export earnings (FAO, 1999). In many countries (such as Bangladesh) more than 30% of the total population are dependent on ground water and underground aquifers for fresh water. These aquifers are, in turn, reliant on flood waters for recharge and replenishment (FAO *et al*., 2003). In Mozambique, after the 2000 flood, new studies on flood forecasting and management were conducted (USGS, 2000a; Artan *et al.,* 2002; DHI, 2006) and new methods for flood forecasting had been put in place. Since the 2000 flood, the government of Mozambique has created more than 200 new resettlement areas to move the population from the flood high-risk areas to safer localities (Arnall *et al.*, 2013). In the study on flooding, resettlement, and change in livelihoods by Arnall *et al.* (2013), evidence from rural Mozambique demonstrated that the developed and implemented policies by the government of Mozambique after the 2000 flood had shown positive impact on communities. Therefore the economy of these communities has moved away from rain-fed subsistence agriculture towards both commercial agriculture and non-agricultural activities, thus improving the living conditions of the poorest and most vulnerable members of society (Pelling and Dill, 2010). Flooding also plays an important role in replenishing wetlands and thereby balancing the health of the ecological status of the wetlands. Healthy wetlands promote healthy water supplies (Kunkel *et al*., 1994; Kolva, 1993; Walker and Kunkel, 1994).

It may reduce political tension among those countries sharing international rivers, by making water available to different users. International river basins (such as the Tigris, Euphrates in the Western Asia, and the Nile in Eastern Africa and other major rivers in the world), are potential sources of conflicts directly related to water scarcity. In the case of the Tigris basin, the Euphrates has been shared by Iraq and parts of Turkey, Syria, Iran, Saudi Arabia, Kuwait and Jordan. Seasonal flooding is a major contributor to the increase in water availability in the region. According to Zentner (2012), the 2008 drought in Iraq sparked political tension; new negotiations between Iraq and Turkey over trans-boundary river flows were then conducted. As a result, Turkey agreed to increase the outflow several times, effectively beyond its means, to supply Iraq with extra water.

The Nile River is shared by eleven countries: namely Rwanda, Burundi, Democratic Republic of the Congo (DRC), Tanzania, Kenya, Uganda, Ethiopia, Eritrea, South Sudan, Sudan and Egypt. Of these countries, Egypt is heavily reliant on water from Nile River, and has asserted natural historical rights on the Nile River. The principles of its acquired rights have been a focal point of negotiations with upstream states. The fact that this right exists means that any perceived reduction of the Nile water supply to Egypt, because of either a reduction of seasonal flooding or through abstractions upstream, is considered to be tampering with its national security and thus could potentially trigger conflict among the countries (Chatteri; 2002). Other positive impacts of floods include: improve navigation; washing out of acidic water; flow carrying salty water toward the sea, etc. (Mays, 1996).

2.3. Flood management

Flood management is the execution of strategic decisions to reduce the negative impact of floods through both structural and non-structural measures (Brakenridge, 1999, Kugler *et al.*, 2007; Hudson *et al.,* 2008). Current approaches for flood management and protection have led to limited success, especially during recent extreme events (INGC, 2009). This is especially so in the developing world, where the risk and vulnerability to flooding is high and the appropriate management and response strategies are not well developed. It is therefore imperative that an integrated flood risk management strategy be developed which will take cognisance of both the hydro-meteorological and the societal processes. At the same time, the real effects of risk mitigation measures need to be critically assessed (ICOLD, 1992; Vaz, 2000; Beilfuss and Dos Santos, 2001; Alexander, 2002a; Artan *et al*., 2001; 2002; Asante *et al.*, 2007c; INGC, 2009). Table 2.2 summarises flood management measures which have been executed in various parts of the world (Vaz, 2000; El-Raey and Beoro, 2003; Jinchi, 2005; Hudson *et al.,* 2008).

Table 2.2: Summary of flood management measures

Structural Measure	Non-Structural Measure
• Construction of dams • River diversion • Construction of river levees and embankments • Widening and deepening of the river bed • Retention of flood water in mining ponds/lakes, water-supply dams, hydroelectric dams, etc.	• Restriction development planning • Water proofing • Flood insurance • Flood forecasting and warning system

Flood management measures can be classified into two categories: (a) a structural engineering–based approach to control floods and (b) the non-structural non-engineering based approach to flood management (Andjelkovic, 2001). Structural measures are associated with the high costs of construction of building new (and/or high maintenance costs of existing) hydraulic infrastructure. Most existing structures were designed for a specific range of floods and thus potentially create a false sense of security (Görgens, 2007a, NR2C, 2008). If the anticipated flood range is exceeded then the flood impact can be even worse and communities are less than well prepared. Viljoen (1999) showed that the Klipfontein dam failed to mitigate flooding in Mfolozi River in 1994; ARA-Sul and DNA (2000) also showed that the Massingir dam failed to mitigate the impact of the 2000 floods on the Limpopo River at Chokwe and Xai-Xai. Non-structural measures can be a less capital-intensive alternative for developing countries where resources are scarce (Artan *et al.*, 2002; Asante *et al.*, 2008). These non-structural measures are also necessary to complement those structural measures proving to be ineffective for excessive floods – levels of water that are beyond the design capacity of the structures. The application of non-structural measures consists of establishing a programme to trigger flood warnings and issue advanced notice that a flood may occur in the near future at a particular geographic point (James and Korom, 2001). The measures would also need to include a plan of action to allow communities to respond in an appropriate way (Grigg *et al.*, 1999; James and Korom, 2001).

2.3.1. Flood forecasting

Flood forecasting is an essential tool for flood risk management, both to reduce the impact on vulnerable communities and as an important component of flood warning (Anderson and Burt, 1985; Yates *et al.*, 2000; Shrestha *et al.,* 2008; WMO, 2011). The outcome of flood forecasting models is a set of forecast time-profiles of channel flows or river levels at various locations; "flood warning" is the task of making use of these forecasts to decide whether flood warnings should be issued to the general public, and to revise and/or update standing warnings (Hernando, 2007). Flood warnings need to be issued when an event is imminent, or is already occurring and must be issued to a range of users, for various purposes, including the following:

- To bring operational teams and emergency personnel to a state of readiness;
- To warn the public of the timing and location of the event;
- To warn of the likely impacts on roads, bridge crossings, dwellings and flood defence structures;
- To give individuals and organizations time to take preparatory action;
- In extreme cases, to give warning to prepare for evacuation and emergency procedures; and
- To provide information for the safe operation of dams (Anderson and Burt, 1985; Hernando, 2007; WMO, 2011).

Flood warning has been going on since floods became problematic to human interests: the ancient Egyptians rowed down the River Nile to warn of coming floods (Keys, 1999). Recently, warnings have become more sophisticated as advances in science and technology have contributed to better systems to predict the severity of floods, their timing and rate of rise, and to assist with the communication of warning messages to communities likely to be affected (Rahman *et al.*, 2002; Maidment, 1996).

2.3.2. Flood forecasting models

Flood forecasting models are useful tools for flood warning (Cannon, 1993; Loumagne *et al*., 2001; Chowdary *et al.*, 2012). The evolution of public weather forecasting during the twentieth century led, inevitably, to the provision of specialist services – including flood forecasting (Maidment, 1996; Loumagne *et al*., 2001; Funk *et al*., 2003). Flood forecasting and warning models are highly data specific (meteorological and hydrological) and demanding in terms of both the quality and quantity of information (Maidment, 1996). The models are dependent on adequate monitoring of the key meteorological and hydrological variables. Thus, one of the main constraints in flood forecasting is the decline of data collection networks and hydraulic infra-structures in developing countries (Funk *et al*., 2004; Asante *et al.,* 2007c; WMO and USAID, 2012). Moreover, many measurement stations in developing countries are manually operated, with little real-time data being collected, affecting the ability of agencies to give proper real-time warnings to the communities. Flood forecasting and early warning systems currently consist of networks of rain and river gauges and hydrologic modelling for the development of general qualitative and quantitative forecasts of flood levels. These early warning systems can often reach high levels of technical accuracy (Keys, 1999; Shrestha *et al.,* 2008). With the passage of time many manual gauges have been linked to telemetry systems to allow remote access to data by telephone and, by the late 1980s, radio-telemetered ALERT (Automated Local Evaluation in Real Time) and similar data collection systems have been established on several of the faster-responding rivers (Keys, 1999).

AWRA (1996) noted that a number of Hydrological models may be used for real-time operation and have been operated in worldwide. In USA for example, the National Weather Service (NWS), through its River and Flood Program (RFP), have developed a watch on the nation's river systems which has been applied for flood forecasts services for approximately 3 000 communities (Fread *et al*., 1995). The NWS relies on a wide variety of sources and techniques to collect data. Many of the ground sensors are owned and operated by major NWS co-operators, including the U.S. Army Corps of Engineers (USACE), the U.S. Geological Survey (USGS), U.S. Bureau of Reclamation (USBR), and the Tennessee River Authority (TVA). In addition to real-time hydrometeorological data, historical data are used in conjunction with hydrologic and hydraulic models for flood forecasting in USA (Fread *et al*., 1995). A study by Hénonin *et al.* (2010) in France demonstrated that the *Evaluation et Suivi des Pluies en Agglomeration pour Devancer l'Alerte* (ESPADA), developed by the local Government in 2010, has been used for real-time flood forecasting and warning for approximately 150 000 people in Southern France. The ESPADA system is based on the local rainfall forecasting, using both radar of 1 km^2 resolution and a measurement network of 10 rain gauges and 11 water levels. The data is transmitted every 15 minutes to the central hub where it is used as input for rainfall-runoff models to forecast the flow, with updates every 30 minutes. In Thailand, MIKE Flood Watch has been installed for real-time flood monitoring and forecasting on the Chaophraya River (Madsen *et al*., 2003).

Mike Flood Watch integrates data management, forecast models and dissemination methodologies in a system within a GIS platform in real-time. Operation of the system is forced by measured rainfall and stream data. These data are measured automatically by telemetric devises installed in the field; the data are then automatically recorded and stored in a data logs and transmitted via an HMF system to the computer servers. The flow is forecast with updates every 30 minutes. In southern Africa, the U.S. Geological Survey (USGS) Earth Resources Observation Systems (EROS) Data Center, as one aspect of its support of the Famine Early Warning System Network (FEWS Net), has developed a flood-monitoring system thereby improving the modelling capabilities of the Southern Regional Water Authority of Mozambique (ARA-Sul). The model has also been applied to the Limpopo River Basin. The model simulates the dynamics of the runoff processes, using precipitation in near-real-time, estimated from remotely-sensed data – the primary dynamic forcing variable (Artan *et al*., 2002; Asante *et al.*, 2007c). The model is currently operational for the Limpopo Basin, and it can be used with catchment modelling units ranging from 10^2 to 10^3 km^2 in area, with a mean area of 3 500 km^2 (Artan *et al.,* 2002). Artan *et al.* (2001; 2002) suggested that the model should be replicated for other River Basins to enable the model to help reduce human and economic losses by providing improved monitoring and forecast information, and to guide relief activities in many African regions.

The model's predictive skills were verified with observed streamflow data from locations within the Limpopo Basin. The model performed well while simulating the timing and magnitude of the streamflow during an episode of flooding in Mozambique in 2000 (Artan *et al*., 2002; Asante *et al.*, 2007c) and for the 2013 floods in the Limpopo Basin (DNA, 2014). This model was used for warning people living in the floodplain areas of the towns of Chokwe, Chibuto and Xai-Xai with 48 hours of advance warning. Elsewhere, Asante *et al.* (2008) demonstrated the ability of the Geospatial Streamflow Modelling system to simulate flow variations, between 1998 and 2005, in the Congo, Niger, Nile, Zambezi, Orange and Lake Chad basins. The resulting simulated flows were compared with the mean monthly values from the open-access Global River Discharge Database. The study demonstrated that most of the severe flood events were independently verified by the Dartmouth Flood Observatory (DFO) and the Emergency Disaster Database (EM-DAT).

In Ethiopia, research in flood forecasting modelling conducted by FEWS-Net and the Ethiopian Government (Moges, 2007), convinced policy makers and planners that there was a clear need to establish a Flood Forecasting and Early Warning System (FFEWS) to mitigate the impact of flood. The study recommended and suggested a possible institutional framework and real-time communication strategy with the stakeholder institutions. It also highlighted the need for research and development support in the process of developing the FFEWS. The need for training and capacity building was also considered a critical element of any successful FFEWS programme (Moges, 2007). Depending on the availability of: hydrological and hydro-meteorological data; basin characteristic information; computational facilities available at the forecasting stations; the warning time required; the purpose of the forecast; various different flood forecasting techniques are being used in Asia and southern Africa (LFEWS, 2012; WMO and USAID, 2012). These techniques include: a simple flow-stage (Q-h) relationship – developed using the measured flow; observed stages and data collected at the sub-basin area. Most of the techniques, however, are suitable for small- to moderate-sized catchments, rather than for large-sized catchments, where hydrologic models are required (Artan *et al.*, 2002). Stochastic models have primarily been applied by researchers and academics for real-time flood forecasting. However, their application is restricted to only a few places, since stochastic models not only try to use models for predicting hydrological variables, but also try to quantify the errors in model outcomes. In practice the exact values of the errors in model predictions are not known; otherwise it would be possible to correct the modelling outcomes (Bierkens, 2002; Singh, 2012). The computing techniques (such as ANN (Artificial

Neural Networks) and Fuzzy logic) are currently in the development stage and their application is primarily by academics and researchers (Lund and Guzman 1999; Dubrovin *et al.,* 2002).

The Fuzzy logic system consists of unsupervised algorithms to solve a clustering problem by classifying a given data set through applying a certain number of cluster priorities. Meanwhile the Artificial Neural Networks model attempts to emulate the architecture and information representation scheme of the human brain (Lund and Guzman, 1999).

Both the Fuzzy logic systems and the Artificial Neural Networks have advantages when unclear or prior knowledge is required (Nasira *et al.,* 2008). In southern Africa basins – for instance the Zambezi Basin – WMO and USAID (2012) recommended that a highly interdependent and fully co-ordinated system needs to be established and should be composed of environmental monitoring, preparation of forecasts and warning and their dissemination. Therefore the Fuzzy logic systems and the Artificial Neural Networks may be a solution for the Zambezi Basin for flood forecasting, rather than using fully co-ordinated and interdependent systems. The commonly used techniques for flood forecasting and early warning system are Climatic Outlooks (SARCOF, CPC, and ECMWF). The Southern African Regional Climate Outlook Forum (SARCOF) is the most commonly used flood forecasting and early warning system in the Zambezi Basin (INAM, 2002; Fonseca, 2012; WMO and USAID, 2012). The SARCOF products issue seasonal rainfall forecasts at the beginning of a rainy season (September) and they are updated throughout the rainfall season in terms of their probability of occurrence. Other products include seasonal outlooks produced by the National Prediction Center (CPC) and from the National Oceanic and Atmospheric Administration (NOAA) and the European Centre for Medium-Range Weather Forecasts (ECMWF). Flood forecasting is associated with many uncertainties and its success depends on following the guidelines proposed by Moges (2007). In the case of the Zambezi Basin, a study conducted by WMO and USAID (2012), recommended the implementation of an Integrated Flood Early Warning System (IFEWS) based on the following guidelines:

- Establishment of a Regional Forecasting and Warning Centre (RFWC) to be responsible for collection, evaluation and issuing of warning messages; monitoring the development of a flood threat and offering advice and assistance to local emergency organisations; and also responsible for the appropriate training of staff;
- Establishment of a Local Emergency Centre (LEC) to be responsible for particular activities in their local areas (such as door-to-door warning, search and rescue, evacuation of residents, moving valuables etc.);
- Establishment of a platform for an active participation of other organisations (including the Red Cross, churches, schools, universities, charity organisations, non-governmental organisations, mass media and the general public).

According to Moges (2007), WMO and USAID (2012), the system status needs to be reviewed on a regular basis and, if necessary, constantly updated. Activities envisaged within the framework will follow the general operation module (Figure 2.5) proposed by Moges (2007). WMO (2011) advised that to form an effective real-time flood forecasting system, the basic structures needed to be linked in an organised manner. This essentially requires:

- The provision of specific forecasts relating to rainfall, for both quantity and timing, for which numerical weather-prediction models are necessary;
- The establishment of a network of manual or automatic hydrometric stations; linked to a central control by a reliable form of telemetric communication;
- Selection of flood forecasting model software, linked to the observing network and operating in real-time.

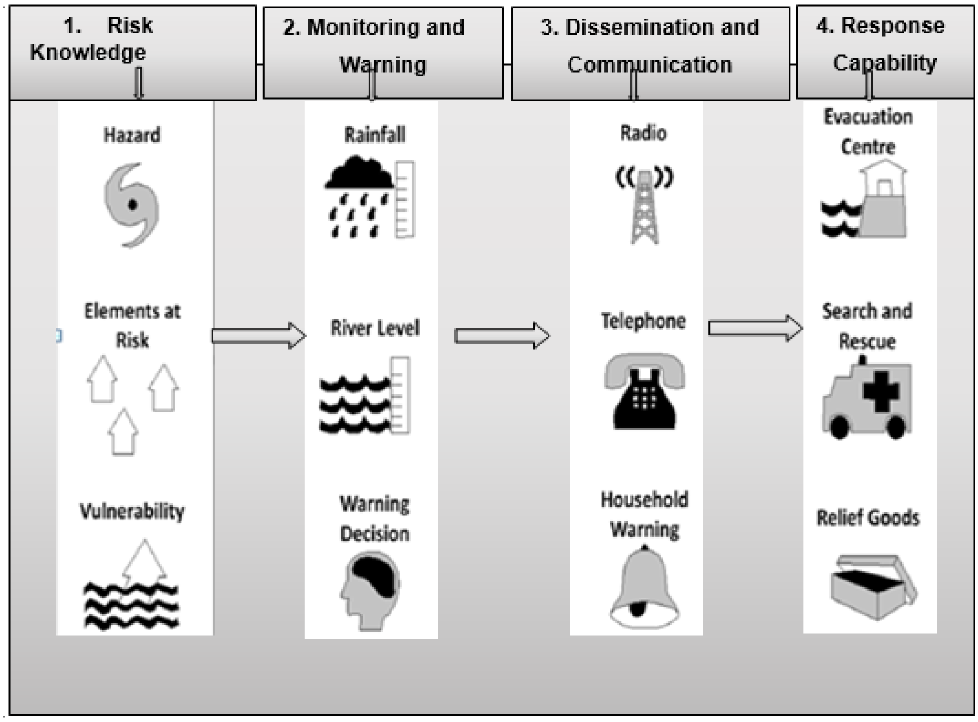

Figure 2.5: An example of typical flood forecasting and warning activities (as proposed by Moges, 2007, which may adopted for the southern Africa River Basin)

2.4. Application of remote sensing to flood hazard and risk Mapping

Most flood studies have primarily focussed on flow forecasting and communication issues, and less on flood risk mapping (Smithers *et al*., 1997; Tanavud *et al*., 2004; Uddin *et al.,* 2013). Islam and Sado (2002) in Bangladesh, Asante *et al.* (2005) in Mozambique, and lately Uddin *et al.,* 2013 in Pakistan, demonstrated that effective communication platforms should also include flood risk mapping. The main objective of flood risk mapping is to prepare flood hazard and vulnerability maps and identify the flood risk areas. Birkmann (2006) and Moel *et al.* (2009) concluded that, in the field of flood management, risk and vulnerability have different meanings. All definitions (e.g. Black, 1994; Islam and Sado, 2002; Tanavud *et al*., 2004; Samuels and Gouldby, 2009; Madsen *et al*., 2007; Samarasinghe *et al*., 2010; Uddin *et al*., 2013) agree that risk is a combination of the physical characteristics of the flood event (the hazard) and its potential consequences: vulnerability is the likelihood that a habitat, community or individual of a species will be exposed to an negative external factor to which it is sensitive (Bohle, 2001; Bogardi and Birkmann, 2004; Kubal, *et al.*, 2009).

According to Bollin *et al.* (2003), Kugler *et al.* (2007) and Ho *et al.* (2010), flood hazard maps contain information about the probability and/or magnitude of a flood event (e.g. flood extent areas generated from DEM or satellites images) and flood risk maps contain additional information about the consequences (e.g. number of people, and socio-economic infra-structure). An example of flood hazard and risk assessment for the Sindh Province in Pakistan is presented in Figure 2.6.

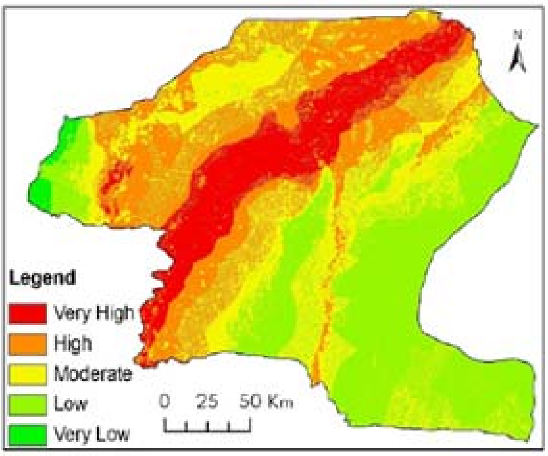

a)

District	Very high	High	Moderate	Low	Very low
Larkana	1335	3087	1706	945	439
Khairpur	1079	1218	4182	9316	0
Jacobabad	944	2788	1840	41	0
Sukkur	941	905	1380	1976	0
Naushahro Feroze	792	1572	666	6	0
Shikarpur	710	1064	770	20	0
Ghotki	355	1647	2351	2070	0

b)

Figure 2.6: Example of flood hazard and risk calculations – Sindh Province, Pakistan. (a) the district-wise flood hazard areas, (b) the total number of affected people, by level of risk (Source: Uddin *et al.,* 2013)

In southern Africa, and Mozambique in particular, there are relatively few studies which relate to the development of frameworks for flood hazard and risk mapping – although three studies by USGS and ARA-Sul (2005), Fonseca (2012), SEMEC (2004) demonstrated the application of Digital Elevation Models (DEMs) in flood risk determination. SEMEC (2004) applied these methods for flood risk analysis in six major river basins in Mozambique: the Maputo; Incomati; Limpopo; Save; Pungue and Zambezi River basins. The extent of inundation by past floods was delineated on digital maps drawn mainly from available data sources. Additional Landsat satellite imagery was acquired for 2001 floods in the Limpopo, Incomati, Zambezi and Licungo Rivers basins. Flood levels, estimated by hydraulic modelling, were compared with digital topographic data to interpret and delineate the expected extent of inundation of 1 in 10, 1 in 25, and 1 in 100 year flood return periods. The benefits of flood mapping using remote sensing techniques in Mozambique were first proposed by INGC (under the FEWS-Net (2000) project funded by USAID) in the Limpopo Basin. The purpose of the mapping was to assess the impact of the year 2000 floods in the Lower Limpopo Basin. Landsat Satellite images were used and combined with flood extent data derived from a Digital Elevation Model of 90 m x 90 m spatial resolution. Such approaches have, as yet, not been used in the flood-prone Lower Zambezi area in Mozambique (INGC, 2009).

2.4.1. Satellites images

A number of high profile flooding events – including Bangladesh in 1987 and 1988 (Islam and Sado, 2002), the Mississippi in 1993 (Kunkel *et al.*, 1994) and the Limpopo, Incomati and Zambezi floods in 2000 (Showstack, 2001) – have drawn attention to the need for new and improved methods for modelling large scale flood events. Reviews conducted after these floods (Kunkel *et al.*, 1994; Droegemeier *et al.*, 2000) identified the need for flood maps to enable hydrologists to predict areas that could be impacted as a result of forecast flows. Rapid progress has been made in the use of remote sensing techniques for flood inundation mapping (Islam and Sado, 2002; Asante *et al*., 2005). The application of satellite imagery from optical sensors including SPOT (Blasco *et al.*, 1992), AVHRR (Zhou *et al.,* 2000) and LANDSAT (Mayer and Tung, 2002) are well documented. The limitation of satellite images is the difference in the dates when images were taken – which may not correspond exactly to the occurrence of a flood event (Hess *et al*., 1995; Ho *et al*., 2010).

2.4.2. Digital Elevation Model (DEM)

Apart from satellite imagery, other methods of flood inundation mapping, based on the topography of the land surface, are required for the development of maps that can be used for flood warning purposes. Digital Elevation Model (DEMs) are the most common method used for representing topography and for visualising inundation in flood mapping applications (Kennie and Petrie, 1990; Bates and DerRoo, 2000; Faber, 2010). Kwak *et al*. (2012) demonstrated DEMs are most preferred for topographic data representation for applications over large areas. During the southern Africa floods of 2000, inundated areas 20 to 30 kilometres wide were observed along major rivers (such as the Limpopo and the Incomati) in Mozambique (Asante *et al.,* 2005). Given that channel or floodplain cross-section data are typically collected, using survey equipment, less than 200 metres apart and that depth estimates along a typical cross-section are spaced at 10 or 30 metres apart (Faber, 2010), a huge volume of data would be required to adequately cover such a vast area. This makes field survey approaches both excessively expensive – the manpower required is extensive – and impractical (because the survey equipment is bulky and the data require a huge amount of computer storage and processing resources) for mapping the flood extent of large-scale flooding events. Mapping of the routed flows onto the floodplain is commonly done using the highest resolution DEM available (Oliveira and Loucks, 1997; and Horritt and Bates, 2001b). Mapping performed in this way takes advantage of the 3D representation of topography, as offered by the DEM, while still using simple, steady state flow computations (Jones *et al.*, 1998). Asante *et al.* (2005) presented one such application: a DEM was used to represent topography in a three-dimensional hydraulic model, for mapping the extent of inundation experienced in past floods in the Incomati River Basin in Mozambique.

2.5. Methods of estimating flood peaks

Flood peaks can be estimated directly as functions of historical streamflow records or by statistical-empirical relationships or by watershed modelling techniques when the whole hydrograph or series of hydrographs are desired (Chow *et al.,* 1988; US Army Corps of Engineers, 2003). This can be done using data generated empirically or through using probabilistic and deterministic methods (Chow *et al.,* 1988; Dillow, 1997, Alexander, 2002a, 2002b).

2.5.1. Statistical or empirical relationship methods

Flood peaks can be determined by early empirical methods*,* basic flow frequency analysis and probability distribution fitting.

Early empirical methods: Empirical methods for estimating floods were first used during the 19th century and were based on delineating homogeneous regions of flood response. The approach was based on plotting the basin's area against observed flood peaks to form an envelope whose upper limit was the expected regional maximum flood peak (Kovács, 1988). However, the value of these approaches is limited and very reliant upon a relatively large number of representative flood observations. Cordery and Pilgrim (2000) recommended that their use be avoided. In South Africa, the Regional Maximum Flood (RMF) method developed by Kovács (1988), in accordance with the Francou and Rodier (1967) approach, is a frequently used empirical method to determine appropriate safety evaluation flood peaks for dams. The mathematical relationship (Francou and Rodier, 1967) is:

$$Q_{peak} = C \cdot A^{n} \qquad \textbf{Equation 2.1}$$

where Q_{peak} is peak flow ($m^3 s^{-1}$), C and n are regional constants, and A is the basin area (km^2).

Kovács (1988) pointed out the following common shortcomings of the empirical approach:

- uncertainty regarding the boundaries of homogeneous regions – this shortcoming is a common drawback of all regional approaches in hydrology (Kovács, 1988);
- very large and very small catchments often cannot be accounted for by the regional approach because of high heterogeneity of hydrological features;
- empirical equations of maximum flood peak envelope curves, dating from the period before 1960, lacked physical meaning and their application was restricted to well-defined areas (Kovács, 1988).

Regional flood frequency analysis is often used to enhance the estimation of flooding probabilities at locations that have short data record length relative to their return periods. In such situations, extreme flow information from a number of sites can be used to compensate for an inadequate temporal representation of the extreme flows at a given location. Regional flood frequency analysis can, therefore, be employed at gauged locations, where information from similar sites that have been gauged is used to assist with the characterisation of the extreme flow regime at the ungauged sites (e.g. Midgley *et al*., 1994, Mazvimavi, 2003; Bergstrom, 2006). The basic tenet in regionalisation is that, if a relationship exists between model parameters and basin properties which holds true for a gauged basin, then peak flow can be achieved in an ungauged basin which has similar physical attributes. The most common basin attributes that have been used include: climate; topography; vegetation; soil properties (e.g. Chiew and Siriwardena, 2005); annual rainfall; areal potential evapotranspiration (e.g. Boughton and Chiew, 2006); basin area and geology. There are various means by which regionalisation of method can be achieved. These methods include statistical methods, parameter mapping and an *a priori* estimation method.

Statistical method is based on the regression relationships developed between optimised model parameters and several basin attributes for a number of gauged basins. Frequently, bivariate and multivariate linear and non-linear regressions are developed and then transferred to the ungauged basin (Boughton and Chiew, 2006). Parameter mapping consists of fixing model parameters to average values for the region. This might achievable if the whole region exhibited the same hydrological response to rainfall input. The parameter mapping method relies heavily on the premise of hydrologic similarity between the gauged and the ungauged basins and therefore the delimitation of hydrological response units (HRUs), based on chosen group-defining signatures (Nathan and McMahon, 1990). While the way to define HRUs has been to use geographical proximity, it is not always a reliable method of judging of hydrologic homogeneity. *A priori* estimation methods fix values based on experience or the use of values adopted from the literature for determining the basin characteristics. The Model Parameter Estimation Experiment (MOPEX) investigated the relationships between physical and hydro-meteorological basin attributes and the parameters of a number of selected hydrologic models (Wagener *et al*., 2006; Ao *et al*., 2006). It is important to note that testing regionalisation approaches involves reserving a proportion of the gauged basins to test the regional parameter estimations. This means that the data set used to establish the regionalisation will be reduced in size. This can be a problem in areas with a limited number of gauged basins – such as in southern Africa. Many regionalisation studies have met with limited success (Franks, 2002). The problems that seem to haunt all the studies are equifinality and parameter interdependence. It has not been easy to be sufficiently confident, with most regionalisation methods, that all the necessary and dominant controls of basin behaviour have been captured in the regionalisation process.

Flood frequency analysis: Design flood estimation approaches can be categorised as either streamflow-based or rainfall-based (Doran and Pilgrim, 1986). Rainfall-based approaches rely on the ability of a model to convert rainfall into streamflow, while a streamflow-based approach may be performed by a frequency analysis of observed flows where the observations are available and adequate in both length and quality (Pilgrim and Cordery, 1993; Bobee and Rasmussen, 1995; Dirceu *et al*., 2005; Faber, 2010; Smithers, 2012). The main characteristic of streamflow-based approaches is the primary reliance on observed streamflow data for the development of the approach. The approach assumes that a series of independent observations of flood characteristics (peak flow, flood volume) fits an underlying probability distribution. Three available approaches include:

- At-Site Analysis – based on data available at site of interest;
- At-Site/Regional Analysis – based on data at site of interest and from other hydrologically similar sites;
- Regional Analysis – based on data from hydrologically similar sites.

The flood characteristic series may consist of annual maxima (annual series) or independent peak flows/volumes over a specified threshold (partial series). The use of an annual series is suitable for the estimation of infrequent floods; the partial series provides useful estimates for frequent floods (Laurenson, 1987). Common to the above approaches is the choice of a suitable probability distribution to describe the series of peak flows/volumes. The distributions employed can range from a simple line-of-best-fit (drawn by hand) to complex multi-parameter theoretical probability distributions (e.g. Chow *et al.*, 1988 Schulze, 2000).

As shown by Schulze (2000) and Smithers (2012), the question of selecting an appropriate distribution has received considerable attention in literature, with diverging opinions expressed by various authors. Schulze (2000) questioned whether a suitable probability distribution could be selected, given that any chosen distribution will vary, *inter alia*, with the season, storm type and duration for each sub-basin. There can also be measurement errors and inconsistency, non-homogeneity and non-stationarity of data – all of which violate the assumptions made when fitting a distribution to the data. The regional frequency approach uses hydrologically and climatologically similar and nearby locations (Schulze, 2000) and uses data from several sites to estimate the frequency distribution of observed data at each site (Hosking and Wallis, 1995, Pegram and Parak, 2006). This approach assumes that the regionalised variable has the same distribution at every site in the selected region and that data from a region can thus be combined to produce a single regional flood, or rainfall, frequency curve that will be applicable anywhere in the region, when used with appropriate site-specific scaling (Gabriele and Arnell, 1991; Hosking and Wallis, 1995).

Probability distribution fitting: These methods relate the historical flood peak records to a probability of occurrence. Both at-a-site and regional flood frequency analysis require the fitting of a probability distribution to the data (Pilgrim and Cordery, 1993). Smithers *et al*., 1997 summarised approaches available for estimating the parameters of a selected distribution which include: Method of Moments (MM); Maximum Likelihood Procedure (MLP); Probability Weighted Moments (PWM); L-Moments (LM); Bayesian Inference and non-parametric methods. The use of L-moments to fit distributions has received extensive coverage in recent literature (Pilon, and Adamowski, 1992; Guttman *et al*., 1993; Gingras and Adamowski, 1994; Karim and Chowdhury, 1995; Seed, 2001; Alexander, 2002b; Görgens, 2007a; 2007b; QFCI, 2011; Smithers, 2012; Opere *et al*., 2012). L-moments are reported to have less bias when compared with other techniques (Bílková and Mala, 2012; Smithers, 2012).

2.5.2. Rainfall-runoff methods

Flood peaks can also be determined by rainfall-runoff modelling (Artan *et al.,* 2002; Entenman, 2005; Asante *et al.*, 2007a, 2007c; Shrestha *et al.,* 2008). A rainfall-runoff model is a mathematical model describing the rainfall to runoff relationship of a drainage basin or watershed (Zeeuw, 1973). The model produces the runoff hydrograph as a response to a rainfall event as input through the conversion of rainfall to runoff. Kokkonen *et al.* (2004) considered rainfall-runoff modelling as a system that transformed the input into output; an example is the unit hydrograph which is a linear transformation of effective rainfall to runoff. When the study area is large, it can be divided into sub-basins and the various runoff hydrographs may be combined using flood routing techniques (Zeeuw, 1973). Walker and Willgoose (1999) and Beven (2012) recognised that the mathematical representations of natural hydrological systems, which can be very variable in space and time, are a major constraint of rainfall-runoff models. USGS (2002) considered the natural hydrological systems as complex and that modelling them involves the need to manipulate vast quantities of data, characterised by large temporal and spatial fluctuations. Hydrological models play an important role in many water resources management functions – generally longer rainfall records are currently available at more sites, with better quality data when compared with earlier records for streamflow(Xu and Singh; 1998; Chowdary *et al.*, 2012).

Measurement errors and other inconsistencies often make streamflow data unsatisfactory for direct frequency analysis. Similarly, non-stationary streamflow records can render the streamflow record unsatisfactory (as a result of changing catchment conditions) for direct frequency analysis (Clarke, 1973; Smithers, 2012).

2.5.2.1. Classification of rainfall-runoff models

Previous reviews have outlined several ways to classify hydrological models (for example – Clarke, 1973; Gosain *et al.*, 2009). There are many types of hydrological models for flow simulation and flood management. Clarke (1973) classified rainfall-runoff models, on the basis of their structure, as either black box (empirical), grey box (conceptual), or white box (physically-based) models; Schultz (1985) presented three categories of classification of models – namely: functional classification (prescriptive and descriptive models); spatial disaggregation classification (lumped and physical distributed models); and structural classification (deterministic, stochastic and parametric or conceptual models). In the current study, the classification system outlined in Pechlivanidis *et al.* (2011) has been used, where models have been classified based on their model structure, spatial distribution, stochasticity, and spatial-temporal application.

Model structure based classification: Based on model structure, rainfall-runoff models can be divided into metric, conceptual, physics-based and hybrid models. Metric models are primarily based on observations and seek to characterise the system response from the available data (Wheater *et al.,* 1993). Metric approaches are essentially empirical. An early example is the unit hydrograph (UH) model for event-based basin-scale simulation developed by Sherman (1932). The simplicity of such models has allowed them to be relatively easily applied to ungauged basins by regional analysis, relating parsimonious model properties (i.e. unit hydrograph time to peak, percentage runoff etc.) to physical and climatic descriptors of the basin (Pechlivanidis *et al.,* 2011). According to Wheater *et al*. (1993), conceptual models are based on two criteria: firstly, the structure of the model is specified prior to any modelling being undertaken; secondly, not all of the model parameters have a direct physical interpretation (i.e. they are not independently measurable). Therefore at least a portion of the conceptual model parameters have to be estimated, through calibration against observed data (Pechlivanidis *et al.,* 2011). The conceptual models generally represent all of the component hydrological processes perceived to be of importance in the catchment scale input-output relationships (Wheater, 2002).

Physics-based models represent the component hydrological processes (such as evapotranspiration, infiltration, overflow, saturated and unsaturated zone flow) using the governing equations of motion (usually formulated as non-linear partial differential equations) based on continuum mechanics (Wheater *et al*., 1993). Generally, the equations of motion of the constituent processes are solved numerically, using a finite difference or a finite element spatial discretisation; however, analytical solutions can exist (Wheater *et al*., 1993). In theory, physics-based models are defined by wholly measurable parameters and can provide continuous simulation of the runoff response without calibration (Beven, 2001). Such models are compilations of the relevant idealised processes but raise a number of important issues. The physics behind the model structure are generally based on laboratory or small-scale *in situ* field experiments (Beven, 2001). Extrapolation to larger scales (e.g. catchment areas) often involves the assumption that the physical processes and properties are independent of scale, raising uncertainty about the applicability of the processes (Beven, 2004). To reduce the computational burden and data requirements, simplified physics or mechanics are sometimes used to represent the processes. Examples include: simplified St. Venant routing equations; the Green-Ampt infiltration equation (Green and Ampt, 1911; Mein and Larson, 1973); leading to a deviation from the physical basis and additional structural uncertainty (Beven, 2004).

Many models are labelled as being one of the types mentioned above but, in truth, the models may include elements of two or more and can be referred to as Hybrid metric-conceptual models (Pechlivanidis *et al.,* 2011). Hybrid metric-conceptual models have been developed to combine the strengths of data-based and conceptual models. They commonly consist of a simple conceptual loss function (*i.e.* a soil moisture accounting module, to produce effective rainfall data) and a simple routing component (i.e. a routing module to transfer the effective rainfall to streamflow) (Wagener, 2007). These models offer scope for dealing with the problems associated with any lack of parameter identifiability and the problem of equifinality, as described by Beven (2006), through the reduction of the dimensionality of the parameter space. Beven and Freer (2001) defined equifinality as the principle that, in open systems, a given end state can be reached by many potential means. Many so-called physics-based models are in fact hybrid physically-based conceptual models; for example SWAT and GeoSFM (Arnold *et al*., 1993). These aim to simplify the model structure by representing the mathematical-physics-based processes in a conceptual manner, particularly in cases where physical parameters are difficult to measure (Wheater and Evans, 2009; Pechlivanidis *et al.,* 2011).

Model spatial distribution based classification: Rainfall-runoff models are further classified on the basis of the scale at which they represent the basin hydrological system, that is, as either lumped or distributed in nature (Pechlivanidis *et al*., 2011). Lumped models treat the basin as a single unit, with state variables that represent averages over the basin area (Beven, 2012), generally expressed by differential or empirical algebraic equations, and taking no account of spatial variability of processes, inputs, boundary conditions and system (basin) geometric characteristics. By contrast, distributed models make predictions that are distributed in space, with state variables that represent local averages, by dividing the basin into a number of elements (or grid squares) and solving the equations for the state variables associated with every element (Artan *et al*., 2004). Distributed models are, to some extent, capable of taking into account spatial variability in processes, inputs, boundary conditions, and basin characteristics. However, all distributed models use average variables and parameters at element or grid scales, and often parameters are averaged over many grid squares, mainly because of data availability (Bandaragoda, 2007). Semi-distributed models represent a compromise spatial structure, and are effectively a group of lumped models that are linked. A semi-distributed model can therefore represent the important features of basin; at the same time these models require less data and lower computational costs than distributed models (Bandaragoda, 2007).

Model stochasticity based classification: Models can also be classified as stochastic or deterministic (Pechlivanidis *et al.,* 2011). A stochastic model tries to predict hydrological variables and to quantify the errors in model outcomes; in deterministic models the results are determined through fixed relationships between the states and the data (Schuurmans, 2007). Stochastic models are black box systems, based on data and using mathematical and statistical concepts to link a certain input (for instance – rainfall) to the model output (for instance – runoff). Commonly used techniques are regression, transfer functions, neural networks and system identification. Stochastic models use random variables to represent process uncertainty and generate different results from one set of input data and parameter values when they run under “externally seen” identical conditions (Beven, 2001). A particular set of inputs will produce an output according to a statistical distribution. This allows variable randomness (or uncertainty) in the possible outcome because of the uncertainty of the input variables, boundary conditions or model parameters.

Deterministic models are process-based and try to represent the physical processes observed in the real world. Typically, such models contain representations of surface runoff, subsurface flow, evapotranspiration, and channel flow, but they can be far more complicated (Pechlivanidis *et al*., 2011). Deterministic hydrology models can be subdivided into single-event models and continuous simulation models. Deterministic models produce a single result from a simulation with a single set of input data and parameter values, and a given input will always produce the same output, if the parameter values are kept constant (Bandaragoda, 2007). Mixed deterministic-stochastic models can also be created by introducing stochastic error models to the deterministic model. For example, stochastic rainfall could be used as an input to a deterministic rainfall-runoff model or a deterministic model may be used to represent a stochastic system using the Monte Carlo simulation as described in Pechlivanidis *et al.* (2011).

Model spatial-temporal application based classification: Spatially, models may be classified into those applicable to various sizes: e.g. small sub-basins (up to 100 km^2): medium-size sub-basins (100 – 1 000 km^2): and large sub-basins (greater than 1 000 km^2) (Young *et al.,* 2000). However, this classification is arbitrary and not conceptual, and ideally the classification should be based on homogeneity and the scale at which processes can reasonably be averaged – referred to by some authors as hydrological response units (Young *et al.,* 2000; Wagener, 2007). Rainfall-runoff models can be classified temporally as continuous simulation models or event-based models. Continuous simulation would typically take into account a time series of rainfall, which may incorporate more than one storm event; event-based models treat each individual event separately (Asante *et al.,* 2007a). Pechlivanidis *et al.* (2011) explained that the time scale may be defined either by the time intervals used for input and internal computations or by intervals used for output and calibration of the model – the choice is usually a function of the model's intended use. Thus, other sub-classifications of the continuous time-based models can be distinguished as sub-daily, daily, monthly, and yearly models.

2.5.2.1. Flow routing in hydrological modelling

There are many simple and more complex flow routing methods in hydrological modelling (Fread, 1993; Mays, 1996; Arora *et al.,* 1999; Asante *et al.,* 2007a). The concept of flow routing in hydrological models was defined by Mays (1996) and USGS (2000), as a way to describe the movement of water from one point to another along a river and to account for delay and attenuation effects. According to Mays (1996) if the flow is a water-excess event (such as a flood) then the procedure is specifically known as flood routing, a method which is most often used to predict flood peaks, water volume, and the timing of the flow. Such predictions are needed when determining the flood peak height at a downstream location, for forecasting how much floodplain inundation may take place and making other flow dependent calculations. It is therefore important to look at the routing techniques used in models in more detail and to assess their adequacy in flood prediction. Hydrological models use a variety of computational linear and non-linear routing methods for simulating the in-channel phase of flow for flood forecasting (Merkel, 2002; Asante *et al.*, 2007c). Linear routing includes a pure translation approach and the diffusion analogue method (Artan *et al.,* 2002; Asante *et al.,* 2007a, 2007b).

Linear routing accounts for the advection of flow and includes attenuation or deformation of the input when the system is considered to be non-linear (Mays, 1996).

The relative simplicity of this model makes it easy to implement and parameterise in a wide variety of settings with little or no calibration necessary (Asante *et al.,* 2008). However, this model is less well suited to high spatial or temporal resolution applications or to settings where a well calibrated model using observed data is required.

In the latter settings, the nonlinear module may be a better option (Asante *et al.*, 2007a, 2007b). The most common known non-linear method is Muskingum-Cunge (Merkel, 2002; Asante *et al.*, 2007a; 2007b). The Muskingum-Cunge algorithm is a non-linear, variable parameter routing method (Mays, 1996). Like the linear routing method, it involves the use of the continuity equation and an empirical storage function. It relies on the Muskingum K coefficient (analogous to flow time) to control the rate of advection and the Muskingum x coefficient to control the rate of attenuation. Cunge proposed to amend the method by allowing the Muskingum x coefficient to vary during each time step based on the condition of flow at the previous time step (Merkel, 2002).The rate of attenuation of flow is dependent on the condition of flow. The Muskingum channel routing method is based on two equations (Merkel, 2002). The first is the continuity equation (or conservation of mass) and the second is a relationship between storage, inflow and outflow. Advanced hydrological modelling for flood forecasting uses both linear and non-linear methods for flood prediction. The main challenge in a hydrological study is to choose which approach to use. Most of these flood routing procedures have been incorporated in the Natural Resources Conservation Service (NRCS) database (Aronica *et al.,* 1998; USGS, 2000b; Merkel, 2002; Entenman, 2005; Shrestha *et al.,* 2008).

2.5.2.3. Advances in hydrological modelling

Many innovations in the application of information technologies in hydrological modelling began in the late 1950s, 1960s and early 1970s (Maidment, 1996), where methods of sophisticated mathematical and statistical modelling were developed and the first remote sensing data became available. Researchers began to envision the development of Geographic Information Systems (GIS) and Hydrologic Model Interface as a result of the new technologies (Maidment, 1996; Chowdary *et al.,* 2012). Developments in remote sensing technology and geographical information systems made it possible to capture and manage a vast amount of spatially distributed hydrological parameter and variable data (Maidment, 1996). Chow *et al.* (1988) considered that linking GIS and hydrological modelling was essential to achieve the desired objectives.

Integrating hydrologic modelling with GIS: GIS is a decision support system involving the integration of spatially referenced data in a problem-solving environment (Chow *et al.,* 1988). The integration of GIS and hydrological models consists of a functional model (that describes the geometrical relationships) and a stochastic model (that describes the probabilistic characteristics of spatial data). Maidment (2002) noted that GIS provides numerous tools, which can enhance the performance of hydrologic modelling. Djokic (2004) classified these integrated technologies as: data management (manipulation, preparation, extraction, etc.); visualisation; and interface development tools. Advances in distributed parameter hydrologic modelling and integration with Geographical Information Systems (GIS) have led to the development of powerful tools for predicting runoff and simulating the physical, chemical and biochemical constituents of basins (Chowdary *et al*., 2012).

Many researchers (Stuebe and Johnston, 1990; White, 1988; USGS, 2000b; Chowdary *et al.,* 2004; Pandey *et al.*, 2008) have used land use/land cover information derived from satellite data collected by Landsat, SPOT, and the Indian Remote Sensing Satellite (IRS) and integrated these data with GIS to estimate SCS CNs (Soil Conservation Service Curve Numbers) and runoff. Several hydrologic models (including ANSWERS (Areal Nonpoint Source Watershed Environment Response Simulation – Beasely *et al.,* 1980); AGNPS (Agricultural Nonpoint Source Pollution – Young *et al.,* 2000); WEPP (Water Erosion Prediction Project – Foster and Lane, 1987); GeoSFM (Geospatial Streamflow Modelling – Asante *et al.,* 2007a); SWAT (Soil Water Assessment Tool – Arnold *et al.,* 1993); and MIKE 11 Flood Watch (Madsen *et al.,* 2003)) have GIS linkages. These models are being extensively used for flood forecasting and sediment simulation in countries such as Bangladesh (Islam and Sado, 2002), Kenya, Mozambique (Artan *et al.,* 2002; DHI, 2006) and Nepal (Shrestha *et al*., 2008).

Flood forecasting models: The *a priori* choice of a flood forecasting modelling for use in the most projects is difficult since these models were not all developed for the same purpose (Loumagne *et al*., 2001). Cheng and Chau (2004) urged that an integrated flood forecast system should include: the choice of hydrologic models; initial condition set and modification of antecedent soil moisture; real-time forecasts; simulation forecasts; and revised forecasts. The basic steps to be followed in selecting the flood forecasting model to integrate with reservoir simulation (Jensen *et al.,* 1999; Loumagne *et al*., 2001; Cheng and Chau, 2004) are as follows:

- use a model (as simple as possible) that can maintain continuity with the existing modelling tools of the project customers;
- ensure the model is not too demanding in terms of input; is easy for the customers to use, understand and implement;

- ensure the model is capable of using the information brought by soil moisture data derived from Earth Observation.

Among the existing flood forecasting models, ranging from purely mathematical (black box) to complex physical methods, a selection should be made considering the four criteria above. Most of the models appear to be able to provide consistent and reliable streamflow results (Franchini and Pacciani, 1991). Considering the results of these numerical tests (Perrin *et al.,* 2003), several model structures are recommended in the context of the flood forecasting and reservoir operation because of their consistent performance and reliability. A list of several of the models is provided here:

IHACRES (Littlewood *et al*., 1997; Kasetsart and Taesombat, 2011) can be applied over a range of spatial and temporal scales – from small experimental catchments to basins; using minute, daily or monthly time steps. The model can be used to fill gaps in data, extend streamflow records, as well as explore the impact of climate change and identify the effects of land use changes (Littlewood *et al*., 1997). IHACRES has been successfully applied worldwide for catchments of different sizes and under different climate conditions from 1 ha experimental catchments to 100 000 km^2 catchments, in various regions across the world – from the Thames River in the UK to the Upper Ping River Basin in northern Thailand (Littlewood *et al*., 1997).

TOPMODEL (Beven, 1997), was originally developed to simulate catchment under humid conditions in the U.K (Beven, 1986; 1987). It is a conceptual model in which the dynamics of surface and subsurface saturated areas are estimated on the basis of storage discharge relationships established from a simplified steady state theory for downslope saturated zone flows. The model has provided good simulation of discharge rates and dynamic saturated areas (as demonstrated by many authors) (Beven, 1986; 1987; Sivapalan *et al*., 1990, Blazkova and Beven, 1997).

GeosFM (Artan *et al*., 2001; Asante *et al*., 2008) is designed to run operationally using widely available remotely sensed data sets and ground observations. The hydrologic analysis module consists of linear soil moisture accounting routine, a more complex nonlinear soil moisture accounting routine. This model has been tested by many authors in many regions (e.g., Limpopo Basin in Mozambique and Bagmati Basin in Nepal) (Artan *et al.,* 2001; 2002; Entenman, 2005; Shrestha *et al*., 2008) and found to generate reliable results. The integration of hydrologic models for streamflow forecasting into reservoir models can help reduce the human and economic losses in many flood prone areas located downstream of major dams (Loumagne *et al*., 2001). Several reservoir model structures are recommended for integration with flood forecasting models (US Army Corps of Engineers, 2003; DHI, 2010).

2.6. *General concepts and evolution of reservoir operation models*

The application of systems analysis techniques for reservoir management and operations has been a major focus of research in water resources engineering during the past four decades (Fenton, 1992; Ahmad and Simonovic, 2000; Chang *et al.*, 2005). Numerous models have been reported in literature for sizing storage capacity and establishing release policies, both at the project planning stage and for real-time operations (Mays and Tung, 1992). Ahmad and Simonovic (2000) considered Inflows (Q_{in}) and outflows (Q_{out}) from the reservoir as the main components of the reservoir model (Figure 2.7). Flow from all tributaries directly contributing to the reservoir is considered as inflow to the entire system. Total reservoir outflow consists of reservoir releases, spill, evaporation, and seepage losses and the reservoir storage is described in terms of the mass balance equation (Keith and Spe, 1982; Mays and Tung, 1992; Ahmad and Simonovic, 2000).

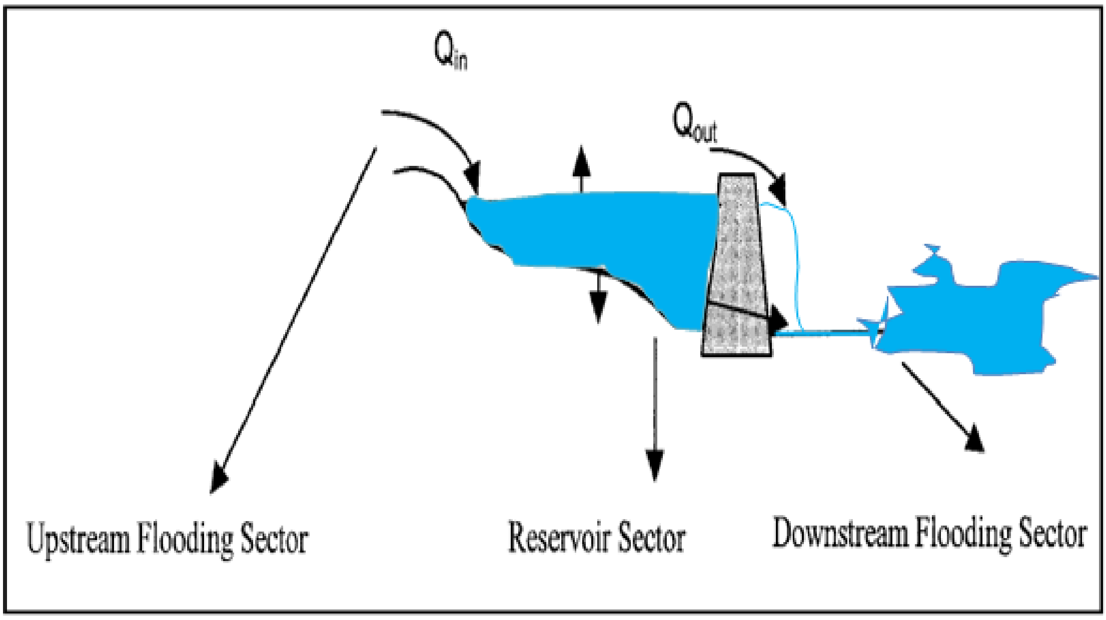

Figure 2.7: Schematic diagrams showing the main components of reservoir model (Source: Ahmad and Simonovic, 2000)

Many reservoirs are operated for multi-purposes which may include: flood control; hydropower generation; water supply; navigation and downstream environmental water requirements. However, in many cases, flood control and hydropower generation are regarded as being the most important factors for the determination of control strategies for reservoirs (Oliveira and Loucks, 1997; Beilfuss and Dos Santos, 2001; Beilfuss, 2009; Nyatsanza and Van der Zaag, 2011; CSIR and WWF, 2012). Approximately 8% of single purpose and 39% of multi-purpose reservoirs have been operated specifically to control floods (ICOLD, 1998) – though for most reservoirs flood mitigation and control remains a secondary purpose. The operation of many reservoirs world-wide includes the release of water for subsequent abstraction downstream for irrigation or water supply, or to maintain ecosystems (DHI, 2010).

However, these flows are almost exclusively well within the capacity of the river channel. Little consideration has been given to the release of high flows to maintain floodplain (out-of-channel) and deltaic ecosystems (ICOLD, 1999). Therefore, to develop reservoir operating objectives to balance water use for the environment and energy generation, and which will also constitute the best compromise solution between upstream and downstream needs, many studies have focussed on how reservoirs can be operated to achieve a balance for environmental flows and hydropower (Beilfuss and Dos Santos, 2001; Beilfuss, 2009; Nyatsanza and Van der Zaag, 2011; CSIR and WWF, 2012).

In recent years, the problem of ineffective operation of existing reservoirs, using out-dated technology and highly subjective management practices, has been repeatedly highlighted (e.g. Oliveira and Loucks, 1997; Lund and Guzman, 1999; Chen, 2003; John, 2004). Because of the variability in hydro-meteorological conditions and the shifting goals of water requirements from one region to another, reservoirs have different operating rules (DHI, 2010). Reservoir simulation models need to take into consideration the operating objectives of the reservoir and the rules that are designed to achieve these objectives. Including appropriate operating rules is a complex problem in reservoir modelling because the decisions often involve many variables and multiple objectives and also need to account for risk and uncertainty (Lund and Guzman, 1999; DHI and Aurecon, 2011).

In addition, the conflicting objectives lead to significant challenges for operators when making operational decisions. Traditionally, reservoir operation models have been based on heuristic procedures, implementation of rule curves and subjective judgements by the operator (Ahmad and Simonovic, 2000). This provided general operational strategies for reservoir releases according to the current reservoir level, hydrological conditions, water demands and the time of the year. Established rule curves, however, do not allow fine-tuning (and hence optimisation) of the operations in response to changes in the prevailing conditions (DHI, 2010).

Therefore, it is necessary to establish an analytical and more systematic approach to reservoir operation, based not only on the traditional probabilistic/stochastic analysis, but also on the information and prediction of extreme hydrologic events and advanced computational technology to increase the reservoir's efficiency in balancing the demands from different users (Vasan and Raju, 2006). Reservoir operation consists of several control variables that define the operation strategies for guiding a sequence of releases to meet a large number of demands from stakeholders, often with different, conflicting and unequal objectives (Lund and Guzman, 1999). These objectives include: flood control, hydropower generation and the allocation of water to the different users (DHI, 2010). It is essential to optimise reservoir operations by determining and setting a workable balance between the conflicting objectives.

Optimisation models are based on clearly defined goals (objective functions), criteria for evaluation of control decisions, and constraints as limitations during optimisation (John, 2004). John (2004) reported that *"…objective functions used in reservoir optimisation models should incorporate measures such as efficiency (i.e., maximising current and future needs), survivability (i.e. assuring future welfare exceeds minimum subsistence levels), and sustainability (i.e. maximising cumulative improvement over time)…"* These criteria address economic, social and environmental issues (Le Ngo, 2006). The typical constraints in a reservoir optimisation model include: conservation of mass and other hydrological and hydraulic constraints; minimum and maximum storage and releases; hydropower and water requirements; and hydropower generation limitations. DHI (2010) identified the following five constraints:

- Hydraulic constraints are defined by the reservoir continuity equation:

$S(t+1) = S(t) + I(t) - R(t) - E(t)$ t = 1,2……..T **Equation 2.2**

where $S(t+1)$ is storage at the beginning of time step t+1, $S(t)$ is storage at time step t; $I(t)$ is the reservoir net inflow at time step t (including reservoir inflow and precipitation), $R(t)$ is the reservoir out flow at time step t, and $E(t)$ is the reservoir evaporation at time step t. T is the total number of time steps in the considered period.

- Constraints on discharge defined by maximum and minimum permissible reservoir releases as described in Equation 2.3.

$TR(1,2..) = R_{min} \leq R(t) \leq R_{max}t$ **Equation 2.3**

where $TR(1,2..)$ is the total number of releases time step, R_{min} is the minimal releases, $R(t)$ is the reservoir out flow at time step t, $R_{max}t$ is the maximum permissible reservoir releases.

- Constraints on storages defined by maximum and minimum permissible (Equation 2.4) reservoir storages:

$TS(1,2\ldots) = S_{min} \leq S(t) \leq S_{max}t$ **Equation 2.4**

where $TS(1,2\ldots)$ is the total number of storages time step, $S(t)$ is the storage relation at time step t, S_{min} is the minimum storage and $S_{max}t$ is the maximum permissible storage in a centime period.

- Constraints on elevations defined by maximum and minimum permissible water level (Equation 2.5) at specified sites:

$Th(1,2..) = h_{min} \leq h(t) \leq h_{max}t$ **Equation 2.5** where $Th(1,2..)$ is the total elevation, h_{min} is the minimum water level; $h(t)$ is the water level at time step t, $h_{max}t$ is the maximum permissible water level.

- Constraints on hydropower generations (Equation 2.6) as defined by the maximum capacity and the minimum requirement for hydroelectricity:

$$THP(1,2..) = HP(t)_{min} \leq HP(t) \leq HP_{max}t \qquad \textbf{Equation 2.6}$$

where $HP(t)$ is a nonlinear function of $S(t)$ and $R(t)$, $THP(1,2..)$ is the total number of hydropower generation time step, $HP(t)_{min}$ is the minimum hydropower generation, $HP(t)$ is the hydropower at time step t, $HP_{max}t$ is the maximum permissible hydropower generation.

2.6.1. Evolution of reservoir simulation models

Research during the 1970s resulted in many significant advances in simulation model formulations and numerical solution methods. These advances allowed simulation of more complex recovery processes and/or reduced computing costs through the increased stability of the formulations and the efficiency of the numerical solution methods. These numerical methods have been applied in an attempt to improve the efficiency of reservoir operation (Kelman *et al*., 1990; Panigrahi and Mujumdar, 2000; Ahmad and Simonovic, 2000). These techniques include: Linear Programming (LP): Nonlinear Programming (NLP): Dynamic Programming (DP): Stochastic Dynamic Programming (SDP): and Heuristic Programming (such as Genetic algorithms, Shuffled Complex Evolution, Fuzzy logic, and Neural Networks etc.) In reservoir operation (Lund and Guzman 1999; Dubrovin *et al.,* 2002), LP is considered the most favoured and well known optimisation method because it is easy to understand and does not require any initial solution (Yeh, 1985; Unver and Mays, 1990). A number of examples of applying LP to reservoir operation were provided by Yeh (1985). Unver and Mays (1990) developed a model for real-time flood control operation for a reservoir system and demonstrated that it is possible to link nonlinear optimisation models with unsteady flow routing models to solve the large-scale LP problems associated with flood control reservoir operation. In this latter method the nonlinear optimisation is performed by using the generalised reduced gradient code (GRG).

Mujumdar and Teegavarapu (1998) developed a deterministic LP model for the short-term annual operation of an irrigation reservoir. Duranyildiz *et al.* (1999) developed a chance-constrained LP model, which takes the random nature of inflows into consideration, to optimise the monthly operation of a real reservoir. Wang and Zhang (2004) studied the optimisation of a short-term hydropower generation and demonstrated that, with the development of a direct search procedure, a reformulated problem (with only linear constraints of outflow release and storage content) can be solved. Another approach for dealing with reservoir operation problems is so-called Dynamic programming. In this method, sequential decision problems are divided into a sequence of separate, but interrelated, single-decision sub-problems.

In this way, large, complex problems can be solved by combining the solutions of the smaller problems (sub-problems) to obtain a solution for the entire problem (Mays and Tung, 2002). Dynamic programming is well suited to deal with short-term operation (hourly or daily) when the hydrologic inputs and water demands are generally considered deterministic.

Solomatine and Avila (1996) used ANN to approximate the hydrodynamic part of the MIKE BASIN river model in optimising reservoir operation. The ANN was based on the water levels given by the MIKE 11 model. A study by DHI (2010) presented the Allocation Pool Reservoir (APR) and Reservoir Rule Curve (RRC) for reservoir operation. APR is effectively a physical storage, but the individual users/stakeholders have been allocated certain storage rights within a zone of water levels. An accounting procedure keeps track of the actual water storage in one pool for downstream minimum flow releases (water quality pool) and in the individual pools allocated for the different water supply users. Operating rules for each user apply to the main storage and the users compete with each other to fulfil their water extraction rights.

2.6.2. Flood control management system scheme for reservoirs

One of the most important aspects of mitigating the damaging impacts of floods is the real-time operation of reservoir flood control systems (Cheng and Chau, 2004). Real-time operation of reservoir systems involves various hydrologic, hydraulic, operational, technical, and institutional considerations, requiring an integrated management framework (Shim *et al*., 2002; Vrugt *et al*., 2003a; 2003b). A flowchart representation of the flood control management system for reservoirs is given in Figure 2.8. The key elements of real-time reservoir system (Figure 2.8) are: data collection; validation and processing of observed data; reservoir forecasting; and flood control operation; and information (Cheng and Chau, 2004). These systems adopt a client/server structure, based on a large-scale database, which includes the following modules: forecast and operation databases: real-time databases; history databases and a results database (Ford and Killed, 1995; Mujumdar and Ramesh, 1997; Shim *et al.,* 2002). The data collection module automatically collects the data from precipitation and streamflow gauges distributed in a specific basin; the data are then transmitted to a central base station through microwave, VHF telemetric, meteor burst and satellite communication systems (Yang *et al*., 1995; Cheng and Chau, 2004). When a flood event happens, the user can invoke the system. All raw data must be validated and processed before data will be stored into a database. The system may automatically process the raw data into hourly/daily precipitation, water elevation and discharge categories after all data have been validated (Ford and Killed, 1995; Shim *et al.,* 2002).

During the past three decades, decision support systems (DSS) have played an important non-structural role in analysing alternative mitigation options, and have been developed to assist flood control decision-making around the world (Ford and Killed, 1995; Cheng and Chau, 2004). For example, Ford and Killed (1995) developed a DSS for flood control operations in Trinity River Basin, Texas. DSS includes the whole support procedure: from retrieving and processing data for rainfall and streamflow to estimating basin averaging rainfall; updating model parameters; forecasting runoff and simulating reservoir operation. DSS integrates a database management system with specialised versions of the HEC-1 and HEC-5 river basin models (Killed, 1995).

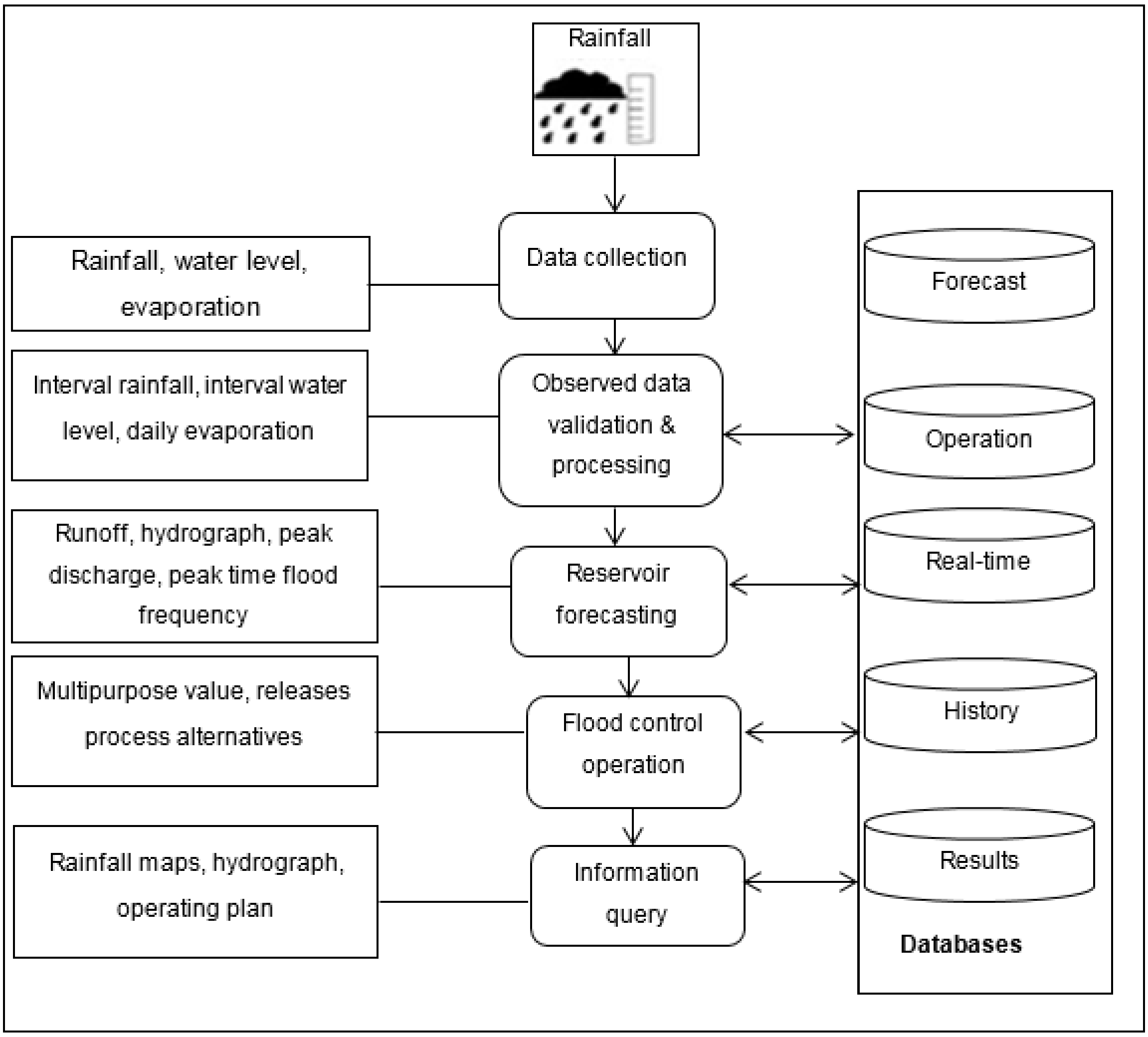

Figure 2.8: Flowchart of a reservoir flood control operation system (Source: Cheng and Chau, 2004)

Simonovic (1999; 2002) developed a Red River Basin Decision Support System that integrates hydrologic models, hydraulic models, economic models and virtual databases for the Red River Basin. Shim *et al.* (2002) developed a spatial DSS for integrated river basin flood control, which integrates several modules including: a relational database management system for hydro-meteorological data; a spatial analysis module using GIS: a flood-forecasting module employing an artificial neural network: a fully dynamic optimisation model incorporating hydrologic routing characteristics of the basin: a dialogue interface module incorporating graphical user interfaces; and graphical display systems supporting all the other modules. This spatial DSS has been applied to the Han River Basin in Korea (Cheng and Chau, 2004). In southern Africa, a recent study conducted by DHI and Aurecon (2011) demonstrated the application of a DSS, integrating GIS, databases and models, to provide a user-friendly tool for evaluating alternative technical operating options for compliance with the Incomaputo Agreements (between South Africa, Swaziland and Mozambique) for the Maputo and Incomati basins. While many reservoir operation software packages are currently available and many varied systems have been deployed in many countries, integrated systems are still subject to research and development, taking advantage of the rapid advances in remote sensing and satellite technology, geographic information systems, database management systems, hydrology modelling analysis and decision techniques (DHI and Aurecon, 2011).

2.7. Uncertainty in flood forecast modelling

Since many decisions in water resources are based on model-generated data, it is prudent to acknowledge the importance of uncertainty in the management process (Vrugt *et al.*, 2003b; Jasper *et al.,* 2005; Moore and Doherty, 2005; Brugnach *et al.*, 2008). The sources of these uncertainties are: the input forcing data (such as rainfall and evaporation demand); the parameterisation process of the models and also the structure of the model (Blasone *et al.*, 2006; Kapangaziwiri, 2008; Kapangaziwiri and Hughes, 2008; Brugnach *et al.*, 2008). Therefore it is important to take into consideration all these uncertainties when a flood forecasting model is being selected and applied.

In hydrology, there are many definitions of uncertainty concerning hydrological systems. In the water management context, uncertainties result from a lack of knowledge regarding the hydrologically correct probabilistic structure of a hydrological model, combined with the uncertainty following from this structure. Beven (2001) demonstrated that uncertainty differs to error because an error represents a specific departure from *"reality"* and uncertainties result from the natural complexity and variability of hydrological systems and a lack of knowledge of the hydrological processes. There have been numerous attempts to distinguish between different types of uncertainty (Vrugt *et al*., 2005; Refsgaard *et al*., 2007; Beven *et al*., 2008; Smith *et al*., 2008).

Input data uncertainty: Input data uncertainty arises from errors in measuring the climatic variables (rainfall, evaporation) and in the observed streamflow (for the gauged catchments). Input data deficiencies arise from limited and infrequent monitoring, sparse and diminishing measuring networks and use of short time series (Vrugt and Bouten, 2002; Wagener and Gupta 2005,). These deficiencies also contribute to uncertainty – this situation is particularly common in developing regions (such as southern Africa) (Hughes and Forsyth, 2006; WMO and USAID, 2012).

Model parameter uncertainty: Parameter uncertainty arises from the manner in which the parameters are estimated, either through regionalisation or *a priori* methods (Kuczera and Mroczkowski, 1998; Liu and Gupta, 2007). Reliance on observed data for calibration inevitably introduces input data uncertainty (Hughes and Forsyth, 2006; 2011) and, according to Knutti (2008), parameter uncertainty arises if the values used in the parameterisations are not adequately constrained by the observed evidence. Equifinality (Beven, 1986) also contributes to uncertainty in the regionalisation of parameters; the lack of appropriate physical basin property data suggests that both regionalisation approaches, and any *a priori* parameter estimation method will be highly uncertain.

Model structure uncertainty: Hydrological models are based on assumptions and simplified representations of the processes that take place in the real world system and will always be associated with some degree of uncertainty (Hughes *et al*., 2010; 2011). The complexity of the underlying hydrological processes has resulted in poor or insufficient knowledge of the processes and, consequently, the use of inappropriate assumptions for model conceptualisation and mathematical formulations (Sorooshian and Gupta, 1993; Beven and Freer, 2001; Beven, 2001, Vrugt *et al*., 2005). Another compounding factor stems from the manner in which the spatial and temporal discretisations are mathematically represented (Refsgaard *et al*., 2007; Beven *et al*., 2008). The focus of this study is on flood forecasting and therefore it is necessary to discuss the uncertainties related to the hydrological forecasting caused by the input of quantitative precipitation forecasts, hydrological and operational uncertainties (Lobbrecht and Solomatine, 2002; Danehelka, 2007) and to identify possible solutions using probabilistic approaches (Krzysztofowicz, 2001).

2.7.1. Quantitative precipitation forecasting (QPF) uncertainty in predicting rainfall

The QPF uncertainty is related to those meteorological models which produce ‘ensemble’ forecasts. Numerical Weather Prediction (NWP) models that generate ensemble forecasts are mostly global ones that operate at quite coarse grid resolutions. The European Centre for Medium Range Weather Forecast (ECMWF) model provides one main run, one control run (both using a 40 km grid) and 50 ensembles runs (80 km grid) with a lead time of 10 days (Krzysztofowicz, 2001). Since the primary input fluxes for most advanced hydrological models are satellite-derived precipitation and evapotranspiration, the operational data processing system supports the daily processing and distribution of these datasets. The Tropical Rainfall Measuring Mission (TRMM) of the U.S. National Aeronautics and Space Administration (NASA) produces merged three-hourly rainfall rates incorporating space borne radar, microwave data and infrared imagery (Barrett, 2001; Artan *et al.,* 2002).

These data are processed at USGS EROS to convert them to daily accumulations and reformatted to GIS-ready images. The NASA TRMM product (version 3B42) covers the tropics between 50^{o} north and 50^{o} south, with grid cells of spatial resolution 8 km by 8 km (Artan *et al.,* 2002). The NASA TRMM products contain constantly updated (current) and daily climatology data ever since the collection of this data was initiated in 1998. Operationally, the most current TRMM products are made available approximately 12 hours after the end of the data collection period. While other satellite-derived rainfall products are also available, the NASA TRMM products are used in this application because of their superior performance in regions with limited *in situ* gauges (Dinku *et al.*, 2007). The operational data processing system also produces and distributes a daily reference evapotranspiration (PET) dataset, with global coverage, as described in Verdin (2000).

The National Oceanic and Atmospheric Administration (NOAA) have developed several satellite-based techniques and an algorithm for rainfall estimation to support weather and flood monitoring activities of USAID. Among them is the system developed at the Climate Prediction Center for Rainfall Estimates known as the CPC-RFE, which was tested and applied in the African region (Funk *et al.*, 2003; Funk and Verdin, 2004; Sawunyama and Hughes, 2010). The CPC-RFE 2.0 is a combined satellite- and surface-based rainfall estimation technique. The CPC-RFE 2.0 product has been available since 2001 on an operational basis and has been applied in South Africa (Sawunyama and Hughes, 2009). It uses a merging technique that increases the accuracy of the rainfall estimates by reducing significant bias and random error when compared with individual precipitation data sources (Xie and Arkin, 1996), thereby adding value to rain gauge interpolations (Shrestha *et al.*, 2008). The disadvantage of this method is the coarse grid cell size of the meteorological output – which is unsuitable for forecasting flows in smaller streams and headwater areas.

Conversely, CPC-RFE 2.0 has a great advantage – the long lead time of the forecast, from daily up to seasonal forecasting (Danehelka, 2007; Shrestha *et al.,* 2008). CPC-RFE 2.0 takes advantage of an Extended Streamflow Prediction (ESP) system of observed historical precipitation time series instead of a Numerical Weather Prediction (NWP) precipitation forecast. Ensembles are based on current initial conditions of the hydrological model and historical weather analogues for the forecasted periods. The results are clearly statistical and are valuable mainly for the longer period (seasonal) forecasts for water supply reservoir operational decision-making. Unfortunately, this method of probabilistic forecasting is often too coarse to resolve the smaller catchments and shorter lead times. Another limitation is the lack of historical daily precipitation data because of the few rain gauges employed in most developing countries – including the Zambezi Basin.

2.7.2. Hydrological uncertainty

As with other hydrological models, flood forecasting models are also affected by hydrological uncertainty (Danehelka, 2007). This may be because of model structure uncertainty or model parameter uncertainty. Flood forecasting models are based on assumptions and simplified representations of the processes that take place in the real world system and will always be associated with some degree of uncertainty (Danehelka, 2007). The complexity of the underlying hydrological processes has resulted in poor or insufficient knowledge of the processes and, consequently, the use of inappropriate assumptions for model conceptualisation and mathematical formulations (Sorooshian and Gupta, 1993; Liu and Gupta, 2007). Another difficulty in the choice of a flood forecasting model is related to the modelling structure, since the mathematical representation of each model differs (Ao *et al*., 2006; Hughes *et al.,* 2006; Refsgaard *et al*., 2007; Beven *et al*., 2008; Smith *et al*., 2008). Uncertainty has been part of all modelling studies because of poor input data, scale and model structure, and the issues related to equifinality, therefore these uncertainties should be taken into consideration when the flood forecasting model is being selected (Vrugt *et al*., 2003a; 2003b; Danehelka, 2007).

2.7.3. Operational uncertainty in predicting flood

Operational uncertainty is caused by unpredictable events during the forecasting process – such as dam breaks, reservoir operations, ice jams etc. (Danehelka, 2007). The *prior* knowledge of the hydrological system and the background of the hydrologists operating the model can both have an important impact on the final hydrological forecast (human impact also belongs to this group of operational uncertainty). Unfortunately, operational uncertainty cannot be quantified in advance and therefore stays unexpressed, not only in deterministic, but also in probabilistic approaches (Danehelka, 2007). The decision-making for flood control is usually effective only for the current period or for the following periods; such decision-making is constrained by the updated results on flood forecasting at each current period on a daily or hourly basis during flood events (ICOLD, 1992; Beilfuss and Dos Santos, 2001; Meier *et al*., 2011).Therefore it is very important to generate the feasible flood control alternatives quickly.

2.8. Hydrodynamic modelling and flood forecasting in southern Africa

Hydrological forecasting models have been used to estimate water resources availability and for impact assessments in southern Africa but the lack of hydro-meteorological data, the problem of ungauged basins and the lack of expertise have made the process difficult (Hughes, 2004a; WMO and USAID, 2012). There is a general consensus that a lack of high quality observations hinders the progression of arid zone hydrology (Pilgrim *et al.,* 1987). Southern Africa is faced with diminishing monitoring networks, whose data are sparse and of poor quality (short time series, missing data and sometimes, unreliable) and also difficult to access. Lack of resources, shifting priorities (especially on the political front) and war in some countries (WMO and USAID, 2012) has resulted in several recording networks going unmonitored for prolonged periods. Although there are a number of hydrological models available, conceptual-type models have been the types commonly applied in southern Africa.

Recent applications of various models are discussed here. Hughes (1997) demonstrated the application of the monthly Pitman model under the Southern African FRIEND project as a contribution to the international FRIEND (Flow Regimes from International Experimental and Network Data) programme (which was part of the UNESCO Fourth International Hydrological Programme), in which the central objective was hydrology and water resources for sustainable development. Beilfuss and Dos Santos (2001) demonstrated the application of HEC5, for studying patterns of hydrological change in the Zambezi delta. Mazvimavi (2003) demonstrated the applicability of the Pitman model, for estimating flow characteristics in ungauged catchments in Zimbabwe. Winsemius *et al.* (2006) presented a GIS-based modelling tool (The STREAM model) to model spatial water balances for environmental studies in the Upper Zambezi.

DHI (2006) introduced a MIKE 11 Flood Watch for flood forecasting and monitoring for the Lower Zambezi and Asante *et al.* (2008) demonstrated the applicability of a linear Geospatial Streamflow Model for flood forecasting for the Zambezi Basin. There has been no standard or unified approach to hydrologic modelling in the Zambezi Basin. No single hydrologic or hydraulic model provides river and flood forecasts throughout the Zambezi river basin, with all its varied characteristics. Therefore the application of models to provide hydrologic forecasts at numerous river gauges and communities throughout the entire basin requires: historical data for calibration; Geographical Information System parameters; real-time rainfall and hydrologic data; and highly trained and experienced operators and forecasters to prepare river-and-flood forecasts (WMO and USAID, 2012).

2.9. Water resources and flood management of the Zambezi River Basin

Almost every year, floods in the Zambezi River Basin claim lives and cause economic losses. Both of these impact negatively on socio-economic development, thereby worsening poverty within the basin. Conditions are particularly severe in Malawi and Mozambique where the flood plains are extensive (WMO and USAID, 2012). The situation is also exacerbated by tropical cyclones. The influence of these cyclones can extend over an area up to 1 500 km in diameter (NGC, 2009; WMO and USAID, 2012). Recent extreme floods in Mozambique and beyond (Limpopo and Zambezi in 2013; Zambezi, 2000, 2001, Limpopo, 2000) have put both community resilience to flood events and the need to predict future flood risks high on research and political agendas in Mozambique. There have been extreme floods in the past (e.g. Zambezi in 1958, 1978) and there is considerable historical evidence about these floods; how the communities remember these events (e.g. in existing high flood marks and community narratives); how people protected themselves – and how the local people built the memories and experiences into their community resilience. Marks, flood records, memories and stories of past flood events might help further develop future community resilience. Hydrometric records available on the Zambezi River in Mozambique show that large floods have occurred on the Zambezi River only six times since records commenced in 1945, and only two of those floods occurred after 1957/58. According to DNA (2014) large floods are defined as occasions when the river stage was equal to or exceeded 7.0 m at Tete (E-320) in the case of the Zambezi basin. The largest recorded flood at Tete (E-320) occurred in 1958 when the river stage reached 10.5 m on the gauge station, corresponding to a flow of approximately 22 500 $m^3 s^{-1}$. Since the Cahora Bassa dam was completed, the largest flood occurred in 1978, when the peak stage at Tete was 8.30 m. Levels in the lower river were also high in 1997. At Caia (E-291), the peak stage in February 1997 was 8.21 m; at Marromeu (E-285), the peak stage in February 1997 was 7.62 m. In 2000 and 2001, the maximum stage at Tete (E-320) was 7.35 m. In 1997 flooding from several of the tributaries downstream of Tete was high, but the effects were mitigated by reducing discharges from Cahora Bassa dam – made possible because inflows from the middle Zambezi (upstream of the dam) were relatively low that year. By contrast, in 2001 a large flood from upstream passed through Cahora Bassa dam, and only minor flooding occurred in the lower tributaries (DNA, 2014).

All eight riparian states have an inadequate capability to predict flooding and issue the timely and accurate flood warnings needed to coordinate disaster prevention and response (WMO and USAID, 2012). Most national meteorological and hydrological services and national disaster management agencies do not have the proper tools and technical capacity to anticipate and plan prevention and response actions for floods (as is possible in Europe and

America). A few local disaster management systems have been developed to provide early warning against these devastating events. However, such systems currently do not provide warnings sufficiently early for mitigating these disasters (Sheila, 2000). The SADC Revised Protocol on Shared Watercourses includes provisions for the sharing of data and information on the water resources of shared river basins. The protocol emphasises the obligation of the SADC states to coordinate and share information in emergencies (such as floods). In addition, Mozambique participates in Permanent Joint Commissions with its neighbouring countries, which provide forums for collaborating and cooperating in endeavours of common interests – including solving flood problems – e.g. the Joint Water Commission between Mozambique and Malawi for cooperation in the development and management of common water resources (which includes flood risk management in the Shire River). The *Direcção Nacional de Àguas (DNA)* and *Instituto Nacional de Meteorologia (INAM)* in Mozambique have the overall responsibility for the management of the Lower Zambezi Basin, assisted by the *Administração Regional de Aguas do Zambezi* (*ARA-Zambeze*). Table 2.3 summarises the stakeholders responsible for operational water resource management systems within the Zambezi Basin.

Table 2.3: Existing water resource and flood management institutions in the Zambezi Basin

Stakeholder	Location of interest	Regime Upstream
Zambezi River Authority (ZRA, Zambia and Zimbabwe) – Operator of the Kariba dam	Inflow (m^3 s^{-1}) into the Kariba dam	Natural
Hidroeletrica de Cahora Bassa (HCB, Mozambique) Operator of the Cahora Bassa dam	Inflow (m^3 s^{-1}) into the Cahora Bassa dam	Natural and regulated
Disaster Management and Mitigation Unit Centre (DMMU) Zambia	Kafue, Siavonga, Luanga and Nyimba	Natural and regulated and flash
Department of Civil Protection (DCP) Zimbabwe	Upstream Victory Falls, Kanyemba area, area of confluence of Sanyati/Gwayi with Zambezi, Chidodo and Muzarambani area	Natural and regulated
The ARA-Zambeze, Mozambique	Downstream of Cahora Bassa dam	Regulated and Natural

2.10. Summary

Understanding concepts, causes, effects and flood management approaches is a prerequisite for the establishment of any integrated flood Management system. Floods cause: the loss of human and animal life; structural damage to bridges, buildings, roads and utilities; result in soil erosion; and massive (and costly) environmental destruction. Floods also bring many benefits – such as the recharge of underground aquifers; restoration of wetlands; increments in fresh water for irrigation and domestic use; improvements in navigation for transport systems, kills insects; washes out acid water; pushes salt water toward the sea; etc.

Therefore the understanding of information from model applications should help to define flood management strategies and identify possible risks, solutions and their impact. This is, indeed, the essence of IWRM, where a holistic approach is required to analyse alternative designs and management strategies for integrated multi-component systems. Many approaches to address the issues of flood forecasting have been developed using hydrological modelling methods. The heterogeneities and variability at spatial and temporal scales remain a major challenge for hydrological modelling methods.

However, the lack of a unifying framework for flood forecasting and early warning systems makes it difficult to select one single method from among the various available approaches. This means that an effective flood forecasting system should integrate several approaches. It is important to ensure that the forecasting estimates are understood by the users and ready to be used for both science-based and operation decision-making in an integrated manner. Hydrological forecasting should also consider the investable uncertainties related to data inputs and model structure, even if these can be quantified and minimised during the calibration and validation stages of the modelling process. Many of the approaches reviewed have addressed the issues of flood forecasting and communication.

Therefore an effective communication platform should include flood risk mapping, to enable to predict and quantity the potential consequences.

3. STUDY AREA, PHYSICAL BASIN CHARACTERISTICS AND DATA SETS

3.1. Introduction

This study was undertaken using two main components. The first component sought to assess the applicability of and analyse the results produced by a selected rainfall-runoff model for natural flow prediction and flood management in the Zambezi River Basin. The second component sought to assess the combination of the chosen rainfall-runoff model with a reservoir simulation model and the ability of the combined models to form an integrated system to be used to predict the impact of activities occurring upstream of the Cahora Bassa dam on downstream flooding. The model also needed to account a number of constraints associated with the available data.

This chapter presents a description of the study area, the data used and the general approach followed to achieve the main objectives of the study. In general, the Zambezi River Basin has a relatively poor quality database for hydrological assessments when compared with the data available for other large basins worldwide (Winsemius *et al.*, 2006; Tilmant *et al.*, 2010). The lack of data makes it difficult to develop guidelines for applying integrated hydrological models for flood prediction for the whole basin.

The general climate, hydrology, soils, vegetation and land use characteristics of the Zambezi River Basin are summarised in the following sections. These characteristics not only affect the total volume of runoff generated from various sub-basins but also the different components of flow regimes (high and low flows, for example) in different ways (Asante *et al.,* 2008; Mul *et al.*, 2009).

3.2. The study area

The Zambezi River Basin covers an area of 1 390 000 km^2, across eight riparian countries – Angola, Botswana, Malawi, Mozambique, Namibia, Tanzania, Zambia and Zimbabwe. Zambia constitutes the highest share of the basin at 40.7% of the total basin area; Namibia is the lowest at approximately 1.2% (Figure 3.1). The other riparian countries constitute the following: Angola 18.2%, Zimbabwe 16.0%, Mozambique 11.4%, Malawi 7.7%, Botswana 2.6% and Tanzania 2.0% (Tumbare, 2004; Tilmant *et al.*, 2010). The main tributaries of the Zambezi Basin cross areas of various heights, slopes, soils and geologies before discharging their flows from the basin into the Indian Ocean.

The altitude of the basin ranges from sea level at the Mozambican coast to 2 960 amsl in the highlands of Angola and Zambia. The Zambezi River Basin is divided into eleven major sub-basins: the Luangingwa (F); Cuando (G); Gwayi (C); Sanyati (D) (all four discharge directly into the Kariba dam): Kafue (H); Luangwa (I); Zambezi, (discharging into the Cahora Bassa dam) and finally: Luia (E); Revubwe (A); Mazoe (B) and Shire (J) (all four discharge downstream of the basin) (Figure 3.1). The last four sub-basins all drain into the main Zambezi River downstream of the Cahora Bassa dam. The Zambezi river basin has two large artificial reservoirs, the Kariba and Cahora Bassa dams, with a combined storage of more than 200 billion m^3, (approximately six times the average annual flow at Victoria Falls and twice the average annual discharge at the sea). Two other reservoirs are located on the Kafue tributary: Ithezi-Tezhi and Kafue Gorge (Tumbare, 2004; Tilmant *et al*., 2010). Since the construction of the Kariba dam in the late 1950s, the river basin has experienced various other infrastructural developments – for energy generation, flood control, recreation, fishing and irrigation (Beilfuss and Dos Santos, 2001). Figure 3.1 shows the Zambezi River Basin selected as the study area for the implementation of the new model.

The lower Zambezi stretches 650 km from the Cahora Bassa dam to the Indian Ocean. This stretch of the river is navigable in the wet season, although the lower Zambezi is shallow in many places during the dry season (Bourgeois *et al.,* 2003). This shallowness occurs as the river enters a broad valley and spreads out over a large area. Only at one point, the Lupata Gorge, 320 km from its mouth, is the lower river confined between high hills. Here it is scarcely 200 m wide. Elsewhere, the width is between 5 and 8 km wide, flowing gently, and composed of many streams (Bourgeois *et al.,* 2003). The river bed is sandy; the banks are low and reed-fringed. At places, however, and especially in the rainy season, the streams unite into one broad fast-flowing river. Approximately 160 km from the sea, the Zambezi receives the drainage of Lake Malawi through the Shire River. On approaching the Indian Ocean, the river splits up into a delta. The Zambezi River basin supports a total population estimated at approximately 38 million and, if the current growth rates are maintained, by 2030 this will reach more than 70 million (Tilmant *et al*., 2010). 5% of the population live on the floodplain areas of the Lower Zambezi, downstream of the Cahora Bassa dam (INE, 2007). This predicted rapid population growth, within the Zambezi Basin, will lead to increased water demands for food and energy, needs which are likely to compete with the minimum and maximum flow requirements for the environment and flood sensitive areas respectively.

The first sections of this chapter provide a general overview of the physical and climatic characteristics of the whole Zambezi River basin; towards the end of this chapter the focus is on Water Resources and flood management of the Zambezi River Basin – the main point of interest in this study.

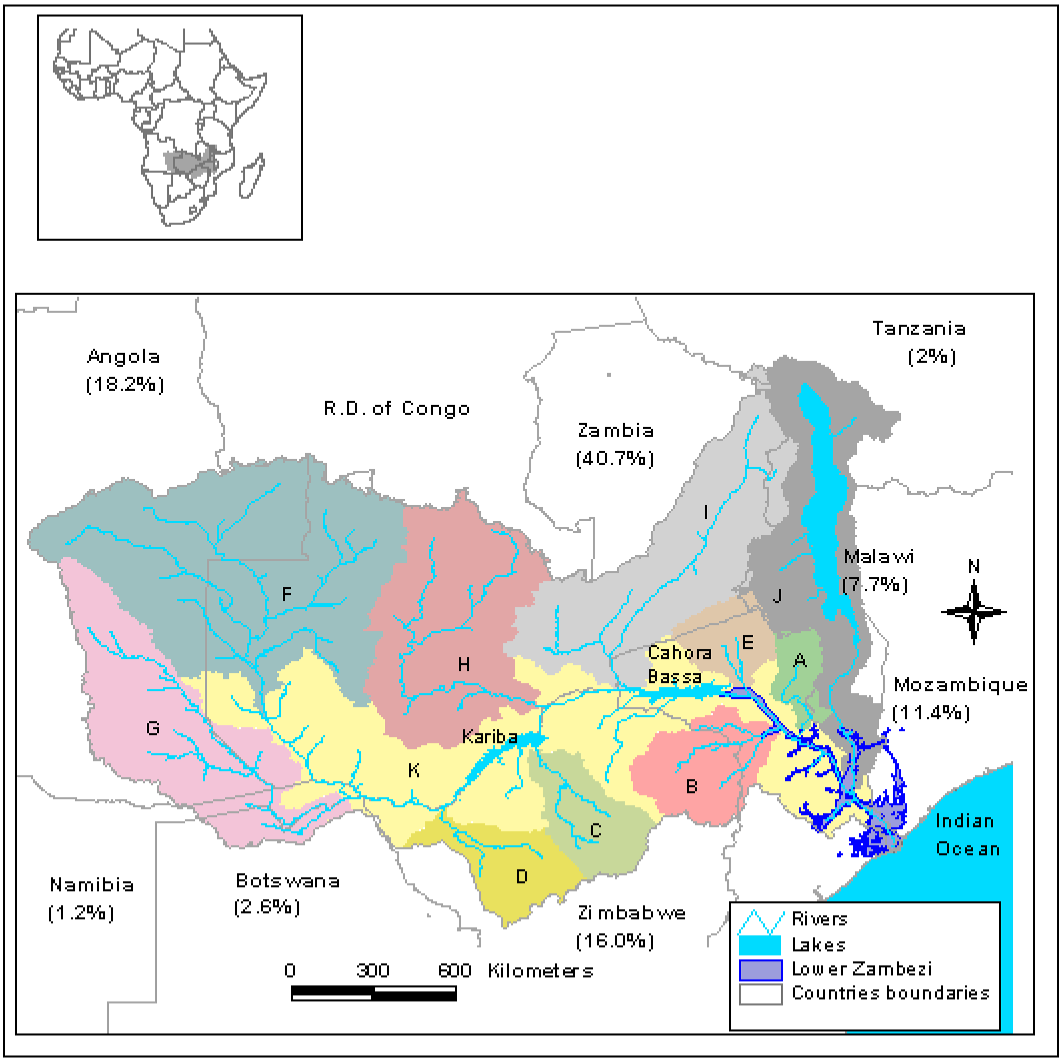

Figure 3.1: The major sub-basins of the Zambezi River Basin. Details of the percentage of total basin area within the borders of each of the riparian countries

3.3. Physical characteristics of the Zambezi River Basin

An understanding or appreciation of the physical characteristics of a basin is important in hydrological studies, to give an indication of the dominant rainfall-runoff processes and such knowledge should, in turn, provide guidance when setting up a hydrological model. For example, the analysis of topographic data gives an indication of water flow direction; the understanding of soil characteristics and land cover (or land use) allows an appreciation of the possible soil moisture and hydraulic conditions (important for the estimation of the hydrologic response of each sub-basin) (USGS, 2000b; Shrestha *et al.,* 2008; Mul *et al*., 2009). From a practical perspective, it is vital that these characteristics be derived from sources (such as topography and soils maps, satellite imagery, and national databases) that are readily available to practising hydrologists, (Artan *et al*., 2001; Mazvimavi, 2003). However, it is also important that the data are available in a formats, scales and resolutions useful for hydrological interpretations (Verdin, 2000). For example, soils data are often compiled for agricultural purposes and do not always contain details of the variables of direct hydrological value (Webb *et al*., 1993).

3.3.1. Topography and relief

Many hydrological models use a grid of elevation data to create topographical characteristics that describe the physical characteristics of each sub-basin to be modelled. A detailed explanation of the process of creating such a grid is described in USGS (2000a) using the digital elevation model (DEM) HYDRO GTOPO30 1 km data (this model is available from the U.S. Geological Survey's Earth Resources Observation System (EROS) Data Center at http://edcdaac.usgs.gov/gtopo30/hydro/africa.html) and the Shuttle Radar Topography Mission (SRTM). The products are available online at http://www2.jpl.nasa.gov/srtm/ and are given in 30 m spatial resolution for the U.S. only and at 90 m and 1 km for other parts of the globe. The GTOPO30 data set was used for terrain analysis of the Zambezi Basin because the model is based on a corrected DEM dataset on a 1 km grid covering the whole of Africa. Howard (2007) recognised that the variations in topographic structure, which lead to differences in drainage networks and efficiency of sub-basins to convey water to the outlet, have pronounced effects on hydrology, particularly on the basins' response to flood events. The relief of the Zambezi Basin can be divided into 5 (five) physiographic regions: flat, with altitude ranging from 0 m – 100 m; low altitude 100 m – 250 m; middle altitude 250 m – 1 000 m; high altitude 1 000 m – 2 000 m and very high with altitudes greater than 2 000 m (Figure 3.2). The SRTM 90 m spatial resolution data were used for the representation and mapping of elevation ranges over the flood plain area downstream of the Cahora Bassa dam. A detailed description of the SRTM project and products can be found in Farr *et al.* (2007).

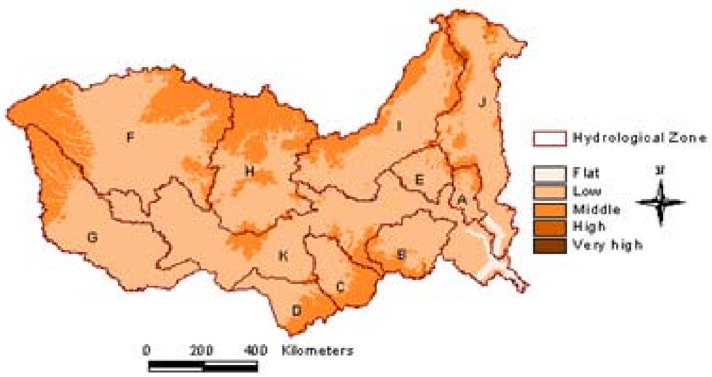

Figure 3.2: Relief map of Zambezi River Basin. Map generated from a 1 km HYDRO DEM (Source: USGS, 2000a)

3.3.2. Slope and geomorphology

Slope is an important characteristic of a basin because it gives an indication of the kinetic energy available for water to move towards the basin outlet (Mazvimavi, 2003; Baumann, *et* *al.,* 2010). One of the main problems for large scale modelling in hydrological studies, before the advent of Digital Elevation Models (DEMs), was the derivation of slopes for all the landscapes within a basin. This is because a single slope index for the whole basin may not be representative of all the landscapes that affect runoff processes. The division of river basins into sub-basins with associated river reaches, and the parameterisation of these modelling units from Digital Elevation Model (DEM) data have been automated in many hydrologic models including the GeoSFM (e.g. USGS, 2000a; Artan *et al*., 2002; Entenman, 2005). The HYDRO 1 km, from USGS EROS, was used to derive slope and river flow because of the model's global coverage. It is a hydrologically-corrected DEM which is devoid of spurious pits that interrupt the hydraulic connectivity over the land surface. These 'pits' are artefacts of the interpolation procedure used in the creation of DEMs, and they result in breaks in the flow network unless they are removed (Asante *et al.,* 2007c; Shrestha *et al*., 2008). HYDRO 1 km data were downloaded from http://edcdaac.usgs.gov/gtopo30/hydro.

Figure 3.3 shows the spatial distribution of slopes within the Zambezi River Basin. Basins located on the Central Southeast, Northeast and East of the basin have the highest median slopes, ranging from 20% to 75%. The lowest slopes are found in basins located in the Southwest and Western regions, ranging from less than 1% to 20%. The spatial variation of slopes is related to the geomorphological features of the river flow. A study conducted by Davies (1986) showed that the Upper Zambezi (located within south-western Zambia, south-eastern Angola, the Caprivi Strip of Namibia, and the northern edge of Botswana) is defined by the floodplains of the Zambezi and Cuando Rivers above Victoria Falls Figure 3.4a). The upper Zambezi receives water from the Cuando and Lungwebungu Rivers and from the Okavango, via the Chobe River, during times of very high rainfall (Davies, 1986). This hydrological zone is predominantly flat, with slopes ranging from 0% to 20%. In the middle Zambezi, the river flows swiftly through the Batoka Gorge, the current being continually interrupted by reefs. Beyond the gorge ,the slopes range from 3% to 36%, except in several isolated areas located in the South West of the basin (where the slopes are less than 1%) and in the Central part of the zone (where slopes are greater than or equal to 36%) (Figure 3.3).The spatial distribution of slopes in the Lower Zambezi is highly variable, ranging from 3% in the Delta to 75% in the Northern and Southern part of the sub-basin.

Figure 3.4 illustrates the changes in configuration of the Zambezi River system, from upstream to downstream, including the Kafue basin. According to the Zambezi Society and the Biodiversity Foundation for Africa (2004), this system has been strongly influenced by tectonic activity (faulting) in an area of low relief. Major wetlands (such as: the Barotse and Chobe floodplains; the Victoria Falls transition from the Upper Zambezi floodplains; the Kafue Flats and the Lower Zambezi Delta floodplains) were all formed in the Pleistocene period (i.e. within the past 2 million years). The area that now forms the Zambezi Basin system is generally accepted to have been a plain of low relief, traversed by sluggish meandering streams.

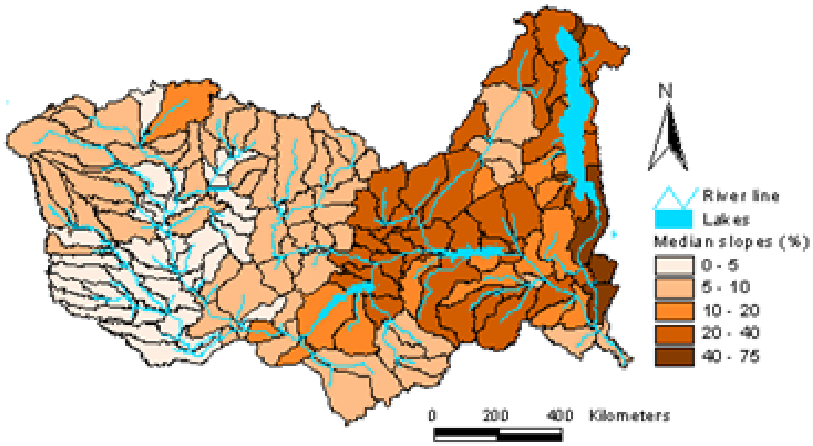

Figure 3.3: Spatial distributions of median slopes of the Zambezi River Basin (Source: USGS, 2000a)

 Upper Zambezi: Chobe floodplain in Upper Zambezi	 Transition Zone Upper to Middle: Victoria Falls transition from Upper to Zambezi floodplains
 Middle Zambezi: Kafue River catchment in Zambia	 Middle Zambezi: Kafue Gorge Dam
 Lower Zambezi: downstream Gorge zone with Luia River inflows in the North of Lower Zambezi	 Lower Zambezi: Delta of Zambezi

Figure 3.4: Overview of the different geomorphologic zones of Zambezi River Basin (Source: Beilfuss and Dos Santos, 2001)

3.3.3. Soils

At the basin scale, soil moisture is the major control for rainfall–runoff response, especially where saturation excess runoff processes dominate (USGS, 2000a; Baumann *et al.,* 2010). Many processes of the basin hydrological response are regulated through the soil medium, which plays a prime role in its capacity to absorb, retain and redistribute water (Schulze, 2007). Soil information is therefore necessary to the understanding of the processes of runoff generation: e.g. saturation excess runoff; interflow; overland flow and the soil moisture. The most relevant factors for understanding the dynamics of hydrological processes are perhaps the four described by Schulze (2007):

- surface properties that regulate the soil infiltrability (such as crusting, sealing, cracking, tillage, macro pores, etc.);
- thickness of various horizons of the soil profile and the distribution of soil particles (soil texture) within the various horizons (which are also related to the soil permeability or hydraulic conductivity);
- soil structure within the profile that may induce drainage, water logging or interflow;
- capacity of the soil to retain water and its behaviour under various conditions (including measures of permanent wilting point, field capacity and saturation).

While the above-mentioned factors are important, the soil characteristics described below were also selected because they have a direct influence on the process of runoff generation. For example, shallow soils can result in higher runoff when compared with the runoff from deep soils – Webb *et al*. (1993) showed that deep soils generate low runoff volumes – which could be explained by lower contributions from the riparian zone. Baumann *et al.* (2010) demonstrated that soil texture influences the hydrological processes within a river basin. Therefore, during tropical rain accumulations over a period of several consecutive days, the progression of the soil water, from the top soil to the deep subsoil, strongly influences the runoff behaviour on soils of coarse texture. Rainstorms up to 70 mm generate more runoff on heavy clay soils than on soils with a sandy clay loam texture (Baumann *et al.*, 2010). Soil and land cover data sets have been used to determine Soil Conservation Service (SCS) runoff curve numbers in GeoSFM – these numbers are used to determine the amount of incident precipitation that becomes surface runoff.

The estimation of soil parameters (such as water holding capacity (WHC); hydrologically active depth (DEPTH); texture (TEXTURE); and saturated hydraulic conductivity (KC)), are used by most hydrological models, including GeoSFM, to estimate the soil moisture conditions of a river basin. These data were extracted from the Digital Soil Map of the World (DSMW) database, jointly produced by the United Nations Food and Agriculture Organization (FAO) and the United Nations Educational, Scientific and Cultural Organization (UNESCO) (FAO, 1995). The data are available in CD-ROMs, in different formats, from ArcInfo Vector Export, ERDAS Raster, and IDRISI Raster (USGS, 2000a). The DSMW database contains over 16 000 different soil mapping units that combine existing regional and national updates of soil information worldwide (Soil and Terrain Database-SOTER, Soil Map of China, World Inventory of Soil Emission Potentials – WISE) with the information contained within the FAO-UNESCO old Soil Map of the World, 1:5 000 000 scale (FAO, 1971 – 1981). This makes the information contained in the database qualitatively variable, with low reliability for the regions in the database that still make use of the FAO data (such as North America, Australia, West Africa and South Asia). The information is considered moderately reliable for those regions of SOTER databases where the scale is smaller than 1:1 000 000. This is the case for South America, the Caribbean, the Congo and Angola.

For the regions where the scale of the original maps was 1:1 000 000, or better, with a complete soil profile database available, the reliability is considered high. Such regions include Southern Africa, Central and Eastern Europe (USGS, 2000a). The regions of the Zambezi basin are 100% covered by the scale of the original maps (1:1 000 000) therefore the soil information is of high reliability. Based on the Digital Global Soil Maps (from the Food and Agricultural Organization (FAO, 1998) of the United Nations) (Figure 3.5), the majority (56.9% of the total area) of the soils in the Zambezi River Basin have poor infiltration capacities, with depths ranging from 100 to 150 cm. These soils occur mostly in the West, Northwest and South of the basin. Very deep soils, with depths ranging from 150 to 225 cm, cover 25% of the area, mainly in the North, Central and Southern parts of the basin.

Other soils are moderately deep ranging from 50 – 100 cm depth, covering 15% of the area and occurring in low-lying areas. The less dominant soils, covering only 3% of the total area, are shallow with very low infiltration capacities and occur around the drainage divides. Figure 3.6 shows the spatial distribution of the soil texture classes in the Zambezi River Basin. In the North and Central parts of basin, loamy soils predominate, with moderate water holding capacity, and cover 48% of the total area: sandy soils are the next most common soils (covering 39%), with poor water holding capacity, in the North and South of the basin (Figure 3.6). Clay soils, with higher water holding capacity, are less dominant (covering 10% of the total area) and located in the floodplain areas of the basin.

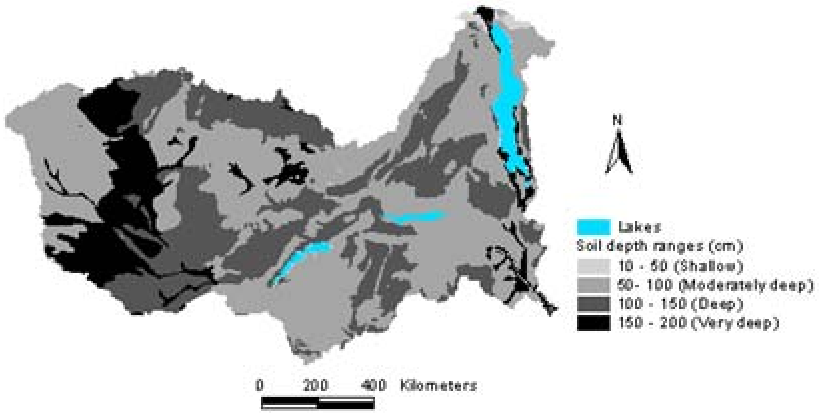

Figure 3.5: Spatial distribution of soil depths in the Zambezi River Basin (Source: FAO, 1998)

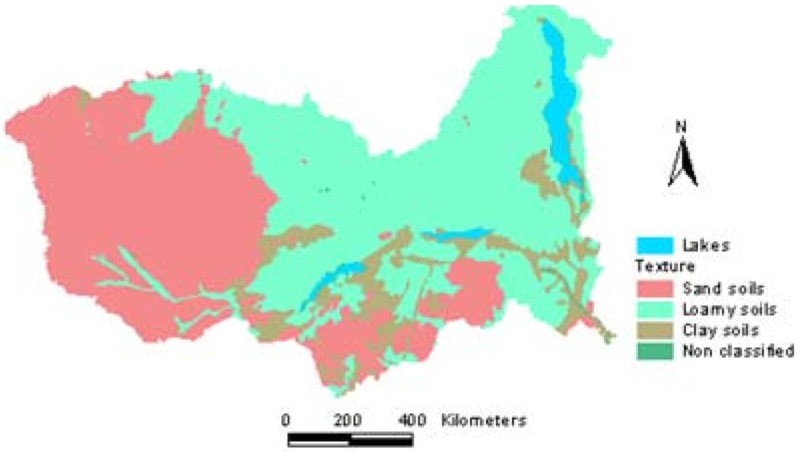

Figure 3.6: Spatial distribution of soil texture classes in the Zambezi River Basin (Source: FAO, 1998)

3.3.4. Land cover and land use

The surface conditions of land cover (i.e. vegetation and/or land use) also have a huge impact on basin hydrological response to rainfall events by separating surface runoff generation from infiltration into the soil. Land use and land cover data are both needed to determine the response of the basin to rainfall events and, along with soil data, are used to estimate the response coefficients used by hydrological models to determine the excess rainfall, recharge to the groundwater system, and the amount of soil water stored. Land cover and land use data include vegetation classification and information about how the land is being used (such as: agricultural croplands or urban and built-up areas). For large regions like the Zambezi Basin, these data are best obtained from satellite observations. One example of satellite-based land cover maps can be found on the Global Land Cover Characterisation (GLCC) webpage (http://edc2.usgs.gov/glcc/glcc.php). A recent product is based on satellites used in the NASA Moderate-resolution Imaging Spectroradiometer (MODIS) sensors, delivering images from 2000 onwards. The land cover products are available at resolutions of 1 km and 500 m. The

USGS Global Land Cover Characterisation (GLCC) database (Loveland *et al.*, 2000) was used in GeoSFM to describe and to generate both the rate of runoff and of overland flow transport.

This study uses the GLCC data derived from the 1 km Advanced Very High Resolution Radiometer (AVHRR) data, available through the Interrupted Goode Homolosine and Lambert Equal-Area Azimuthal projections (USGS, 2000b; Loveland *et al.*, 2000), to estimate the effect of rainfall events within different land cover types/classes. The GLCC dataset was validated by the Land Cover Working Group (LCWG), through the International Geosphere Biosphere Programme (IGBP) DISCover, established by the researchers of the University of California, Santa Barbara (UCSB) (Belward *et al.,* 1999; Scepan, 1999). The IGBP DISCover accuracy approach was derived using a random sample stratified by land cover type (Belward *et al.,* 1999).To determine the true cover type, three interpreters independently interpreted either Landsat TM or SPOT images covering each sample. The AVHRR pixels were corrected by the majority vote of the three interpreters – at least two of the three had to agree on the land cover type, as interpreted from Landsat or SPOT images – for each sample point. In the Zambezi River Basin the dominant land cover type (Figure 3.7) is savannah covering 58% of the area; followed by deciduous broadleaf forests (covering 15%). Other land cover types in the basin include: cropland/woodland mosaic (covering 14%); dry land cropland and pasture (5%); evergreen broadleaf forests (4%); water bodies (3%); barren or sparsely vegetated surfaces; grassland; urban and built-up surfaces; irrigation areas; shrub land and herbaceous wetlands; each cover less than 1% of the total area.

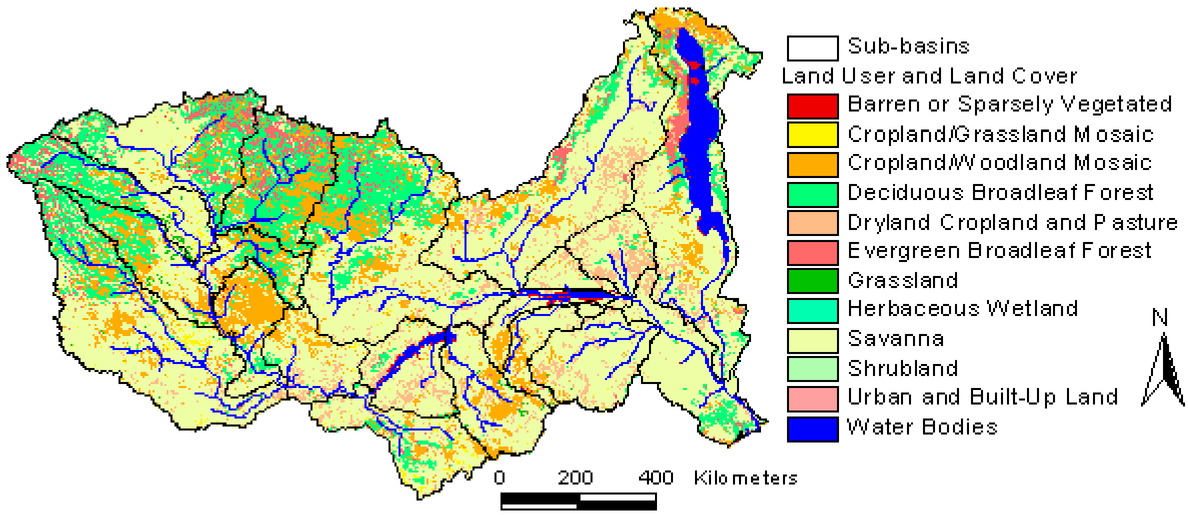

Figure 3.7: Spatial distribution of land cover land use classes in the Zambezi Basin (Source: USGS, 2000b)

3.4. Climatic characteristics

Temperature, through its influence on evapotranspiration and rainfall, are the key driving meteorological variables in a hydrological model. Among other factors the lack of adequate hydrological and meteorological data forms an impediment to economic growth and poverty eradication in developing countries, and therefore handicaps the achievement of the UN Millennium Development Goals in these countries (Bogaard *et al.,* 2010). Currently, data are primarily collected by advanced electronic equipment, often installed in data collection networks. The hydrological data collection in the eight riparian countries within the Zambezi Basin is managed by the respective hydrological service agencies (WMO and USAID, 2012).

In the absence of access to ground-based observation data, satellite-derived rainfall may provide a suitable alternative. The Tropical Rainfall Measuring Mission (TRMM) satellite was launched by NASA and JAXA (Japan) at the end of 1997 and data and documentation can be downloaded from the TRMM homepage at http://trmm.gsfc.nasa.gov/. An additional advantage for operational use is that the products are available in near real-time. Other rainfall and evaporation estimates that can be used are the FEWS RFE 2.0 data (Herman *et al*., 1997), generated by the Climate Prediction Center (CPC, NOAA) for the Famine Early Warning System (FEWS) for Africa (accessible at the following websites:(http://www.fews.net and http://www.cpc.ncep.noaa.gov/products/fews/)).

3.4.1. Temperature

Temperature variations over the Zambezi River Basin are mostly determined by altitude, latitude, and proximity to large water bodies. Leenaer (1990) showed that, towards the coast, the climate in this region is continental in character with appreciable seasonal variations in temperature. There is a fair amount of sunshine and during the cool season, from May to August, the day temperatures are moderate, with continuous sunshine; the night temperatures are low and ground frost may occur in sheltered valleys. The drier hot season is from September to November. Temperatures and atmospheric humidity progressively increase until the onset of the wet season. The average annual temperature in the basin is between 16ºC and 26ºC. However the monthly maximum temperatures occur between October and February; the monthly minimum temperatures occur in June and July (Figure 3.8). In general, the average annual thermal amplitude is around 10ºC. Spatially, the mean annual temperature ranges from 16ºC in the Southern part of the basin to 26ºC in the South East. The areas that experience the highest temperatures are the central and lower parts of the basin. The variation of temperature in the basin is influenced by the elevation above mean sea level, affecting the air temperature of the surrounding areas. The general trend in temperature is that it decreases with increasing latitudes in the Zambezi Basin; these temperature variables influence the evaporation rates.

3.4.2. Rainfall

The Zambezi Basin experiences highly variable rainfall, both spatially and temporally, which contributes to risk in the availability of sustainable water resources (World Bank, 2006). This situation impacts on the runoff regime experienced in the area, resulting in a concentration of high flows in the wet season and relatively frequent drought conditions. The probability of the occurrence of floods is also high during the wet season in the Zambezi Basin. There are two main rain seasons strongly related to the spatial and temporal distribution of rainfall within the basin. The wet season occurs from November to March (Figure 3.8), with mean rainfall between 250 and 1500 mm yr^{-1} – the rainfall levels generally decrease from north to south. In the central part of the region, dry-season precipitation is rare, and there is usually no measurable rain for six months or more. In the Zambezi Basin, rainfall intensity is the major problem – for example, in March of 2009 torrential rains of more than 100 mm in 24 hours, across Angola, Namibia, and Zambia, increased water levels in the Chobe, Kunene, Kavango and Zambezi Rivers to such an extent that the north-central and north-eastern regions of Namibia experienced the worst flooding in decades (Katjavivi, 2009).

The damage affected 60% of the total population, destroying critical infrastructure, washing away crops and livestock, damaging homes, and causing widespread displacement. A similar situation was observed in 2008 in Mozambique, where intense rainfall associated with the Cyclone Jokwe caused extensive flooding, destruction of property and displacement of more than 1 000 000 people (INGC, 2009). The rainfall within the Zambezi River Basin during the hot summer season is associated with the Inter Tropical Convergence Zone (ITCZ), which moves North-Westward from the Southeast to the higher altitude in the Northern part of the basin bringing both conventional and cyclonic rainfall. The rainfall has a high inter-annual variability expressed in terms of rainfall anomaly, i.e. the deviation of the mean annual rainfall from the long-term average rainfall (Figure 3.9).

Spatially, the mean annual precipitation (MAP) ranges from 570 mm yr^{-1}, in the Southern part of the basin, to 1 180 mm yr^{-1} in the North-West. The highland areas in the North-West, the North, and small parts in the South East of the basin, receive higher rainfalls when compared with the mean annual rainfall in the low-lying Southern and Central parts (World Bank, 2006). The concentration of high rainfall in the North Western part of the basin is also a result of the influence of the Inter Tropical Convergence Zone (ITCZ) whose location varies seasonally. The majority of the national rainfall data is recorded at a daily time-step; only a few sites are able to record data at finer intervals (using continuously recording instruments). In the past, rainfall was measured at a relatively large number of daily total recording stations; many records extend back into the 19th century (Asante et *al.*, 2008).

However, recently many of these stations have been closed and a gradual decline in data collection continues as a result of financial and human resource constraints (WMO and USAID, 2012). The quality of the available data is made worse by frequently missing data. Dense rain gauge networks are needed to obtain accurate estimates of areal rainfall for input into water resources estimation methods (Schulze, 2005; Cooper and Fernando, 2009). Most national meteorological services and national disaster management agencies do not have proper rainfall networks and lack the technical capacity to measure rainfall in real-time as is required to measure and/or anticipate the probable impact of rainfall (WMO and USAID, 2012). The problems are most critical in high runoff mountainous areas where point rainfall measurements display considerable spatial variability (Liechti *et al.*, 2011).

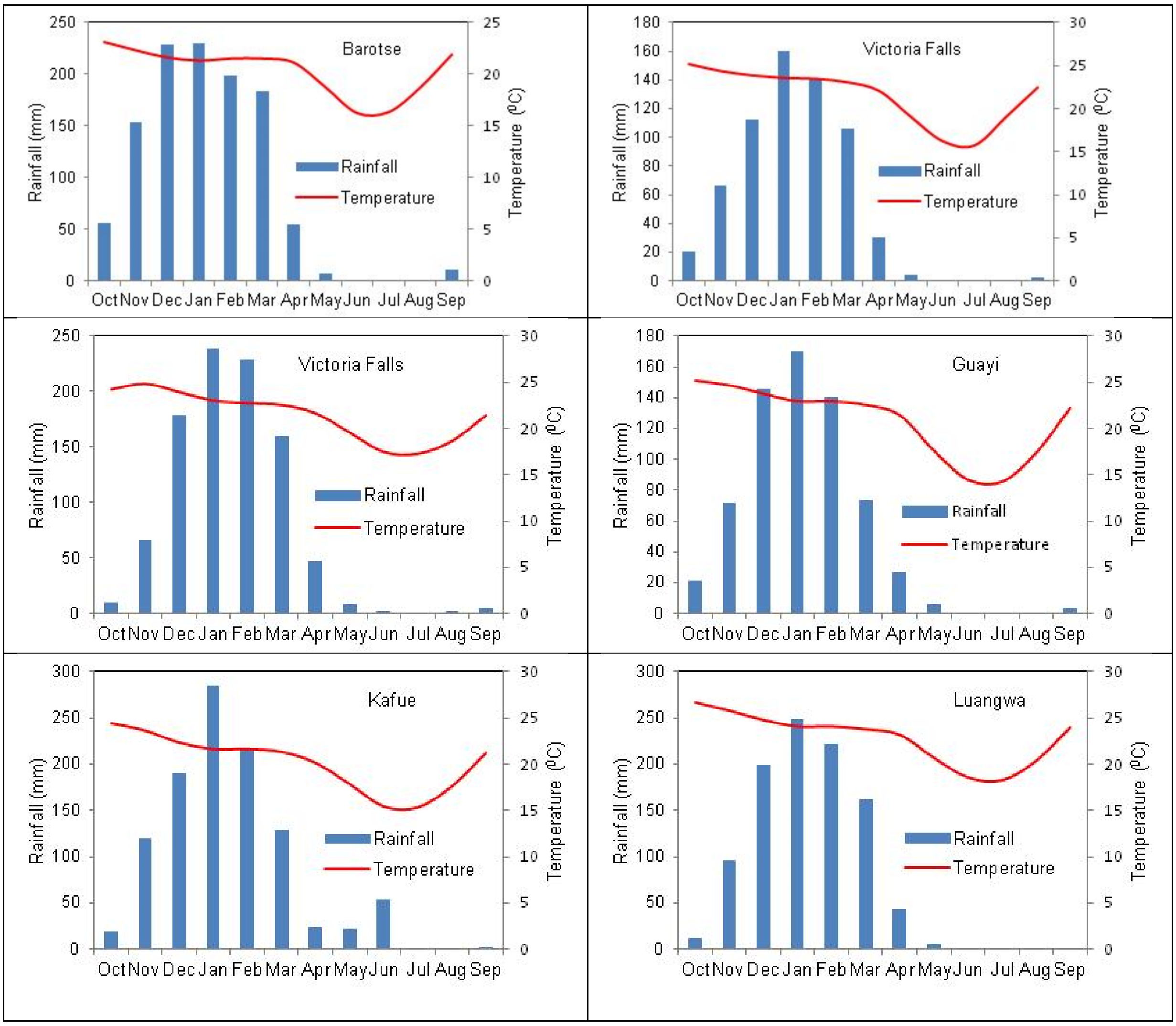

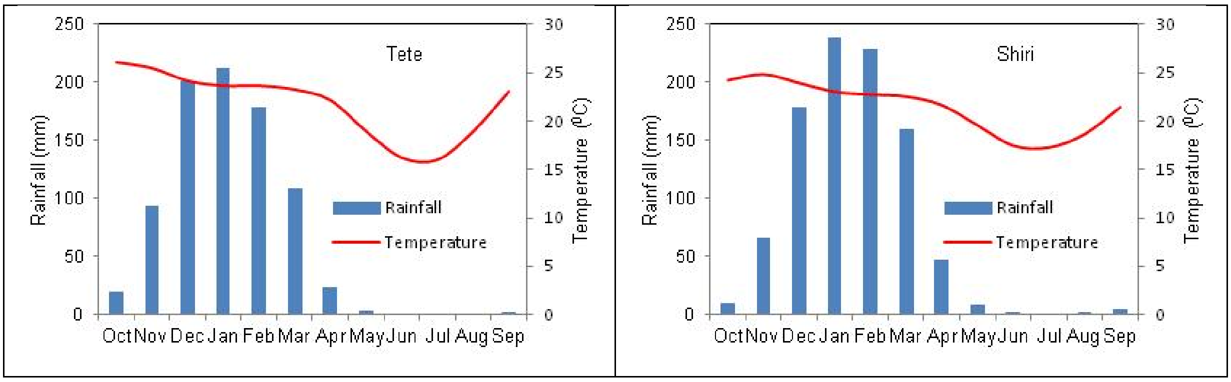

Figure 3.8: Seasonal distribution of monthly mean temperature and rainfall. Rainfall at selected locations in the Zambezi River basin, based on data for the period 1960 – 2000 (Source: IWRI, 2000)

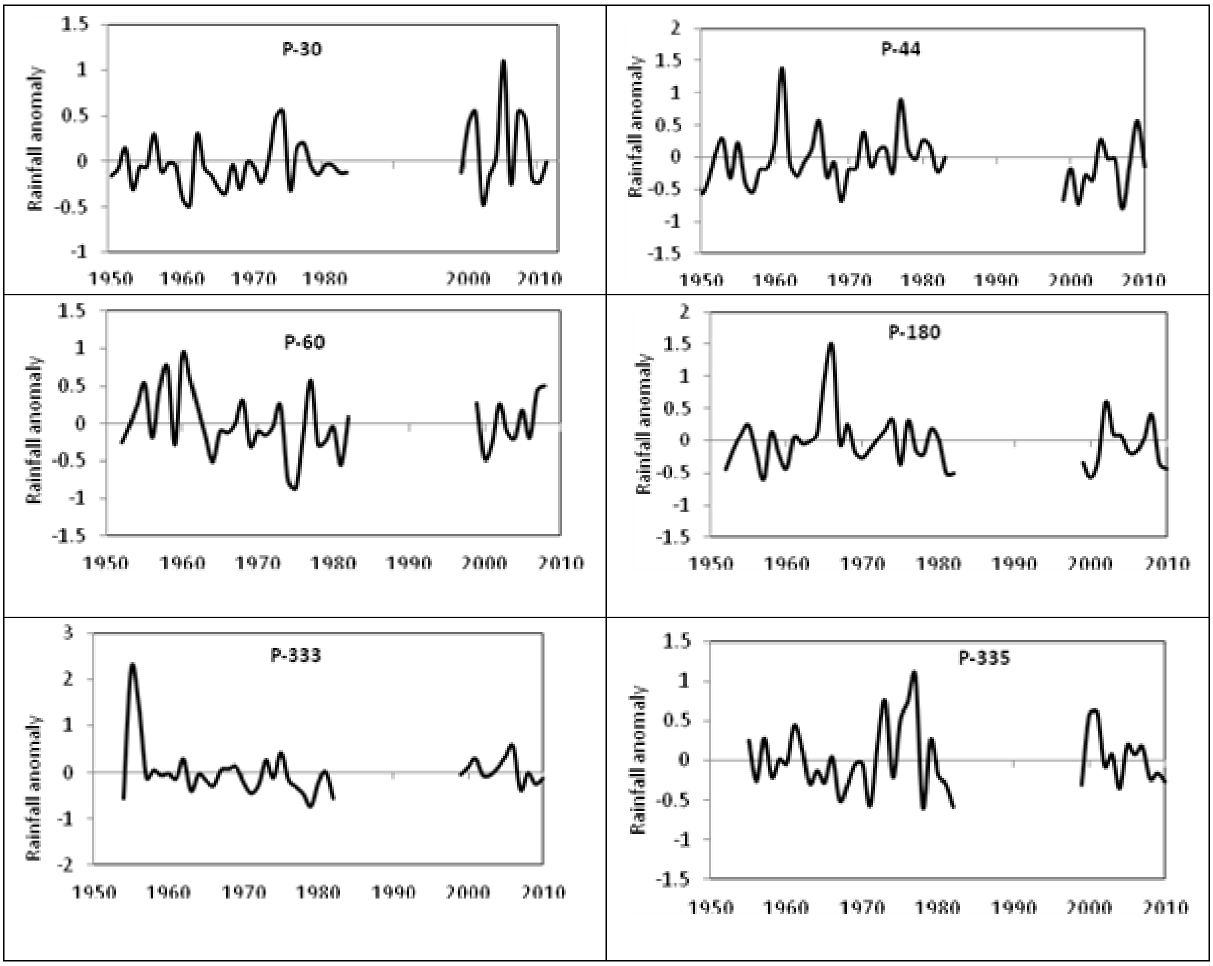

Figure 3.9: Inter-annual variability of annual rainfall in the study area using the (P-30), (P-44) (P-60), (P-180), (P-333), (P-335) rainfall stations expressed in terms of rainfall anomaly (Source: National Directory of Water Database, 2009)

3.4.2.1. Ground-based rainfall data

In many river basins around the world, the inaccessibility of rainfall data is an obstacle to water resource studies and operational monitoring. Therefore the assessment and planning of water resources, forecasting of extreme events and decision-making can be improved by access to reliable rainfall data (Asante *et al.,* 2008). In the Zambezi basin, rain gauge networks were established during colonial times and many rain gauges implemented since this period have suffered from lack of monitoring and maintenance, because of both difficulties related to political and economic situations and a lack of expertise among the riparian countries. To date, efforts are being made, in collaboration with various international agencies, to increase the capacity of information and database management of water resources in the Zambezi Basin (WMO and USAID, 2012).

One of the main objectives of this study was to assess all the sources of the available ground rainfall data for the Zambezi Basin – this data can then be used to validate and select the most appropriate satellite rainfall data for setting up models for flood forecasting within the basin. Four main sources have been identified: the Climate Explorer of the Royal Dutch Meteorological Institution (http://climexp.knmi.nl/); the Global Historical Climate Network (GHCN v. 2) (ftp://ftp.ncdc.noaa.gov/pub/data/ghcn/v2); the Climate Research Unit (CRU) (http://www.cru.uea.ac.uk/) and the database available from the National Observation Agencies (NOA). Most of these sources have the rainfall data formatted in monthly time steps. The National Observation Agencies (NOA) database of riparian countries is of high reliability, effectively a global database that contains rainfall data for the Zambezi Basin, formatted in a daily time step. In practice, the Zambezi Basin is limited in climatic data – the major challenges being the sparseness of observed data, missing values and short hydrological records. This problem has been exacerbated by deteriorating gauging networks, reduced budgets and the lack of adequate monitoring capacity within the national hydrological agencies – all issues that are partly related to the recent history of civil wars in countries like Angola in the North West (covering 18% of the total area of the Basin) and Mozambique (covering 11%) in the East. The Zambezi Water Information System (ZAMWIS), a web-based and information systems portal for the Zambezi basin, is purportedly in place but was difficult to access at the time this study was conducted. The dataset acquired consists of daily rainfall records from 1998-2008, collected at more than 50 rain gauges over the Zambezi Basin. One of the major constraints in this study was availability of the most recent data corresponding to the period of available satellite images (1998 - 2008). A strict quality control process was applied (by the Meteorological Office of each country) to check and validate rainfall extreme values. Most of the selected rain gauges have records from 1999 - 2008.

Figure 3.10 shows the spatial distribution of the selected rain gauges for the Zambezi Basin, based on the availability and reliability of the data used to evaluate the satellite data. Spatial and temporal characteristics of these gauging sites are presented in Table 3.1.

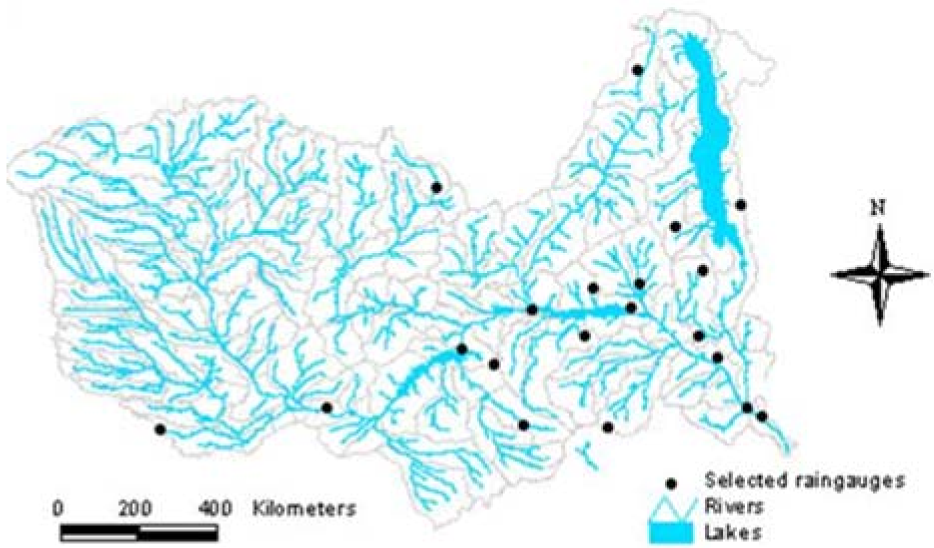

Figure 3.10: Location of the existing and selected rain gauge network in the Zambezi Basin (Sources: National Directory of Water Database, 2012; WMO and USAID, 2012)

The observed daily rainfall data in the Mozambican section of the Zambezi Basin are collected by the *Administração Regional de Aguas do Zambeze (ARA-Zambeze)* and the National Directorate of Water (DNA). In other riparian countries (such as Zimbabwe, Zambia and Malawi) rainfall data are collected by District meteorological stations that are run and maintained by the Provincial Meteorological Office. Each province also has several registered volunteer observation stations (collaborating stations) that collect daily rainfall. Usually a hard copy of all the collected data is regularly sent to the central headquarters of the Meteorological Service in the capital of each country. The data are then computerised, verified and archived. For the Upper Zambezi, three stations (one located in the Kafue basin, one in the Cuando and the last one in the Zambezi before the Kariba dam) were used to represent the Upper Zambezi. In the Lower Zambezi there are 56 rain gauges – 60% of these have less than 6 years of continuous time series data and most of them do not have recent data (1998 - 2008). Rainfall stations missing at least ten days of continuous data records were omitted from the study to minimise errors or bias in analysis. As a result, only 20 (Table 3.1) of the existing rain gauges have data of reasonable quality for the period in question.

Table 3.1: A summary of the data on the rain gauges selected for the analysis

ID	Rain gauge ID	Gauge Name	Latitude	Longitude	% missing data	Mean Elevation (m)	Mean annual precipitation (mm)
1	639320	Mbeya	-8.93	33.46	5.2	2 385	1 878
2	675610	Ndola	-13	28.65	5.8	1 269	1 211
3	675860	Lilongwe	-13.78	33.77	4.9	1 218	1 008
4	677430	Belvedere	-17.83	31.07	6.4	1 460	900
5	678810	Rusape	-17.42	32.22	3.8	1 558	1 007
6	680260	Shakawe	-18.42	21.88	4.3	1 003	618
7	677610	Rukomiche	-16.13	29.39	0	1 135	795
8	677650	Monapools	-15.73	29.34	0	860	860
9	P-44	Zumbo	-15.6	34.43	0	339	695
10	P-50	Caia	-15.62	30.45	0	30	647
11	P-60	Zambue	-17.82	35.38	0	900	695
12	P-176	Doa KM 100	-15.12	30.8	0	126	854
13	P-180	Necungas KM 138	-16.18	34.4	0	280	745
14	P-218	Mopeia	-17.97	35.7	5.5	260	739
15	P-325	Songo	-15.58	32.75	0	900	881
16	P-333	Vila Mouzinho	-14.76	34.4	0	1 270	890
17	P-335	Bene	-15.06	34.26	0	950	858
18	P-786	Fingoe	-15.17	31.88	0	857	974
19	P-829	Morrumbala	-17.35	35.58	0	250	763
20	P-893	Mucumbura	-16.18	31.68	0	450	720

3.4.2.2. Satellite rainfall data

In large scale southern African river basins (such as the Zambezi Basin) a consistent platform for data collection and transmission is currently under development (WMO and USAID, 2012). Modelling the hydrology of the Zambezi Basin is a challenging task because of its size and heterogeneity, but mostly because of the lack of reliable input data for calibration (Asante *et al*., 2008; Liechti *et al*., 2011). With regard to hydrological model performance, the type and quality of the input rainfall data are considered as equally – or even more – important than the choice of the hydrological model (Shrestha *et al.,* 2008; Liechti *et al*., 2011). Satellite data is a viable option for use in data-scarce regions such as the Zambezi River Basin. However, the application of satellite derived rainfall data has not been adequately evaluated in the Zambezi River Basin (Winsemius *et al*., 2006). For most satellite rainfall products, data from two types of sensors are commonly used in the estimation algorithms – these are the Passive Microwave (PM) and the Visible and Infrared Radiance (VIS/IR).

The PM sensors identify the precipitation particles by the scattering caused by large ice particles present in the clouds (Kummerow *et al*., 1998; Xie *et al*., 2007). These sensors are installed on Earth-orbiting satellites which offer only intermittent coverage of a given region of interest (currently approximately ten observations per day). Therefore, the estimation of rainfall from proxy parameters (such as cloud top temperature which can be inferred from geo-stationary observations) has been developed (Kummerow *et al*., 1998). The algorithms based on Infrared Radiance (IR) data relate rainfall to the cloud top temperatures and cloud optical properties through a precipitation index. The indexing method assigns a fixed rain rate to each identified cloud type (Kidd, 2001). This assumption is most effective for convective conditions but can yield crude estimates because of the weak link between cloud properties and precipitation (Asante *et al*., 2008; Liechti *et al*., 2011). With the multiple products currently available (Table 3.2), it is important to evaluate their precision and uncertainty, as well as their advantages and drawbacks, before opting for a specific application. Several studies have been conducted aiming at comparing rainfall estimates derived from satellite observations against locally observed data (Demirtas *et al.,* 2005; Layberry *et al*., 2006; Winsemius *et al*., 2006).

Given that the national networks of ground-based rainfall observations are sparse in the Zambezi River Basin, the potential for using relatively easily accessible satellite rainfall products – towards improving streamflow forecasting and early warning systems in the Zambezi River Basin – was investigated. Similar work has already been done in the basin by several researchers (for example: Winsemius *et al.,* 2006; Beilfuss and Dos Santos, 2001; Beilfuss *et al*., 2009). There are several methods for correcting satellite rainfall (which are being used to derive final operational satellite rainfall datasets) that have been reported in literature (Sawunyama and Hughes, 2009; Thiemig, 2012).

A detailed evaluation of each of the sources and the methods used for all the datasets is beyond the scope of this study – reference can be made to the literature sources given in Table 3.2 for more details. In this study the focus was on the Climate Prediction Center (CPC) Rainfall Estimates product (CPC-RFE 2.0), and Tropical Rainfall Measurement Mission (TRMM 3B42). These methods were chosen for further analysis because of their spatial resolution and wider coverage in Africa. Two studies – conducted by ICIMOD and USAID (2008) (in the Hindu Kush-Himalayan Region) and Liechti *et al*. (2011) (for Southern Africa) – showed that the CPC-RFE 2.0 provided reasonable rainfall estimates when compared with the TRMM 3B42 and other satellite products – but CPC-RFE 2.0 still needed to be improved before being used for operational flood forecasting. Similar results were found in this study. Sawunyama and Hughes (2009) demonstrated that the original satellite estimates needed to be corrected, especially in areas where rainfall spatial variability is high because of topographic influences. The satellite data correction algorithm – developed by Sawunyama and Hughes (2009) at a monthly time step – and/or the Linear Interpolation Estimator (LIE) method (Morrissey *et al*., 1995) may be a valuable contribution toward introducing an integrated early warning system for the Zambezi Basin. To validate these data, both visual verification and comparisons of maps of satellite estimates with observations within the Zambezi Basin were conducted (Chapter 5).

Table 3.2: An example of available global satellite rainfall products and their temporal and spatial coverage

Product	Provider	Spatial coverage	Temporal coverage	Spatial resolution	Temporal resolution	Reference
RFE 2.0	NOAA-CPC	40°N - S, 20° W - 55°E	since 01.01.2001	0.25°	24h	Xie *et al*., 2002
TRMM 3B42 v6	NASA	50°N - S, globally	since 01.01.1998	0.50°	3h	Kummerow *et al*., 1998
PERSIANN	University of Arizona	60°N - S, globally	since 01.03.2000	0.25°	6h	Sorooshian *et al*., 2000
PERSIANN-CCS	University of Arizona	50°N - S, globally	since 01.03.2000	0.04°	0.5h	Sooroshian *et al*., 2000
CMORPH	NOAA-CPC	60°N - S, globally	since 06.12.2002	0.25°	3h	Dinku *et al*., 2008
CMORPH	NOAA-CPC	60°N - S, globally	1.1.2006 - 31.12.2008	0.08°	0.5h	Joyce *et al*., 2004

The Climate Prediction Center (CPC) Rainfall Estimates product (CPC-RFE 2.0)

The CPC-RFE 2.0 is computed by the National Oceanic and Atmospheric Administration Climatic Prediction Center (NOAA/CPC) (Herman *et al.,* 1997). The African Rainfall Estimation Algorithm Version 2 (CPC-RFE 2.0), which became operational from 1 January 2001, and integrates PM estimates is used. The output daily rainfall data is a combination of PM and IR precipitation estimates, merged with daily rain gauge data from the Global Telecommunication System (GTS) records and is available from the website ftp://ftp.cpc.ncep.noaa.gov/fews/fewsdata/africa/rfe2/bin/. The algorithm has at times, however, resulted in rare high spikes in the precipitation estimates.

The Tropical Rainfall Measuring Mission (TRMM 3B42)

The TRMM 3B42 is computed jointly by the National Aeronautics and Space Administration (NASA) and the Japan Aerospace Exploration Agency (JAXA, Kummerow *et al*., 1998). The data are available from http://disc.sci.gsfc.nasa.gov/precipitation/trmm3b42.

3.4.3. Potential evaporation estimation method and data sets

3.4.3.1. Potential evaporation estimation method

Evaporation is one of the most important fluxes in the hydrological cycle. Recently, there has been a wide interest in estimating evaporation fluxes, on both continental and global scales, for a variety of purposes (Mueller *et al*., 2011; 2013; Marshall *et al.,* 2013). According to Yates and Strzepe (1994), potential evapotranspiration (PET) is a process by which water is extracted from the soil column. The data represents the atmospheric demand for water from the Earth's surface as a function of: solar radiation; air temperature; wind; humidity and atmospheric pressure and factors like soil moisture availability and vegetation type. Actual evapotranspiration (AET) depends on the water present in the soil column. Literature reviews of regional to global scale PET modelling techniques can be found in Diak *et al.* (2004), Glenn *et al.* (2007), Jimenez *et al.* (2011) and Mueller *et al.* (2011). Among these techniques, remote sensing methods have been gaining popularity, because they do not suffer from the same scale dependencies and can readily be driven by global scale data (Oudin *et al.,* 2005; Miralles *et al.,* 2011a; b; Jimenez *et al.,* 2011).

Remote sensing based modelling techniques use near real-time visible, near infrared, and/or thermal sensor and, typically, certain amounts/types of meteorological data to estimate PET as a residual of the energy balance. The vegetation fraction, the primary control factor for PET, can be updated with readily available remote sensing data; meteorological forcing can be estimated from ground, meteorological satellite, and surface climate re-analysis data. Operational Land Surface Models (LSMs), like remote sensing based methods, provide near real-time continuous and global estimates of PET using process based techniques driven by assimilated ground, satellite and surface climate reanalysis data (Rodell *et al.,* 2004).

Because of the above, PET data (produced by remote sensing based modelling techniques) were used as input for Geospatial Stream Flow Modelling (GeoSFM) (Verdin and Klaver, 2002). The method consists of solving the Penman–Monteith model (Verdin and Klaver, 2002), which uses GIS routines to ingest grids of input variables – produced by NOAA's Global Data Assimilation System on a 11 grid for the entire globe. The dataset is compiled by using output fields from NOAA's Global Data Assimilation System (GDAS) as inputs into the Penman-Monteith equation (Equation 3.1); (Asante *et al.*, 2008; Shrestha *et al.,* 2008). NOAA's output parameters include: air temperature; fluxes of long-/short-wave radiation; atmospheric pressure; relative humidity and wind speed. The approach assumes: a hypothetical reference crop with an assumed crop height of 0.12 m; a fixed surface resistance of 70 s m^{-1} and an albedo of 0.23 (Asante *et al.*, 2008). The computation is performed at an hourly interval and aggregated to obtain a daily value of PET. However, the input fields remain constant for at least 6 hours during the computation when applying the Penman-Monteith equation (Equation 3.1) because GDAS data are updated every 6 hours.

$$PET = \sum_{t=1}^{24} \frac{1}{(\Delta+\gamma(1+0.34\mu 2))} * \left[\left(0.408\Delta(Rn-G)\right) + \left(\frac{37\gamma\mu 2(e_s-e_a)}{(T+273)}\right)\right] \qquad \textbf{Equation 3.1}$$

where *PET* is the potential evapotranspiration [mm day^{-1}]; Δ is the slope of the saturation vapour pressure [kPa $^oC^{-1}$]; γ is the psychrometric constant [kPa $^oC^{-1}$], *μ2* is the wind speed at 2 m above the ground surface [m s^{-1}], *Rn* is the net radiation [MJ m^{-2} dyr^{-1}]; *G* is the soil heat flux [MJ m^{-2} dyr^{-1}]; T is the air temperature [°C]; e_s is the saturation vapour pressure [kPa°C^{-1}] and e_a is the actual vapour pressure [kPa°C^{-1}].

The radiation and heat fluxes are generated by the GDAS model; the vapour pressure terms (γ, e_s and e_a) are computed from GDAS temperature and humidity fields. Wind fields computed by GDAS at 10 m heights are downscaled to obtain 2 m wind fields for use in the evapotranspiration computations. The resulting product has a spatial resolution of 1° by 1° and has a global spatial extent in Geographic projection (and is available for downloading by users from: http://earlywarning.usgs.gov/fews/pet/).

However, the accurate estimation of these parameters on large scales has always been a difficult (Verdin and Klaver, 2002). Direct measurements of evaporation are only possible over small regions – e.g. using flux towers – and are limited to only a few sites, particularly in certain developed regions (Oudin *et al.,* 2005; Marshall *et al.,* 2013). Conversely, most of the existing global products are verified only in those particular regions with available (and reliable) data – generally in North America and Europe (Alton *et al*., 2009; Zhang *et al*., 2010; Miralles *et al*., 2011b).

In developing countries, taking for example the Zambezi Basin, the availability and accessibility of the potential evapotranspiration data is far worse than that for the rainfall data – even recognising that PET is the second most important component of the water balance in the Zambezi River Basin after rainfall (Mazvimavi, 2003). Surface runoff (a dependent variable) from a river basin can be regarded as the by-product of two large processes: precipitation and evapotranspiration (independent variables). Using the USGS PET data, the Mean Annual Evaporation (MAE) in the Zambezi River Basin increases generally from West to South and ranges from 1 200 mm yr^{-1}, to 1 700 mm yr^{-1} (Figure 3.11).

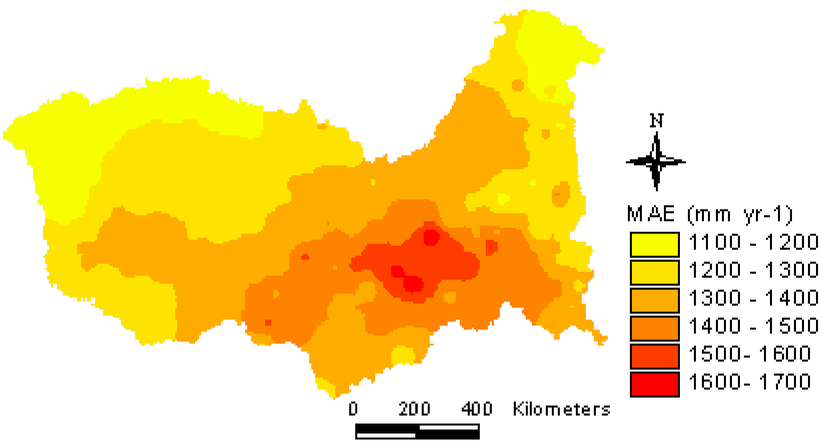

Figure 3.11: Spatial distribution of mean annual evaporation in the study area (accessed from: http://earlywarning.usgs.gov/fews/africa/**)**

3.4.3.2. Potential evaporation data sets

Potential Evaporation (PET) is a measure of the ability of the atmosphere to remove water through Evapo-Transpiration (ET) processes. The FAO introduced the definition of PET as the ET of a reference crop under optimal conditions, having the characteristics of: well-watered grass, with an assumed height of 12 centimetres; a fixed surface resistance of 70 seconds per meter and an albedo of 0.23 (Allen *et al.,* 1998). Among several equations to estimate PET, a FAO application of the Penman-Monteith equation (Allen *et al*., 1998), is currently widely considered as the standard method (Walter *et al.,* 2000). The Penman-Monteith method is predominately a physically based approach, which can be used globally because it does not require estimations of additional site-specific parameters. However, a major drawback of the FAO-PM method is its relatively high need for specific data for a variety of parameters (i.e. wind speed, relative humidity, solar radiation, etc.). These parameters are reliably observed by a limited number of meteorological stations around the globe, and are especially lacking in developing countries (Verdin and Klaver, 2002, Droogers and Allen, 2002). Table 3.3 summarises the sources of evaporation data available globally. All these global products can be extracted for Africa at a daily temporal resolution, with the exception of the MOD16 product, (a monthly product) (Mu *et al*., 2011).

Table 3.3: An example of available global evaporation products, listing the providers of the datasets and their spatial coverage and lengths of data

Product	Provider	Input precipitation data	Potential evaporation-method	Spatial resolution	Time periods of data	Reference
PCR-GlobWB	PCR-GLOBWB	ERAI + GPCP	Hargreaves	0.50°	1 Jan 1979-31 Dec 2010	van Beek and Bierkens, 2009
PCR-PM	PCR-GLOBWB	ERAI + GPCP	Penman-Monteith	0.50°	1 Jan 1979-31 Dec 2010	Hargreaves and Allen, 2003
PCR-TRMM	PCR-GLOBWB	TRMM 3B42 v6	Hargreaves	0.50°	Since 1 Jan 1998	Thiemig *et al*., 2012
PCR-Irrig	PCR-GLOBWB	ERAI + GPCP	Hargreaves	0.50°	1 Jan 1979-31 Dec 2010	Van Beek , 2011
ERAI	ECMWF	ERAI	No PE Input	0.70°	1 Jan 1979-near-real-time	Dee *et al*., 2011
ERAL	ECMWF	ERAI+GPCP	No PE Input	0.70°	1 Jan 1979-31 Dec 2010	Balsamo *et al*., 2012
MOD16	University of Montana	NASA's GMO	Penman-Monteith	1.00°	Since 1 Jan 2000	Mu *et al*., 2011, 2007
GLEAM	VU Amsterdam	PERSIANN	Priestley and Taylor	0.25°	Since 1 Jan 1998	Miralles *et al*., 2011a,b
USGS-PET	USGS	CPC-RFE	Penman-Monteith	1°	Since 1 Jan 1998	Verdin and Klaver, 2002

From this information, it can be seen that the potential evaporation data is primarily derived using the Penman–Monteith and Hargreaves equations. A study conducted by Trambauer *et al.* (2014), aiming at comparing different evaporation estimates over the African continent, demonstrated that potential evaporation derived from the Penman–Monteith and Hargreaves equations resulted in very similar values throughout the continent. The small differences between the two methods are because of their different formulations and the greater number of input parameters that the Penman-Monteith requires (Section 3.4.3.1) when compared with the more simplified Hargreaves method (Oudin *et al.,* 2005; Senay *et al.*, 2007; Trambauer *et al.*, 2014). Furthermore, Trambauer *et al.* (2014) reported that, in general, the differences between evaporation products is much smaller in humid areas than in arid areas – where the MOD16 product is commonly 20–30% higher. This difference is probably primarily because of the difference in temperature data sets used in the estimates.

3.5. Streamflow characteristics

3.5.1. Flow measurement infrastructure

An ungauged basin is defined as the one with inadequate data to support the understanding of the basin's hydrological processes and enable predictions. However, in the past two decades there has been a serious decline in global streamflow monitoring infrastructures, particularly in the developing countries – because of the lack of finance and civil wars – which, in turn, are the countries most vulnerable to changes in water quantity and hazard characteristics (Asante *et al*., 2008).

In the Zambezi Basin, most National Hydrological Services (NHS's) of the eight riparian states do not have proper flow data collection networks and technical capacity to record hydrological data in real-time (EU and SADC, 2002; WMO and USAID, 2012). Very few local hydro-stations have the ability to collect suitable flow data measurements and thereby issue early warning notices against devastating events. The majority of these flow data collection sites are located in Kafue in Zambia, Mazoe and Sanyati in Zimbabwe. In Mozambique, downstream of Cahora Bassa dam, there are only four (4) flow data collection sites for flow measurement. Most of measurement sites available during colonial times were destroyed during civil war which lasted from 1977 to 1994. Table 3.4 shows the number of existing flow measurement stations, with different lengths of recorded flow data, within the riparian countries. An effort has been made by the SADC to establish a Hydrological Cycle Observing System (HYCOS), and to install telemetric stations in all the riparian countries of the Zambezi Basin. Currently the system is working in Malawi, Namibia, Tanzania, Zambia, and Zimbabwe and provides real-time data and information on the Zambezi River and its tributaries. However, in other countries, the SADC-HYCOS regional network is not yet complete. 79% of existing stations are experiencing operational problems in collecting and transmitting real-time data (WMO and USAID, 2012). Operation and maintenance of these stations are the responsibility of each country. Because of financial constraints; the lack of training and experienced personnel; and the lack of local technological support (to provide spare parts, field service and programming); the countries do not have the capacity to continue operating and maintaining the network. At most of the stations, staff members manually collect and transmit data and information to the National Hydrological Services (NHS's). Data are also retrieved during periodic data collection trips to the gauge sites. Other sources of data are the Zambezi Water Information System (ZAMWIS), a web-based and information systems portal for the Zambezi basin, Flow Regime in Experimental and Network Data (FRIEND) and the Global Runoff Data Centre (GRDC). Although FRIEND data are not available after 1994, the ZAMWIS and GRDC were purportedly in place but both were difficult to access at the time this study was conducted.

One of the main objectives of this study has been to assess all the available hydrological data for the Zambezi Basin suitable for use to set up models for hydrological flood control in the basin. Given the issue of data paucity in Southern Africa, only a few streamflow gauging stations in the Zambezi Basin have data of reasonable quality and time series length. For example, advice was sought from the *Administração Regional de Aguas do Zambeze (ARA-Zambeze*) office in Tete for identifying flow measuring stations with reasonable flow data. Normally, *ARA-Zambeze* should have, for each station, a file documenting the maintenance of the station and, most importantly, a rating curve.

Table 3.4: Existing flow measurement stations and collected data. (H) is water level (m) and Q is streamflow (m^3 s^{-1}) and measurement type and *N/I* = Non-Information (Source: WMO and USAID, 2012)

Id	Country	Station No.	Data availability		Data Type	Measuring
			1900 - 1998	1998 - 2010		
1	Angola	3	*N/I*	*N/I*	H,Q	Natural Control and Weir
2	Botswana	14	*N/I*	*N/I*	H,Q	Natural Control and Weir
3	Malawi	16	*N/I*	*N/I*	H,Q	Natural Control and Weir
4	Mozambique	102	6	4	H, and H,Q	Bridge piers and Natural Control
5	Namibia	*N/I*	*N/I*	*N/I*	H, and H,Q	Natural Control and Weir
6	Tanzania	45	45	0	H, and H,Q	Bridge piers and Natural Control
7	Zambia	180	175	5	H, H,Q, H. Sediment and H,H. Sediment	Natural Control and Weir
8	Zimbabwe	381	317	64	H,Q	GP on Dam, Natural Control, Parched flume, Recording on Dam wall and Weir
Total	**-**	**741**	**543**	**69**	**-**	**-**

However, not all existing flow gauges had accurate and reliable flow rating curves. Of the 36 stations in the Lower Zambezi, only four (4) stations have rating curves. Figure 3.12 shows the four rating curves that were deemed unreliable. The rating curves used in the Lower Zambezi are relatively sensitive to changes in cross section width and depth during the high and low flows, which means that the use of these rating curves needs to take into consideration the uncertainty associated with observed streamflow information. It is essential for the streamflow data to be carefully assessed (for errors, upstream development effects and possible non-stationary factors) before the data are used in the model. In this study an assessment of the consistency of the observed data was done through analytical checking of the historical maximum observed flood data from the *ARA-Zambeze* records. These checks were performed on the higher resolution daily data, rather than the aggregated monthly streamflow volumes. Because of the uncertainties with the rating curves for the selected sites, a hydraulic model, developed at Rhodes University in 2011, was used to correct the rating curves, using the relationship between channel width and maximum channel depth. The channel widths were estimated from Google Earth and the maximal channel depth from DNA historical record data base. A detailed explanation of this process is presented in this study in Chapter 4 (Section 4.6.1).

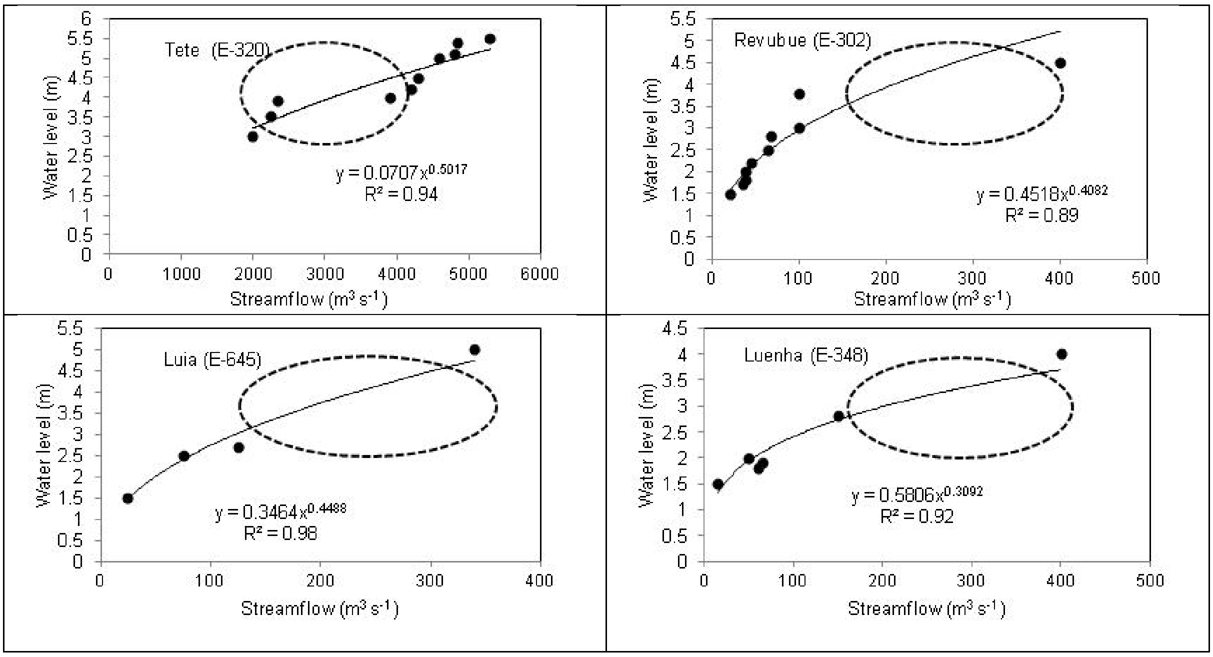

Figure 3.12: Inadequacies of rating curves of hydrometric stations at Lower Zambezi (Source: *ARA-Zambeze* database, 2010)

The observed streamflow records were obtained from the National Directorate of Water database and *Hidroeletrica de Cahora Bassa* in Mozambique, and the Zambezi Water Authority in Zambia and Zimbabwe. Most of the stations have long periods of missing data for the period of analysis. The other stations (Figure 3.13) only have reasonably good data quality, with no missing data, spanning the 11 years between 1998 to 2008. It is important to recognise that most of the observed streamflows are regulated from three hydropower dams: Kariba, Kafue Gorge and Cahora Bassa. Eleven (11) sites were selected to carry out model calibration and validation based on historical observations in the Zambezi Basin (Figure 3.13 and Table 3.5). The Kariba and the Cahora Bassa observed water levels were also used for comparison with the simulated water level from the MIKE BASIN reservoir model for the period 1998 to 2008.

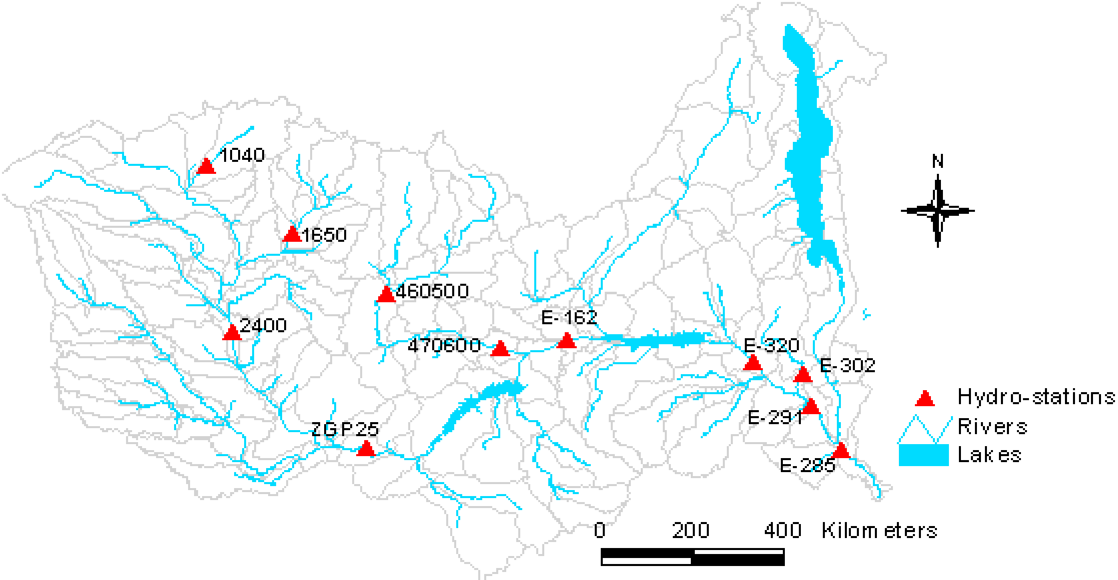

Figure 3.13: Streamflow gauging stations used for model calibration (Source: National Directory of Water Data base, 2012)

Sawunyama (2008) considered three main factors that can affect the use of observed data for assessing outputs from hydrological models: (i) poorly defined artificial upstream influences (upstream reservoir storage, dynamic patterns of abstractions, return flows and land use modifications notably commercial afforestation); (ii) gauge inaccuracies (particularly in the low flow parts of hydrographs) and (iii) the inability of particular gauging structures to measure flows above certain thresholds. In the case of the Lower Zambezi, the liberation, civil war (1977-1994) and the inability of the structures to measure high flows during flooding events, were found to be the major limiting factors of the data set. The majority of the observed streamflow data in the Lower Zambezi reflects anthropogenic influences on the main river.

Table 3.5: Characteristics of streamflow gauging stations selected for calibration in the Zambezi Basin (Source: National Directory of Water Database, 2012)

ID	Sub-basin Name	Station	Location		Area (Km^2)	Data availability	1998 - 2008		CV (%)
			Latitude	Longitude			Daily Mean streamflow (m^3s^{-1})	Daily Maximum streamflow ($m^3 s^{-1}$)	
1	Luanginga	1040	-11.23	24.22	24 484	2000-2005	-	-	-
2	Kabompo	1650	-13.6	24.3	42 740	2000-2005	-	-	-
3	Barotse	2400	-16.1	23.16	4 749	1998-2001	-	-	-

ID	Sub-basin Name	Station	Location		Area (Km^2)	Data availability	1998 - 2008		CV (%)
			Latitude	Longitude			Daily Mean streamflow (m^{3}s^{-1})	Daily Maximum streamflow (m^3 s^{-1})	
4	Victoria Falls	ZGP25	-17.9	25.85	56 878	1998-2008	1 085.2	4 567.9	94
5	Lupata	E-162	-15.74	29.68	6 290	1998-2008	1 960.89	18 859.9	93
6	Kafue-Hook at Bridge	460500	-15.74	29.68	6 990	1998-2008	236.3	1 473.85	93
7	Kafue-Gorge	470800	-15.74	29.68	20 420	1998-2008	253.8	1 085.9	76
8	Tete	E-320	-16.2	35.58	9 649	1951-2008	1 938.2	11 492.9	65
9	Revubue	E-302	-17.01	34.78	19 402	2000-2008	-	-	-
10	Caia	E-291	-17.8	34.02	9 904	1998-2008	2 747.8	13 586.6	71
11	Marromeu	E-285	-15.6	34.79	5 316	1991-2008	3 383.8	10 897	50

3.5.2. Seasonal distributions

The Zambezi River Basin system is composed of eleven main tributaries (Section 3.2) that drain the primary basins into the downstream basin of the Zambezi River. Figure 3.14 shows the mean daily distribution of the streamflow for selected parts of the Zambezi Basin. The mean daily streamflow distribution in the northern part of the basin is different from that of the southern part of the basin. These streamflow patterns are essentially driven by the rainfall pattern over the basin.

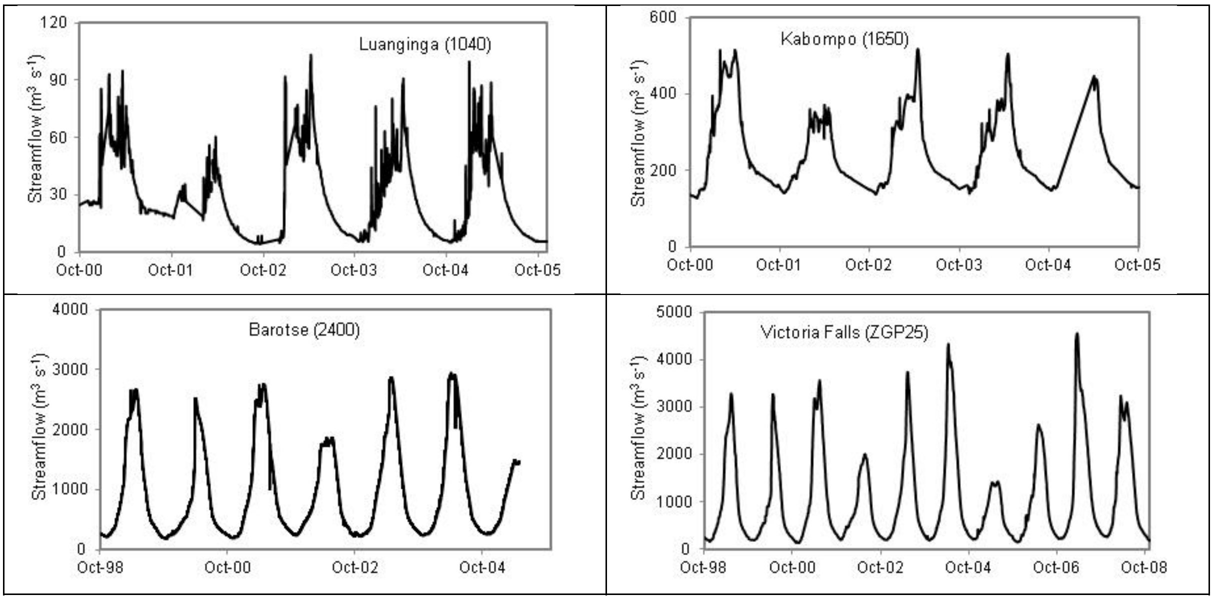

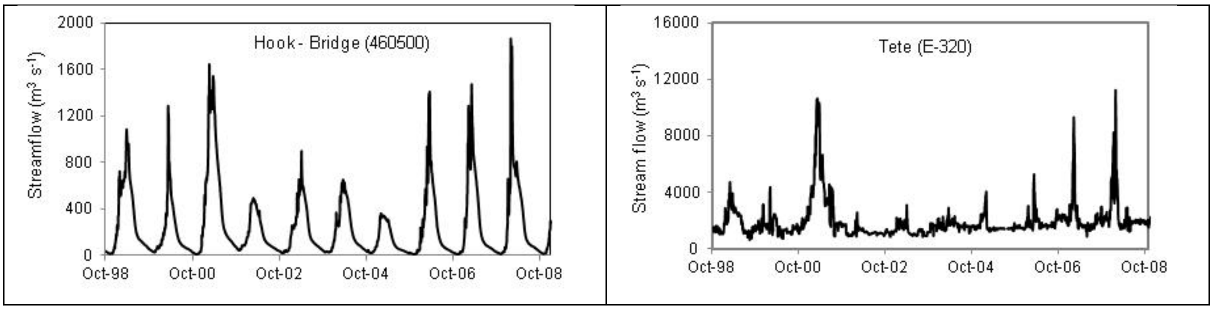

Figure 3.14: Sample of available mean daily streamflow using daily streamflow with reasonable good quality data at Upper (Luanginga (1040), Kabompo (1650) and Barotse (2400); Middle (Victoria Falls (ZGP25) and Hook-Bridge (460500)) and Lower Zambezi at Tete (E-320)

General observations on river streamflow indicate that the streamflow peaks on different days, moving from upstream to downstream. These streamflow variations can be attributed to the basin storage and attenuation effects, which tend to increase from upstream to downstream. For example, Beilfuss and Dos Santos (2001) stated that the attenuation effect of the Barotse floodplain results in a delay of the runoff of 4 to 6 weeks and the peak discharge only reaches the catchment outlet in April or early May (instead of in February/March – as would be expected in most parts of the north-western parts of the basin). It is also known that the presence of wetlands and other storage (such as the Kafue Flats floodplain area) delay the response for each sub-basin and these factors would need to be taken into account when analysing the final results. Upstream impacts, particularly those from human activities, have great potential for impacting the downstream streamflows – if future developments are to be sustainable, it is necessary to know how the hydrological regime can be affected by climatic and non-climatic changes (such as land use changes) (Tilmant *et al*., 2010). Tirivarombo (2012), for example, evaluated the percentage of change in river streamflow over the Zambezi Basin, at monthly time step between the periods 1931 - 60 and 1961 - 90, and demonstrated that the change in streamflow varies from 1 to 19%, increasing from upstream to downstream.

Apart from rainfall streamflow is also impacted by the reservoir regulation. Bain *et al.* (1998) considered that the streamflow is regulated when it is being managed to achieve various goals – for example, for maintaining a minimum flow downstream of a reservoir or for maintaining a minimum depth for shipping. This regulation of streamflow is in contrast to a natural streamflow, which refers to a river's naturally occurring changes in water flow through the course of the year. Many regulated streams are characterised by high variable and unpredictable flow regimes (Bain *et al*., 1998). Traditionally the Zambezi River has had a highly seasonal flow, with a clear low flow in winter and a high flood-inducing flow in summer (Beilfuss and Dos Santos, 2001). The Cahora Bassa dam has changed this through releasing stored water for power generation during the dry season and using the high flood inducing summer streamflows to fill the reservoir in preparation for the low winter flows. Even though the Kariba dam is also on the Zambezi, the flow pattern entering the Cahora Bassa reservoir is seasonal – unlike its releases which are regulated and constant. The lower Zambezi no longer follows the natural flooding regime with the floodplains remaining dry throughout the hot summer in all but the wettest years. There are several large reservoirs which impact on the seasonal streamflow variation. Among these reservoirs, the Kariba dam between Zambia and Zimbabwe, and Cahora Bassa dam in Mozambique are both very large dams developed primarily for hydropower generation.

Kariba is a double curvature concrete arch dam with height of 617 m, with a storage capacity of 185 000 m^3x10^6. The length of the reservoir is 280 km, with the minimum and maximum operating levels of 475.50 m and 487.8 m respectively. It is the second largest reservoir in Africa (and one of the largest in the world). It was commissioned in 1957. It has a gated spillway with a discharge capacity of 9 500 m^3 s^{-1} – however in many years/instances the spillway gates remain closed (DNA, 2014). It is only in years of very high flow that releases need to be made. Other large upstream storages are the Ithezi-Tezhi , Kafue and Lunsemfwa dams on the Kafue River in Zambia, the Mulungushi dam (also in Zambia), and the Manyame, Masvikadei, Sebakwe and Chivero dams in Zimbabwe – all of which are in excess of 200 m^3 x 10^6 (Beilfuss and Dos Santos, 2001; Mwelwa, 2004). Within Mozambique, the Cahora Bassa dam, commissioned in 1976, has a gross storage capacity of 65 000 m^3x10^6. At Full Supply Level the impoundment extends up the river approximately 270 km, virtually to the border with Zimbabwe and Zambia. The Cahora Bassa is a double-arch dam 170 m high, with a crest length of 303 m. Releases are made through up to eight large radial gates. The design capacity of the outlet works are 16 250 m^3 s^{-1}, at a maximum water level of 329 m. Normal Full Supply Level is 326 m.

The important regulating effect of Lake Malawi deserves mention. Lake Malawi has a storage capacity of approximately 8 400 000 m^3x10^6, and is larger than any man-made reservoir. The flows along the Shire River downstream are substantially mitigated by this huge natural storage. Kariba and Cahora Bassa Dams have an important flood mitigation effect on floods downstream, therefore because of limitations on time and resources only two artificial reservoirs (Kariba and Cahora Bassa) were analysed for their impact on downstream floods. However, this study recognises that there are other reservoirs which can produce relatively rapid rises in river streamflows, typically superimposed on a larger steadier streamflow from the regulated upstream sub-basins. Then, if the operations of the Kariba and Cahora Bassa dams in the Upper Zambezi Basin are integrated with other systems in the river basin, this study believes that it may be possible further mitigate flooding downstream.

3.6. Selection of sub-basins for GeoSFM calibration

In this study, the sub-basins were generated from the analysis of topography in GeoSFM (Section 4.3.1).The selected sub-basins for modelling performance testing, was based on the location of the main rainfall and streamflow sites and the importance of each site for flood monitoring and forecasting in the Zambezi Basin, are shown in Figure 3.15. The selected gauging stations are representative of the main drainage systems of the Zambezi Basin. Each sub-basin was assigned an ID number for reference purposes (Figure 3.15) – Luanginga (54), Kabompo (100), Barotse (148), Victoria Falls (227), Kafue-Hook at Bridge (136), Kafue-Gorge (169) Lupata (162), Tete (180), Caia (205), Revubue (144) and Marromeu (235).

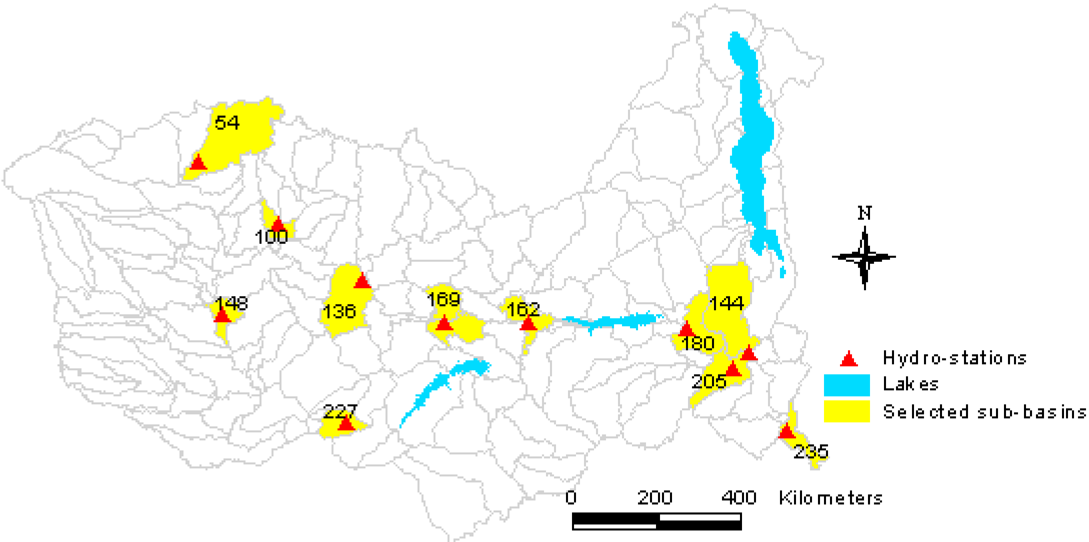

Figure 3.15: Selected sub-basins based on the location of the main rainfall and streamflow sites

While the general physical basin characteristics of the various sub-basin areas are described in detail in Sections 3.1 to 3.5, below is a brief outline of the physical basin characteristics which were used to inform the initial parameter ranges for each of the selected sub-basins and for ungauged sub-basins in the Zambezi Basin from Upper Zambezi to Lower Zambezi. Knowing the initial parameter ranges is an important stage to inform the lower and higher parameters' values, to which the model may be calibrated (Section 6.2).

Upper Zambezi and Barotse

The Upper Zambezi and Barotse drainage area includes the Kabompo, Luanginga, Lungue Bungo, Cuando and all areas upstream. The region is a flat plateau at an elevation of approximately 900 m. The area is characterised by high mean annual rainfall of 1 200 mm (mainly occurring in the rainy season from October to May), and the headwaters rise on the higher ground to the North. A flood moves down the river reaching a flat region, composed of Kalahari sands, approximately 500 km wide. High values of the soil moisture holding capacity

(SoilWHC) (to reflect the high storage capacity of the deep sand soils) are assigned and the initial parameters range between 100 and 280 mm m^{-1}. The Cuando drainage flows through Angola and Namibia's Caprivi Strip into the Linyanti Swamp on the Northern border of Botswana. Below the swamp, the river is initially called the Linyanti River, and further east it is known as the Chobe River, before it flows into the Zambezi River. The area is characterised by elevations ranging from about 700 to 1 600 m above mean sea level (amsl). The mean annual rainfall in the upper reaches of each sub-basin is above 1 100 mm and below 600 mm in the downstream areas. High values of the soil moisture holding capacity (SoilWHC) that reflect the high storage capacity of the deep sands soils are assigned and the initial parameters range between 150 and 250 mm m^{-1}. The Victoria Falls and Lupata drainage includes all areas downstream of the Barotse, after the confluence with Cuando, together discharging directly into the Kariba dam. The area is characterised by elevations ranging from about 500 to 1 400 m amsl. The mean annual rainfall in the upper reaches of each sub-basin is above 900 mm. High values of the soil moisture holding capacity (SoilWHC) that reflect the high storage capacity of the deep sands are assigned and the initial parameters range between 110 and 250 mm m^{-1}. In general the land cover and land use in the Barotse, Cuando and Upper Zambezi regions, are mainly savanna, small village settlements and subsistence farming, with minimal developmental activities, which have resulted in almost no water withdrawals in this part of the basin (Tirivarombo, 2012).

Kafue and Luangwa

The sub-basins considered under the Kafue basin (whose outlet is at Kafue-Hook Bridge) includes the Lufwanyama, Luswishi, Lunga sub-basins and the Lukanga swamps and Kafue Gorge in the Lupata sub-basin. The Kafue basin has an elevation extending from 1 700 m amsl in the middle of the sub-basin down to 400 m amsl in the low-lying Kafue flats area and the downstream sub-areas. It receives a mean annual rainfall ranging from 700 to 1 000 mm. The soils are well drained, moderately deep to deep sandy soils which have high soil moisture holding capacity. The Luangwa River is one of the major tributaries of the Zambezi River, and one of the four biggest rivers in Zambia (Sheila, 2000). The main tributaries of the Luangwa are the Lukusashi and the Lunsemfwa and the river generally floods in the rainy season (December to March); flow decreases considerably in the dry season (Nyambe and Feilber, 2007). In its lower reaches the Luangwa meets the Lupata River before draining into Cahora Bassa dam. Along the Luangwa the elevation ranges from 2 000 m amsl in the North of the sub-basin down to 300 m amsl downstream of the sub-basin. The Luangwa drainage system receives a mean annual rainfall of between 700 and 1 000 mm. The initial SoilWHC ranges from 110 to 180 mm m^{-1}. The land cover and land use in Kafue and Luangwa are mainly miombo woodland, dry ever-green forests, many large lakes, and vast floodplains. There are commercial plantations in Kafue, and the largest of these is the Nakambala Sugar Estate.

Lake Kariba

The sub-basins considered under the Lake Kariba drainage area include Gwai, Mupfure, and Sanyati. There is a wide variation in topography which extends from approximately 1 600 m amsl in the southernmost areas to approximately 400 m amsl, both in the area dominated by Lake Kariba and downstream of the Lake. The drainage area receives rainfall with mean annual values between 500 and 900 mm. The drainage area has moderately deep Kalahari Sands which suggest moderate SoilWHC values ranging between 100 and 150 mm m^{-1}. This sub-basin is dominated by dense natural vegetation (for conservation purposes) implying high infiltration capacity.

Lower Zambezi

The Tete, Caia and Marromeu drainage area is located downstream of Cahora Bassa dam. The sub-basins considered under the drainage area include the Luia, Revubue and Shire at the left river bank of main Zambezi River in Mozambique and Mazoe in the right river bank in Zimbabwe, before the river ends in the Zambezi Delta in Marromeu. There is a wide variation in topography which extends from approximately 2 400 m amsl in the Northern and, in the southernmost areas, down to 0 m amsl in the area dominated by floodplains downstream of Tete. The region experiences a mean annual rainfall between 600 to 900 mm. The soils are generally coarse-grained sands, characterised by shallow to moderately deep sandy clays, with low to high soil water capacity. The majority of the drainage area is covered by woodland and savanna, interspersed with grasslands and wetlands where soil drainage is poor. These sub-basins are the most prone to flooding.

Lake Malawi and Shire

The Shire River is located in Malawi and Mozambique and forms the outlet of Lake Malawi. The altitude varies from 30 to 3 000 m amsl. The steep slopes suggest high streamflow velocity ranging between 0.8 and 1.5 m s^{-1}. The initial SoilWHC parameter range (30 to 180 mm m^{-1}) reflects the low and moderately deep sandy loams soils that are dominant in the sub-basin. High mean annual rainfall is observed at the North end of the Lake which receives between 900 to 1 000 mm. Most of the gauging stations in the Lake Malawi sub-basin, including the Shire River, have very poor data.

3.7. Summary of datasets

The datasets used in this study are: ground and satellite rainfall; potential evapotranspiration; observed streamflow and stage; basin physical property (soils, vegetation, and topography); and reservoir characteristics (rule curve, minimal and maximal operation level and flood control level). Data on infrastructure (schools, hospitals and Villages) were also used to quantify the impact of flooding downstream of Cahora Bassa dam. SRTM 90m Digital Elevation, was used to produce flood maps and was obtained from the National Cartography and Remote Sensing Center of Mozambique. Finally, the satellite image captured on 03/03/2001 (and obtained from the Famine Early Warning System Network) was used to assess the performance of the integrated model.

3.8. Summary

This chapter has presented the background of the study area, data collection and processing approaches and the summary of the methodology set up to derive catchment, physical, hydrologic and hydraulic statistics from Earth Observation (EO) data. It provides an explanation of the assumptions used for modelling integration and an explanation of the existing water resources and flood management system within the Zambezi Basin. The strength and weakness of the models, the main challenges in setting up an operational hydro metrological network to allow the implementation of an effective and integrated early warning system in the Zambezi Basin are also discussed. The chapter also reviews the existing opportunities for the riparian states to cooperate by applying existing water resource management tools (such as the SADC Protocol and Zambezi Joint Technical Commission). Chapter 3 also summarises the methods followed for flood mapping and impact assessment. Data analysis shows that there is high temporal and spatial variability in climatic and the physiographic properties of the Zambezi Basin, which reflects the variability of processes occurring at the various spatial scales in the basin. The lack of observed data (data essential to the implementation of an effective and integrated early warning system in the Zambezi Basin) remains a major constraint. Flood management has been the most critical issue in the Zambezi basin but little has been done in terms of actual implementation – except in Lower Zambezi where there has been some testing of experiential flood management measures which have not been integrated with releases from the Kariba, Cahora Bassa and Kafue system dams.

4. APPLICATION OF THE GEOSPATIAL STREAMFLOW AND MIKE BASIN MODELS

4.1. Introduction

This chapter provides an overview of the modelling approach used to simulate basin hydrology and the flood mapping methods applied for the assessment of the impact of different levels of flooding on the Lower Zambezi. Two models were used in this study, one for rainfall-runoff and the second for reservoir simulation. The rainfall-runoff model was the Geospatial Streamflow Model (GeoSFM); and the reservoir model was the MIKE BASIN.

The selection of a rainfall-runoff model was taken into consideration that most of the sub-basins in the Zambezi Basin are ungauged, and the rainfall-runoff model selected within the study should comply with the following requirements:

(a) produce reliable results in terms of streamflow compatible with the reservoir manager requirements;

(b) be as simple as possible, thereby maintaining continuity with the existing modelling tools of the project customers;

(c) require a large amount of input data;

(d) be easy to use, understand and implement; and

(e) be capable of using the information brought by soil moisture data derived from earth observation data.

From among the existing rainfall-runoff models, ranging from purely mathematical (black box) to complex physical methods, GeoSFM was selected (because of lack of available physical data and because the model allows the use of remote sensing data).

The GeoSFM was used in this study to simulate the daily streamflow to feed the MIKE BASIN reservoir model, with the intention to optimise the operation of the Kariba and Cahora Bassa dams. GeoSFM is a physically-based, semi-distributed hydrological model developed by the United States Geological Survey (USGS) in 2001. The model simulates the dynamics of runoff processes using remotely sensed and other global datasets.

MIKE BASIN (Section 4.4) is a quasi-steady-state mass balance modelling tool for integrated river basin modelling and management, developed by the Denmark Hydraulic Institute (DHI) in 2003 (DHI, 2010). The simulation time step can be any positive time span, ranging from a second to a month. Because of the need for integration with the GeoSFM model, the MIKE BASIN for the Zambezi Basin was run at a daily time step for the entire Zambezi Basin. MIKE

BASIN was chosen since its conceptual structure accommodated the multi-purpose, interconnected reservoir systems. It was fed through the cumulative streamflow for the entire Zambezi Basin, routed by calibrated GeoSFM and then used for optimising the Kariba and Cahora Bassa reservoir operations.

These linked models were adopted for implementation in the Zambezi Basin because both have been demonstrated (and documented) in previous studies (Artan *et al*., 2002; Asante *et al.,* 2008; Shrestha *et al*., 2008; DHI and Aurecon, 2011). These studies found the models to be robust enough for supporting raster operations of large amounts of data and the selection of these models was decided by the following needs: to establish a common visual environment for topographic analysis; geospatial data processing; time series manipulation and the presentation of results in a simple integrated system tool.

4.2. GeoSFM conceptual structure

The conceptual representations of the GeoSFM processes involved are the logical (i.e. conditional) and mathematical expressions that describe the hydrological processes occurring within streamflow events (USGS, 2000a). The logical expressions are related to retrieval, classification, measurement, overlaying, neighbourhood and connectivity operations used to perform the terrain analysis for flow routing, quantifying basin characteristics and the generation of rainfall and evaporation files.

The mathematical expressions require the equations and functions applied to be able to calculate the soil water balance and streamflows (USGS, 2000a; Artan *et al.*, 2001; 2002; USGS, 2002). The main structure of the processes within GeoSFM is shown in Figure 4.1.

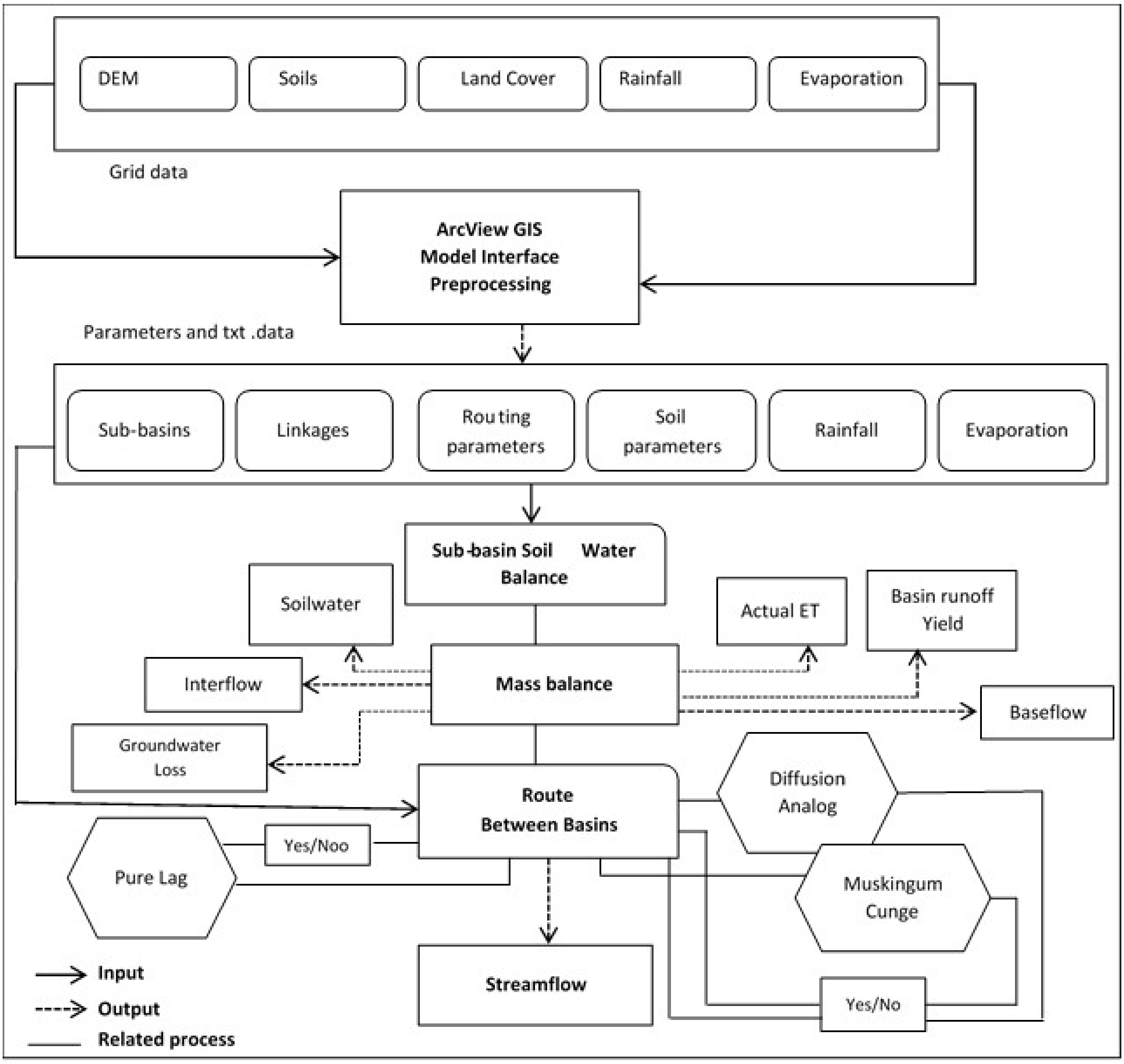

Figure 4.1: Main structure of the Geospatial Streamflow Flow Modelling (Source: Asante *et al.*, 2007a)

4.2.1. Physical parameters in GeoSFM

In the pre-processing, the basin was subdivided into several sub-basins based on the Digital Elevation Model (DEM) data. The characteristics generated by the topographical and terrain analysis routine are presented in Table 4.1. The topographic parameters were used by GeoSFM during the water balance and routing phase.

Table 4.1: Basin characteristics derived from the topographical and terrain analysis routine in GeoSFM

Grids	Description	Unit
Flow Direction	Flow Directorate grid consists of numeric values assigned using the eight Directorate pour point model. Each cell is assigned one of eight compass Directorates	cell
Flow Accumulation	Flow accumulation grid defines the number of contributing cells draining into each cell. Values range from 0 at topographic highs to large numbers at the mouths of rivers	Number of cells
Slope	Hill slope grid describes the maximum change in elevation between each cell and its eight neighbours	%
Basins	Sub-basin grid assigns a unique ID value to each sub-basin	
Flow Length	Downstream flow length grid defines the distance from the cell to the basin outlet	m
Streams	Stream grid defines stream cells. Value 1 = stream, No data = land	-
Stream Links	Stream link grid assigns a unique value to each stream ID	-
Outlets	Outlet grid defines number of outlets; one outlet per sub-basin, each outlet assigned a unique value	-
Hill Length	Hill length grid defines distance to stream, from cell to nearest stream	m
Downstream	Downstream grid assigns a unique ID number of the sub-basin immediately downstream	-
Big Basins	Basin boundary polygon	-
Basin Polygon's	Shape file defining all sub-basins with unique ID and Grid codes	-
River Line	Shape file defining streams with unique IDs, grid codes and from node and to node	-

The response of a river basin to a rainfall event depends on the nature and condition of the underlying soils (Artan *et al*., 2002; Wilk *et al.,* 2006; Shrestha *et al*., 2008). The global Digital Soil Map of the World (DSMW, FAO, 1995), at a scale of 1:5 000 000 (Section 3.3.3), is used by GeoSFM to calculate the physical parameters (such as texture, hydraulic conductivity, soil water holding capacity, hydrological active soil depths, average saturated hydraulic conductivity, Soil Conservation Service (SCS) runoff curve numbers and percentage of impervious cover for each sub-basin). The saturated hydraulic conductivity (Ks) (measured in cm hr^{-1} for the predominant soil type) is an important input variable which is used by GeoSFM model in the runoff generation process algorithms (Asante *et al.,* 2007b). GeoSFM model generates Ks values for each sub-basin using the soil texture classes and each basin's boundary grids as input (Table 4.2).

Table 4.2: Hydraulic conductivity values (Ks) based on seven texture classes defined by the class code (Source: FAO, 1995)

Zobler Class Code	FAO Texture	Porosity (%)	Matrix Potential (Ψ_m)	Ks (cm hr^{-1})	BSlope (%)	USDS Soil Texture (-)	Soil Hydraulic Class Group (-)	Numeric soil Hydraulic Class Values (-)
1	Coarse	0.42	0.04	5.08	4.26	loam sand	a	88
2	Medium or coarse	0.43	0.14	1.88	4.74	sandy loam	a	88
3	Medium	0.44	0.35	1.22	5.25	loam	b	89
4	Fine medium or heavy	0.40	0.13	1.60	6.77	sandy clay or loam	c	90
5	Heavy or Fine	0.47	0.26	0.88	8.17	clay or loam	d	91
6	Ice	0.00	0.00	0.00	0	ice	-	-
7	Organic	0.44	0.35	1.22	5.25	loam	b	89

The GeoSFM model uses a grid of soil depth values to determine the average soil depth in each of the sub-basins. The process is based on median soil depth for each soil depth category and the percentage of each mapping unit that is in the depth category as taken from the FAO digital soil map (Entenman, 2005). The depth categories, their depth ranges, and the median depth are shown in Table 4.3, which also includes the percentage of the depth categories assigned to the different parts of the particular basin. The GeoSFM model also yields a runoff curve number (RCN) by intersection of the land cover and soil group classes (using the U.S. Department of Agriculture's (USDA) soil classification system) (Asante *et al.,* 2007b). In this classification system, the hydrologic soil group A, corresponds to the excessively drained, somewhat excessively drained and well drained soils of the FAO classification; the hydrologic soil group B is related to the moderately well drained soil at FAO classes; the hydrologic soil group C links to the imperfectly drained soils and group D to the poorly and very poorly drained of the FAO classes (Table 4.3 and Table 4.4).

Table 4.3: FAO soils depth category, class's depth range, and the class's median depth (Source: FAO, 1995)

Depth category	Range of depth (cm)	Median soil depth (cm)	Mapping unit (% of area)		
			A	B	C
Very Shallow	< 10	5	10	40	5
Shallow	10 - 50	30	20	30	5
Moderately Deep	50 - 100	75	20	10	5
Deep	100 - 150	125	30	10	15
Very Deep	100 - 300	200	20	10	70

Table 4.4: SCS runoff curve numbers used for various soil and land cover classes in GeoSFM

Anderson Code	Land Cover Description	Soil Class A	Soil Class B	Soil Class C	Soil Class D
0	Unclassified	54	70	80	85
100	Urban and Built- Up Land	81	88	91	93
211	Dryland and Cropland Pasture	68	79	86	89
212	Irrigated Cropland and Pasture	62	71	78	81
213	Mixed Cropland and Pasture	65	75	82	85
280	Cropland/Grassland Mosaic	65	75	82	85
290	Cropland/woodland Mosaic	45	66	77	83
311	Grassland	54	70	80	85
321	Shrubland	45	66	77	83
330	Mixed Shrubland/Grassland	49.5	68	78.5	84
332	Savannah	57	73	82	86
411	Deciduous Broadleaf Forest	45	66	77	83
412	Deciduous Needle leaf Forest	45	66	77	83
421	Evergreen Broadleaf Forest	25	55	70	77
422	Evergreen Needle leaf Forest	25	55	70	77
430	Mixed Forest	35	60.5	73.5	80
500	Water Bodies	98	98	98	98
620	Herbaceous Wetland	30	58	71	78
610	Wooded Wetland	25	55	70	77
770	Barren or sparsely vegetated	68	79	86	89
820	Herbaceous Tundra	98	98	98	98
810	Wooded Tundra	98	98	98	98
850	Mixed Tundra	98	98	98	98
830	Bare Ground Tundra	98	98	98	98
900	Snow or Ice	98	98	98	98

4.2.2. Soil water balance

The GeoSFM rainfall-runoff component has two main modules: (a) a water balance module, and (b) a catchment and distributed channel routing module. In the water balance module, a daily water balance calculation determines how much water enters the stream network from each sub-basin. The soil conceptualisation is composed of two zones: (i) an active soil layer where most of the soil–vegetation–atmosphere interaction processes take place, and (ii) the groundwater zone. The active soil layer is divided into an thin upper soil layer where evaporation and transpiration both occur and a lower layer where only transpiration takes place. The catchment runoff mechanisms considered in the model are: excess precipitation runoff; direct runoff from impermeable areas of the basin; rapid subsurface flow (interflow), and baseflow contribution from groundwater. Figure 4.2 shows a schematisation of transferring fluxes in the two layered model in GeoSFM.

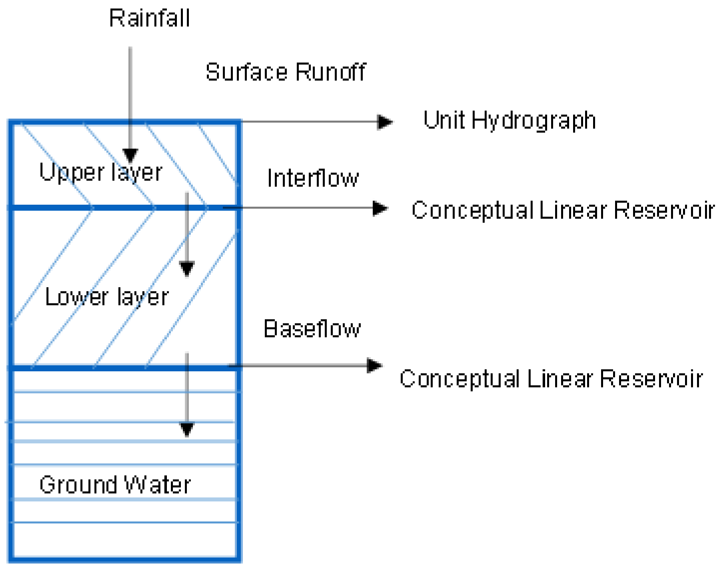

Figure 4.2: Partitioning fluxes in the two layered GeoSFM model

The model has several options for simulating excess precipitation runoff. In this study the Soil Conservation Service Curve Number (CN) method was used because of its potential to assess the impact of variation in physical parameters on flood frequency distribution (Morris, 1980; Klemes, 1982; Muzik, 1993; Shrestha *et al*., 2008). Curve Numbers were estimated from a land use and land cover data layer and were dynamically updated to reflect the state of the soil moisture. At each time step, the default curve number is adjusted based on the percentage saturation of the upper soil layer (*Upper Layer SWCX*), as shown in Equation 4.1 (Asante *et al.,* 2007a).

$$CN = \begin{cases} 1.95 \cdot CN_o \cdot 2.718282^{(-0.00663 \cdot CN_O)} & (0.9 < SWCX_{UpperLayer} < 1) \\ CN_O & (0.6 < SWCX_{UpperLayer} <= 0.9) \\ 0.39 \cdot CN_o \cdot 2.718282^{(0.009 \cdot CN_O)} & (0 < SWCX_{UpperLayer} < 0.6) \end{cases}$$

Equation 4.1

The adjusted curve number is used to generate excess precipitation when the daily rainfall is higher than 20% of SCS runoff, using Equation 4.2 in Asante *et al.* (2007a).

$$RUNOFF \cdot EXPRP = \frac{\left(PRECIP - 0.2 \cdot \left[\left(\frac{1000}{CN} - 10\right)\right]\right)^2}{\left(PRECIP + 0.8 \cdot \left[\left(\frac{1000}{CN}\right) - 10\right]\right)}$$

Equation 4.2

where $PRECIP$ is rainfall and CN is the default curve number.

4.2.3. Catchment and distributed channel routing

The runoff produced by the water balance module is routed in two phases. The catchment runoff is routed at the sub-basin level to its outlet (using the catchment routing module) and thereafter the flow is routed through the main river channel network (using a distributed channel routing module). The subsurface runoff is routed using a set of two conceptual linear reservoirs; the surface runoff routing is carried out using a diffusion wave equation as described by Artan *et al.*, (2002). The DEM and land cover data are used to determine the rate at which runoff is routed from the point of generation to the catchment outlet. Routing is the process of predicting the shape of a hydrograph at a particular location in a channel, reservoir, or lake (Merkel, 2002; Asante *et al.*, 2007a). It is often used to predict flood peaks, water volume, and the timing of the flow. It is therefore important to look in more detail at the routing techniques available in GeoSFM and assess their adequacy in flood prediction. GeoSFM uses a variety of computational linear (pure translation and diffusion analogue) and non-linear (Muskingum-Cunge routing) routing methods for simulating the in-channel phase of flow for flood forecasting.

Pure Translation method: The Pure Translation method accounts for the advection of flow but does not include any attenuation or deformation of the input (Artan *et al.,* 2002). Consequently, the input flow remains unaltered in magnitude at the discharge point, and a single flow parameter (namely travel time between the input and discharge locations) is required for the computation. Mathematically, lag routing can be expressed as Equation 4.3.

$$Q(t) = I(t - t') \qquad \textbf{Equation 4.3}$$

where *Q(t)* is the discharge at time, *t; t'* is the travel time between input and discharge locations and *I(t–t')* is the input at time *(t–t').*

Diffusion Analogue method: The Diffusion Analogue is a linear routing method which accounts for both flow advection and attenuation. This method includes one parameter for flow translation (flow time or celerity) and another for the attenuation (or spreading out) of flow (dispersion coefficient). The diffusion analogue equation is the linear solution of the Advection-dispersion equation (also known as the Navier-Stokes equation for a simple plane rectangular source. The relative simplicity of this model makes it straightforward to implement and parameterize in a wide variety of settings with little calibration (Artan *et al.,* 2002; Asante *et al.,* 2008). Mathematically, diffusion analogue method can be expressed as Equation 4.4.

$$Q(x,t) = I(0,0)\left(\frac{x}{\sqrt{4\pi D t^3}}\right) * exp\left[-\left(\frac{(Vt-x)^2}{4Dt}\right)\right] \qquad \textbf{Equation 4.4}$$

where $Q(x,t)$ is the discharge at time t at a distance x from the origin; I (0,0) is the input at time zero at the origin; D is the dispersion coefficient in $m^2 s^{-1}$; V is the flow celerity in $m s^{-1}$; x is the distance from the origin in m; t is the time elapsed since the input in seconds; π is the numerical constant Pi and has a value of 3.14159.

Muskingum-Cunge method: This is a non-linear, variable parameter routing method (Asante *et al.*, 2007a). Like the linear routing method, it involves the use of the continuity equation and an empirical storage function, relying the Muskingum K coefficient (analogous to flow time) to control the rate of advection and the Muskingum x coefficient to control the rate of attenuation (or spreading out). Cunge proposed to amend the method by allowing the Muskingum x coefficient to vary during each time step, based on the condition of flow at the previous time step. In effect, the rate of attenuation of flow is dependent on the condition of flow. The Muskingum channel routing method is based on two equations (Merkel, 2002). The first is the continuity equation or conservation of mass and the second equation is a relationship of storage, inflow and outflow of the river reach. However, the Muskingum-Cunge model is suited to high spatial resolution applications or to settings where a well calibrated model with observed data is required. Mathematically, Muskingum-Cunge routing can be expressed using Equation 4.5, Equation 4.6 and Equation 4.7.

$$\frac{\mathrm{I1+I2}}{2}\cdot\Delta t-\frac{\mathrm{O1+O2}}{2}\cdot\Delta t=S2-S1 \qquad \textbf{Equation 4.5}$$

where I1 and I2 are inflow discharges at time 1 and time 2, $m^3\ s^{-1}$; O1 and O2 are outflow; discharges at time 1 and time 2, $m^3\ s^{-1}$; Δt is time difference between time 1 and time 2; *S1* and *S2* are values of reach storage at time 1 and time 2, m^3.

The second equation is a relationship of storage, inflow, and outflow of the reach.

$$S=K\cdot\{XI+(1-X)\cdot O\} \qquad \textbf{Equation 4.6}$$

where S = reach storage, m^3; I is inflow discharge, $m^3\ s^{-1}$; O is outflow discharge, $m^3\ s^{-1}$; K = storage constant S; X= weighting factor, dimensionless.

Combining Equations 1 and 2 and simplifying results (Ponce, 1981) can be as shown in Equation 4.7.

$$\mathrm{O2}=\mathrm{C1\,I1}+\mathrm{C2\,I2}+\mathrm{C3\,O1} \qquad \textbf{Equation 4.7}$$

where C0, C1, C2, and C3 are dimensionless parameters:

$$C1=\frac{\left[\left(\frac{\Delta t}{K}+2X\right)\right]}{CO}\ ;\quad C2=\frac{\left[\left(\frac{\Delta t}{K}-2X\right)\right]}{CO}\ ;\ C3=\frac{\left[2\cdot(1-X)-\frac{\Delta t}{K}\right]}{CO}$$

An approximation for *K* is the travel time through the reach (length of reach divided by the average flow velocity). The value of *X* is between 0.0 and 0.5. A value of 0.0 gives maximum attenuation from the procedure and 0.5 provides the minimum attenuation. Linsley *et al.* (1982) described a procedure to determine *K* and *X* from hydrographs. Cunge (1969) developed equations to estimate *K* and *X* from hydraulic properties of the reach. The mathematical derivation has been condensed and presented by Ponce (1981).

The main challenge in a hydrological study is to choose the most suitable approach to use. Most of these flood routing procedures have been incorporated into the Natural Resources Conservation Service (NRCS) Technical Release (Merkel, 2002, Asante *et al.*, 2007a). This study used the translation approach in GeoSFM for daily flow forecasting because many studies (e.g. Artan *et al.,* 2002; Asante *et al.*, 2007c; Macuacua, 2012) on hydrological simulation in Southern Africa have demonstrated this approach to be relatively suitable (for implementation and parameterising in a wide variety of settings with little required calibration) in a data scarce river basin such as the Zambezi.

4.3. GeoSFM application in flood forecasting in the Zambezi Basin

The choice of a rainfall-runoff model for use in this study was difficult since models are not all developed for the same purpose. The success of hydrological modelling for a river basin depends on an appropriate conceptualisation of the dominant processes of the basin hydrology. There are currently a large number of hydrological models being used for flood forecasting at the basin scale. Hughes *et al*. (2006), stated that the focus when selecting a hydrological modelling should be on improving the existing models that have performed moderately successfully across different climate conditions rather than developing new models. Therefore, the existing models can be selected and improved upon, using specific requirements based on the prevailing hydrological processes, availability of data, modelling purpose, cost and expertise for implementation (Beven, 2001). Past experience with hydrological modelling studies in the Zambezi Basin (e.g. Beilfuss and Dos Santos, 2001; Winsemius *et al.,* 2006; Asante *et al.,* 2008) suggests that the initial consideration of the hydrological processes in the modelling exercise is crucial.

An assessment of the physical basin characteristics (Chapter 3) revealed that the Zambezi Basin contains massive areas of savanna, extensive soils with moderate water holding capacity, floodplains areas and large lakes, for which knowledge of both the surface and subsurface processes is important. This study presumes that an adequate conceptual representation of storages (such as soil moisture and groundwater, lakes, wetlands and river systems) would represent the hydrological behaviour of the system under study.

Based on the above-mentioned prerequisites and because of their demonstrated applicability to other parts of the Southern African region (Artan *et al.,* 2001; 2002), the GeoSFM rainfall-runoff model was chosen for flood forecasting modelling of the Zambezi Basin. The model remains the most widely used hydrological model for research and practical flood forecasting in Southern Africa. It has been shown to be robust enough for simulating hydrological processes in different hydroclimatic conditions, notably in southern Africa (Artan *et al.,* 2002; Vilanculos, 2006; Asante *et al.,* 2007c; 2008; Macuacua, 2012). Figure 4.2 shows a flow chart of the methodological approaches based on developments of the GeoSFM model at the United State of Geological Survey (USGS), which were adopted for use in this study. All these procedures have been implemented within the ArcView GIS-Model Interface software package – a modelling framework designed to make use of graphical display and database management routines for hydrological and water resources applications (Artan *et al.,* 2002; Asante *et al*., 2007a).

One of the issues taken into consideration in this study was how to investigate a combination of remote sensing linked with available ground-based observed data sets, can best be used in hydrology for flood forecasting in data scarce basins such as the Zambezi. Certain research models may be capable of taking advantage of the new information generated by remote sensing. Therefore these data were used as input into GeoSFM to simulate daily streamflow for the Zambezi Basin. The topography, soil characteristics, land cover, rainfall and evaporation information were input used to parameterise the hydrologic modelling units and to set the hydraulic properties that govern subsurface water movement and changes in soil moisture content (Shrestha *et al.,* 2008; Asante *et al*., 2008). The generated daily streamflow was compared and then calibrated with the observed streamflow (Figure 4.3) at a daily time step.

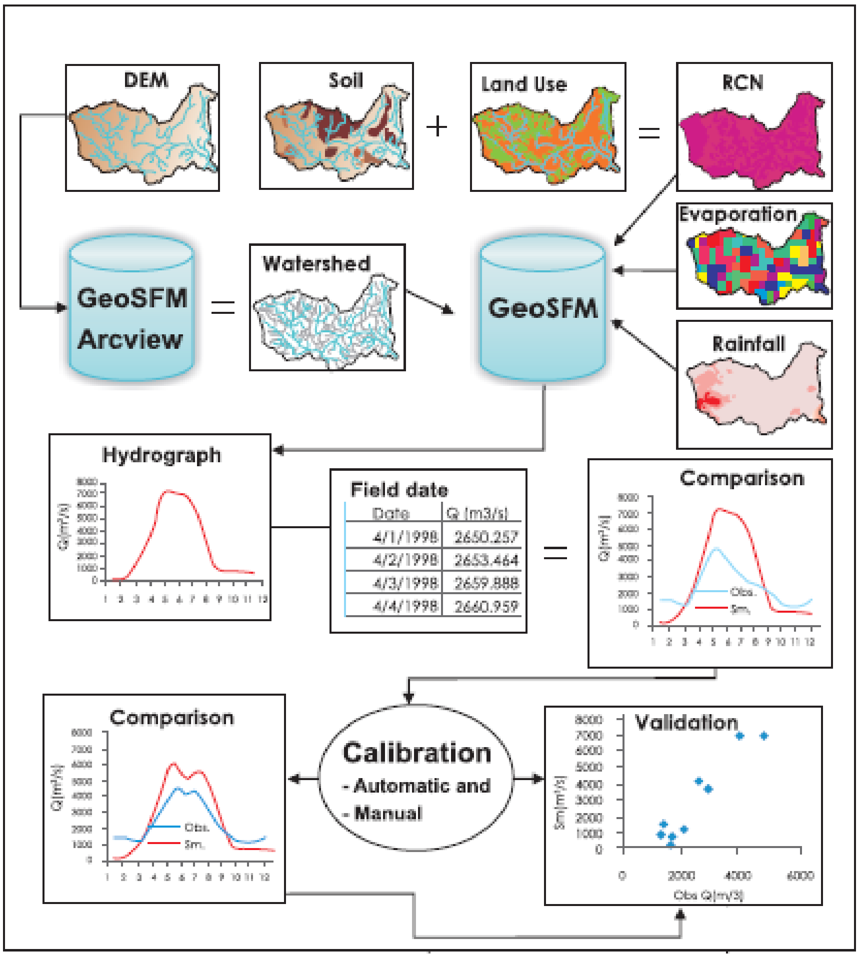

Figure 4.3: Processing steps using GeoSFM-ArcView and GeoSFM for hydrologic modelling simulation and data analysis in the Zambezi Basin

4.3.1. Physical property parameterisation data in GeoSFM

The first pre-processing step in GeoSFM is a terrain analysis undertaken to subdivide the study area into river modelling units and to extract terrain-dependent parameters from a Digital Elevation Model (DEM). The HYDRO1K global elevation dataset (Verdin and Greenlee, 1996) is the standard dataset for baseline parameterisation. Other higher resolution elevation datasets (such as the Shuttle Radar Topography Mission (SRTM) data, available from the USGS EROS site), can also be used in GeoSFM. For the Zambezi Basin, the HYDRO1K (Verdin and Greenlee, 1996) was used for the physical property parameterisation data because it is more comprehensive and has consistent global coverage of topographically derived data sets, including stream lines (river channels), drainage basins and ancillary layers derived from the USGS 30 arc-second digital elevation model of the world (GTOPO30 – Verdin and Greenlee, 1996; Shrestha *et al.,* 2008). The analysis of catchment physical properties of the Zambezi Basin is described in the following sections.

4.3.1.1. Topography

The analysis of topographical data for hydrologic modelling applications relies on the simple assumption that water flows in the direction of steepest descent. By comparing the elevation of a given cell with that of the eight surrounding cells, it is possible to determine in which direction water would naturally flow (Kennie and Petrie, 1990; Maidment, 1993; 2002; Entenman, 2005). GeoSFM uses an 8-direction geographic flow algorithm with each cell value corresponding to one of the following: 1 (East), 2 (Southeast), 4 (South), 8 (Southwest), 16 (West), 32 (Northwest), 64 (North) and 128 (Northeast) (Figure 4.4a). Figure 4.4 shows the process of creating flow directions and accumulation grids in GeoSFM.

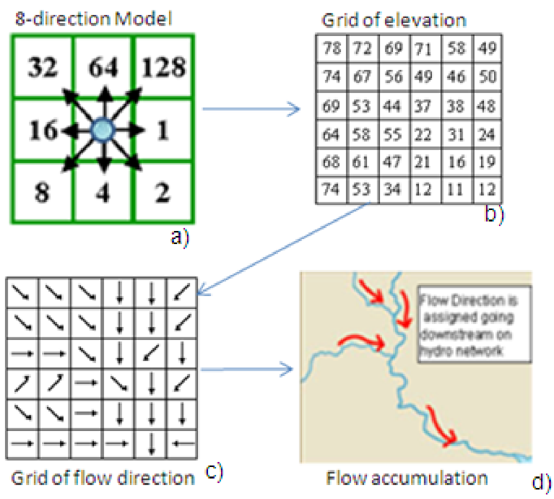

Figure 4.4: Methodology for creating the flow direction grid (a, b and c) and example of flow accumulation representation network (d) (Source: Maidment, 2002)

The calculation of a flow direction grid is important in GeoSFM, because it determines several other parameters of hydrologic interest (such as upstream contributing area, distance to the basin outlet and the slope of the land surface). It also enables the definition and delineation of hydrologic modelling units (such as sub-basins and river reaches) (Asante *et al.,* 2007a).

4.3.1.2. Slope

Slope is another important variable generated from topography for the model initialization stage. A 1 km-HYDRO DEM from USGS was used to estimate slopes for all pixels within the basin. GeoSFM used slopes, in conjunction with Manning roughness and hydraulic radius, to estimate overland velocity from land cover. GeoSFM calculated slopes for each sub-basin in the Zambezi River Basin using the ArcView Spatial Analyst function, by solving the Equation 4.8.

$$Rise_{rum} = SQRT\left(\frac{dz}{dx}\right) + SQRT\left(\frac{dz}{dy}\right)$$ **Equation 4.8**

where $\frac{dz}{dx}$ and $\frac{dz}{dy}$ for cell "e" of a 3x3 grid is calculated by the equations below:

$$\begin{bmatrix} a & b & c \\ d & e & f \\ g & h & i \end{bmatrix}$$

$$\frac{dz}{dx} = \left[\frac{(a+2d+g)-(c+2f+i)}{(8*xmesx_{spacing})}\right]$$ **Equation 4.9**

$$\frac{dz}{dy} = \left[\frac{(a+2b+c)-(g+2h+i)}{(8*ymesh_{spacing})}\right]$$ **Equation 4.10**

where: $xmesh_{spacing}$ is the horizontal distance of the grid and $ymesh_{spacing}$ is the vertical distance of the grid.

A terrain analysis for the Zambezi Basin was undertaken with a minimum contributing area threshold of 25 km^2 for stream network initiation. Figure 4.5a shows the elevation; the slopes and river network delineations for the Zambezi Basin are shown in Figure 4.5b. The analysis of topography in GeoSFM, generated 150 sub-basins (Figure 4.6) with an average area of 8 750 km^2 and an associated river reach approximately 110 km in length.

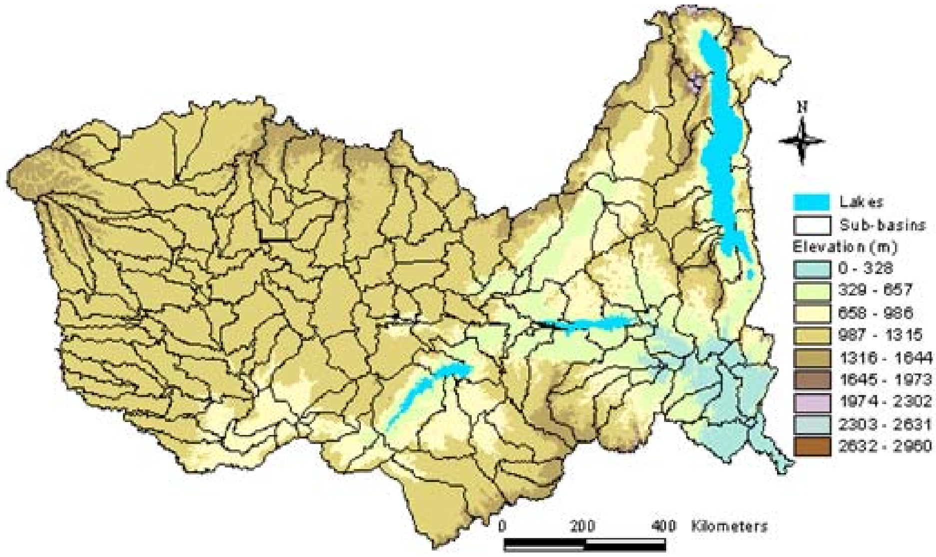

a)

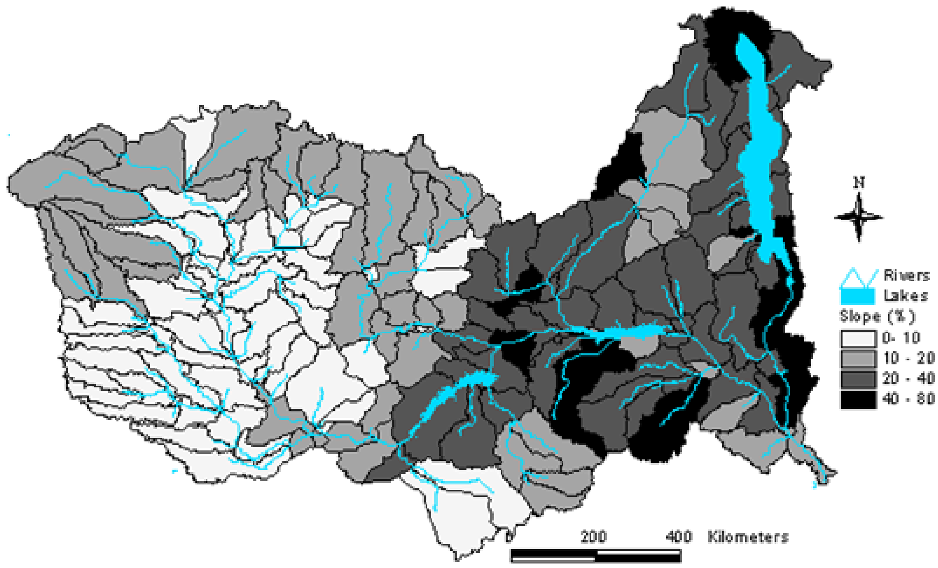

b)

Figure 4.5: Sub-basins delineated based on the areas of dominant elevation (a) dominant elevation (b) slope and the main tributaries

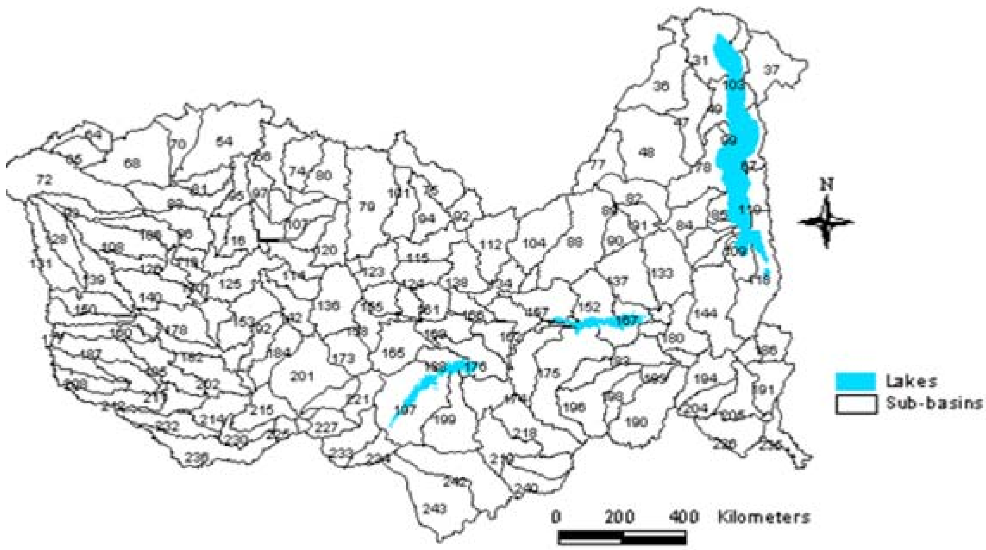

Figure 4.6: Sub-basins identification numbers

4.3.2. Rainfall-runoff parameterisation data in GeoSFM

The second pre-processing task in the GeoSFM model was the parameterisation of the hydrologic modelling units. The terrain analysis parameters (described in the preceding paragraphs) were aggregated to obtain a single value for each parameter for each sub-basin. Additionally, remotely sensed vegetation (from the Global Land Cover Characteristics (GLCC) database) (Loveland *et al.*, 2000; USGS, 2000b) and digital soil data (from the Digital Soil Map of the World) (FAO, 1995; 1998) and the World Soil File (Zobler, 1986) have been used to determine the predominant land cover and soil texture classes in each sub-basin. The published values of Manning roughness coefficient (McCuen, 1998), together with the land cover and texture classes and soil parameters (such as water holding capacity and hydraulic conductivity) (Webb *et al.*, 1993) have been used to determine the initial parameter ranges for each sub-basin.

4.3.2.1. Soils

The soil properties (Section 4.2.1) were then used by the GeoSFM to set the hydraulic parameters that govern the subsurface water movement and changes in soil moisture content over the Zambezi Basin. For soil depth characterisation, the Global Data Set of Soil Particle Size Properties produced by Webb *et al.* (1993) was used. The data set specifies the top and bottom depths and the percentage of the texture type (sand, silt, and clay) of soil horizons in 106 different soil types, catalogued for nine regions. Detailed procedures for extracting the required grids from these data sets have been described in USGS (2000a) and the procedures are performed outside of GeoSFM. Below is a description of the derivation processes for the parameters for the study area.

Soil Texture: The soil texture class was generated for each sub-basin using the GeoSFM and the FAO soil data attributes were used as input. The FAO soil data attributes contain a record number, and the percentages mapping unit for each sub-basin (Table 4.2 Section 4.2.1). The criteria defined in USGS (2000a) and USGS (2002) to identify the soil texture type are:

- “1" sandy (coarse) soils;
- "2" loamy (medium) soils, and
- "3" clay (heavy) soils.

The governing equation for soil texture calculation for each sub-basin (as described in USGS (2000a) and Entenmanns (2005)) was based on the soil data attributes and one assumption. For example: if it was assumed that a mapping unit *"A"* in the Western and Southern parts of the Zambezi River Basin was *95% coarse, 4 % medium, and 1% heavy then the calculation for the estimated soil texture was:*

*Estimated Soil Texture = ((95/100) * 1) + (4/100) * 2) + (1/100) * 3)*
Estimated Soil Texture = 0.95 + 0.08 + 0.03
Estimated Soil Texture = 1.06
Estimated Soil Texture = 1

- In the Northern and Eastern parts of the basin the mapping unit was based on 40% coarse, 20% medium and 20% heavy giving a soil texture index of 2.0.
- For the wetland areas the mapping unit was calculated as 1% coarse, 4% medium, and 95% heavy soil texture giving a soil texture index of 2.85.

The soil texture data (Figure 4.7a) was used in the GeoSFM model as an input value to estimate the hydraulic conductivity – which plays an important role in the estimation of soil water holding capacity – by accounting for the amount of water being retained by different soils texture types according to their infiltration rate capacity over the Zambezi Basin. The texture is also used in conjunction with land cover type to generate the SCS Runoff Curve Number.

Hydraulic conductivity: The empirical approach (similar to the one used for the calculation of soil texture described above and in USGS (2000a)) was used by the GeoSFM model to estimate the spatial distribution of saturated hydraulic conductivity in the Zambezi Basin. The approach estimates Ks by correlating the various soil properties (such as porosity and matrix potential distribution and soil texture). The range of values of soil properties used to estimate the Ks for each sub-basin within the Zambezi Basin are described in Table 4.2, Section 4.2.1. The Ks was calculated for each region (Figure 4.7b) as follows:

- In the Western and Southern parts of the Zambezi River Basin the mapping unit "A" in the FAO soil parameters was *95% coarse (sand), 4% medium (loamy), and 1% heavy (clay)* then the calculation for the estimated hydraulic conductivity was:

*Estimated hydraulic conductivity = (95/100) * 1) + ((4/100) * 0.01) + ((1/100) * 0.001)*
*Estimated hydraulic conductivity = (0.95 * 1) + (0.04 * 0.01) + (0.01*0.001)*
Estimated hydraulic conductivity = (0. 0.95) + (0. 0.0004) + (0.00001)
Estimated hydraulic conductivity = 0.95 hr^{-1}

- In the Northern, Central and Eastern parts of the basin the mapping unit "A" was based on 40% coarse, 40% medium and 20% heavy giving an average estimated sutured hydraulic conductivity of 0.44 cm hr^{-1}.

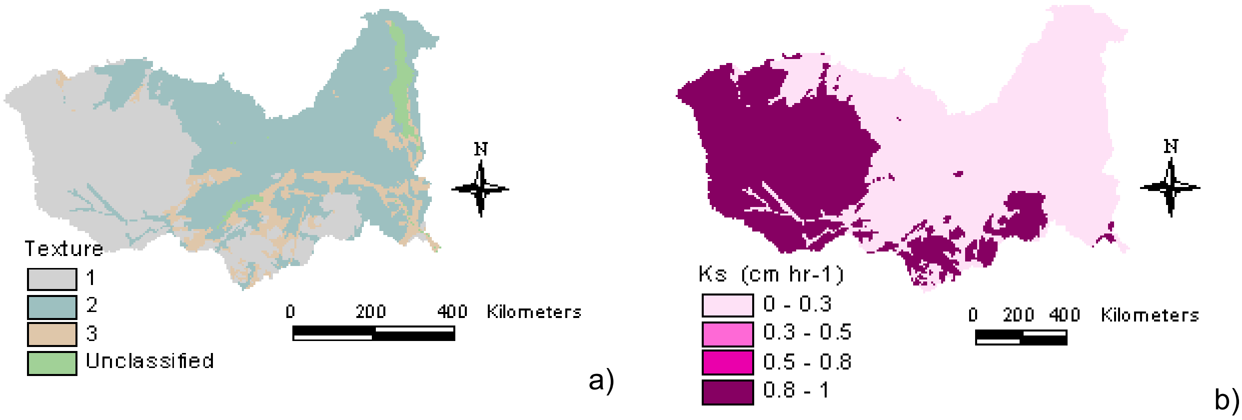

Figure 4.7: Spatial distribution of soil texture class (a) and saturated hydraulic conductivity (b) in the Zambezi Basin (FAO, 1995)

Soil depth: The soil depth data are used by the GeoSFM model, together with the daily available soil water (estimated by the daily water balance and Ks) to estimate the rate of percolation to deep groundwater (USGS, 2000a; Entenman, 2005). The soil depth classes were calculated for each region Figure 4.8a) as follows:

- In the Western and Southern part of the basin the spatial distribution of the soil depth (Unit "A") was calculated as 50% shallow, 60% moderately deep, 20% deep, and 15% very deep, giving an average soil depth of 101.5 cm;
- In the North-East and certain areas of Central of the basin, the spatial distribution of soil depth (Unit "A") was calculated as 5% moderately deep, 15% deep, and 80% very deep, giving an average soil depth of 182.5 cm;
- For the large areas of Central and South-East of the basin, the spatial distribution of soil depth (Unit "A") was calculated as 10% very shallow, 50% shallow, 10% moderately deep, 10% deep, and 20% very deep, giving an average soil depth of 75.5 cm.

Soil Water Holding Capacity (SoilWHC): The GeoSFM model used the soil depth values, in conjunction with soil texture data, to determine the average soil water holding capacity (SoilWHC) in each of the sub-basins within the Zambezi Basin. Based on FAO data for the Zambezi Basin, the GeoSFM classified SoilWHC into four hydrologic soil groups (Figure 4.8b) according to their soil water holding capacity as follows:

- Group "A" consists of soils that have a high soil moisture capacity, low runoff potential and high infiltration rates. The soil textures included in this group are sand, loamy sand, and sandy loam. This group of soils is mainly predominant in the North and Central areas of the Zambezi Basin;
- Group "B" consists of soils that have moderate moisture capacity and infiltration rates. The soil textures included in this group are silt loam, and loam. This group of soils occurs in the Western, some areas of the Central, East and South East regions of the basin;
- Group "C" consists of soils that have low moisture holding capacity. The only soil texture included in this group is sandy clay loam. Spatially, this soil occurs in the West, Central and North-East of the Basin;
- Group "D" consists of soils that have very low moisture holding capacity. The soil textures included in this group are clay loam, silty clay loam, sandy clay, silty clay, and clay. These soils predominantly occur in the West and North-West of the basin.

Based on the above assessment it was assumed that, in the North-East and small areas of the Central part of the Zambezi Basin, the predominant hydrological soils are very deep with high infiltration rates; in the West and South and large areas of the Central areas and along the river banks, the predominant soils are deep and moderately deep with high to moderate infiltration rates (Figure 4.8).

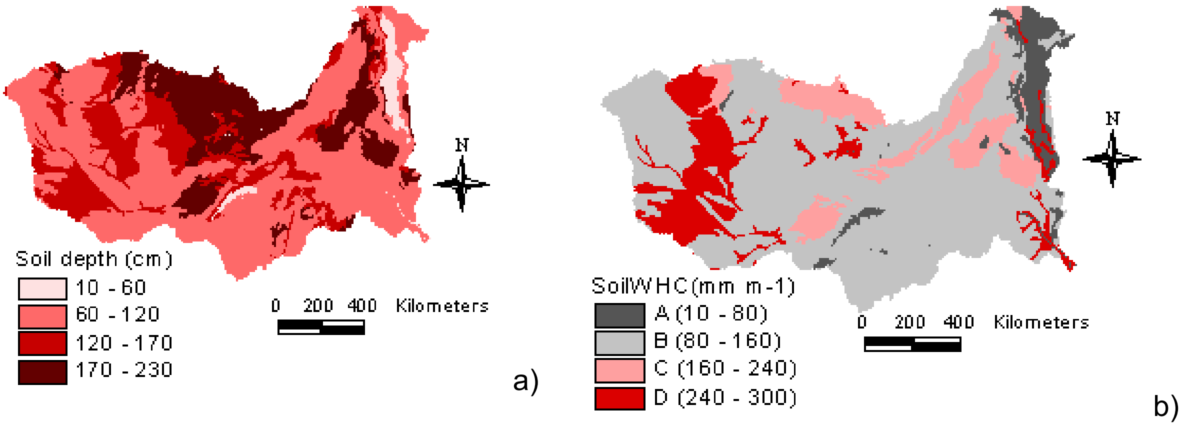

Figure 4.8: Spatial distribution of soil depth classes (a) soil depth in (cm) and (b) soil water holding capacity in (mm m^{-1}) for the Zambezi Basin (Source: FAO, 1995)

4.3.2.2. Land cover

The USGS Global Land Cover Characteristics (GLCC) database, derived from 1 km Advanced Very High Resolution Radiometer (AVHRR) data, was used to generate the flow velocity and hydrographs for the entire Zambezi River Basin. Considering that land surface influences the flow velocity and hence the runoff generation and overland flow processes, the non-uniform velocity grids approach (USGS, 2000a) is applied by the GeoSFM model to generate the unit hydrographs representing the response of each basin to rainfall input events. The land cover and soil water holding capacity were used in combination to estimate the Soil Conservation Service (SCS) runoff curve numbers in GeoSFM as follows:

Unit hydrograph: As a semi-distributed hydrologic model, GeoSFM requires a single input value of precipitation and other forcing data for each sub-basin during each modelling time step. A unit hydrograph is developed to simulate the typical response of the basin to a uniformly distributed rainfall input event for each sub-basin. According to Ramírez (2000), three types of synthetic unit hydrographs are possible: (1) those relating hydrograph characteristics (time to peak, peak flow, etc.) for watershed characteristics (Snyder, 1938; others); (2) those based on a dimensionless unit hydrograph (Soil Conservation Service, 1972), and (3) those based on models of watershed storage (Clark, 1943). GeoSFM uses the Soil Conservation Service approach and generates watershed storage hydrographs to describe a typical response for each sub-basin to rainfall events. The default approach for estimating overland velocity from land cover uses the Manning's Equation, with values of hydraulic radius assigned to each cell based on drainage area, as shown in Equation 4.11 (Asante, *et al*., 2007b).

$$\mathbf{Velocity} = \frac{1}{\mathbf{MANNINGN}} * \mathbf{RH}^{\frac{2}{3}} * \sqrt{\mathbf{HILLSLOPE}} \qquad \textbf{Equation 4.11}$$

where *RH* = hydraulic radius; *HILLSLOPE* = average elevation change divided by the average flow length from each cell to the basin outlet; *MANNINGN* = Manning roughness for the dominant land cover in the sub-basin; *Velocity* = Average overland velocity in the sub-basin.

Cells with drainage areas greater than 5 000 km^2 were assumed to be river cells and velocities ranging from 0.3 m s^{-1} to 1.5 m s^{-1} are directly assigned, based on drainage and slope (USGS, 2000a). For non-river cells, Manning's roughness values were estimated based on the land cover type related to the soils group as identified by the Anderson Code (Asante *et al.,* 2007a). Therefore the distribution of discharge at the catchment outlet is given by the probability density function (PDF) of travel times in the basin (Equation 4.12), as described in USGS (2000a) and which is the time taken to cover the distance of a certain (given) flow length.

$$t_i = \frac{l_i}{v_i}$$ **Equation 4.12**

where t_i is the travel time from a given grid cell to the basin outlet in days; l_i is the flow length in m from a given grid cell to the basin outlet and v_1 is the average overland velocity in $m^3 s^{-1}$ for the basin.

SCS Runoff Curve Number: The RCN is used by GeoSFM to generate a unit hydrograph and simulate the typical response of the sub-basin to a uniformly distributed rainfall event for each sub-basin. The SCS curve numbers assigned to the different soil hydraulic classes were described in Section 4.2.1. Figure 4.9 shows a sample of simulated hydrograph results based on the capability of each selected sub-basin to respond to the rainfall events. The approach is represented in GeoSFM model by the hypothetical unit response of each sub-basin in terms of runoff volume and timing to a unit input of rainfall, in daily time scale. The odd shapes of the hydrographs may be explained by taking into the consideration that way the model is integrating different responses over large areas.

It can be seen in Figure 4.9 that the Mazoe (185), Tete (180), and Marromeu (235) sub-basins are releasing, on average, 40% of the effective rainfall received during the first day. These sub-basins have smaller drainage areas, with higher peak flow than the median and large sub-basins (such as the Upper Zambezi (227), Cuando (230), Lupata (162), Luangwa (151), Barotse (148), Manyame (175) and Revubue (144) sub-basins) which release between 15% and 35% of the rainfall during the first day. In this application the responses were used to identify sub-basins with similar responses at the calibration stage. Therefore, in this study, sub-basins with similar responses were assumed to have similar parameters.

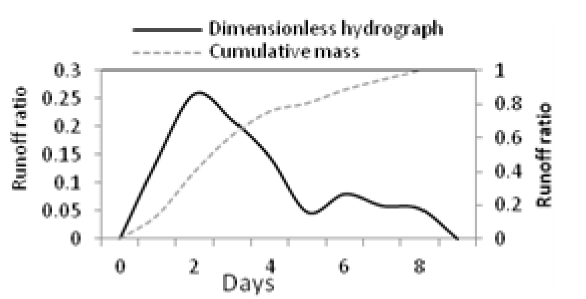

162)

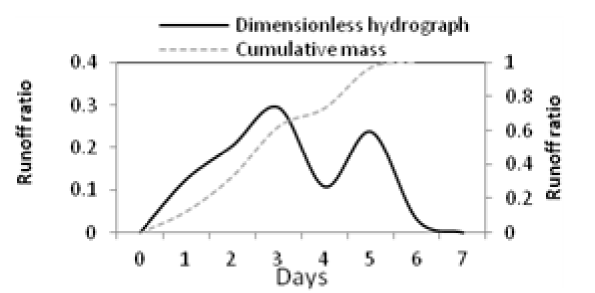

157)

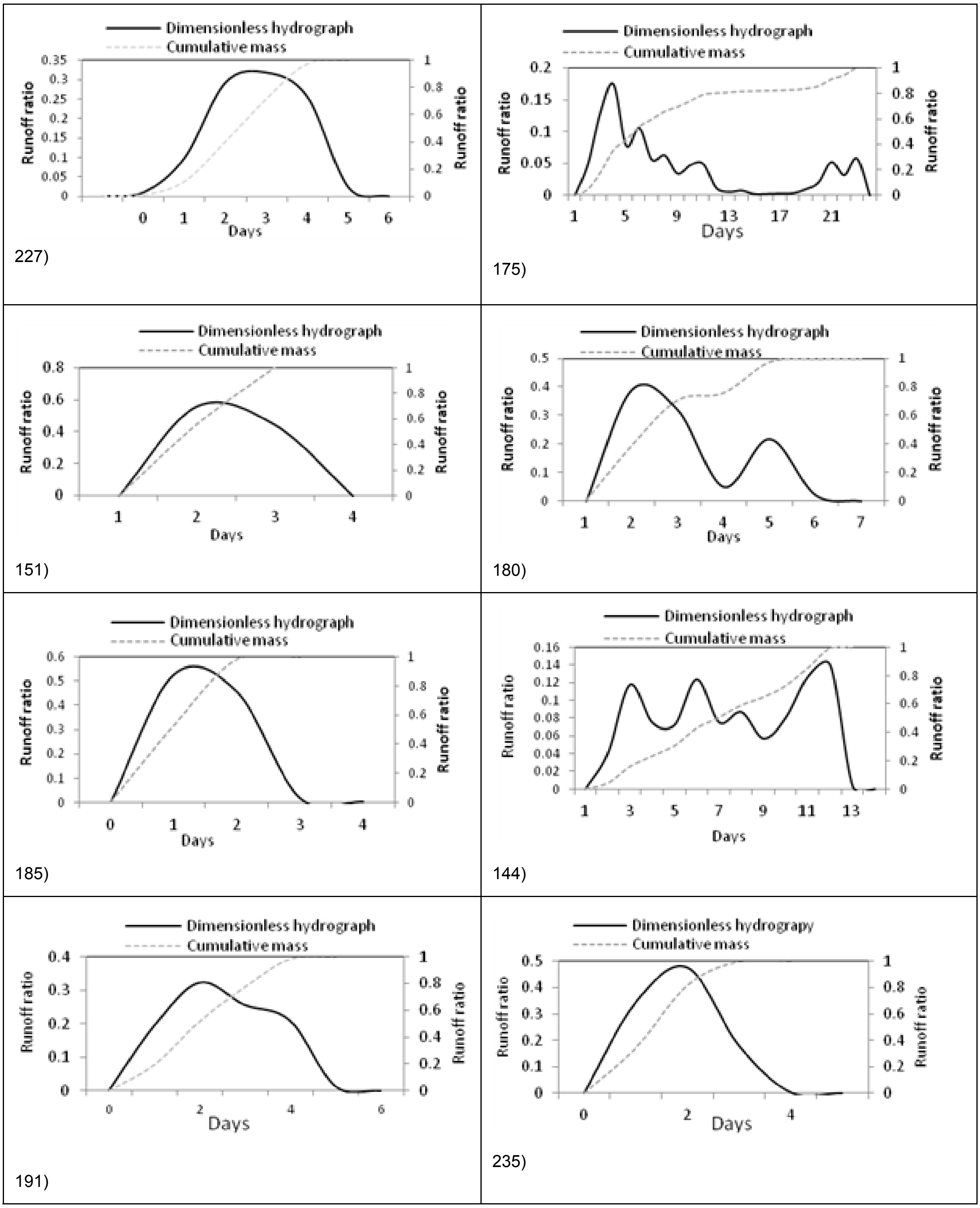

Figure 4.9: A dimensionless unit hydrograph and cumulative mass curve. Graphs generated using various soil classes and land cover types for each selected sub-basin namely: Cuando (230), Barotse (148), Upstream Zambezi (227), Kafue (169), Lupata (162), Luangwa (157), Manyame (175), Luia (151), Tete (180), Mazoe (185), Revubue (144), Shire (191) and Marromeu (235)

Maximum cover: GeoSFM used the GLCC data to represent the impervious area (MAXCOVER) when accounting for the presence of water bodies in each sub-basin. In

GeoSFM, the default MAXCOVER is 1 for areas which represent water bodies and MAXCOVER=0 for impervious areas. The model uses the MAXCOVER results to determine the excess amount of precipitation (in (mm) millimetres) on each sub-basin being modelled where the precipitation cannot be infiltrated into the soil layer or used by evapotranspiration processes. As the upper soil layer becomes wetter, a larger percentage of the basin acts as if it was impervious, contributing to surface runoff generation (in mm) in the model. For this study all the existing water bodies (such as lakes, rivers, and large wastelands) were parameterised using the land cover land use classification data. On areas classified as impervious in the land cover maps, runoff (in mm) is generated directly by GeoSFM. The approach generates many uncertainties – because the GLCC data and the modelling structure are not considering the processes of expansion and contraction of the areas covered by the water (USGS, 2000b; Asante *et al.,* 2007b). Another shortcoming of this approach relates to the spatial resolution of the land cover data, which makes it impossible to represent all existing water bodies in the Zambezi Basin – this may result in an indeterminate amount of direct runoff not being included in the calculations.

4.3.2.3. Climate data processing

GeoSFM requires daily rainfall and evaporation data to simulate streamflow conditions at the daily time scale. However, the spatial coverage of ground-based gauges with adequate rainfall and evaporation data is sparse in the study area, making it difficult to adequately support hydrologic modelling needs (WMO and USAID, 2012). Therefore, the satellite rainfall estimates (RFE) and evaporation (PET) estimates from The Climate Prediction Centre of the National Oceanic and the Atmospheric Administration (NOAA) were used to calculate daily soil water conditions and flow prediction – this was the only available source of precipitation data with reasonable spatial and temporal coverage (Artan *et al*., 2002; Verdin and Klaver, 2002; Joyce *et al*., 2004; Shrestha *et al*., 2008). The GeoSFM used daily estimates of precipitation (these estimates are available for the period January 1998 to January 2008). GIS was used to convert the rain satellite images into a grid and the grid for each day of the simulation period was named in Julian days as “rain – year and day of the year”.

Another important model input for daily water balance estimates in GeoSFM is the daily potential evapotranspiration (PET) data, produced by the Early Warning Group at the United States Geological Survey of Earth Observation Science (USGS EROS) Center (Verdin and Klaver, 2002). Data from the Global Data Assimilation System (GDAS) (Kanamitsu, 1989) was used to solve the Penman-Monteith equation to generate grids of PET at a daily time step (Section 3.4.3.1). In this study PET values were available from January 1998 to January 2008. GIS was used to convert the evaporation PET images into a grid and the grid for each day of the simulation period was named in Julian days as “evap – year and day of the year”. GeoSFM contains procedures for assimilating the resulting PET grids and computing actual daily evapotranspiration (AET) based on antecedent soil moisture conditions. Within the GeoSFM AET is estimated from PET (computed with the Penman Montieth equation) by limiting AET to moisture available in the soil. Therefore the potential evapotranspiration is first adjusted by a pan coefficient (pancoef) to account for known biases in satellite imagery or pan-based estimates supplied in the PET values during the estimation, with a default value of 0.95. Then, the conversion of potential to actual evapotranspiration is based on the relationship between the antecedent and actual soil moisture conditions as given by Equation 4.13 in Asante *et al*. (2007b). To ensure that the conservation of mass is maintained throughout the simulation, a temporary storage term called "STORETEMP" (USGS, 2000a, Artan *et al*., 2002; Asante *et al*., 2007b) in GeoSFM, is used to track the moisture remaining in storage after each flux extraction or addition during the simulation time step, as shown in Equation 4.14. The antecedent soil moisture is the water present in the soil profile before any additional rain event and the actual soil moisture refers to the water present in soil profile, resulting from any event of rainfall, at a given date and time.

$$\text{AET (B,T)} = \text{MIN}\begin{pmatrix} \text{PET (B,T)} \\ \text{STORE (B,T-1) + RAIN (B,T) – EXCESSRAIN (B,T)} \end{pmatrix}$$ **Equation 4.13**

$$\text{STORETEMP} = \text{STORE (B,T-1) + RAIN (B,T) – EXCESSRAIN (B,T) – AET (B,T)}$$ **Equation 4.14**

where AET is actual evapotranspiration; STORE (B,T-1) is antecidente soil moisture, calculated by multiplying maximum storage by the infiltration fraction, where the maximum storage is calculated by multiplying its soil water holding capacity by the depth of the soil column, RAIN (B,T) is soil moisture from rainfall; EXCESSRAIN is the fraction of rainfall (RAIN) landing on the permanent impervious area and the partial contributing area created by the saturation from subsurface storage. So, the EXCESSRAIN is generated when the soil storage capacity, is exceeded.

4.3.2.4. Soil water balance and runoff generation

In simulating flow, GeoSFM uses mean areal precipitation and evapotranspiration (*PET)* values for each sub-basin, determined by spatial averaging of daily rainfall and *PET* grids. For both soil moisture accounting and in-streamflow routing GeoSFM uses two routines: the Linear Soil Moisture Accounting (LSMA) and Nonlinear Soil Moisture Accounting (NSMA) routines. The LSMA routine is used as a bucket model in which surface runoff is generated with a partial contributing area formulation. Interflow is generated from the bucket, and baseflow from an unbounded storage below the bucket. The soil layer acts as a single control volume, with rainfall as the only input and evapotranspiration, surface runoff, subsurface runoff, and percolation as outputs (Asante *et al.*, 2008). The NSMA module provides a more complex representation of subsurface processes by creating separate soil layers within which interflow and baseflow processes occur (Artan *et al.,* 2002; 2004). For each daily time step, the change in soil moisture storage in each catchment was calculated for each sub-basin from the continuity Equation 4.15 and the parameters and the schematic representation of the process are shown in Figure 4.10.

$$\frac{\Delta s}{\Delta t} = P - E - R - G$$ **Equation 4.15**

where P is the precipitation in mm at time, E is the actualevapotranspiration in mm computed as the lower of P and available soil moisture, R is the total runoff in mm, G is the deep percolation to ground water in mm and s is the availablesoil moisture in mm.

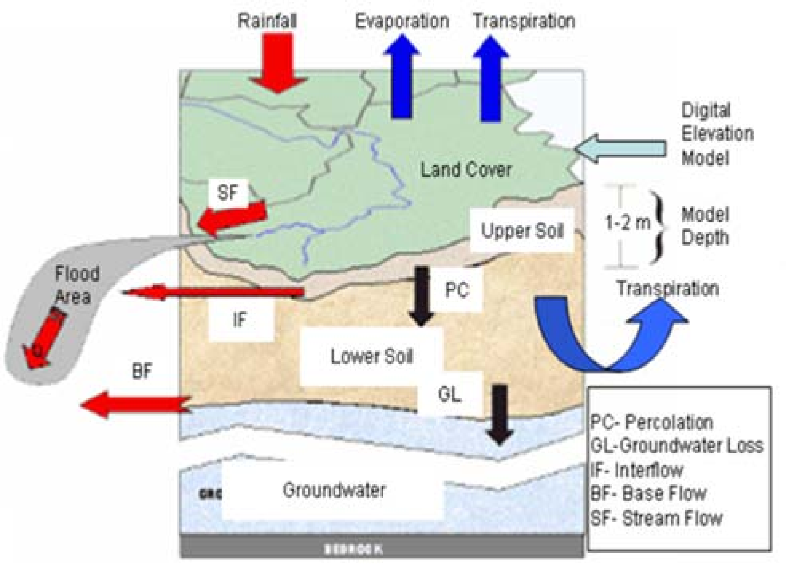

Figure 4.10: Schematisation of the conceptual processes involved in GeoSFM to estimate the soil water content (Adapted from USGS, 2000a)

Percolation: The rate of percolation to deep groundwater is calculated by a linear reservoir equation with residence time estimated in the GeoSFM model as the total soil depth divided by the saturated hydraulic conductivity as shown in Equation 4.16.

$$G = S * \frac{KS}{SDEPTH} * exp\left(-\frac{KS}{SDEPTH}\right)$$ **Equation 4.16**

where G is the percolation for each day in mm, S is the available soil moisture in mm, $SDEPTH$ is the soil depth in mm and Ks is the saturated hydraulic conductivity in mm day^{-1}.

Runoff generation: The total runoff is calculated as a summation of the excess precipitation and the baseflow generated from soil storage using linear reservoir functions with quick and slow components. For the saturated soil column, all excess precipitation is converted to runoff, while partial contributing areas. Equation 4.17 was used to estimate runoff for unsaturated soil conditions.

$$\mathrm{R} = \mathrm{P} * \mathrm{f}\left(\frac{\mathrm{S}}{\mathrm{SMAX}}\right) \quad \textbf{Equation 4.17}$$

where R is the runoff for each day in mm, S is the available soil moisture in mm, SMAX is the soil water holding capacity in mm and f is a function defining the relationship between percent soil saturation and percent impervious cover.

A dimensionless unit hydrograph generated for each sub-basin by discretizing the flow times for grid cells within the sub-basin is used to route runoff from the water balance to the catchment outlet where it enters the next downstream river reach (Equation 4.18) (Asante *et al.,* 2008).

$$q_j^i = 0.001 * \mathrm{A} * \mathrm{R} * \sum_{\mathrm{i}=1}^{\mathrm{m}} \mathrm{U_j} \quad \textbf{Equation 4.18}$$

where q_j^i is the overland flow in $m^3 s^{-1}$ arriving at the catchment outlet *j* at time *i*, A_j is the surface area of the runoff generating unit in m^2, U_j is the dimensionless unit hydrograph for catchment *j*, and * is the symbol representing convolution integral.

Streamflow: GeoSFM supports two linear routines (Pure Lag and the Diffusion Analog) and one nonlinear method (i.e. the Muskingum Cunge) for simulating the in-channel phase of streamflow. The present study uses Diffusion Analog routing (Section 4.2.2).

The discharge at the downstream end of each river reach is computed by convolving the diffusion analogue response function with the flow entering the upstream end (Equation 4.19) and the discharge is passed on as inflow to the next downstream river reach (Asante *et al.,* 2008).

$$Q_j^i = h_j(t) * \sum_{k=1}^{n} q_k^i \quad \textbf{Equation 4.19}$$

where Q_j^i is the discharge arriving at the outlet of river reach *j* in $m^3 s^{-1}$ q_k^i is the inflow from each river entering the upstream end of reach *j* in $m^3 s^{-1}$, *n* is the number of river reaches immediately upstream of reach *j*, and $*$ is a symbol representing the convolution integral.

4.3.2.5. Assessing GeoSFM model performance

Various objective functions are used to assess the performance of the model for both the uncalibrated results and the calibration process and these can be calculated in GeoSFM. Detailed results obtained from modelling calibration are presented in Chapter 6. The objective functions include: the Coefficient of Determination R^2; Root Mean Square Error (RMSE); Standard Deviation (STD); Maximum Likelihood Error (MLE); Nash-Sutcliffe Coefficient of Efficiency; NSCE, Number of Sign Changes (NSC) and BIAS. The GeoSFM outputs were evaluated using the Coefficient of Determination (R^2), Nash–Sutcliffe Coefficient of Efficiency (NSCE) (Nash and Sutcliffe, 1970), and the Root Mean Square Error (RMSE). R^2 describes as the amount of variance in the observed data that is explained by the simulated data and is given as:

$$R^2 = [\Sigma(Qo - \bar{Q}o) * (Q_S - \bar{Q}_S)]^2 / [\Sigma(Qo - \bar{Q}o)^2 * (Qs - \bar{Q}s)^2]$$ **Equation 4.20**

where Qo is the observed discharge, $\bar{Q}o$ is the mean of the observed discharge and Q_S is the simulated discharge and $\bar{Q}o$ is the mean of the simulated discharge. R^2 has values between 0 and 1 and a value of 1 indicates that the simulated value has incorporated all the variability in the observed data, while a value of 0 shows a poor correlation of the variability.

Typically any values calculated as greater than 0.5 can be considered acceptable (Santhi *et al*., 2001; Van Liew *et al*., 2007). However, for hydrological purposes the function tends to be over-sensitive to outliers and insensitive to the systematic differences between the observed and simulated values (Legates and McCabe, 1999). To circumvent the problem of systematic bias, the NSCE has commonly been used in rainfall-runoff modelling to evaluate the predicted flow hydrographs (Nash and Sutcliffe, 1970). The NSCE is an improvement (over the coefficient of determination for streamflow comparison) because it accounts for model errors in estimating the mean of the observed datasets (Shrestha *et al*., 2008). This accounting enables the efficiency of the model to be compared with the initial variance as defined by the observed datasets. An efficiency value of 1 implies a perfect match between the observed and simulated values; values less than 0 indicate an undesirable outcome (in which the observed mean is deemed to be a better predictor than the model) as calculated in Equation 4.21 (Nash and Sutcliffe, 1970). When the two statistics are used together, large differences between NSCE and R^2 are indications of systematic errors. The ideal value for the NSCE is 1 and its range is -∞ to 1 (Moriasi *et al*., 2007).

$$NSCE = 1 - \left[\frac{\sum_{i=1}^{n}(S_i - O_i)^2}{\sum_{i=1}^{n}(O_i - \bar{o})^2}\right]$$ **Equation 4.21**

where O_i is the observed discharge, S_i is the simulated discharge and ō is the mean value of the observed discharge.

The RMSE (Equation 4.22) is a measure of the differences between the values predicted by a model (or an estimator) and the values actually observed. These individual differences are called residuals (Moriasi *et al*., 2007). The RMSE are used to aggregate the magnitudes of the errors in predictions for various times into a single measure of predictive flow. The ideal (Moriasi *et al.,* 2007) value is ≈ 0 and the range is$[0, \infty]$.

$$RMSE_m = \sqrt{\frac{1}{N}\sum_{t=0}^{N}[F_m(Z_t) - f_m(Z_t)]^2} \qquad \textbf{Equation 4.22}$$

where N is total number of observations; F_m is the observed data and f_m is the forecasted data.

The model results obtained for this research were also compared using time series plots and flow duration curves (FDC) for both the observed and modelled streamflows. The FDC is defined as the cumulative frequency distribution of the percentage of time a given flow magnitude in a river channel is equalled or exceeded (Searcy, 1959; Mays, 1996; Moriasi *et al.,* 2007). Visual comparison of observed and simulated FDCs provides a qualitative evaluation of the model performance, based on the frequency distribution of high, medium and low flows. More quantitative assessments can be achieved by determining the differences in the frequency of exceedence at specific flows, or differences in flows at specific frequencies of exceedence.

4.4. MIKE BASIN conceptual structure

The MIKE BASIN (DHI, 2010) is a conceptual model that is fully integrated into the ArcGIS environment. It is a river management model addressing water allocation, reservoir operation, or water quality issues. The model is builds on a network model in which branches represent individual stream sections and nodes represent confluences, diversions, reservoirs, or water users. The catchment is divided into sub-catchments belonging to the specific river reaches. In situations of water excess or shortage, a conflict arises of how to distribute the water available in river among the stakeholders (users of water). MIKE BASIN solves this distribution problem by setting up priority rules on a local or global scale allocating different priority levels. The overall modelling concept in MIKE BASIN has been to find a stable solution for each time step, and through this step to make reasonable and stable assumptions. The simulation time step can be set to cover any positive time span, ranging from seconds to months. To meet any pre-defined objectives, MIKE BASIN may be used together with optimisation algorithms, to solve any particular constraint (DHI and Aurecon, 2011). MIKE BASIN comprises three main modules: water quality; groundwater and reservoir simulation modules (DHI, 2010).

With the water quality module, MIKE BASIN can simulate steady-state reactive transport of the most important nutrient substances affecting water quality. Point sources, as well as non-point pollution, can be modelled and this facilitates integration with other GIS-based data for automatically calculating the non-point nutrient loads from catchment areas. The groundwater module in MIKE BASIN is represented by a linear reservoir where the groundwater interacts with the surface water via groundwater recharge and stream seepage.

Moreover, when the depth of the water table of the upper reservoir reaches the land-surface, the water starts to spill directly into the river. MIKE BASIN also accommodates multiple multi-purpose reservoir systems. Reservoirs can simulate the performance of specified operating policies using associated operating rule curves (Section 4.5.2).

The main conceptual structure of MIKE BASIN reservoir model is shown in Figure 4.11. The conceptual structure of the MIKE BASIN (MB) reservoir model can accommodate systems ranging from simple lakes to complex multi-purpose, interconnected reservoirs. MIKE BASIN covers three different types of reservoirs namely:

(i) Allocation pool reservoirs;

(ii) Lakes;

(iii) Rule Curve Reservoirs.

All reservoir types are characterised by geometry: Volume-Area-Height (VAH) *relationship* and the discharge- height *(Q-h)* relationship for the individual reservoir (Figure 4.11). Losses and gains (represented by precipitation, seepage, evaporation and releases or abstractions) may also be included. Runoff from individual catchments can be specified either in time series from historical flow or as generated by hydrological models. Rule curve reservoirs are a single physical storage and all users are drawing water from the same storage point. Operating rules for each user apply to that same storage and the users compete with each other to fulfil their water extraction rights. An Allocation Pool reservoir has also physical storage, but the individual users have been allocated certain storage rights within specific zones of water levels (DHI, 2010; DHI and Aurecon, 2011). Lakes are specific reservoirs for which no operation rules apply. The outflow from a lake can be restricted by a spillway relationship. If no such spillway exists, and the water level is at the top of dead storage, all inflow to the lake will flow out immediately. In this study, the rule curve reservoir model was chosen to represent the operating rules for Kariba and Cahora Bassa dams (Section 4.5.1), because both the Kariba and Cahora Bassa dams are being operated based on the maximum rule curve (Section 4.5.2).

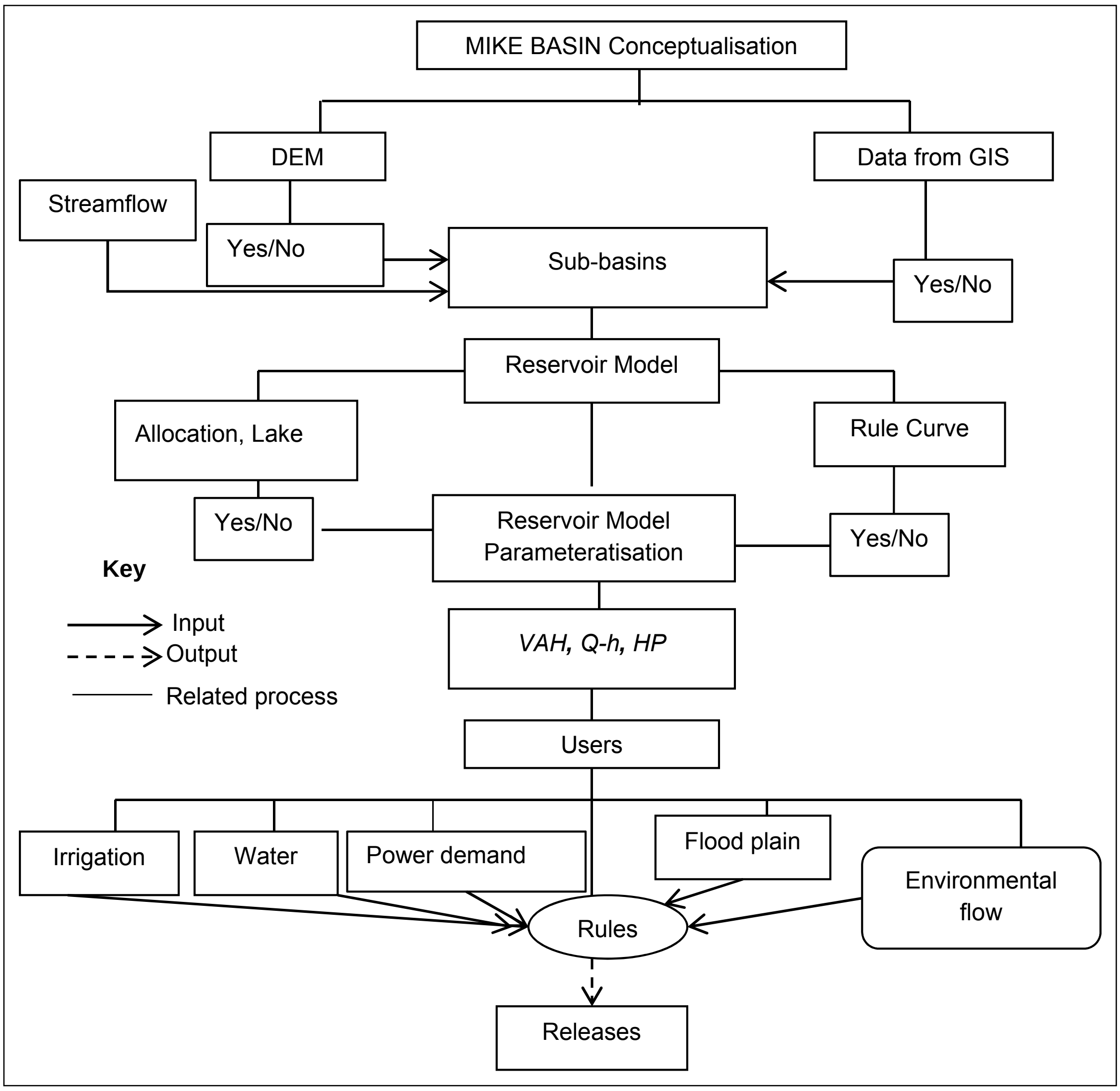

Figure 4.11: Main structure of the MIKE BASIN Reservoir model (Source: DHI, 2010)

4.5. MIKE BASIN reservoir simulation for Kariba and Cahora Bassa

The choice of a reservoir model for use in this study was difficult since reservoir models are not all developed for the same purpose. The success of reservoir modelling for a dam management depends on an appropriate conceptualisation of the dominant processes of the basin hydrology and physical conceptualization of the reservoir. There are currently a large number of reservoir models being used for dam operation. Past experience with reservoir modelling studies in the Zambezi Basin (e.g. Davies *et al*., 2000; Beilfuss and Dos Santos, 2001; Beilfuss, 2009) suggests that the initial conceptualization of the reservoir processes in the modelling exercise is crucial. In this study, the MIKE BASIN model was chosen for reservoir simulation modelling of the Kariba and Cahora Bassa dams. This model has been shown to be robust enough for simulating reservoir processes in different reservoirs conditions, notably in Southern Africa (DHI, 2010; DHI and Aurecon, 2011). Figure 4.12 shows a simplified flow chart of the methodological approaches based on the development of the MIKE BASIN model at the Denmark Hydraulic Institute (DHI) and gives an indication of why this model was adopted for use in this study. All these procedures are implemented within the ArcGIS-Model Interface software package – modelling framework designed to make use of graphical display and database management routines for hydrological and water resources applications (DHI, 2010). The model set up was achieved through using sub-basins and rivers shapefiles imported from GIS ArcView 3.2.

The rivers and sub-basins were same as used for parameterisation of the GeoSFM for the Zambezi Basin. Therefore the total of 150 sub-basins, with an average area of 8 750 km^2 and an associated river reach of about 110 km in length, were imported from the GIS-GeoSFM interface to the MIKE BASIN. The assumption used was that the imported sub-basins shape would conserve the sub-basin boundaries in terms of ID codes and areas to allow for data exchange processes when the GeoSFM and MIKE BASIN were integrated. The behaviour of the individual building blocks, and the interactions between them, was defined using built-in operation rules, or through the creation of customized rules in a macro program, designed to access the MIKE BASIN engine through its *"COM interface".* All information regarding the configuration and the linkages between the model building blocks were defined through on-screen editing in ArcMap and through the data exchange by the macro developed in Microsoft Excel. The releases were then parameterised to be controlled by minimum and maximum streamflow. Because this study addresses the issue of forcing Kariba and Cahora Bassa dams to release artificial floods, mainly in the rainy season, on the hydropower production, the rule curve reservoir model was chosen in MIKE BASIN to connect the users and to set up appropriate operation rules for Kariba and Cahora Bassa dams. However, this study recognises the role that other dams (such as Itezhi-Tezhi and Kafue) may play in flood management in the Zambezi basin.

These dams were not included in this analysis because of three main reasons:

- first: the assumption based on study Tilmant *et al*. (2010) which consider that the Kariba and Cahora Bassa dams together are able to store more than 200 * 10^9 m^3, which is about six times the average annual flow at Victoria Falls and two times the average annual discharge flowing to the sea, while Beilfuss and Dos Santos (2001); Beilfuss *et al*. (2009), considered that the peak flow at the Zambezi delta have been reduced in 50% since the Kariba dam have been completed in 1959. Then including Cahora Bassa dam which was concluded in 1975 and from arithmetical calculations was concluded that these two dam may able to store approximately 80% of the peak flow generated upstream if are well operated and release it in optimised manner.

- second: the Kariba and Cahora Bassa dams are operated based on the maximum rule curves: the Itezhi-Tezhi and Kafue dams are operated on minimal rule curves. Maximal rule curve is a tool used for dam operating curve which objectives is to meet hydropower production and flood control, while minimal rule curves has been used as a tool for meeting hydropower production and environmental flow requirements on regulated rivers, (Beilfuss and dos Santos, 2001; Beilfuss *et al*., 2009; Nyatsanza and Van der Zaag, 2011) – therefore the operation of the dams based on the minimal rule curves may offer an option to predict the high streamflow based on the rainfall-runoff model (by considering these dams as impervious areas where the high streamflow can be generated by the model without considering any abstraction), since their objective is not regulating flow for flood control.
- third: because of limited funds and the lack of time to develop a more complete model (in which all water users in the basin should be integrated) this research, therefore, should not be considered a conclusive study but a move towards improving the flood forecasting and early warning systems in the Zambezi Basin by integrated modelling systems and by making use of the new developments in the field of remote sensing and hydrological modelling for the Zambezi Basin.

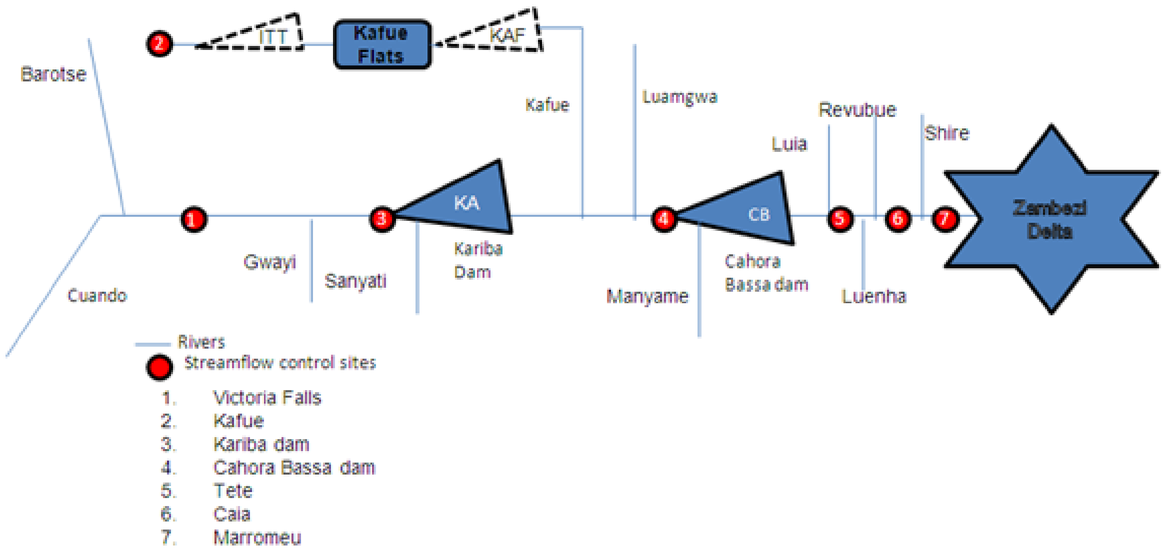

Figure 4.12: Simplified schematisation of MIKE BASIN configuration for the Zambezi Basin

4.5.1. MIKE BASIN parameterisation

This study tests the applicability of the MIKE BASIN reservoir simulation model to address the issue of near real-time operation for flood control and hydropower generation. The Kariba and the Cahora Bassa reservoirs, are an ideal case study for this testing.

MIKE BASIN parameterisation: To parametarise the MIKE BASIN, the water level time series of the Kariba and Cahora Bassa reservoirs were modelled and curtailed when the water level was within the zones defined by the rule curves (Figure 4.13 and Figure 4.14). To accurately model the releases from the different outlets (e.g. conduits; gates; spillways); evaporation (a function of surface area); and hydroelectric power generation (a function of reservoir elevation); a number of basic physical relationships for the Kariba and Cahora Bassa reservoirs were established. These included: water level-area; water level-volume; and discharge -water level (*Q*-*h*) capacity curves (Figure 4.15 and Figure 4.16).

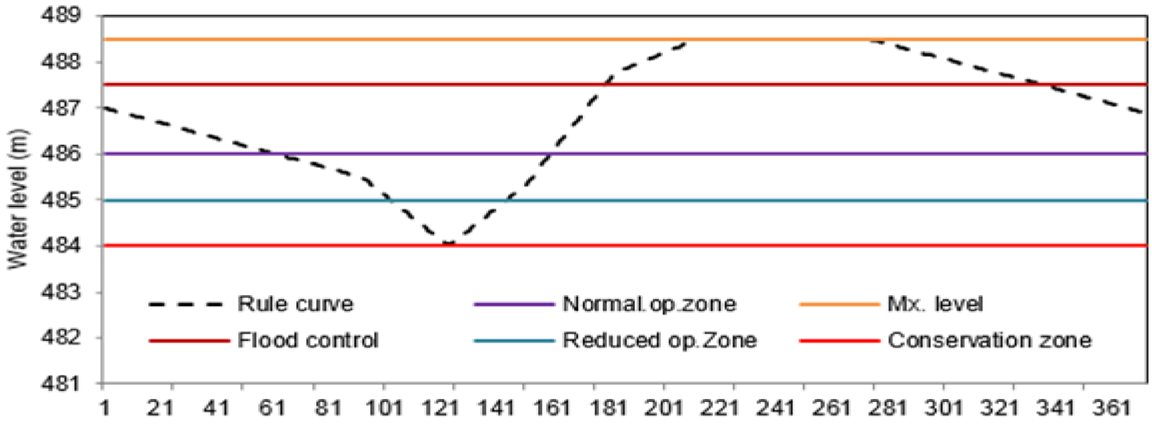

Figure 4.13: Processing steps using MIKE BASIN flood rule curve for Kariba reservoir model

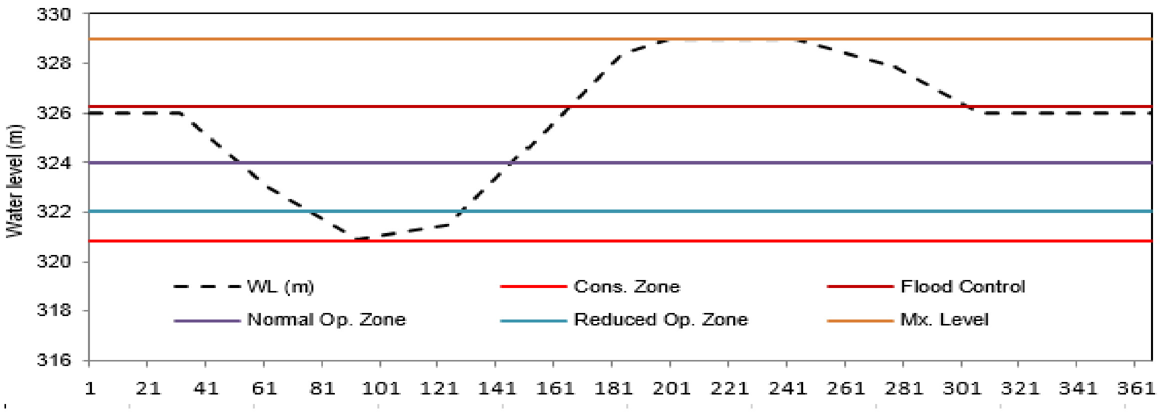

Figure 4.14: Processing steps using MIKE BASIN flood rule curve for Cahora Bassa reservoir model

MIKE BASIN computed the water levels for the Kariba and Cahora Bassa reservoirs by establishing a relationship - Volume-Area-Height (VAH). During the simulation, linear interpolations (between the user-specified neighbouring data triplets in the table) were performed to arrive at a piece-wise linear VAH function (Equation 4.23) in DHI (2010).

$$V\big(H(i+1)\big) \geq V\big(H(i)\big) + A\big(H(i)\big) \cdot \big(H(i+1) - H(i)\big)$$ **Equation 4.23**

where *i* is the value of increasing water level elevations. It implies that for every step in elevation, the increase in volume (*V*) should be at least equal to the base area (at the previous level (*H*)) times the increase in height.

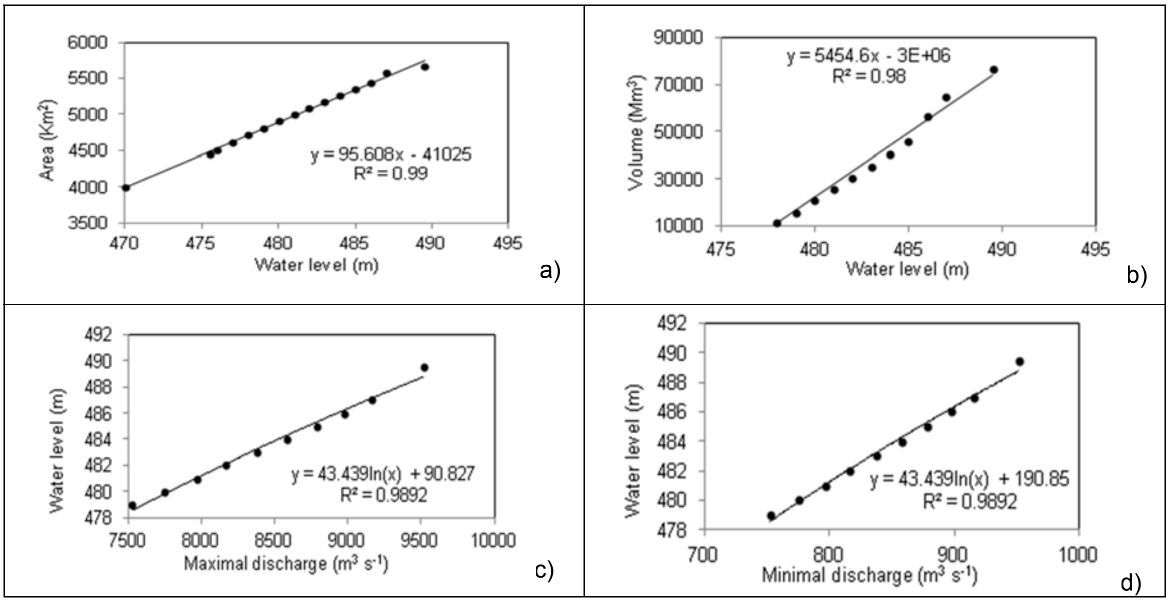

Figure 4.15: Reservoir relationships for Kariba dam. (a) Water level-area, (b) Water level-volume, (c) Water level-minimal discharge and Water level-maximal discharge

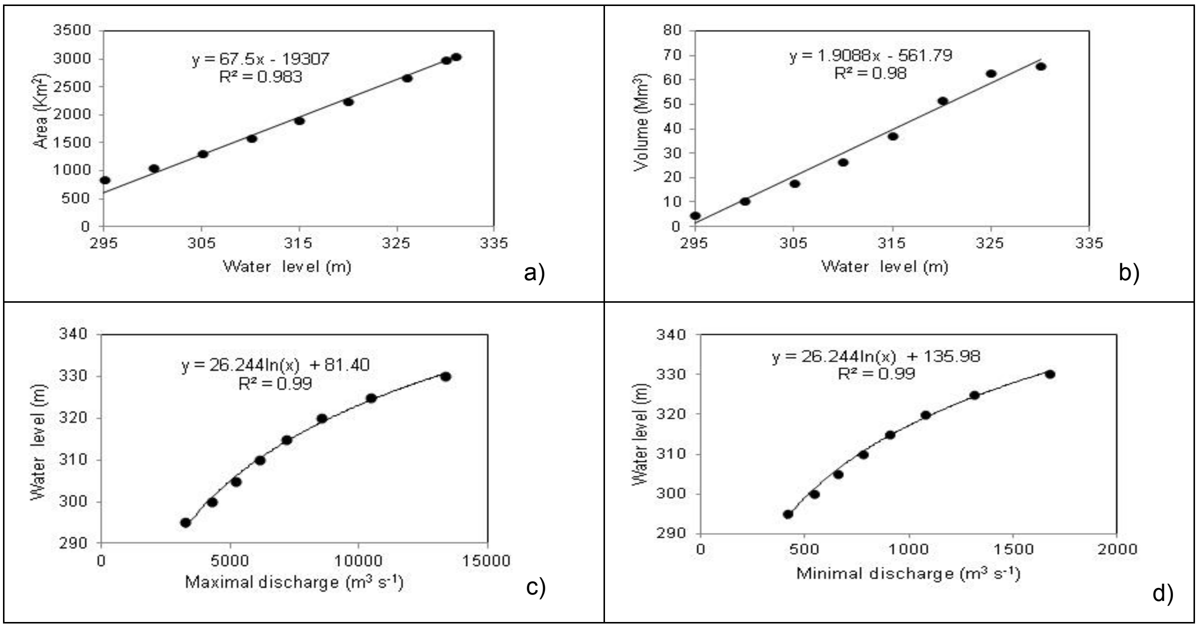

Figure 4.16: Reservoir relationships for Cahora Bassa dam. (a) Water level-area, (b) Water level-volume, (c) Water level-minimal discharge and Water level-maximal discharge

Hydropower: With the rules thus defined, the MIKE BASIN Reservoir model was set to perform a hydropower simulation as a first objective; the second objective was to simulate minimising flood levels at the dam site and at selected downstream flood control points. During periods of high electricity demand, the stored water is released through turbines to produce electric power. In this application, hydropower is represented in MIKE BASIN as a user that extracts water from the Cahora Bassa reservoir (and produces power according to effective head difference and turbines efficiencies), and thereafter calculates the hydroelectric effect produced. The effective head difference (Δh) was computed using Equation 4.24.

$$P = HI(Q) * Q * \varepsilon(\Delta h) * g * \rho hHIco$$ **Equation 4.24**

$$\Delta h(Q) = hreservoir\ (Q) - \Delta hconveyance(Q)$$ **Equation 4.25**

where *P*(MW) is the power generated, Δh is the effective head difference (L), Q is the discharge/release through turbines ($m^3\ s^{-1}$), ε is the turbine efficiency (%), and g is the gravitational constant ($m\ s^{-2}$).

Figure 4.17 illustrates the relationship between turbine efficiency and the effective head of the Cahora Bassa plant used for model parameterisation. The turbine efficiency is high at an effective head between 201 m and 211 m, and low at an effective head of 199 m and 226 m. These were defined to vary in time as described by the rule curve. The rule curve approach was also used to maintain certain defined minimum and maximal flows at a number of downstream control locations. In this study, flood control points were selected at Tete (E-320), Caia (E-291) and Marromeu (E-285), with a maximum flow of 5 000 $m^3\ s^{-1}$, 6 000 $m^3\ s^{-1}$ and 6 500 $m^3\ s^{-1}$ respectively. The FCL and MRR were defined to check whether the current rules were being met by the rule curves to control dam operations. Minimum downstream release is required to meet hydropower demand and is not the same as the minimum environmental release required to support the flow in the river downstream of the reservoir during critical periods of drought. These rules were input to the MIKE BASIN model (Table 4.5). The hydropower demand and flood control flow were defined as first priority users; secondary priority was given to the downstream users. This means that the water from the Cahora Bassa reservoir should first be delivered to satisfy higher priority users and thereby meet the pre-defined operation rules.

ID	Effective head (m)	Turbine efficiency (%)
1	190	0.0
2	194	89.3
3	199	92.7
4	201	95.6
5	204	95.8
6	207	95.9
7	211	95.6
8	216	95.2
9	222	94.2
10	226	92.9

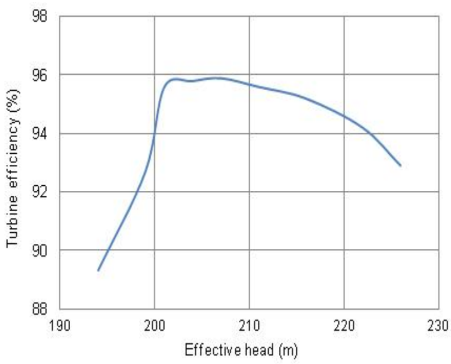

Figure 4.17: Representation of the relationship between turbine efficiency for the Cahora Bassa hydroelectric plant. (a) tabular and (b) graphical representation of the relationship between turbine efficiency and the effective head (m) for the Cahora Bassa hydroelectric plant

4.5.2. MIKE BASIN operating rules for Kariba and Cahora Bassa dams

In this study, a two-step approach was undertaken to develop appropriate flood operating rules for both the Kariba and Cahora Bassa dams:

1. Definition of operating objectives for Kariba and Cahora Bassa in MIKE BASIN;
2. Determination of flood release rules, taking into account the operating objectives of the Kariba and Cahora Bassa dams.

Operating objectives of Kariba and Cahora Bassa dams: Because the focus of this study has been on the Kariba and Cahora Bassa dams, an analysis of daily reservoir operations was carried out comparing the daily discharges for the pre- and post-flooding periods from 1998 to 2008. Literature reviews were also conducted – including literature on the Kafue and Itezhi-Tezhi dams (Beilfuss, and Dos Santos, 2001; Beilfuss *et al*., 2009; Nyatsanza and Van der Zaag, 2011). From the analysis, it was observed that the reservoirs primarily operate on rule curves, with Kariba and Cahora Bassa using maximum rule curves; conversely the Itezhi-Tezhi and Kafue dams operate on minimum rule curves. The main operation objectives in the Zambezi basin are:

- to maximise hydropower production;
- to ensure dam safety;
- to ensure sufficient storage for flood protection (both at the Kariba and Cahora Bassa dams and the downstream communities).

Operating flood releases rules: To use the Kariba and Cahora Bassa reservoirs efficiently, operating rules were specified to define the storage target levels and various storage allocation zones and, through a definition of a relationship, to determine the water level minimum and maximum releases (Section 4.5.1, Figure 4.15, Figure 4.16) and Table 4.5. Three releases – namely release 1, release 2 and release 3 – were defined in MIKE BASIN to determine the availability of water for flood releases from the Kariba and Cahora Bassa reservoirs. These release levels were set for the optimum operating objectives of the Kariba and Cahora Bassa dams and status of the inflows and water levels at the dams (Section 6.3.2.2) where:

For Kariba, release1 was defined to take place if the water level reaches set levels at Kariba of 477.5 m and sequentially incremented or reduced according to the amount of inflow. So, release 2 to be applied when the water level is 488.5 m. Release 3 may only take place if the water level is 489 m, where the maximum dam discharge (9 500 $m^3 s^{-1}$) may be released.

For Cahora Bassa, release 1 was defined as the top of the flood control level (326 m); release 2 is applied when the water level rises to 2 m above the top of the flood control level (328 m).

Release 3 is applied at the top of the crest level (329 m) where the maximum dam discharges (16 250 $m^3 s^{-1}$) may be released.

Table 4.5: Modelling operating parameters for Kariba and Cahora Bassa reservoirs

Parameters	Kariba dam	Cahora Bassa dam
Minimal Release Requirement (MRR)	750 $m^3 s^{-1}$	1 750 $m^3 s^{-1}$
Maximum Release	9 500 $m^3 s^{-1}$	16 250 $m^3 s^{-1}$
Power Demand (PD)	750 $m^3 s^{-1}$	1 750 $m^3 s^{-1}$
Minimal Operating Level (MOL)	475.5 m	295 m
Flood Control Level (FCL)	485 m	326 m
Dead Storage (DS)	470 m	280 m

Downstream flood control: In this study downstream flood control is defined as controlled release of water from upstream reservoirs to inundate a specific area of the floodplain (or river delta) downstream to restore and maintain ecological processes and provide natural resources for dependent livelihoods – such release measures are undertaken in collaboration with stakeholders. Flood control, in the context of this study, should be considered to be distinctly different from the sudden, unplanned releases which are sometimes made from reservoirs to prevent dam failures – these unplanned release are made without any warning to downstream communities. The new paradigm contests that, while large floods may always have a proportion of positive impact, all floods play an important role in maintaining the structure, processes and resources of a river system (Ward and Stanford, 1995; ICOLD, 1999). A study conducted by Beilfuss in 2001, in the Zambezi basin, revealed that there are relatively few alternatives available for restoring the natural rhythms of the river-floodplain system. Therefore, dam removal has gained worldwide attention as an important tool for restoring the hydrological regime of rivers (Shuman, 1995; ICOLD, 1999). However, the removal of the Cahora Bassa dam is not an option given the current development objectives of Mozambique will require intensive hydroelectric power generation, transportation, and commercial irrigation in the lower Zambezi Valley (Beilfuss and Dos Santos, 2001). The once-annual discharge of surplus reservoir waters at the end of the dry season, to increase storage capacity for the rainy season (*i.e.,* a variation on management practices currently in place) will produce mistimed flooding patterns which will only worsen conditions for people and wildlife downstream. Conversely the release of scheduled floods during the normal (historical) period of flooding offers enormous potential for benefiting farming systems and floodplain ecosystems, all while continuing to meet the demands for hydropower, flood mitigation, and other economic development objectives. This study is aimed at resolving the problem of sudden, unplanned releases from the Kariba and Cahora Bassa dams (at the end of the dry season, intended to increase their storage capacity for the rainy season) through the development of an integrated and improved forecasting tool which will result in reduced uncertainties in the information available to the reservoir manager, and thus lead to improved reservoir operation.

In this study, flood control downstream of the Cahora Bassa dam was parameterised in the MIKE BASIN model through devolving logical relations between defined reservoir rules and flood control locations in the lower Zambezi River system. These locations were defined to be controlled by minimum and maximum flow requirements. Tete (E-320), Caia (E-291) and Marromeu (E-285), were the selected locations because of:

i. the availability and reliability of data;
ii. the persistence of flooding and flooding disasters in the area;
iii. the importance of the selected points for flood forecasting and management; and
iv. the absence of an integrated model for flood forecasting.

The maximum flow control was determined as the flow which corresponded to the flood alert level – i.e. the flow that can be released with minimal impact on the communities living in the floodplains.

4.6. Integrating GeoSFM and MIKE BASIN

A fundamental principle of the flood pulse concept is that the natural (unregulated) flood regime of large rivers is predictably unpredictable (e.g. Davies *et al.,* 1998). The characteristics of any given flood event are uncertain and depend on the regional climatic conditions and other factors. But the magnitude, timing, duration, and frequency of hydrological conditions over time fall within a predictable range and pattern (Beilfuss and Dos Santos, 2001). This predictability is derived in part from the persistence of natural flow patterns in large river systems. As the annual flood levels build up over the rainy season, the characteristics of the flood hydrograph, the magnitude, extent, duration, and timing of peak flooding conditions, is increasingly revealed. When the flooding regime is disrupted because of dams, embankments, or diversions, the hydrological connection between river and floodplain is altered or severed (Kennie and Petrie, 1990; Ward and Stanford, 1995). Social and economic impacts may include: loss of life; damage to property; negative socio-economic impacts and damage to manmade cross-country infra-structure (rail lines), etc. To mitigate the impact of floods, a reliable flood forecasting system is important to enable the establishment of a reliable early warning system that can be rapidly transmitted down to the vulnerable community. Apart from mitigating the impacts of floods downstream of the Zambezi basin, this study investigated the applicability of an integrated flood forecasting system in the Zambezi Basin. Operationally, the system simulated and tested the hypothesis which claims that the flooding downstream of Cahora Bassa dam is impacted by the operation of the dam. The hypotheses were tested by examining the operating rules described in Section 4.5.1, during the reservoir model parameterisation. Releases were defined to take place as long as the water level remained above the dead storage level. Two tasks were undertaken to test the hypothesiss:

- The first task sought to evaluate the performance of the integrated the GeoSFM and MIKE BASIN for streamflow and flood forecasting and flood management in the Lower Zambezi sub-basin;
- The second task aimed at assessing the impact of the different levels of flooding downstream of the Cahora Bassa dam.

A number of steps were undertaken to integrate the GeoSFM into MIKE BASIN reservoir simulation. These steps were:

- The GeoSFM was parameterised (Section 4.3) and calibrated for the entire Zambezi River Basin;
- Then, after calibration of GeoSFM, a reservoir simulation model was selected and based on the criteria that the reservoir model should be robust enough and capable of using the streamflows generated by GeoSFM (therefore the MIKE BASIN model was selected);
- MIKE Basin was parameterised first by importing details of both the rivers and sub-basins (from the GIS-GeoSFM interface) and the physical characteristics of the Kariba and Cahora Bassa reservoirs;
- A macro in Microsoft Excel was developed to automatically import the daily streamflows from GeoSFM into MIKE Basin reservoir model. A total of 150 automatically timed series were imported, corresponding to one for each of the 150 sub-basins created during GeoSFM and MIKE BASIN parameterisation phase. Each sub-basin was linked to a single ID;
- Rules (Section 4.5.1) were defined in MIKE BASIN for flood control downstream, taking into account the operating objectives for Kariba and Cahora Bassa reservoirs (Section 4.5.2);
- The Lower Zambezi sub-basin was selected for testing the integrated modelling for the reasons mentioned in Section 4.5.1 and also because of its irregularity in seasonal rainfall which results in fluctuations in river flow – and frequent dry spells and floods (as reported in a study on climatic change disaster risk conducted by INGC (2009);
- Operationally, the reservoir inflow generated by the calibrated GeoSFM was fed into MIKE BASIN resulting in a GeoSFM-MIKE BASIN integrated model. The data exchange process was achieved by calculating the simulated streamflows from

GeoSFM (using a Microsoft Excel Macro) as daily flow input for the water balance calculations of the Cahora Bassa reservoir. The Macro changes the ".txt" files from GeoSFM to the "ds" file format required by MIKE BASIN. The integrated modelling system simulated streamflow between 1998 and 2008 and was validated for the period from 2009 to 2011. The performance was assessed using the objective functions described in Section 4.3.2.5.

4.6.1. Prediction of water level

To define alternative measures for reducing the impact of flooding downstream of the Cahora Bassa dam, two calculations were necessary:

i. the water level and discharge relationship;
ii. the prediction of flood peak flows travel time.

The first calculation was done by establishing a relationship between the different water storage levels in the Cahora Bassa dam and the maximum flow that may occur at Tete (E-320), Caia (E-291) and Marromeu (E-285), using Cahora Bassa Reservoir integrated models if the following factors applied:

i. the water level in the dam was between the minimum operation level of 319 m – 324 m;
ii. the water level in the dam was between normal operation zone of 324 m – 326 m; and
iii. the water level in the dam is between flood control zone of 326 m – 329 m.

There are no reliable flow measurement systems downstream of the Cahora Bassa dam and the measured stages were thus assumed to be more reliable than the measured flows. Therefore, the calculated daily discharges were converted to water levels in the river. The water level measurements are the common method used for river monitoring in the Lower Zambezi (practically all on the Mozambican side of the Zambezi Basin). The flow measured at the Lower Zambezi is influenced by the predominance of flat topography with large cross sections, which makes the flow measurement difficult. To address this issue the following steps were followed:

- because of the lack of the cross-section data for Tete (E-320), Caia (E-291) and Marromeu (E-285), Google Earth was used to measured channel widths;
- estimation of the maximum observed water level data from 1998 to 2008 – for each flood control site the value of maximum observed water level (m) was obtained from a database of the National Directorate of Water in Mozambique;

- use of the Hydraulic Cross Section Generator, developed at Rhodes University in 2011 (Figure 4.18), to generate the necessary river cross-sections (which could then be used to estimate the stage of water using the available rating curves);
- use of the channel widths and maximum water levels as the main input data and, by applying the Manning's approach in the Hydraulic Cross Section Generator, it was possible to establish a relationship between the maximum depths (m) and the discharge ($m^3\ s^{-1}$).

The approach described above was necessary to calibrate the existing rating curve (Section 3.5) and reduce the levels of uncertainty at selected sites. The maximal channel depth was assumed to be the highest historical observed water level recorded from the highest flood event for each selected site, for the period 1998 to 2008. The calibrated rating curves for Tete (E-320) Caia (E-291) and Marromeu (E-285) are shown in Figure 4.19. These 'modified' rating curves show the relationship between the flow and water level for each flow control site. This was the best that could be achieved with the available data; however there will always be uncertainties associated with using these 'modified' rating curves.

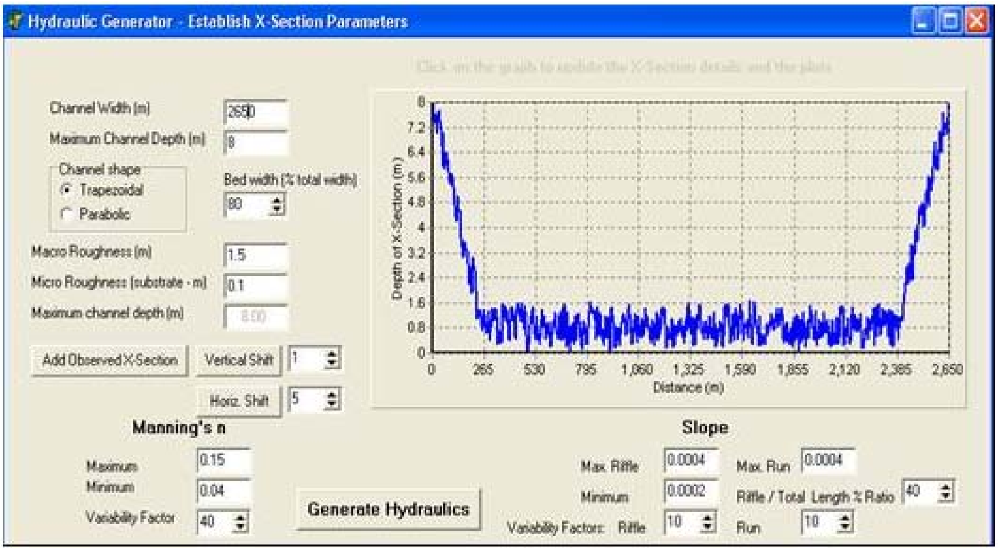

Figure 4.18: A screenshot of the hydraulic model developed at Rhodes University showing the screen area for generating channel cross-sections

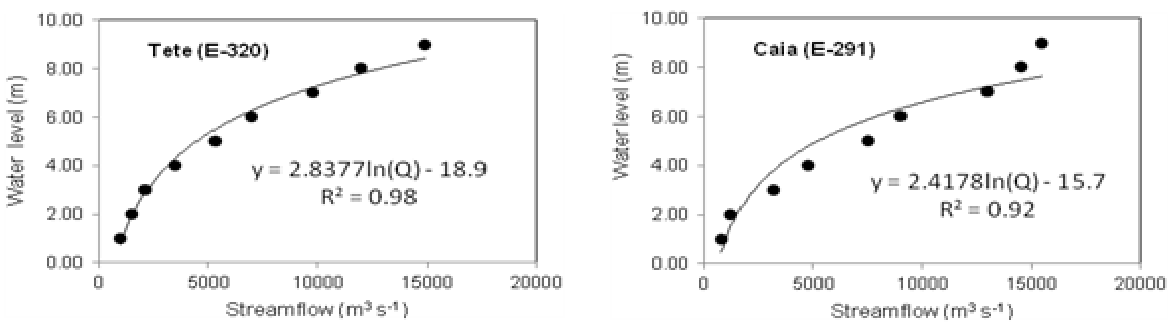

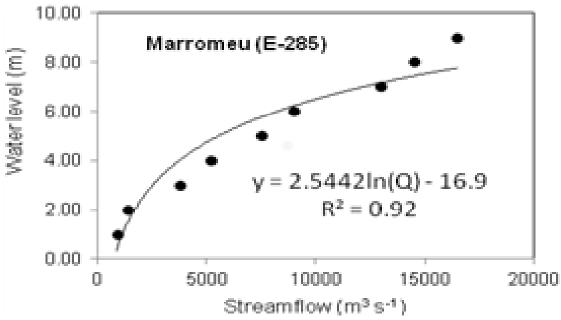

Figure 4.19: Modified discharge rating curves located downstream of Cahora Bassa dam Tete (E-320a) Caia (E-291b) and Marromeu (E-285c) selected as flood control sites. The streamflow ($m^3 s^{-1}$) was simulated by the model and the points in the graphs are measured water levels at the gauging stations

4.6.2. Prediction of flood peak flows travel time

Since the objective of the integrated hydrological modelling system is to predict floods downstream of Cahora Bassa dam, the calculation of the flood flow travelling time is required to make it possible to give timely warning to the vulnerable communities before the flood arrives. This calculation was done by comparing the sequential interval flood peak using hydrographs generated from the integrated model. Flood peak is the highest point on the hydrograph when the rate of discharge is greatest; lag time is the time interval from the center of mass of the rainfall excess to the peak of the resulting hydrograph (Kennie and Petrie, 1990). Given the peak discharge of Cahora Bassa and the lag time (which was a day) for the duration of the excess rainfall, the peak flow travelling time was estimated for Tete (E-320), Caia (E-291) and Marromeu (E-285). In each case the interval flood peak flow travelling time for Tete (E-320, Caia (E-291) and Marromeu (E-285) was estimated by comparing hydrographs of Cahora Bassa dam, Tete (E-320), Caia (E-291) and Marromeu (E-285), plotted on the same graph (Figure 4.20). Then the *Time to Peak* (*tp)* from Cahora Bassa dam to Tete (E-320), Cahora Bassa dam to Caia (E-291) and Cahora Bassa dam to Marromeu (E-285) was captured by counting the number of days that the peak flow would take to travel from one site to another. Therefore *tp* is the time from the beginning of the rising level to the occurrence of the peak discharge at a given measurement site. The time to peak can be largely determined by drainage characteristics (such as drainage density, slope, channel roughness, and soil infiltration characteristics of each location) and by rainfall distribution.

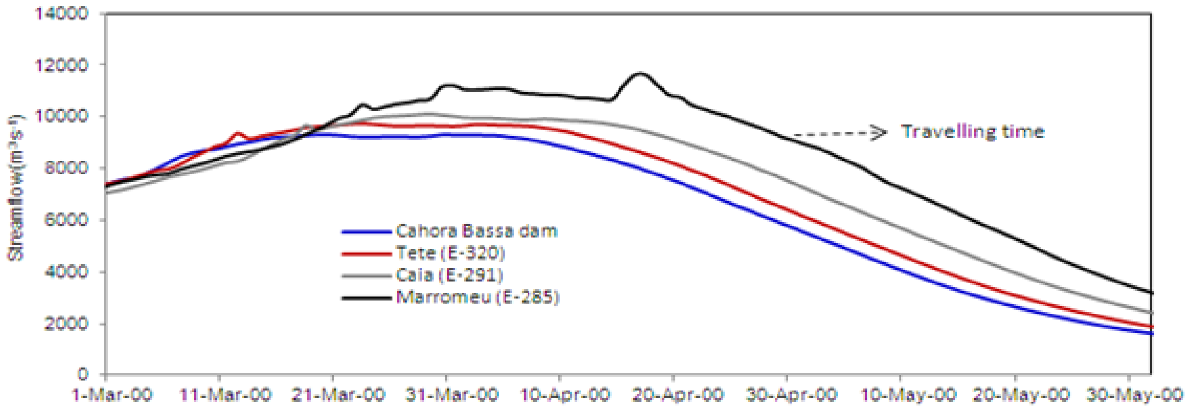

Figure 4.20: Comparison of the temporal distribution of the streamflow flood wave hydrograph. Flood waves from the Cahora Bassa dam to Tete (E-320), Caia (E-291) and Marromeu (E-285) respectively from 1st March to 31st May 2001 using simulated flow.

4.7. Flood risk maps

Flood area mapping: Rather than the mere identification of severe flood events from the integrated GeoSFM and MIKE BASIN simulation results, flood risk maps are an important tool for flood prediction and management because they complement the information predicted from hydrological models and allow the development of relief profiles. These flood risk maps can serve as a basis for designing measures to minimize the loss of life in the Lower Zambezi sub-basin. There are several methods for flood mapping, ranging from Landsat images for flood inundation mapping to Digital Elevation Models (DEMs). This study used the DEM method (USGS, 2000a; Asante *et al*., 2005) for flood mapping in Lower Zambezi. This method was chosen because it is easier to use and to understand. The method establishes a relationship between the water level (m) at a given location and the elevation (m). The application of the method consists of using predicted flow, expressed in terms of water level (m), and the corrected Digital Elevation Model (DEM) data to map the water level on the terrain and thus identify the areas where flooding may occur. Flood risk maps, prepared using GIS ArcView 3.2a tools and remote sensing (RS) data, form part of the early warning system for eleven districts located downstream of the Cahora Bassa dam. These districts are: Cidade de Tete, Guro, Chemba, Chindi, Chiringoma, Marrínguè, Marromeu, Mopeia; Morrumbala, Mutarara and Tambara (Figure 4.21). Similar approaches were used by ARA-Sul (2005) for the Limpopo river basin in Mozambique. Figure 4.22 shows the data required and the methodology followed to process the flood risk maps. The process of flood hazard delineation has been based on DEM and GIS analysis, and the vulnerability to flood based on the analysis and identification of the population density, the land use and the infrastructure (roads, hospital and schools) likely to be inundated. The overlaying of GIS flood hazard and vulnerability maps results in flood risk maps.

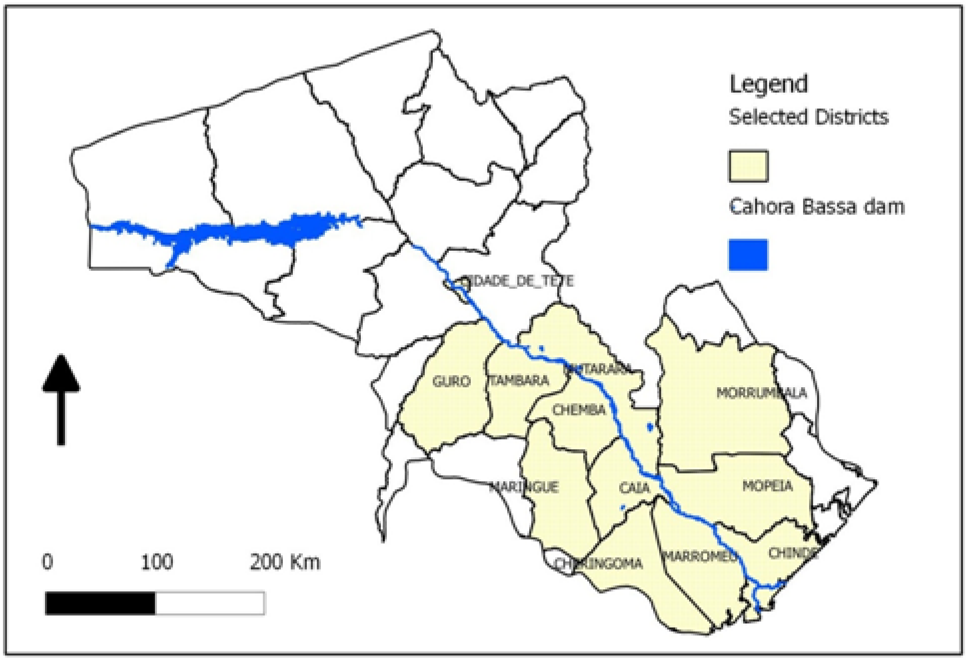

Figure 4.21: Location of the elevation (11) selected districts in the Lower Zambezi sub-basin for flood impacts assessment

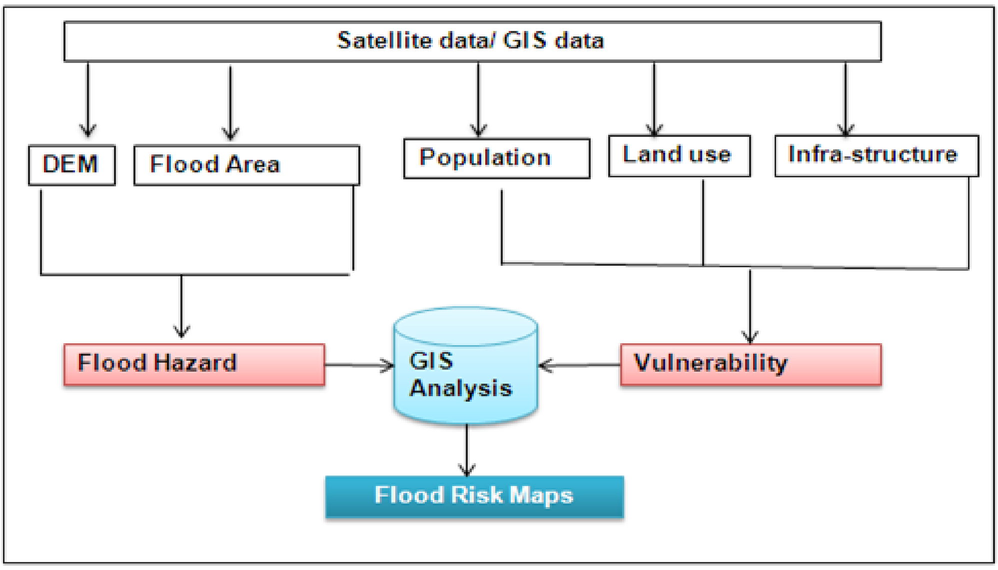

Figure 4.22: Schematisation of the main flow chart method followed for flood risk maps for the Lower Zambezi

The methodology, recommended by USGS (2000a) and Asante *et al.* (2005), was used to map the flood area and quantify the predicted impact of flooding. For this study, the flood area mapping was implemented combined with both GIS ArcView 3.2a and Spatial Analyst 1.1. The governing equation in this process is the energy Equation given in Asante *et al.* (2005)

Equation 4.26). The function uses the forecasted flow depths and the DEM (Digital Elevation Model) at 90 m x 90 m (Section 3.7) data to identify the area where flooding may occur.

$$H = z + y + \frac{v^2}{2g} \qquad \textbf{Equation 4.26}$$

where z is the elevation of the riverbed above datum (m), y is the depth of flow or pressure head (m); v is the flow velocity at the river cross-section (m s^{-1}) and g is the gravitational force. The sum of the pressure head (y) and elevation above datum (z) constitutes the river stage while the third term $\frac{v^2}{2g}$ is the velocity head.

A detailed example of flood levels mapping is given in (Appendix 1).

Flood impacts assessment: The flooding extent mapping generated a total of 15 flooding areas for the Lower Zambezi. The different areas which are likely to be inundated as a result of rising water levels at selected sites downstream of the Cahora Bassa dam were obtained by applying the following empirical equation (Equation 4.27) proposed by ARA-Sul (2005):

$$\begin{aligned} \Delta X &= 10.5 - X \\ N1 &= 10.5 - \Delta X \\ N2 &= N1 + \Delta X \\ N3 &= N2 + \Delta X \end{aligned} \qquad \textbf{Equation 4.27}$$

where Δx is a constant which indicates the water rising difference between the initial flood level and the maximum observed historical flood record in meters (which in this study was observed at 10.5 m in Tete (E-320) in the hydrological year 1957/1958) (Section 2.9); x is initial flood level; N1-Level 1; N2-Level 2 and N3-Level 3.

The assumption is that, having the initial and maximum references of a flood record, it is possible to estimate the other flood extent areas (which might be inundated) in between. In this study the initial level was fixed at 5 m on the reference scale and the maximum observed flood of 10.5 m at the Tete (E-320), Caia (E-291) and Marromeu (E-285) hydro-stations. The initial flood levels and maximum flood levels recorded for these hydro-stations were obtained from DNA flood records database. Three levels of flood were defined namely:

i. Flood Level 1 (N1), which corresponds to moderate flooding;

ii. Flood Level 2 (N2), which is major flooding;

iii. Flood Level 3 (N3) which is extreme flooding.

Data on villages, schools and hospitals were overlaid with flood areas using GIS to identify those that were likely to be inundated at different water level rises for each of eleven selected districts (Appendix 2).

Verification of flood risk maps: The accuracy of the flood risk maps was verified by comparing them with Landsat satellite images of flooded areas (obtained from the Famine Early Warning System Network on the 3rd of March, 2001) and by visits to villages, schools and hospitals which the results had classified, using the actual data from the flood in 2000/2001, as being within the high flood risk area (according to the DNA and ARA-Sul, DNA, 2014 reports on the impact assessment of the 1977-2013 floods).

4.8. Summary

This chapter presents descriptions of the application of the GeoSFM and MIKE BASIN numerical models for streamflow forecasting and reservoir modelling in the Zambezi Basin. The chapter describes the methods followed to calculate and predict water levels at different ranges of flow releases; explains the method used to estimate the flood peak travelling time, and demonstrates the method followed for flood risk mapping, using both Remote Sensing (RS) data and GIS. These methods were then used to test the performance modelling at four selected flood control sites. From the four sites, one is located at the dam site and three are downstream of the Cahora Bassa dam (Section 7.3.1 and Section 7.3.2).

Eleven districts located downstream of the Cahora Bassa dam, i.e. those areas considered the most exposed to flood risks, had flood extent maps produced for their areas.

5. RAINFALL ANALYSES

5.1. Introduction

The results and discussion of rainfall data, including the criteria for selecting remote sensing products for hydrological forecasting, are presented. The comparison between satellite rainfall estimates and observed point rainfall and the extent to which they were used as input for the stream flow predictions is also presented. Two satellite derived estimates were evaluated against the observed rainfall data in terms of spatial and temporal resolution and these were: the Climate Prediction Centre (CPC-RFE 2.0) and Tropical Rainfall Measuring Mission (TRMM 3B42) products. The comparison was done for the period 1999 – 2008. This process was first done by comparing the daily CPC-RFE 2.0 and TRMM 3B42 data (extracted from pixels where the station is located, with the station data itself after interpolated to ensure use of the same pixels). The interpolation of observed data was done at 8 km x 8 km and 25 km x 25 km, using the Kriging method in GIS, chosen to optimise the smoothness of the fitted values. Secondly, a continuous verification statistic (which included the Coefficient of Determination (R^2), Relative bias (Rbias), Relative Root Mean Square Error (RRMSE) and the Index of Agreement (IA) was carried out to obtain a quantitative assessment for each set of validated data (Ebert, 2007; Ebert *et al.,* 2007). The validated Satellite Rainfall Estimate (RFE) data are of fundamental importance in this study because they were used to fill in data missing from the observed records for the modelling application/s. Fundamental difficulties existed when comparing gauge measurements and satellite estimates and these included: retrieval errors of satellite algorithms; sampling errors caused by different sampling schemes; and systematic gauge errors related to instruments (Ciach and Krajewski, 1999; Bowman, 2005). The aim of this study, however, is not to quantify the errors of satellite estimates in individual rain events, but to evaluate the overall performance of the two satellite products when compared with using rain gauge data as input into hydrological model. This evaluation was used to gather information on the type of product to recommend for input into hydrological modelling studies in the Zambezi River Basin. In the Zambezi Basin, the comparison of TRMM 3B42 and CPC-RFE 2.0 estimates with the *in situ* station records, at a monthly time scale, indicated that TRMM often underestimates (by up to 50%) during the wet season and overestimates (by up to 50%) during dry months, whereas the CPC-RFE 2.0 showed less bias (Winsemius *et al*., 2006; Liechti *et al*., 2011). Based on the divergent results obtained from previous studies and the lack of validation at the daily time scale, one of the objectives of this study has been to provide a comparison and evaluation of the different sources of input data that can be used for the hydrological modelling and flood forecasting of the Zambezi Basin at the daily time step.

5.2. Statistical methods for comparison of rain gauge and satellite rainfall estimates

The first part of the analysis focused on the comparison of the different satellite estimates against rain gauge based rainfall estimates to highlight both the similarities and the discordances. The Pearson Correlation Coefficient (R^2) was used to compare the time series between the rain gauge data and the satellite data in the same pixel from 1999 – 2008. Twenty selected rain gauge stations were analysed (Table 3.1, Section 3.4.2.1). For these rain gauge stations, the Global Telecommunication System (GTS) was excluded from the analysis, because GTS may have influenced the statistics agreement when compared with the CPC-RFE 2.0. The original grid size for each product was used to extract the satellite rainfall values. As most of the observed rain gauge data contains large gaps, only those time series with a minimum of at least 20 continuous daily values were used in the analysis at a daily time step. The correlation between satellite products and rain gauge data was evaluated by applying the Coefficient of Determination (R^2), Bias and Relative bias, the Relative Root Mean Square Error (RRMSE), and the Index of agreement (IA) (Daren and Smith, 2007) (Equation 5.1 to Equation 5.5).

$$R^2 = \frac{\sum_{i=1}^{n}(0_i - \bar{0})(S_i - \bar{S})}{\sqrt{\sum_{i=1}^{n}(O_i - \bar{0})^2 \times \sqrt{\sum_{i=1}^{n}(S_i - \bar{S})^2}}}$$ **Equation 5.1**

$$Bias = \sum_{i=1}^{n}(S_i - 0_i)$$ **Equation 5.2**

$$Relative\ bias = \frac{\sum_{i=1}^{n}(S_i - 0_i)}{\sum_{i=1}^{n}\bar{0}}$$ **Equation 5.3**

$$RRMSE = \frac{\sqrt{\frac{1}{n}\sum_{i=1}^{n}(S_i - O_i)^2}}{\bar{0}}$$ **Equation 5.4**

$$IA = 1 - \left[\frac{\sum_{i=1}^{n}(S_i - O_i)^2}{\sum_{i=1}^{n}(|S_i - \bar{O}| + |Oi - \bar{O}|)^2}\right]$$ **Equation 5.5**

where "S_i" is the satellite data, "o_i" the observed data and "$\bar{0}$" the mean of the observed data.

The Coefficient of Determination: R^2 is a standard correlation statistic designed to determine the strength of the linear relationship between simulated and observed data (Legates and McCabe, 1990; Ebert *et al.,* 2007; Moriasi *et al.*, 2007). This statistic describes the proportion of the total variance in the observed data which can be explained by the model and the ranges is expressed between 0 and 1, with higher values indicating the ability of the model to explain more variance in the observed data.

The Bias: Bias is the difference between the estimator's expected value and the true value of the parameter being estimated. An estimator (or decision rule) with zero bias is called unbiased – otherwise the estimator is said to be biased. For this study the acceptable range for data validation was chosen to be ±0.50.

The Relative bias (Rbias): Rbias is an error index that measures the individual and average deviation of the satellite mean daily rainfall from the observed rain gauge data (Moriasi *et al*., 2007). Zero is the optimal value of both bias and relative bias and the deviation from this value, whether positive or negative, indicates errors in the model prediction. For this study the acceptable range for data validation was chosen to be ±0.20.

The Relative Root Mean Square Error (RRMSE): RRMSE is used to measure the differences between values predicted by the satellites and those by observed rain gauge data. If the RRMSE is high, then the observed rain gauge values are not close to the satellites values; if the RRMSE is low, the satellite values are well predicted (Moriasi *et al*., 2007).

The Index of Agreement (IA): IA is a standardised measure of the degree of model prediction error and varies between 0 and 1 (Legates and Willmott, 1990). A value of 1 indicates a perfect match, and 0 indicates no agreement at all. For this study the acceptable range for data validation was ≈ 0.5.The comparison between satellite and rain gauge data was also done temporally through a time series comparison and a probability of exceedence, from October 1999 to 2008. Spatial comparisons were also performed for the wet seasons from 1999 to 2008.

5.3. Comparative analysis of rainfall inputs

5.3.1. Daily temporal rainfall assessment

To enable a reasonable graphical analysis, a sample comparison of time series of rain gauge and satellite rainfall data is shown in Figure 5.1. The detailed statistical comparison based on R^2 for CPC-RFE 2.0 and the rain gauge data was above 0.5 for most of the stations, (with the exception of P-176, P-218, P-325, P-333, P-829 and P-893, where the correlation coefficients were low) (Table 5.1). Therefore, the CPC-RFE 2.0 is significant when correlated with observed rainfall data at $P < 0.00001$. The bias between the daily observed and CPC-RFE 2.0 ranged from -1.42 to +0.6. These findings are in agreement with those obtained by similar studies in the East and Western Africa (Dinku *et al.,* 2008; Roca *et al.,* 2010). The other statistics also showed that the satellite products were reasonably good (Table 5.1). At a daily time step, reasonably significant correlation existed between the satellite estimates and the rain gauge data at 639320, 678810, 677430, 675860 and 675610, where R^2 was above 0.5

when compared with the TRMM 3B42 data). The bias between the daily observed and TRMM 3B42 data ranged from -3.43 to +0.4.

Therefore, overall the CPC-RFE 2.0 data were reasonably significant when correlated with observed rainfall data at $P < 0.00001$, but were relatively more biased when compared with the TRMM 3B42 correlations. The analysis also demonstrated that CPC-RFE 2.0 and TRMM 3B42 occasionally failed to register any significant rainfall amount on a particular day, even though the rain gauges registered the occurrence of rainfall on the same day – and vice versa. In some situations, the rain gauge network may have registered high values while the CPC-RFE 2.0 and/or TRMM 3B42 had both registered low values (Figure 5.1) and these findings have influenced the trend of the probability of exceedence curves (Figure 5.2). The results are consistent with the findings of other recent studies on satellite rainfall estimation which concluded that satellite-based precipitation underestimates heavy precipitation in comparison with the rain gauge-based observations on a daily basis (e.g. Liechti *et al*., 2011; Gao and Liu, 2013). The CPC-RFE 2.0 showed improved statistics, with R^2 ranging between 0.2 and 0.77 when compared with TRMM 3B42. The TRMM 3B42 displayed a R^2 ranging between 0.1 to 0.72. These results were obtained when both sets of satellite data were being compared with the rain gauge data for the same period. The CPC-RFE 2.0 underestimated the rainfall by approximately 0.17 and the TRMM 3B42 by approximately 0.5, as shown by the relative bias for each station (Table 5.1). The results are consistent with previous findings by Romilly and Gebremichael (2011), who concluded that the CPC-RFE 2.0 underestimated the rainfall by 0.11 on daily time step. Using the Agreement Index criteria, CPC-RFE 2.0 showed good performance, with an average of approximately 0.52; whereas the TRMM 3B42 had an average value of 0.18. Therefore, CPE-RFE 2.0 is a more reliable product to use in the Zambezi Basin when compared with TRMM 3B42.

Table 5.1: Statistical comparison of the satellite products (at daily time step) to rain gauge estimates at selected rain gauges

Rain gauge ID	Satellite data	Statistics				
		R^2	Bias	Relative bias	RRMSE	IA
639320	CPC- RFE 2.0	0.70	0.64	0.52	2.00	0.68
	TRMM 3B42	0.51	-0.10	-0.10	2.40	0.50
675610	CPC- RFE 2.0	0.64	0.28	0.15	3.40	0.63
	TRMM 3B42	0.62	0.03	0.03	3.90	0.59
675860	CPC- RFE 2.0	0.71	0.58	0.53	3.00	0.70
	TRMM 3B42	0.61	-0.03	-0.08	3.40	0.61
677430	CPC- RFE 2.0	0.63	0.55	-0.09	2.78	0.58
	TRMM 3B42	0.50	0.20	0.90	0.51	0.64
678810	CPC- RFE 2.0	0.77	0.17	0.13	2.30	0.74
	TRMM 3B42	0.72	-0.40	-0.30	2.30	0.68
680260	CPC- RFE 2.0	0.64	0.56	0.78	3.70	0.58
	TRMM 3B42	0.51	0.10	0.10	3.70	0.45
677610	CPC- RFE 2.0	0.70	0.10	0.01	1.60	0.68
	TRMM 3B42	0.40	-1.10	-0.60	4.30	0.35
677650	CPC- RFE 2.0	0.57	-0.04	-0.02	1.00	0.53
	TRMM 3B42	0.40	-1.10	-0.60	4.10	0.38
P-44	CPC- RFE 2.0	0.57	0.28	0.15	3.76	0.53
	TRMM 3B42	0.20	-0.81	-0.45	5.25	0.13
P-50	CPC- RFE 2.0	0.45	-0.86	-0.47	5.19	0.14
	TRMM 3B42	0.01	-1.24	-0.68	4.81	0.14
P-60	CPC- RFE 2.0	0.66	-0.20	-0.09	2.78	0.58
	TRMM 3B42	0.20	-1.18	-0.52	4.32	0.19
P-176	CPC- RFE 2.0	0.33	-0.80	-0.33	4.35	0.45
	TRMM 3B42	0.01	-1.84	-0.76	4.80	0.14
P-180	CPC- RFE 2.0	0.72	-0.13	-0.07	3.38	0.61
	TRMM 3B42	0.20	-1.22	-0.64	5.09	0.15
P-218	CPC- RFE 2.0	0.43	-0.57	-0.22	4.01	0.42
	TRMM 3B42	0.03	-1.95	-0.76	3.79	0.22
P-325	CPC- RFE 2.0	0.27	0.08	0.04	4.75	0.25
	TRMM 3B42	0.02	-0.89	-0.52	4.90	0.17

Rain gauge ID	Satellite data	Statistics-Continued				
		R^2	Bias	Relative bias	RRMSE	IA
P-333	CPC- RFE 2.0	0.20	-1.06	-0.41	3.49	0.18
	TRMM 3B42	0.10	-1.42	-0.55	4.02	0.19
P-335	CPC- RFE 2.0	0.55	-0.44	-0.19	3.74	0.49
	TRMM 3B42	0.40	-1.29	-0.55	4.56	0.20
P-786	CPC- RFE 2.0	0.51	-1.19	-0.43	3.59	0.47
	TRMM 3B42	0.30	-3.27	-1.17	4.24	0.21
P-829	CPC- RFE 2.0	0.39	-2.18	-0.54	3.11	0.24
	TRMM 3B42	0.20	-3.43	-0.85	3.33	0.23
P-893	CPC- RFE 2.0	0.28	-0.17	-0.10	3.99	0.35
	TRMM 3B42	0.01	-0.84	-0.48	5.00	0.17

The following five graphs show the sample of comparisons between in-situ rain gauge measurements and satellite-derived rainfall estimates.

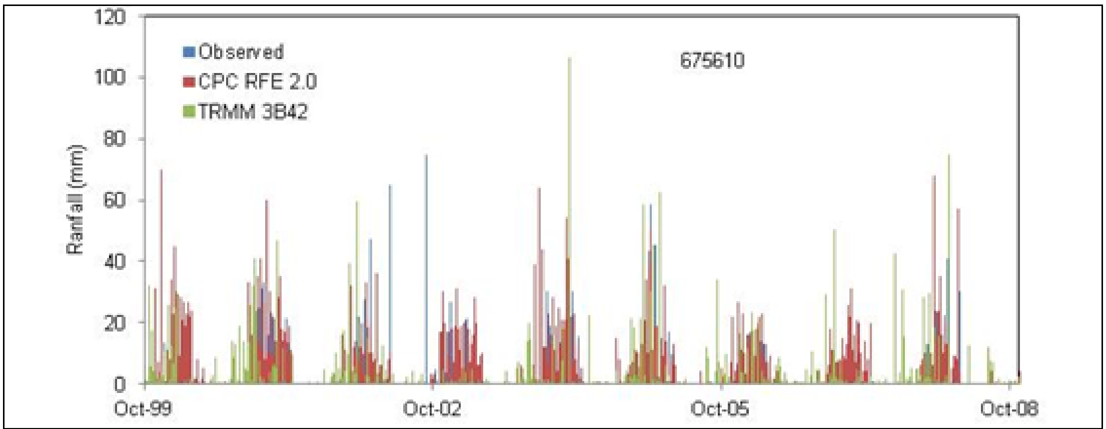

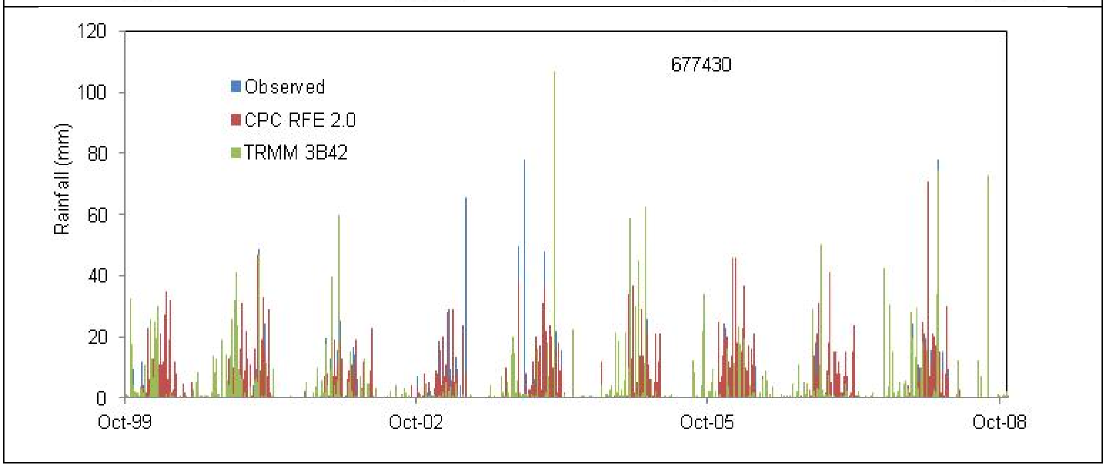

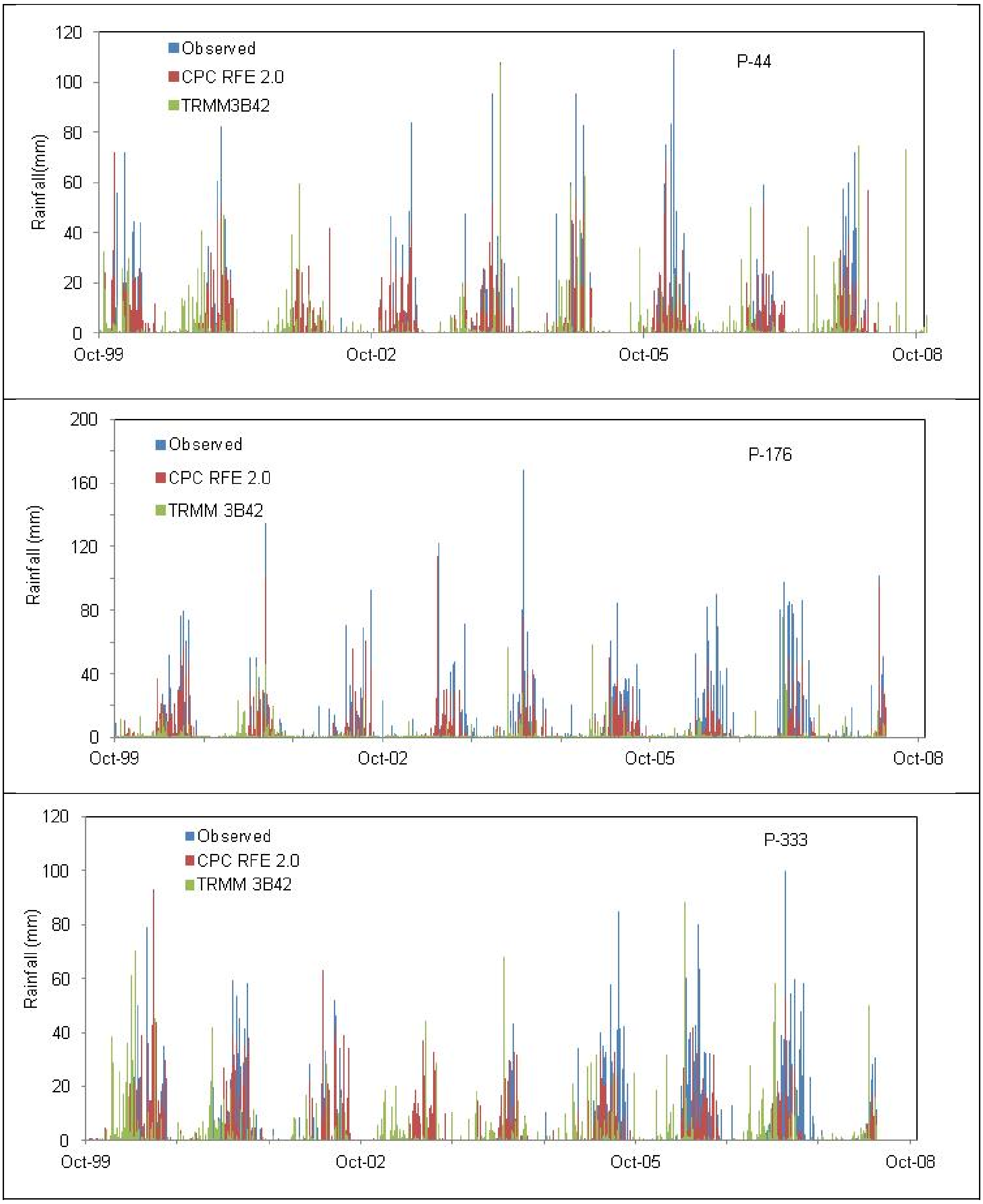

Figure 5.1: Sample comparisons of daily rain gauge observed and satellite-derived rainfall estimates (CPC-RFE 2.0 and TRMM 3B42), displayed in mm day^{-1} from 1 October 1999 to 31 October 2008

The following nine pairs of graphs demonstrate the rainfall frequency of exceedence curves, also between 1 October 1999 and 31 October 2008.

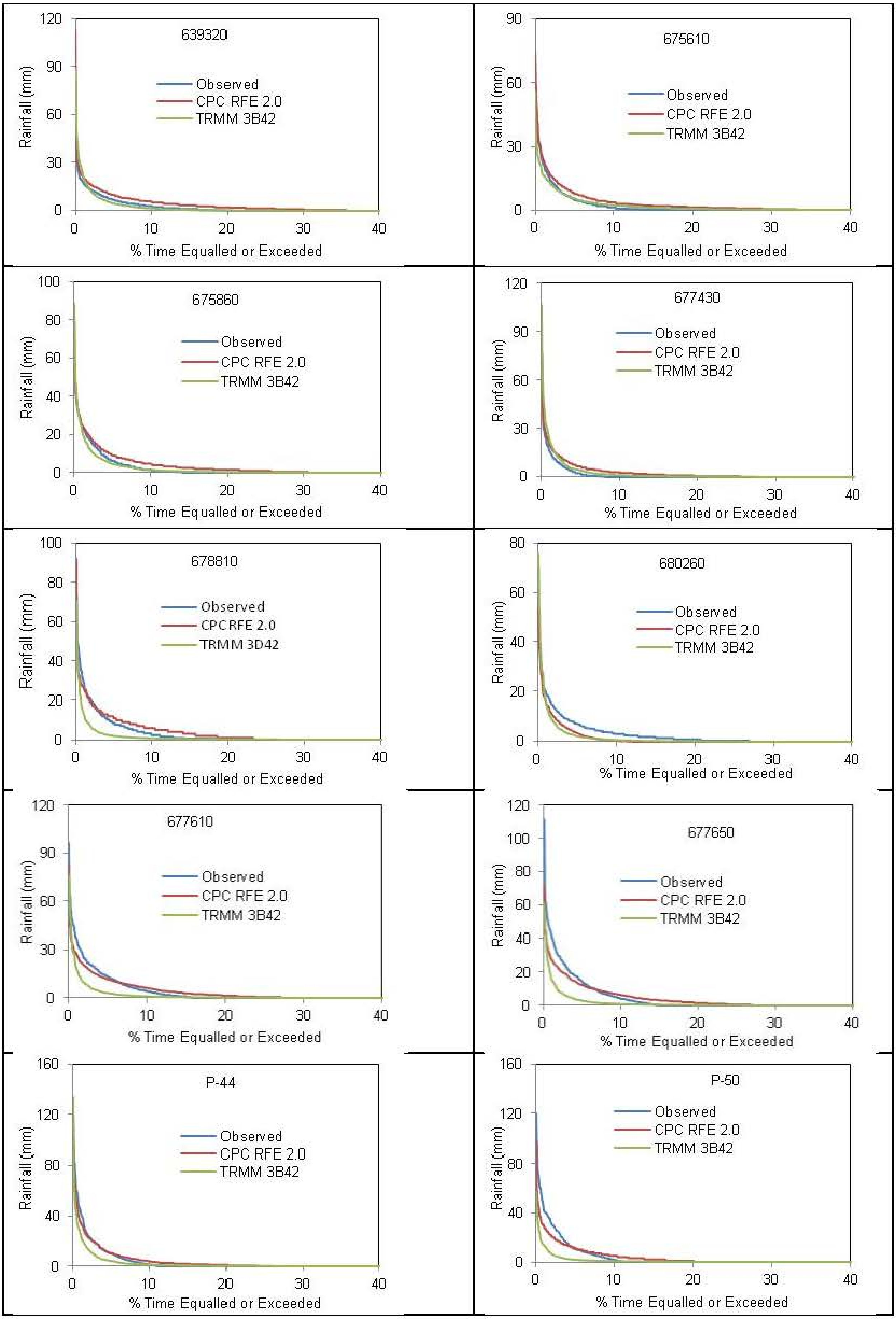
639320
Observed
CPC RFE 2.0
TRMM 3B42
Rainfall (mm)
% Time Equalled or Exceeded
675610
Observed
CPC RFE 2.0
TRMM 3B42
Rainfall (mm)
% Time Equalled or Exceeded
675860
Observed
CPC RFE 2.0
TRMM 3B42
Rainfall (mm)
% Time Equalled or Exceeded
677430
Observed
CPC RFE 2.0
TRMM 3B42
Rainfall (mm)
% Time Equalled or Exceeded
678810
Observed
CPC RFE 2.0
TRMM 3D42
Rainfall (mm)
% Time Equalled or Exceeded
680260
Observed
CPC RFE 2.0
TRMM 3B42
Rainfall (mm)
% Time Equalled or Exceeded
677610
Observed
CPC RFE 2.0
TRMM 3B42
Rainfall (mm)
% Time Equalled or Exceeded
677650
Observed
CPC RFE 2.0
TRMM 3B42
Rainfall (mm)
% Time Equalled or Exceeded
P-44
Observed
CPC RFE 2.0
TRMM 3B42
Rainfall (mm)
% Time Equalled or Exceeded
P-50
Observed
CPC RFE 2.0
TRMM 3B42
Rainfall (mm)
% Time Equalled or Exceeded

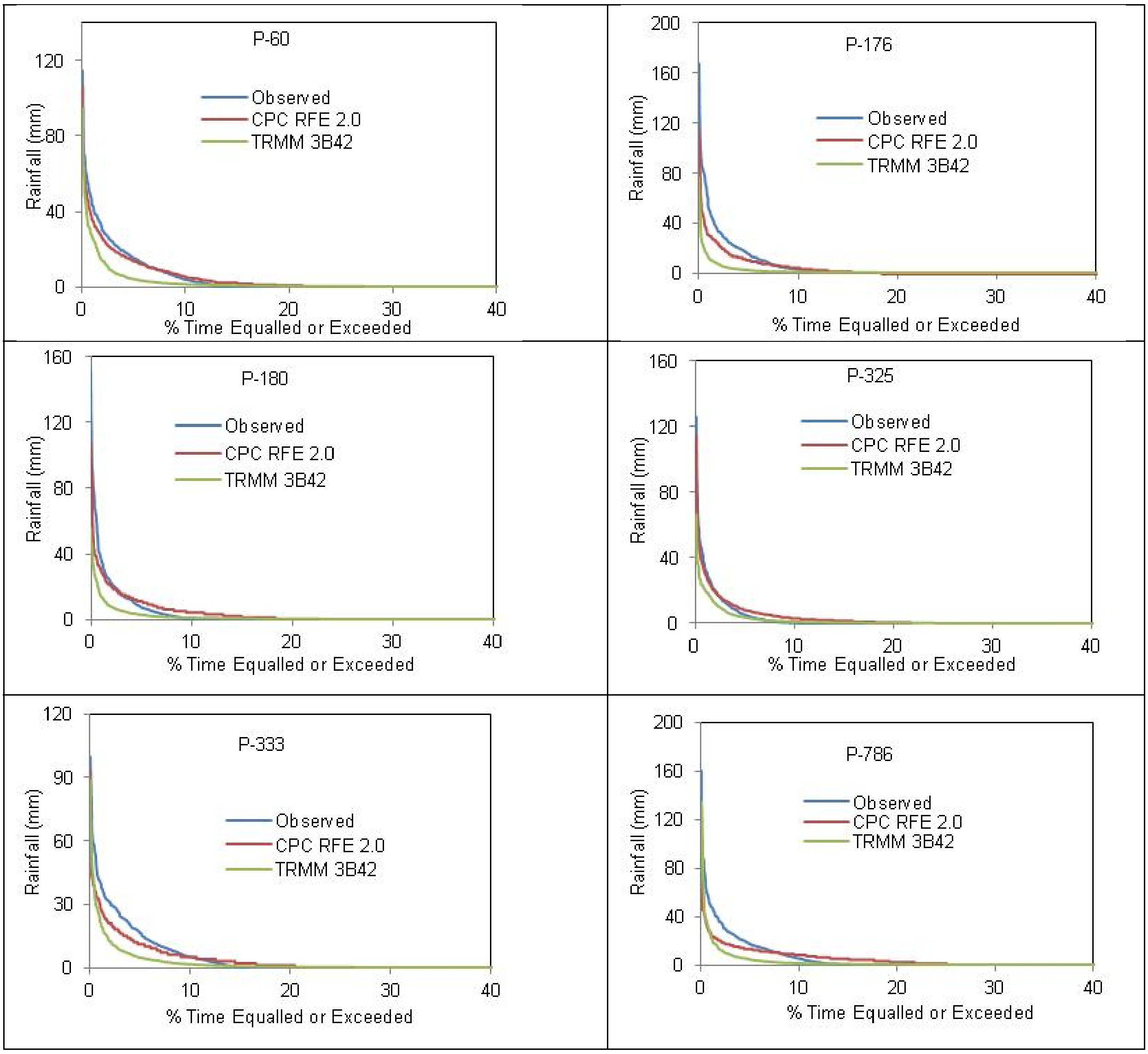

Figure 5.2: Comparison of rainfall frequency of exceedence curves, 1 October 1999 to 31 October 2008

5.3.2. Spatial rainfall assessment

In this study, the spatial variation analysis was performed to capture the spatial agreement between observed rainfall and predicted by the satellite products. While recognising that there are a number of alternative spatial interpolation approaches, the Inverse Distance Weighting procedure (IDW) has been used throughout this study. This technique was chosen because it is simple and efficient and forms part of widely available Geographic Information Systems (GIS) software (Artan *et al.,* 2007). This study used the availability reasonably good quality rainfall data as the criteria to include key rain gauges for data analysis and validation. When there were missing data in the records, the interpolation approach used the next closest rain gauge, but only if the gauge lay within the defined searching radius. This approach prevented rain gauges which are too far from the sub-basin being used – even when optimally located rain gauges have missing data periods. In this application, the rain gauge rainfall data were interpolated at 0.25^0 by 0.25^0 grids of spatial resolution. The data were compared by means of maps of mean rainfall for the daily rain, from 1 October 1999 to 30 September 2008, to evaluate the spatial distribution of the satellite precision. The sampling results (Figure 5.3), show a general North-South gradient in the intensity of precipitation for the period of the analysis.

The CPC-RFE 2.0 and TRMM 3B42 datasets registered lower rainfall intensities than the observed rain gauge dataset. The region of Lake Malawi, located in North-East side of the Zambezi Basin, is characterised by lower rainfall in comparison with the Central and North-West areas. The grid pixels above the ocean (South-East corner) revealed lower rainfall than those of the coastal. The ground gauge data showed the highest spatial variability of rainfall. The rainfall varied from 600 to 1 800 mm for the total annual accumulated rainfall and seemed to overestimate the precipitated amount in the North-West and South-East regions. The bias in the satellite rainfall estimates depends on both the rainfall regime and, in certain regions, the elevation. In the North-West region (which is characterised mainly by three factors: highland topography; a humid climate and a strong Inter Tropical Convergence Zone (ITCZ) effect) the elevation had a strong influence on the accuracy of the CPC-RFE 2.0 and TRMM 3B42 – at higher elevations the satellite products underestimated rainfall. In the South-East region (characterised mainly by lowland topography), elevation did not appear to have a significant influence on the accuracy of satellite products. Regardless of the product, the central part of the basin seems to be homogeneous; the region over Lower Zambezi seems rather heterogeneous. In terms of spatial comparison, CPC-RFE 2.0 predicted rainfall better than TRMM 3B42. The following twelve figures show the spatial comparison of daily observed CPC-RFE 2.0 and TRMM 3B42 data for the period 26 February 2000 to 29 February 2000.

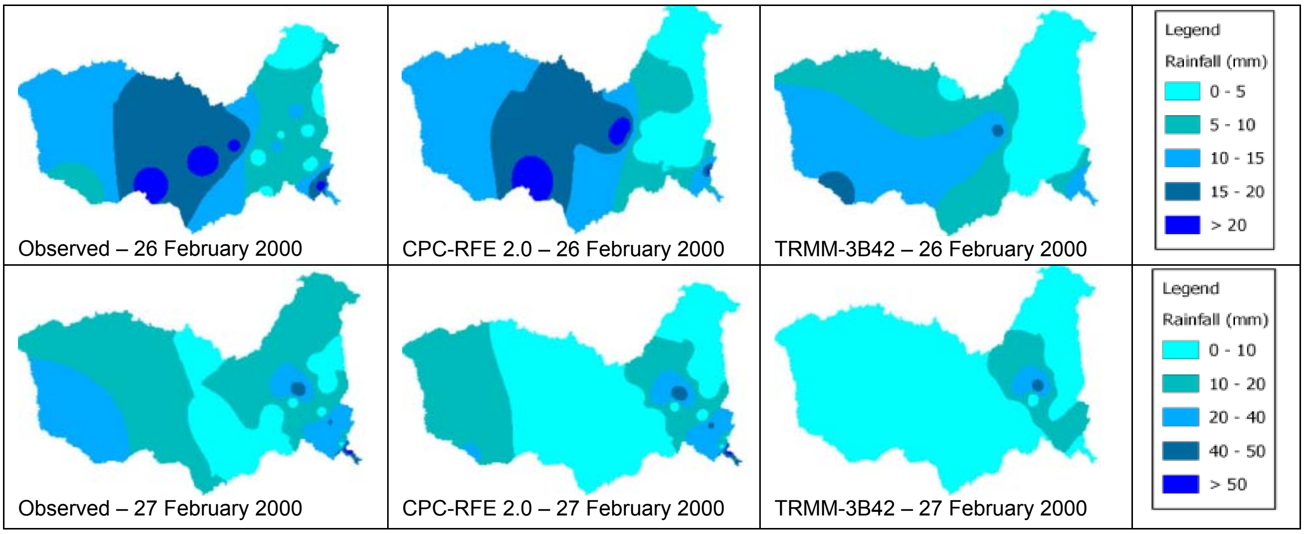

Observed – 26 February 2000
CPC-RFE 2.0 – 26 February 2000
TRMM-3B42 – 26 February 2000
Observed – 27 February 2000
CPC-RFE 2.0 – 27 February 2000
TRMM-3B42 – 27 February 2000

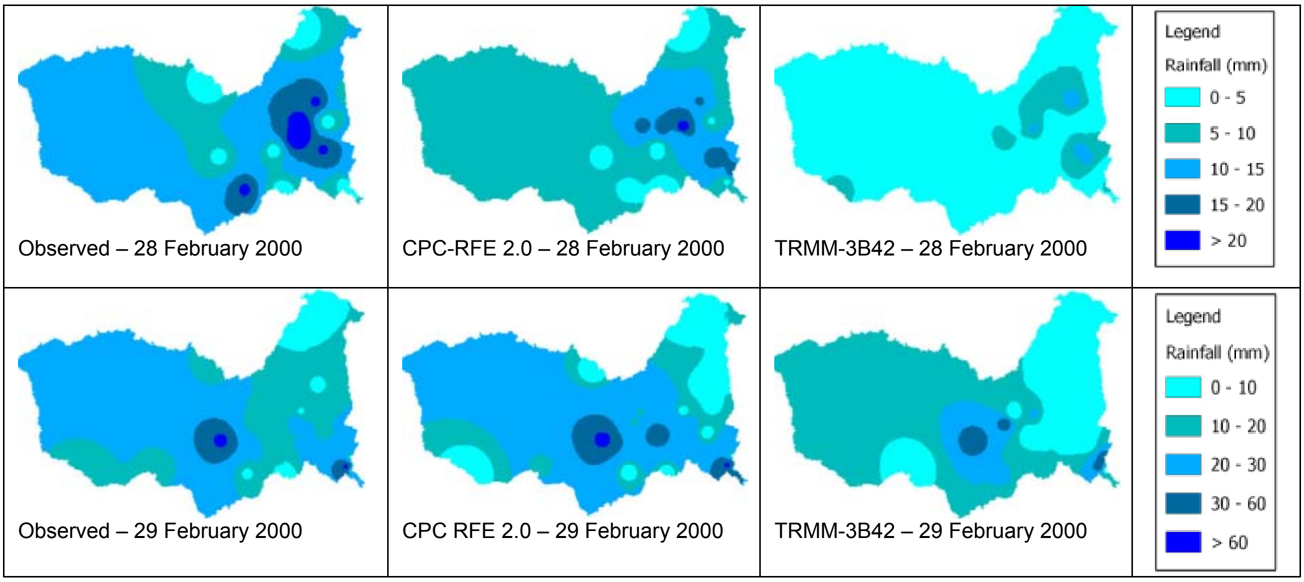

Figure 5.3: Sample of spatial comparison of daily observed CPC-RFE 2.0 and TRMM 3B42 data for the Zambezi Basin displayed as mm day^{-1} from 26 February 2000 to 29 February 2000

5.4. Correction of satellite rainfall

Previous studies (Sawunyama and Hughes, 2008; Liechti *et al.,* 2011) have demonstrated that, in some parts of Southern Africa, satellite rainfall underestimates real rainfall and thus this study recognised the need to correct satellite estimates before they were used as input to a hydrological model. As a consequence, this study used a sample of rain gauges, assumed to provide the best estimate of the true rainfall values, to test a method that can be applied for adjusting satellite rainfall. Various techniques of rain gauge point value interpolation have been developed to estimate not only area-averaged ground rainfall accumulation but also to define the sampling errors associated with the interpolation of the point values over their surrounding spatial domain (Hughes and Smakhtin, 1996; Sawunyama, 2008; Roca *et al.,* 2010). The accuracy of most of the standard methods used to interpolate point rainfall estimates (such as point to pixel, Inverse Distance Weighting, Theissen polygons and Kriging) varies, depending on basin topographical characteristics and the density of the gauge network within the basin (Schäfer, 1991; Liechti *et al.,* 2011). These methods usually fail to yield accurate estimates of spatially averaged (areal) rainfall in basins where there is a marked variability in relief, experiencing strong orographic rainfall influences and they often lead to smoothing errors.

Frequently inadequate rain gauge distributions in elevated areas fail to capture systematic spatial variations of rainfall. Interpolation methods also generally fail to give accurate rainfall estimates in areas experiencing convective rainfall with typically high degrees of spatial variation within individual storms. The ground-based and satellite rainfall products, both TRMM 3B42 and CPC-RFE 2.0, are also subject to uncertainties. Within the Zambezi Basin, most of the rainfall is measured using non-recording rain gauges, where errors in measuring rainfall normally arise from human error in taking readings, faulty instruments and damage to the collectors. Other errors are related to incorrect calibration of instruments and a lack of training of the staff. The satellite-based precipitation estimates are affected by false precipitation artefacts (often over mountainous regions). The underestimation of shallow orographic and monsoon system rainfall, compared with observations on a daily basis, is because of the difference in the Infra-Red (IR) based estimates used in the algorithms. Among the techniques used to correct satellite rainfall data are the Linear Interpolation Estimator (LIE) (Morrissey *et al*., 1995) and the patching method in SPATSIM (Sawunyama and Hughes, 2008). These two techniques appear to be options that could be explored for satellite data correction at the daily time step in the Zambezi Basin. LIE is a method of curve fitting, using linear polynomials (Morrissey *et al*., 1995; Roca *et al*., 2010). The detailed unweighted LIE method of rain gauge accumulations and comparison of the sampling errors associated with various geometries of networks is presented in Morrissey *et al*. (1995). Generally the data correction approach using the LIE can be given by expressions shown in Equations 5.6 and 5.7 and Figure 5.4 which show an example of the application of the Linear Interpolation Estimator method.

$$\frac{\text{Satellite}_{\text{daily}}}{\text{Satellite}_{\text{monthly}}} = \frac{\text{Raingauge}_{\text{daily}}}{\text{Raingauge}_{\text{monthly}}}$$ **Equation 5.6**

$$\text{Satellite}_{\text{correction}} = \text{Raingauge}_{\text{daily}} * \left(\frac{\text{Satellite}_{\text{monthly}}}{\text{Raingauge}_{\text{monthly}}}\right)$$ **Equation 5.7**

According to Morrissey *et al.* (1995) linear interpolation is a method for obtaining values at positions between the data points. The points are joined by straight line segments (Figure 5.4). Each segment (bounded by two data points) can be interpolated independently. The method uses a sample of control points in estimating an unknown value, so a change in an input value will only affect the result within the neighbouring points. The advantage of LIE is that the values of the known points stay unchanged in the process of interpolation allowing LIE to can display the spatial anomalies of a phenomenon. The two disadvantages of local interpolation are that, even if the method displays the spatial anomalies of a phenomenon, the LIE does not explain the causal factors and LIE needs a dense network of points with known values.

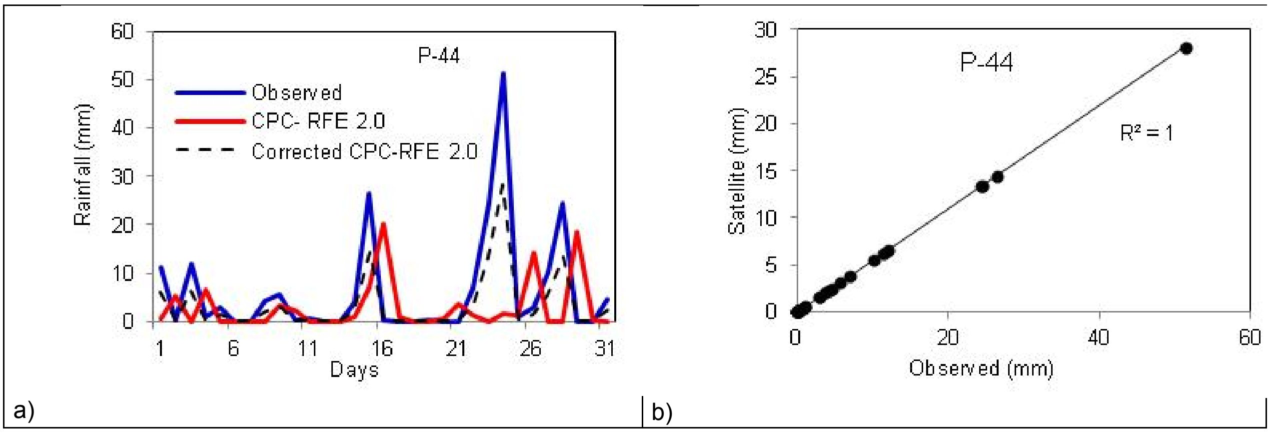

Figure 5.4: Application of the Linear Interpolation Estimator method, shown as a graph (a) and a scatter plot (b) on corrected satellite and observed data, at P-44 as an example, for the month of December, 2008

In this study, the entire recorded dataset for the period 1999 – 2008 for both CPC-RFE 2.0 and TRMM 3B42 was used in the analysis when applying the LIE method for error correction. This was the longest period, spanned by all the rain gauge records that were available, with reasonably continuous daily time series and quality data for use in this study. The results are presented in Table 5.2 and illustrated, using gauges P-44, P-50, P-176, P-325, and P-786 in Figure 5.5. The LIE approach appeared to work satisfactorily with almost all of the satellite corrections, showing good agreement with the rain gauge data, based on several performance criteria. The right hand side of Figure 5.5 illustrates that the frequency of exceedence characteristics of the corrected satellite data were much improved when compared with the uncorrected satellite data (Figure 5.5). The CPC-RFE 2.0 satellite results were better than the TRMM 3B42 results in most cases. Given that the spatial analysis presented in Section 5.3.2 also favoured the CPC-RFE 2.0 product, these data were selected for further use with the hydrological model (Chapter 6).

Table 5.2: Statistical analysis of corrected satellite rainfall estimates compared against actual rain gauge observed rainfall in mm day^{-1} for selected rain gauges

Rain gauge ID	Satellite Data	Statistics				
		R^2	Bias	Rbias	RRMSE	IA
639320	CPC-RFE 2.0	0.93	0.10	0.01	0.80	0.89
	TRMM 3B42	0.94	0.10	-0.30	2.30	0.91
675610	CPC-RFE 2.0	0.99	-0.04	-0.02	1.00	0.98
	TRMM 3B42	0.98	-1.10	-0.60	4.10	0.96
675860	CPC-RFE 2.0	0.91	0.28	0.23	1.80	0.87
	TRMM 3B42	0.91	-0.01	-0.08	2.40	0.81
677430	CPC-RFE 2.0	0.94	0.10	0.01	0.70	0.87
	TRMM 3B42	0.90	0.10	-0.30	2.30	0.86
678810	CPC-RFE 2.0	0.97	0.07	0.03	1.30	0.94
	TRMM 3B42	0.97	-0.10	-0.30	1.30	0.93
680260	CPC-RFE 2.0	0.91	-0.04	-0.02	1.00	0.83
	TRMM 3B42	0.92	-1.10	-0.60	3.10	0.88
677610	CPC-RFE 2.0	0.95	0.10	0.01	0.80	0.90
	TRMM 3B42	0.98	0.10	-0.30	1.30	0.92
677650	CPC-RFE 2.0	0.83	-0.04	-0.02	1.00	0.83
	TRMM 3B42	0.73	-1.10	-0.60	4.10	0.68
P-44	CPC-RFE 2.0	0.96	-0.70	0.20	0.50	0.88
	TRMM 3B42	0.97	-2.20	-0.60	1.10	0.93
P-50	CPC-RFE 2.0	0.93	-0.90	-0.90	0.60	0.90
	TRMM 3B42	0.98	-2.30	-2.30	1.10	0.91
P-60	CPC-RFE 2.0	0.95	-0.70	-2.00	0.50	0.90
	TRMM 3B42	0.97	-2.20	-0.60	1.10	0.91
P-176	CPC-RFE 2.0	0.95	-1.20	-0.30	0.60	0.90
	TRMM 3B42	0.94	-3.00	-0.60	0.40	0.89
P-180	CPC-RFE 2.0	0.95	-1.40	-0.30	0.80	0.90
	TRMM 3B42	0.98	-2.10	-0.50	1.10	0.90
P-218	CPC-RFE 2.0	0.88	-2.10	-0.40	0.80	0.88
	TRMM 3B42	0.96	-3.60	-0.70	1.20	0.79
P-325	CPC-RFE 2.0	0.98	-2.10	-0.40	0.80	0.82
	TRMM 3B42	0.91	-2.80	-0.60	1.00	0.76

Rain gauge ID	Satellite Data	Statistics-Continued				
		R^2	Bias	Rbias	RRMSE	IA
P-333	CPC-RFE 2.0	0.98	-0.30	-0.30	0.60	0.80
	TRMM 3B42	0.91	-0.60	0.60	0.90	0.70
P-335	CPC-RFE 2.0	0.93	-0.90	-0.20	0.60	0.90
	TRMM 3B42	0.80	-2.60	-0.60	1.00	0.70
P-786	CPC-RFE 2.0	0.94	-1.20	-0.20	0.50	0.90
	TRMM 3B42	0.80	-2.90	-0.60	0.90	0.72
P-829	CPC-RFE 2.0	0.92	0.40	-0.50	1.00	0.78
	TRMM 3B42	0.91	0.50	-0.70	1.10	0.76
P-893	CPC-RFE 2.0	0.83	0.10	-0.34	0.70	0.90
	TRMM 3B42	0.73	-0.50	-0.10	0.40	0.90

The following seven pairs of graphs detail the comparisons, through scatter plots and frequency of exceedence curves, of daily rainfall for the period 1999 to 2008.

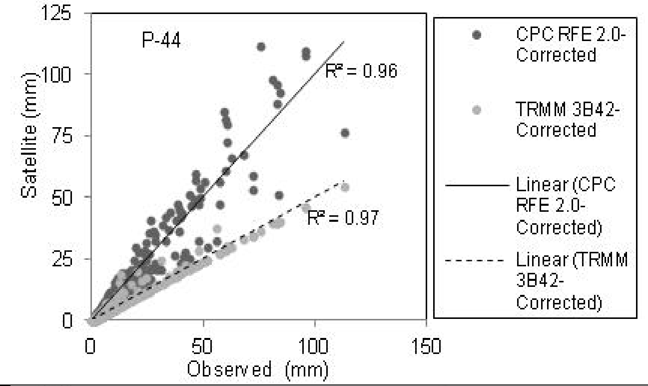

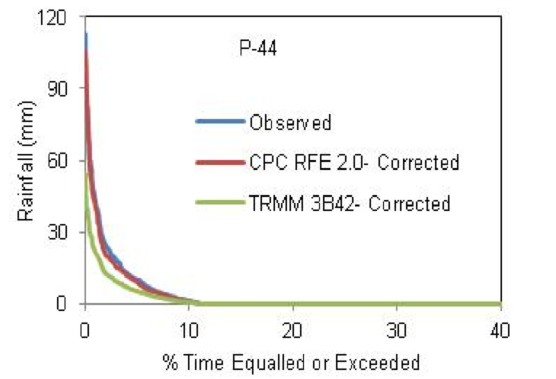

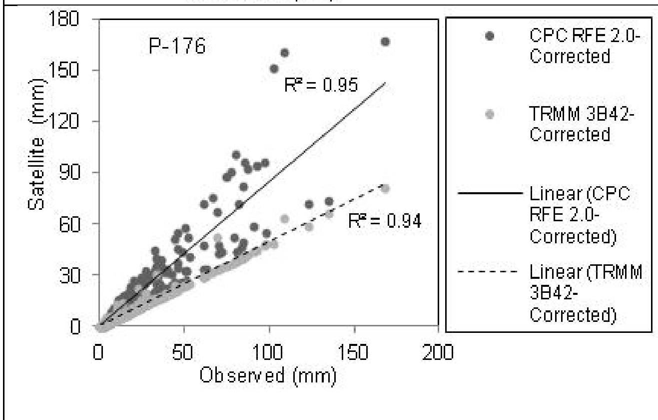

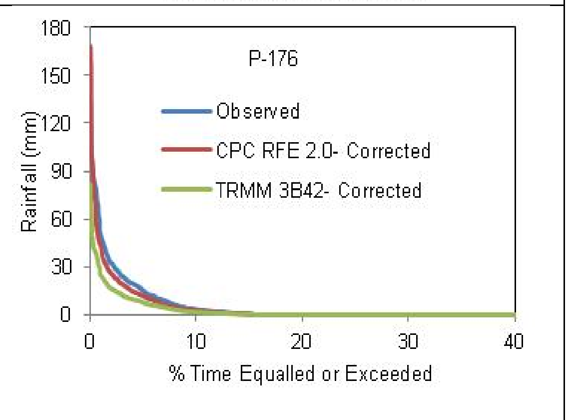

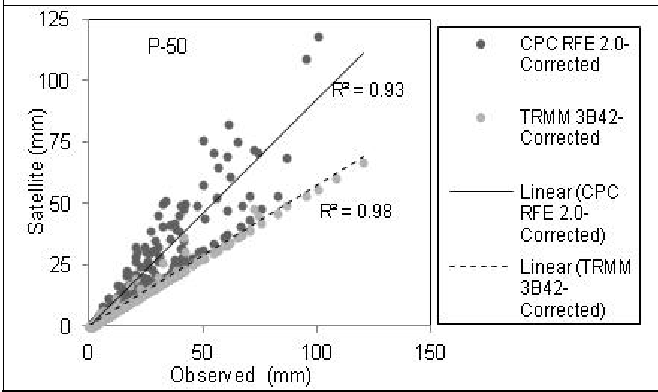

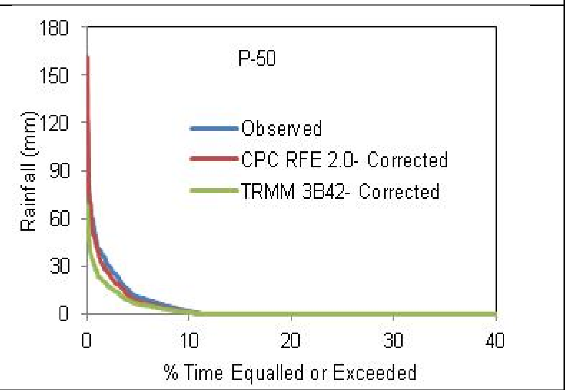

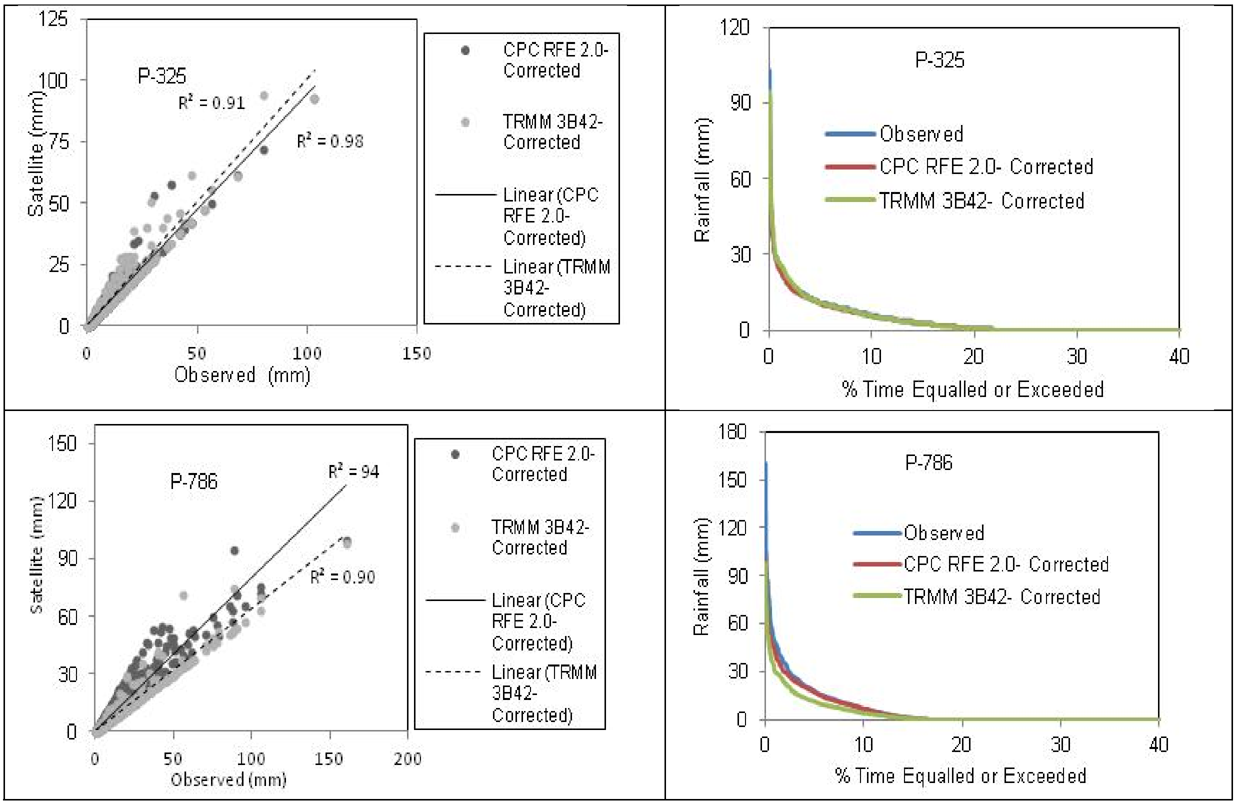

Figure 5.5: Comparison of scatter plots and frequency of exceedence curves of daily rainfall. The above graphs detail the observed data and satellite-based estimates for the selected sampling rain gauge stations, showing CPC-RFE 2.0 (black points) and TRMM 3B42 (gray points) versus ground observed data for daily (mm day^{-1}) time step for the period 1999 to 2008

5.5. Summary

Satellite-based estimates were compared with ground-based observed data on a daily time step. Clearly, the comparison was not expected to provide results identical to the gauge measurements because both the temporal and the spatial samplings were different. The gauge stations provided point measurements observed over continuous periods of time; the satellites delivered spatial averages based on intermittent rain rate estimates. Furthermore, the satellites produce estimates over a broad area, thus having a tendency to smooth localised phenomena – a smoothing process which can substantially affect the interpretation of data from the gauging stations. Given that CPC-RFE 2.0 data have been demonstrated to show better statistics (compared with the TRMM 3B42), these data were chosen as the input data for hydrological modelling for flood forecasting in this study. The results presented underline the fact that rainfall input data have to be studied before modelling the hydrological behaviour of a basin to calculate the size of rainfall events and their distribution through space and time. Moreover, the results illustrate a very strong dependency on the quality of the satellite product within the region of interest.

6. FLOOD FORECASTING MODEL CALIBRATION FOR THE ZAMBEZI BASIN

6.1. Introduction

This chapter presents the results and discusses the model application exercise in the Zambezi Basin. The results are presented as comparisons between simulated and observed streamflow. The chapter also shows how the simulated streamflow from GeoSFM was used for flood prediction through the integration into a reservoir and hydropower model (MIKE BASIN) for operating the Cahora Bassa dam. The Geospatial Streamflow Model (GeoSFM) and MIKE BASIN Reservoir models were evaluated against the observed streamflow data in terms of magnitude and time to peak. The comparison was done for data collected over a period of 11 years (from 1998 to 2008) on a daily time step. The GeoSFM makes use of 20 parameters to quantify the main hydrological processes at the basin scale. As with other conceptual models (e.g. Beven, 2006; Hughes *et al.,* 2010) the large number of parameters in GeoSFM has been identified as a major cause of equifinality (Artan *et al*., 2004). This problem is expected to be more pronounced in large basins (such as the Zambezi basin) where there is insufficient data to constrain the model predictions (WMO and USAID, 2012). Therefore equifinality was taken into consideration in the analysis of the final results. Lastly, flood risk maps are presented as a tool for flood prediction and management, to complement the predictions from hydrological models and allow the development of flood relief profiles.

6.2. The calibration approach

Calibration was achieved through a sequential combination of the Multi-objective Shuffled Complex Evolution Metropolis Algorithm within GeoSFM and manual methods. Tests on this automatic calibration procedure (Gupta *et al*., 1998; Vrugt *et al*., 2003a; Vrugt *et al*., 2003b; Schoups *et al.,* 2005) have shown that the method will provide reproducible results for the model. Three objective functions were used – the Nash-Sutcliffe Efficiency (CE, Nash and Sutcliffe, 1970) of the daily streamflow predictions; the Root Mean Square Error (RSR); and the Coefficient of Determination (R^2). A measure of bias (Bias) was also used. The procedures used to establish the GeoSFM for the Zambezi Basin are listed below; Figure 6.1 is a flow chart illustrating the process:

1. Using terrain analysis to extract model parameters from land surface data and assessing the initial ranges (minimum and maximum) of model parameters using *a priori* knowledge of the basin processes and guided by physical basin property information;

2. Testing the un-calibrated model to compare how the model matches with the observed values;
3. Performing sensitivity analysis, using the routines available within GeoSFM, to measure the impact on the model outputs caused by changes in the model inputs;
4. Using the Multi-objective Shuffled Complex Evolution Metropolis Algorithm within GeoSFM and manual calibration to obtain optimum parameter values;
5. Testing the calibrated model using performance statistics R^2, CE, RSR and Bias;
6. Fixing the calibrated model parameters that may be used for operational purposes.

The information used to determine the initial values of the parameters and their ranges included topography (USGS, 2000a); soil types (FAO, 1998); and land use land cover from the USGS-NASA databases (USGS, 2000b). This information formed part of the input-data files to the user interface of the GeoSFM. The model, using the input-data files and the mathematical equations describing the movement of water through the basin, simulates daily streamflow and soil-water conditions (Section 4.3.1 and Section 4.3.2). Table 6.1 shows the parameter values and the maximum range of calibrated parameters values for Zambezi Basin. Although the scale of the FAO soils (1:1 000 000) is too coarse, the information obtained was valuable in providing a baseline indication of the soil types in a given area and it was considered a good starting point for the calibration process. Other physical basin information was obtained from previous studies in the basin (such as Mazvimavi (2003) for several of the sub-basins that lie in Zimbabwe; Mwelwa (2004) and Ndiritu (2009) for the Kafue sub-basin in Zambia; Winsemius *et al.* (2006) for the Luangwa sub-basin; Asante *et al.* (2008) and Tirivarombo (2012) for the Zambezi Basin and for general physical property data covering most parts of the Zambezi Basin.

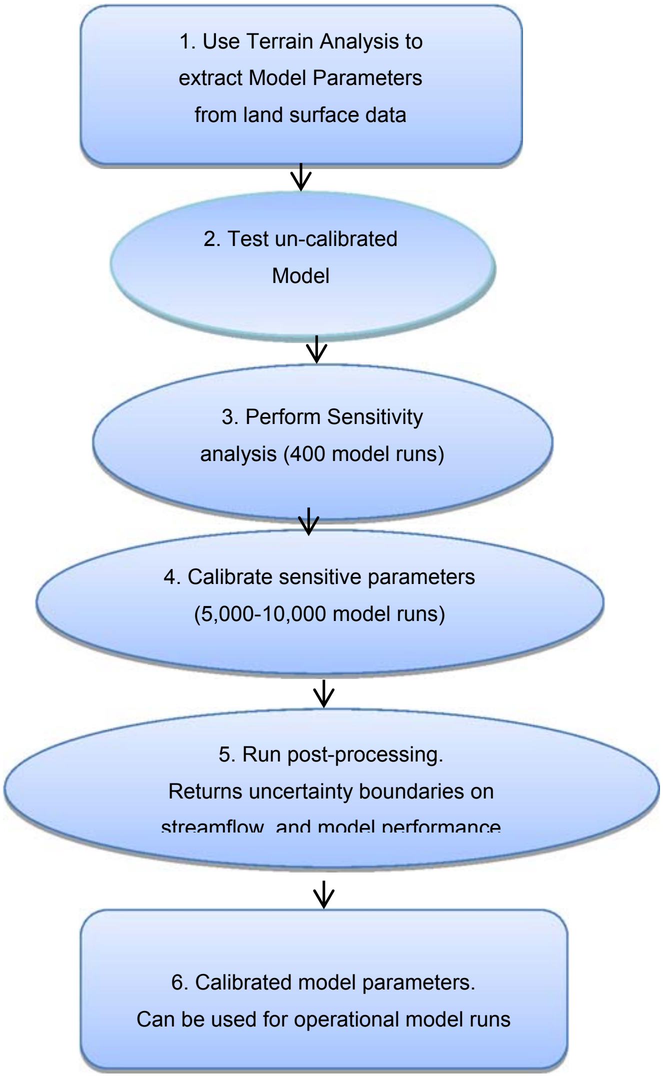

Figure 6.1: Flow chart of the calibration process followed in this study (Source: Asante *et al*., 2007b)

6.2.1. Assigning the initial parameter ranges

Given the limitations of available physical property data in the Zambezi Basin, a subjective ‘rule based’ approach was undertaken to assign the initial parameter ranges for each sub-basin. Based on various established calibration principles for the GeoSFM (e.g. Artan *et al*., 2004; Asante *et al.,* 2007a), and from the conceptual understanding of the model parameters and a qualitative interpretation of the physical basin characteristics, it was possible to derive the initial ranges of the model parameters for the Zambezi Basin (Table 6.1). The parameter value ranges for the main model parameters (Soil Depth; Texture; Hydraulic Conductivity (Ks); Soil Water Hold Capacity (SoilWHC); Top Soil; RC Number; Maxcover; Pan Coefficient; Interflow; Hill Slope; Baseflow; Basin Loss; Celerity; River FP Loss; River Loss Coefficients; River Rough; Diffusion) were estimated, based on an interpretation of the definition of the model parameters in physical hydrology terms. The division of the river basin into sub-basins, with their associated river reaches and hillslopes, and the parameterisation of these modelling units, was estimated using Digital Elevation Model (DEM) information in GeoSFM. For estimating soil parameters (Soil Depth; Texture; Hydraulic Conductivity (Ks); Soil Water Hold Capacity (SoilWHC); Top Soil; RC Number) GeoSFM uses the information from the global Digital Soil Map of the World (DSMW) (jointly produced by the United Nations Food and Agriculture Organization (FAO) and the United Educational, Scientific and Cultural Organization (UNESCO) (Section 4.3.2).

Each sub-basin was assigned a fixed MaxCover value, based on the Global Land Cover classification data (USGS, 2000a) to represent the impervious area. Aridity and Pancoeff parameter values, unique to each sub-basin (USGS, 2000a; 2002), were allocated. The MaxCover parameter was fixed at 1 for the Barotse, Kafue, Kariba, Cahora Bassa and Lake Malawi regions because of the existence of large water bodies. Establishing the parameter ranges and the model calibration process was based on the following principles:

- large differences in the Baseflow and Basin Loss values are to be expected in basins which have a large variation in soil properties;
- both SoilWHC and Basin Loss are assigned higher values for coarse textured and well drained soils (sands); low values are assigned to soils of a finer texture (clays and loams);
- arid basins with thin soils are expected to have low infiltration capacities and therefore low values of Baseflow and Basin Loss;
- the soil moisture runoff parameter (SoilWHC) is partly guided by soil characteristics and influenced by topography, whereby the runoff rate is increased in areas of steeper gradients – high SoilWHC values are therefore assigned for high gradients and high relief areas – because slope is a good indicator of the kinetic energy available in moving the water towards the downstream outlet (Mazvimavi, 2003);
- Groundwater is guided by the moisture state SoilWHC, and Basin loss percolation and the underlying geology.

The excess rain parameter is associated with the relationship between SoilWHC, (explaining the amount of water that percolates down to groundwater) and the Pan Coefficient (Pancoeff) which expresses the amount of rainfall that becomes evapotranspiration. Low values are expected in areas of deep rooted vegetation (bushland forest); high values are expected in areas of less dense vegetation (urban and built-up areas, grassland and savanna).

The initial parameters, their influence on the water balance and the range of parameter values applied for model calibration for the Zambezi Basin are presented in Table 6.1. The initial parameters' ranges for all the basins are important to inform the minimum and the maximum values that can be expected during the calibration of each sub-basin.

Table 6.1: Parameters, their influence on the water balance and the minimum and maximum values used for the modelling of the Zambezi Basin

ID	Parameter	Water balance Component	Minimal and Maximum range	Description
1	SoilWHC (mm m^{-1})	Soil moisture	(20-300)	Mean soil water holding capacity for each sub-basin
2	Soil Depth (cm)	Soil moisture	(20-230)	Mean soil depth for each sub-basin
3	Texture	Soil moisture	(1-3)	Predominant soil type class
4	Ks (cm hr^{-1})	Runoff	(0.01-1)	Coefficient value of saturated hydraulic conductivity for the predominant soil type in each sub-basin
5	Interflowlag	Runoff	(2-120)	Interflow residence in days calculated as the time it would take water to drain from the sub-basin area to the river
6	Hill Slope (%)	Runoff	(0.011-1.0)	Coefficient to calculate average sub-basin slope for each sub-basin, as the average change in elevation between sub-basin cells and their associated outlet divided by the average streamflow length between the same cells and outlets
7	Baseflowlag	Runoff	(8-360)	Baseflow residence time in days for each sub-basin
8	RCNumber	Runoff	(50-100)	SCS runoff curve number for each sub-basin
9	MaxCover	Runoff	(0.001-0.0087)	Fraction of sub-basin covered by a water body or other impervious area
10	Basin Loss (%)	Runoff	(0.95-0.99)	Coefficient to route water from sub-surface reservoir to groundwater reservoir
11	Pancoeff	Evapotranspiration	(0.85-0.95)	Pan evapotranspiration coefficient
12	Celerity (m s^{-1})	Kinematic Wave	(0.3-5)	Celerity (the rate at which a flood wave is propagated) through the reach
13	River Manning	River response	0.035	Value of Manning's n for the river reach
14	River Loss (%)	Water balance	0-1	Fraction of the river water lost to evaporation
15	Diffusion	Streamflow routing	45-42695	Streamflow attenuation (or dispersion) coefficient of the reach
16	River Loss (%)	Runoff	0-1	Channel infiltration loss factor for each river

6.2.2. Generating the parameter space using automatic calibration in GeoSFM

Using the previously generated minimum and maximum parameter values (Table 6.1) as input for GeoSFM, the second step was a parameter sensitivity analysis, using an internal model routine. The sensitivity analysis was used to measure the impact of any changes in the model inputs on the model outputs (Bahremand and DeSmedt, 2008). Twenty parameters (including the area of each sub-basin in GeoSFM and all the model parameters) were tested (over the ranges specified in Table 6.1) to explore the parameter space. GeoSFM uses the One-At-a-Time (OAT) method to carry out model parameter sensitivity for choosing the more sensitive parameters to be calibrated (Asante *et al*., 2007a). The OAT method (Morris, 1991) is a localised test because, in each model run, only one parameter is changed; all other parameters are held constant. With this method, changes in the output for each model run can be unambiguously attributed to each change of any given parameter. To ensure that the parameters were tested over the full range, parameter values were taken for 20 equal intervals samples for each of the 20 parameters. This sampling resulted in a total of 400 model runs (Asante *et al*., 2007a). The sensitivity analysis gave the mean absolute difference of test results over the parameter range for each parameter. The greater the differences (measured by the largest standard deviations) the more sensitive the parameter was. In this study, nine (9) of the 20 parameters were found to be more sensitive than others and were used in the calibration. These sensitive parameters included: the Soil Water Holding Capacity (SoilWHC); Soil Depth; Hydraulic Conductivity (ks); Interflow; Hill slope; Baseflow; Basin Loss; River width and Celerity. Figure 6.2 shows an example of the sensitive analysis results at Barotse (148) sub-basin.

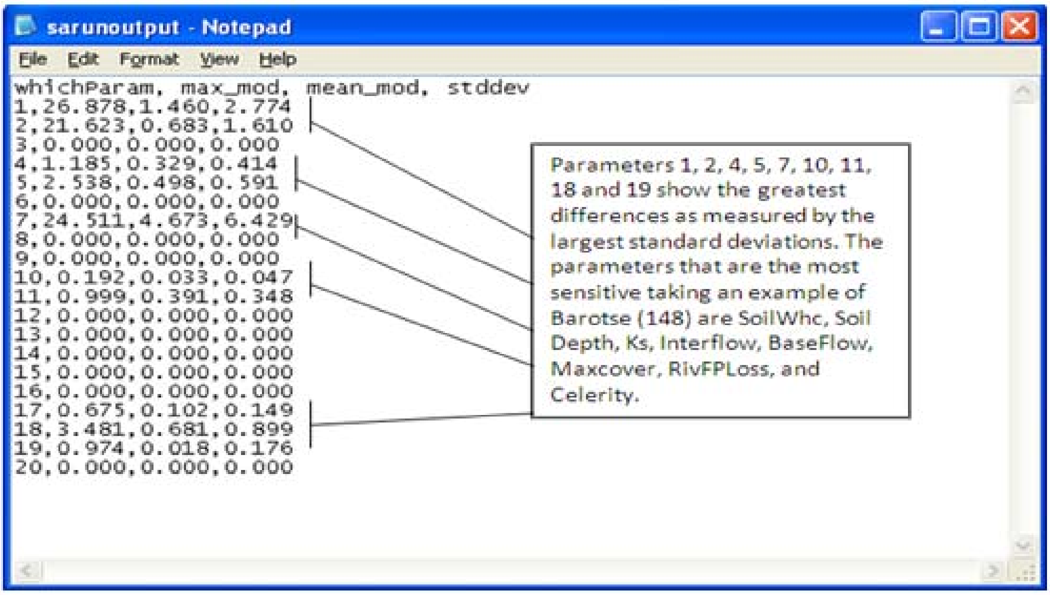

Figure 6.2: Results of a sensitivity analysis for the Barotse (148) sub-basin. The sensitivity analysis provided information on which parameters should be the main focus points during the calibration process

To achieve a calibrated model, a sequential combination of the Multi-objective Shuffled Complex Evolution Metropolis Algorithm (MOSCEM) was used – first to explore the parameter space (with a total of 400 runs (Figure 6.3) and, second, to establish the convergence from the optimum parameter set (depending on the length of stream streamflow record and the number of parameters being tested). The MOSCEM algorithm was chosen for this study because of its ability to consistently find optimum parameter sets requiring the least number of model runs (Asante *et al*., 2007a). Several studies have been conducted with the aim of evaluating the applicability of MOSCEM in model calibration (Gupta *et al*., 1998; Vrugt *et al*., 2003a; Vrugt *et al*., 2003b; Schoups *et al.,* 2005) and they have all provided reproducible results.

Automatic calibration in GeoSFM started with the selection of the parameters obtained from the sensitivity analysis results. The relationship between the streamflow model and the calibration algorithm is presented in Figure 6.3. By the end of a successful calibration, the streamflow model will have been run many times, tracking information from the parameter values input for each of the model runs. Finally the values that gave the best model performances were considered as the optimal parameter set for this study. The GeoSFM was linked to the spatial input data through the basin and river basin attribute files that listed parameter values for each sub-basin. In this study, these attribute files (basin and river) were rewritten with new parameter values each time the model was run, and the performance of the model was evaluated using: R^2; the RSR; the CE; and the percentage bias (PBIAS) as objective functions. Based on these objective functions, the output ensembles were apportioned into behavioural and non-behavioural ensembles. The behavioural parameter sets were then refined, using manual calibration, to establish the regional scheme of the model parameters for the basin, including the ungauged sub-basins.

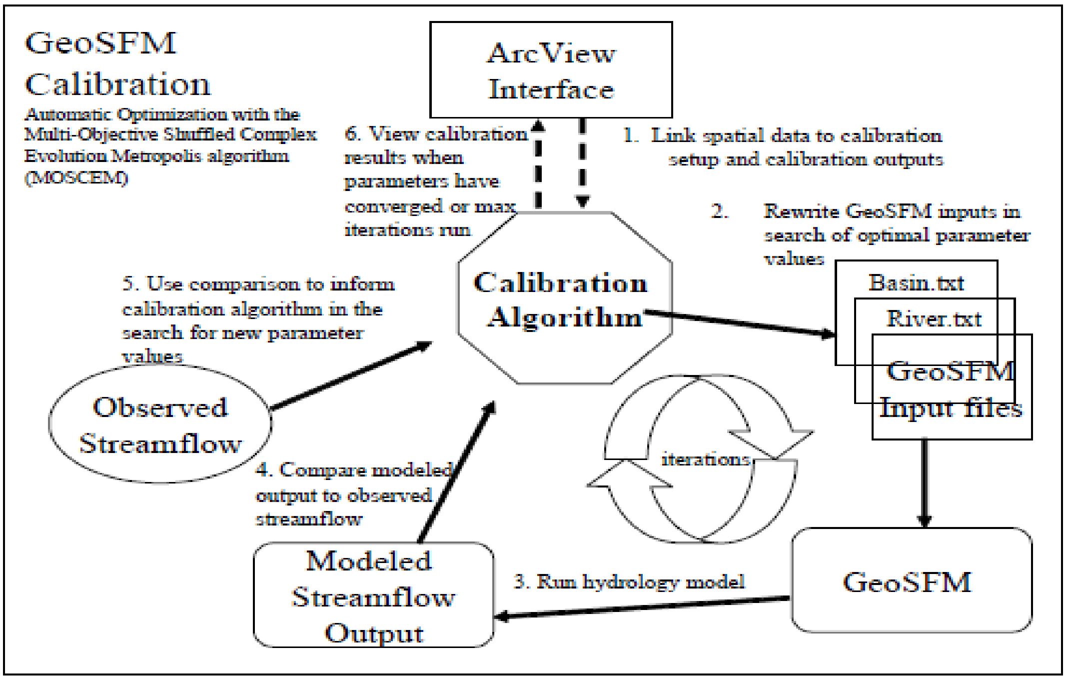

Figure 6.3: Calibration module relationships between the GeoSFM and the Multi-objective Shuffled Complex Evolution Metropolis Algorithm (Source: Asante *et al.*, 2007a)

Figure 6.4 shows a sample of the practical application of the beginning of the objective function results, a list of the nine (9) parameters chosen to be calibrated, together with the lower and upper values using the Barotse (2400) sub-basin as an example. Each sample can display the number of fluxes selected, and in this particular example only one flux was selected. When the sampling had been completed, the next process was labelled “Begin Metropolis Shuffled Complex Evolution,” for which 5 000 iterations were selected – to explore the parameter and convergence with or from the optimum parameter set. Because of the poor reliability of the observed data (which were mainly affected by measurement errors) and the fact that what the data actually represented in terms of developments existent within a sub-basin was not known (Hughes *et al.*, 2011), an acceptable model performance was regarded as CE > 0.5, and 10% ≥ PBIAS ≥ -10%. These criteria were used for model performance testing and validation.

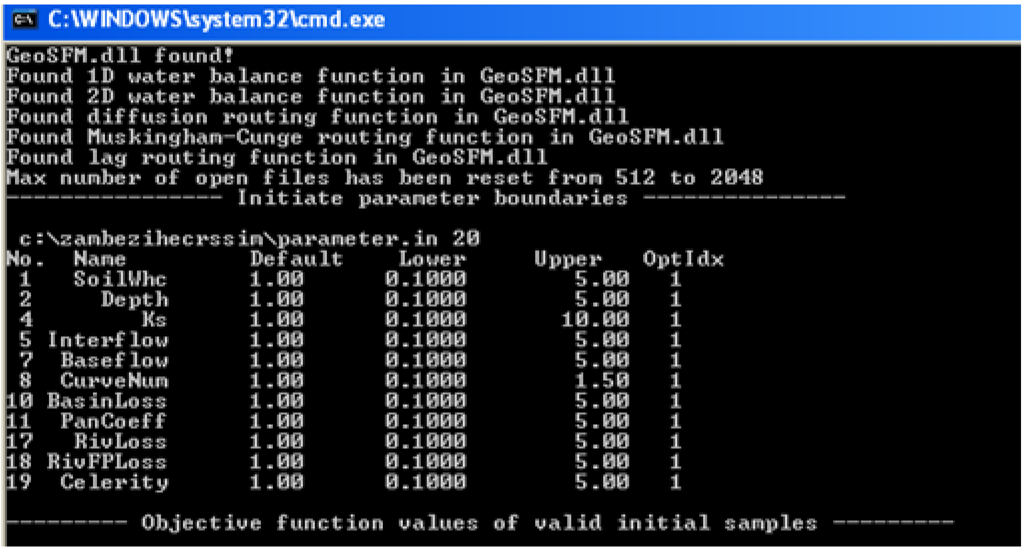

Figure 6.4: An example of the calibration process runs at Barotse (2400)

6.3. Calibration results

This section presents and discusses the results related to the prediction of streamflow, based on the assimilation of Earth Observation (EO) data into the hydrological Geospatial Stream Streamflow Model (GeoSFM). Daily rainfall data obtained from the Climate Prediction Center (CPC-RFE 2.0) were used to drive the GeoSFM and to generate daily streamflows in the Zambezi Basin. Since the testing of the un-calibrated GeoSFM was the first stage of model calibration, the comparison of un-calibrated model with observed data has been presented first. Secondly, the calibrated results of the GeoSFM and its performance are presented. Thirdly, results of the integration of the calibrated GeoSFM into the MIKE BASIN Reservoir model are also presented. Lastly, the flood risk mapping and quantification of the socio-economic impacts related to different flood levels are presented.

6.3.1. Testing the un-calibrated model

The GeoSFM was used to simulate streamflow for all the sub-basins between 1998 and 2008, and the resulting streamflows were compared with mean daily values from the national river discharge database for those sites where observed daily streamflow data were available and considered to be of acceptable quality. For each simulation time step, daily streamflow values, in $m^3 s^{-1}$, for the downstream end of more than 100 river reaches in the study basin were estimated. While the un-calibrated model could not predict the absolute magnitude of streamflow, the model was a valuable tool for rapid characterisation of the relative magnitude of flood hazards and seasonal streamflow changes in data-sparse settings like the Zambezi Basin. Six streamflow gauging stations (Figure 6.5 and Table 6.2) were used to evaluate the simulated hydrographs. These streamflow gauging stations were selected because they have data of acceptable quality and are located in areas with less anthropogenic impact. All selected streamflow stations were located either along the main Zambezi River or on the tributaries without any hydraulic infrastructure (i.e. without infrastructure which might regulate the stream flow). The simulations were compared against the observed record, using both graphical plots and flow duration curves.

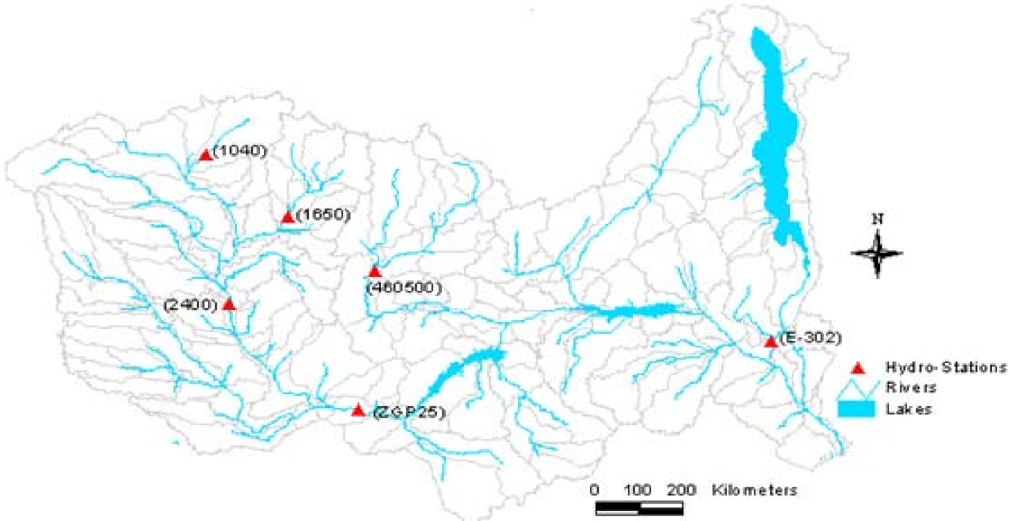

Figure 6.5: The location of the streamflow gauges selected for testing of un-calibrated model

The time series plots and flow duration curves for observed and simulated streamflows before model calibration are presented in Figure 6.6 and Figure 6.7. The simulated streamflows over the 4 010 days (from 1st October 1998 to 31st October 2008) were based on satellite rainfall data, showing significant differences with the observed peak streamflows. The magnitude of the daily simulated streamflow did not match the observed streamflow magnitude – but the timing during the high-streamflow period did match. The un-calibrated model generally over-estimated the peak streamflow for the selected streamflow gauging stations but the over-estimations were within the acceptable behavioural range for PBIAS and RSR. In general, a ±25% PBIAS and a 0.70 ≥ RSR are considered satisfactory for un-calibrated models (Van Liew *et al.,* 2007; Singh *et al*., 2005; Moriasi *et al.,* 2007).The results are presented in Table 6.2.

Table 6.2: Results of statistical comparison between observed and simulated time series of streamflows before model calibration

Location	Goodness-of-fit indicator			
	R^2	CE	RSR	PBIAS
Luanginga (1040)	0.58	0.52	1.0.	9.4
Kabompo (1650)	0.72	0.55	1.3	8.6
Barotse (2400)	0.81	0.62	0.61	-7.3
Victoria Falls (ZGP25)	0.87	0.76	0.48	-6.9
Kafue Hook at Bridge (460500)	0.91	0.87	0.35	-3.3
Revubue (E-302)	0.64	0.5	1.9	8.6

Luanginga (1040), Kabompo (1650), Barotse (2400) and the Victoria Falls (ZGP25)

Figure 6.6 shows the comparison results using hydrographs (left side) and flow duration curves (right side). From the graphical analysis, the results illustrate that the model was over-estimating the high streamflows and under-estimating the low streamflows in all streamflow measurement sites, except at the Victoria Falls (ZGP25). Here the model closely matched the timing and the magnitude of observed streamflows, as shown by the flow duration curve. The assessment demonstrated that it is not adequate to apply the un-calibrated model for daily stream streamflow forecasting and therefore a model calibration process (to achieve reasonably good simulations) is required (Section 6.3.2).

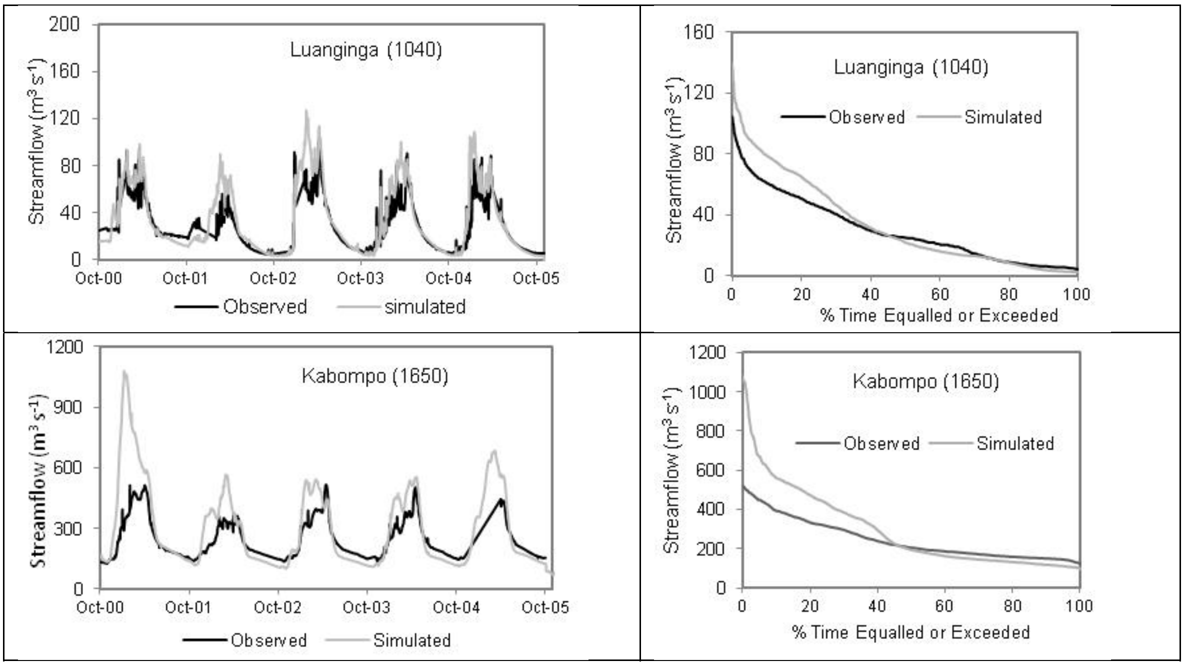

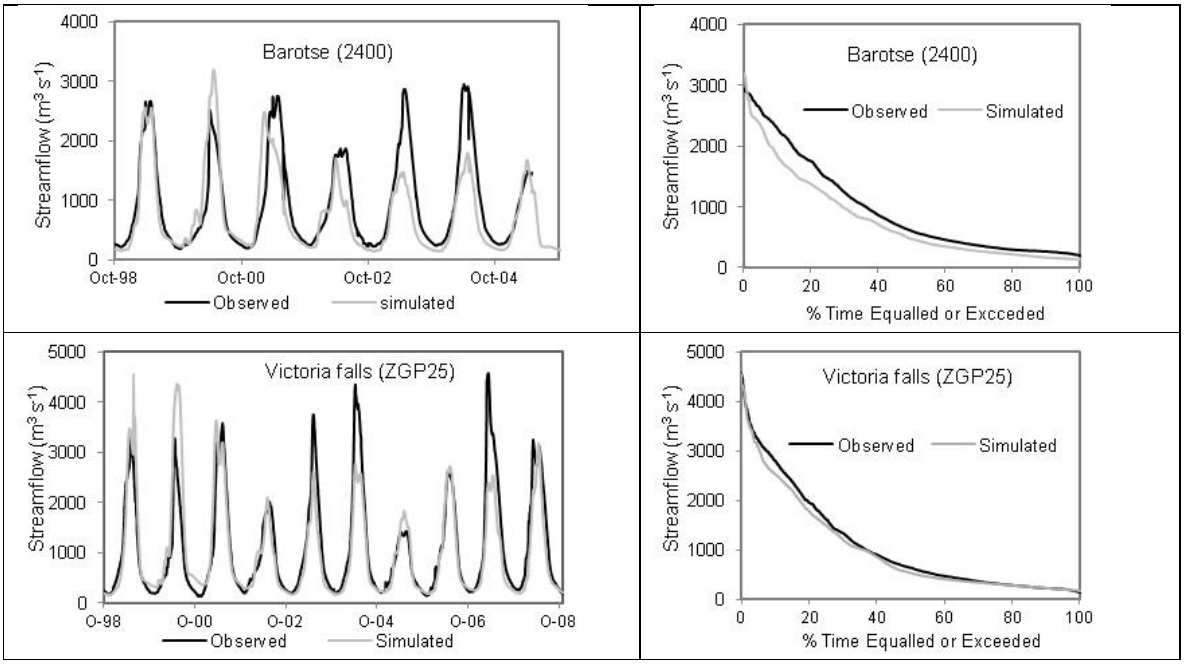

Figure 6.6: Comparisons between simulated and observed streamflow time series – Luanginga, Kabompo, Barotse and Victoria Falls. Streamflow time series (left side) and flow duration curves (right side) at Luanginga (1040), Kabompo (1650), Barotse (2400) and the Victoria Falls (ZGP25) before model calibration

Kafue-Hook Bridge (460500) and Revubue (E-302)

Figure 6.7 shows that the simulated streamflows closely matched the magnitude and the timing of observed streamflows and the flow duration curves illustrate an agreement between observed and simulated streamflows at Kafue-Hook Bridge (460500). At Revubue (E-302) results show that the simulated streamflows did not match the magnitude of observed streamflows; but closely matched the timing of the streamflows. This means that reasonably good simulations results may be achieved by the model calibration process (Section 6.3.2).

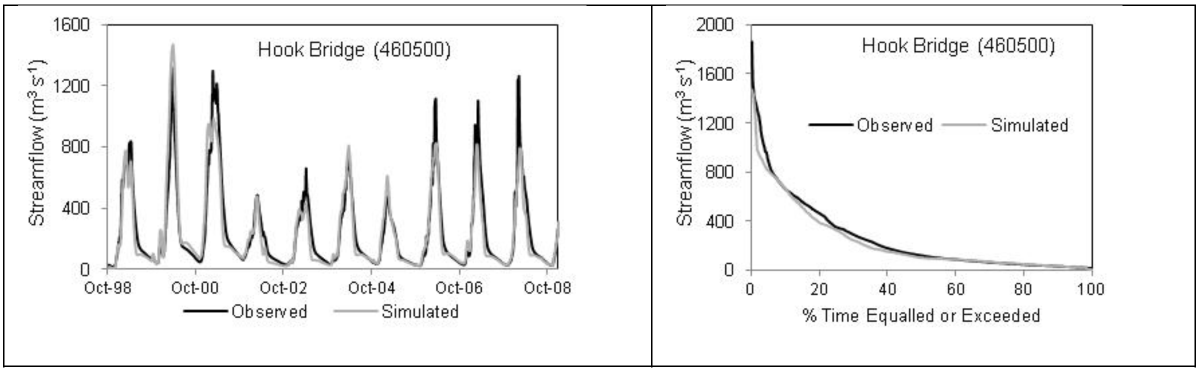

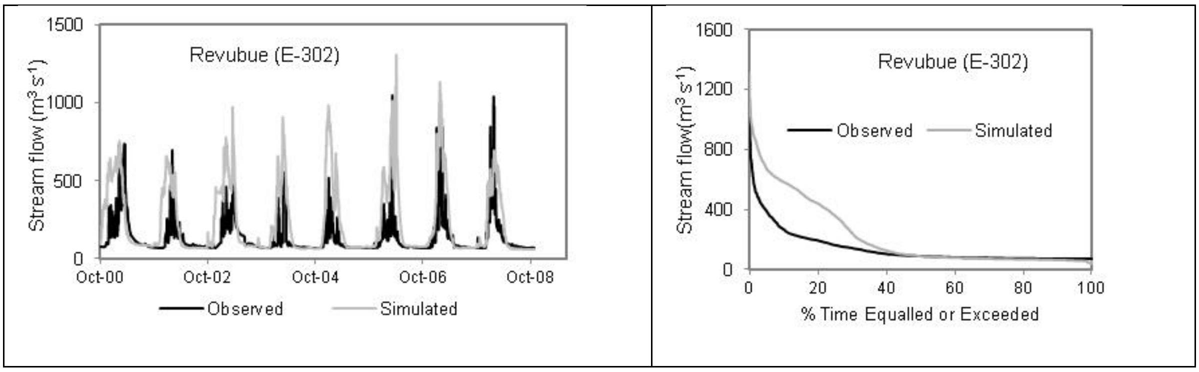

Figure 6.7: Comparisons between simulated and observed streamflow time series – Hook Bridge and Revubue. Streamflow time series (left side) and flow duration curves (right side) at Hook Bridge (460500) and at Revubue (E-302) before modelling calibration

6.3.2. Testing the calibrated model – introduction

To test the performance of the calibrated GeoSFM, three analyses were performed. For the first the observed daily streamflow were compared with the observed record for a period of 11 years (1998 – 2008), using time series plots and flow duration curves. Seven (7) streamflow gauging stations were selected to evaluate the calibrated model. The selected stations were: Luanginga (1040), Kabompo (1650), Barotse (2400), Victoria Falls (ZGP25), Kafue-Hook at Bridge (460500), Kafue-Gorge (470800) and Revubue (E-302). These stream gauging stations were selected because they have data of acceptable quality and are located at strategic sites for flood forecasting and the early warning system in the Zambezi River Basin. There was no common comparison period between observed and simulated streamflow so the comparisons between observed and simulated streamflow were based on the time series available at the different streamflow gauging stations (Section 3.5).

The second analysis was the comparison of the results of the integrated model against observed data at three selected streamflow gauging stations, located downstream of the Cahora Bassa dam. These stations were Tete (E-320), Caia (E-291) and Marromeu (E-285). It is important to note that these stations are the key streamflow gauging sites for flood control downstream of the Cahora Bassa dam, and all have data of acceptable quality. Visual inspections of time series plots, flow duration curves and statistical objective functions (R^2, CE, RSR and PBIAS) were used to evaluate the performance of the integrated modelling system. The integrated rainfall-runoff and reservoir simulation models were used for streamflow estimation downstream of the Cahora Bassa dam. Through the rule curves the reservoirs are operated to regulate flow for both hydropower production and flood control downstream. Because, downstream of Cahora Bassa dam, the systematic flow monitoring tool has been based on the water stage (Section 3.5 and Section 4.6.1), in the third analysis, two approaches for flood monitoring and forecasting at the Lower Zambezi were tested:

- the establishment of the elevation, volume, and area relationship to allow the monitoring of the water level (WL) at the dam site – the practical application of this approach is the translation of predicted streamflow to water levels to provide guidance related to potential flooding at different dam levels;
- the establishment of relationships between predicted streamflow (m^3 s^{-1}) and observed water level (m) for three downstream streamflow gauges (E-320, E-291 and E-285) – the practical application of this approach is the prediction of flood levels downstream of Cahora Bassa dam.

6.3.2.1. Evaluation of daily streamflow after model calibration

Table 6.3 summarises the performance of the model for the calibration of the various sub-basins. The streamflow hydrographs and flow duration curves obtained from the calibrations are also presented in Figure 6.8, Figure 6.9, Figure 6.10 and Figure 6.11. The calibration statistics (Table 6.3) indicate good simulations where both the R^2 and CE values are generally above 0.5. The RSR shows good performance which values below 0.7, except at Revubue (E-302). The unsatisfactory value of RSR at Revubue (E-302) could be related to the poor quality of the observed streamflow data and also to the fact that the GeoSFM does not perform well for small sub-basins.

Table 6.3: Results of statistical comparison between observed and forecasted time series of streamflows after model calibration

Location	Goodness-of-fit indicator			
	R^2	CE	RSR	PBIAS
Luanginga (1040)	0.85	0.69	0.64	6.1
Kabompo (1650)	0.87	0.68	0.69	4.9
Barotse (2400)	0.9	0.81	0.43	-4.3
Victoria Falls (ZGP25)	0.91	0.84	0.4	-4.5
Kafue-Hook Bridge (460500)	0.91	0.88	0.35	1.5
Kafue-Gorge (470800)	0.86	0.51	0.69	4.3
Revubue (E-302)	0.66	0.52	0.55	7.5

The assessment demonstrated that, in the upper Zambezi, the model calibration produced acceptable simulations.

Upper Zambezi and the Barotse

The final calibration parameters for the Luanginga (1040), Kabompo (1650) and Barotse (2400) are presented in Table 6.4. Reasonably good simulations were achieved for the low and high flows – as indicated by R^2 and the CE, whose values were both above 0.6. The high SoilWHC (which was above 170 mm m^{-1}) was indicative of the deep Kalahari sands that dominate the area and the high absorption rate parameters (Soil Depth Min. and Soil Depth

Max.) reflected the highly permeable nature of these soils. The predominant soils in the Barotse (2400) are sands and sandy loams, which are not as deep as in the upper catchments. In addition the area is extensively occupied by marshland, resulting in a moderately high SoilWHC and lower absorption rate parameters, indicative of the less deeply rooted vegetation characteristic of swampy areas. The higher Hill Slope value for the Kabompo (1650), when compared with the downstream sub-basins, suggested differences in the topographical conditions – i.e. higher in the upper Zambezi (compared with the downstream region, which is relatively is flat and dominated by wetlands). Although a Maxcover value of 1 has normally been assumed for the channel routing parameter and for the presence of a water body, the Celerity parameter has been calibrated at an average value of 0.45 to obtain a good calibration.

Table 6.4: Initial parameter ranges and calibrated parameters for selected sub-basins of the Upper Zambezi and the Barotse drainage area

ID	Parameters	Zambezi and the Barotse Sub-basins								
		Luanginga (1040)			Kambopo (1650)			Barotse (2400)		
		Min.	Max.	Calibrated	Min.	Max.	Calibrated	Min.	Max.	Calibrated
1	SoilWHC	140	200	170	150	200	172.6	140	280	146.5
2	Soil Depth	120	200	133.4	120	200	133.4	110	200	133.4
3	Ks	0.13	1	1	0.13	1	1	0.13	1	1
4	Interflowlag	3	120	32.84	3	120	32.84	3	120	32.84
5	Hill Slope	0.01	0.18	0.04	0.01	0.18	0.04	0.01	0.18	0.04
6	Baseflow	8	360	49.3	8	360	49.3	8	360	49.3
7	Basin Loss	0.95	0.97	0.95	0.95	0.97	0.95	0.95	0.97	0.95
8	Celerity	0.15	0.45	0.3	0.15	0.45	0.45	0.15	0.45	0.45
9	River width	118	478	478	121	385	369	118	478	478

The time series plots and flow duration curves are presented in Figure 6.8. The low flow has been reasonably well simulated; the high streamflows have been over-simulated. Attempts to reduce the over-simulations in very high flows resulted in worse under-simulations of the lower flows. Part of this problem could be related to the uncertainties in the observed high flow measurements – however without more data this cannot be confirmed. The percent bias differences between the means of observed and simulated streamflows ranged from -4.5% to +6.1%. The RSR at the Upper Zambezi and the Barotse were within the acceptable range of 0.1 to 0.7 (Table 6.3). The relatively higher RSR at Barotse can possibly be explained by the effect of both the expansion and contraction of the wetlands on the streamflow regime (which is not well captured by the model) and at Luanginga (1040) and Kabompo (1650) the high values of RSR may be related to the poor quality of observed data.

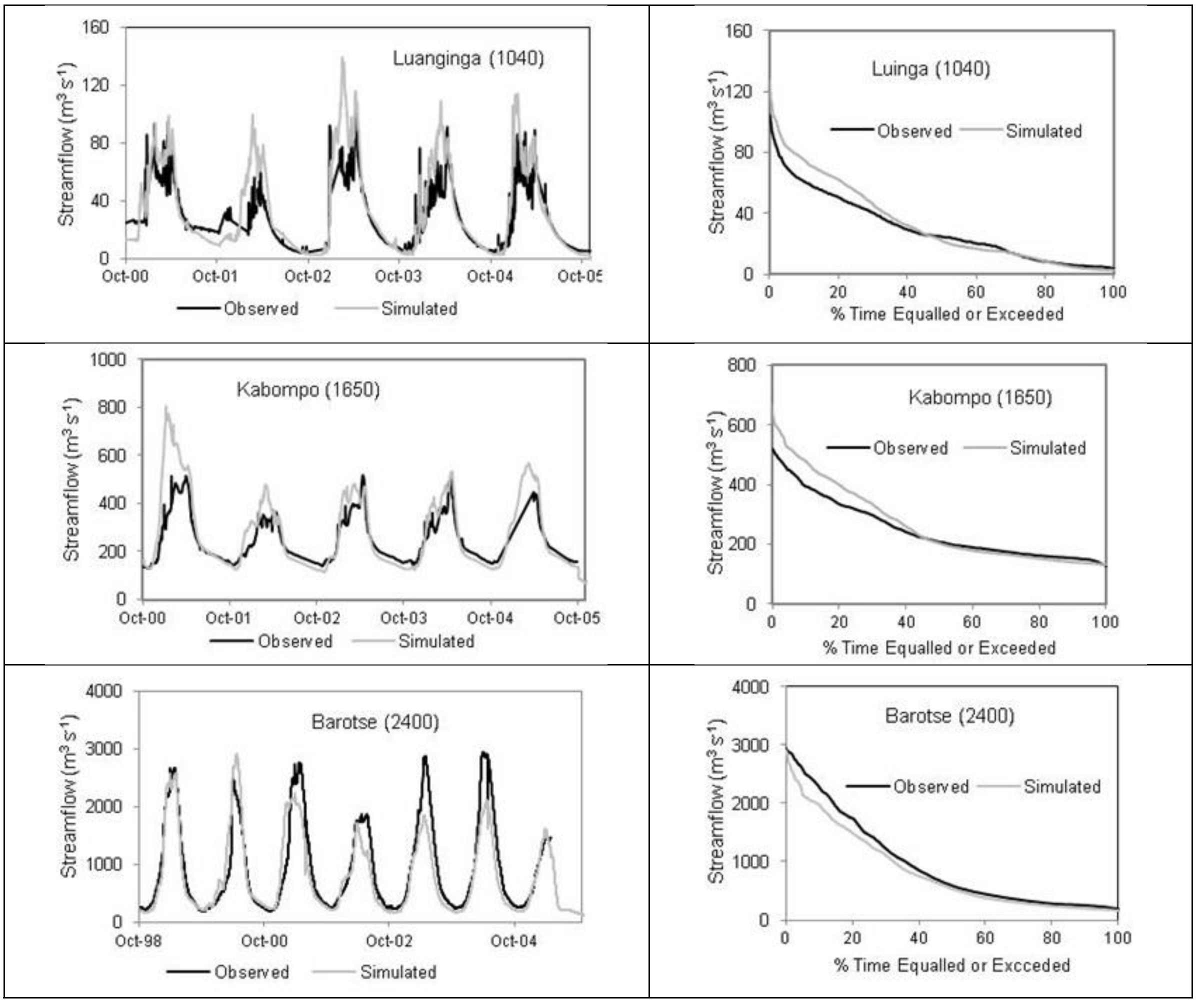

Figure 6.8: Comparison between simulated and observed streamflow time series – Upper Zambezi and the Barotse. Streamflow time series (left side) and flow duration curves (right side) at Upper Zambezi and the Barotse after modelling calibration

Lake Kariba

The Victoria Falls station (ZGP25) was used to calibrate the Lake Kariba sub-basin. Another station, considered in the calibration process after modelling integration, was Lutapa (E-162) located downstream of Kariba. The sub-basin is underlain by deep Kalahari sands which resulted in a high SoilWHC parameter value. The final calibration parameters for the Lake Kariba sub-basin at Victoria Falls (ZGP25) streamflow gauge station are presented in Table 6.5. Because of the size of the catchment (Section 3.5), the Celerity value of 0.45 indicated a large attenuation of flow and this was appropriate for all the large sub-basins found in the western part of the Zambezi Basin. This sub-basin is directly downstream of the Barotse, where the Celerity parameter value was also calibrated at 0.45. In this study, the Gwai and Mupfure sub-basins in Zimbabwe were modelled as ungauged. These two sub-basins are dominated by Kalahari sands and very shallow gravel soils, resulting in lower SoilWHC values and they are located in the dry and low rainfall (500 to 700 mm yr^{-1}) areas of the basin. These results are similar to those in earlier studies (Tirivarombo, 2012), which concluded that the prevailing dry conditions resulted in low antecedent soil moisture conditions, therefore most of the runoff was being generated from the northern sub-basins (rather than in the dry southern areas such as the Gwai and Mupfure). The Kariba dam has been modelled as an impervious area (Section 4.3.2.2), where the runoff (in mm) was generated directly by GeoSFM. This approach made it quite difficult to maintain high streamflow at gauging stations located downstream of the dam. Part of this problem has been related to operating rules of the Kariba dam, which do not follow the patterns of the rainfall season and therefore alter the natural streamflow regime. This problem was solved by the integration of GeoSFM with MIKE BASIN (Section 6.3.2.2).

Table 6.5: Initial parameter ranges and calibrated parameter for example of Lake Kariba drainage area

ID	Parameters	Lake Kariba sub-basin					
		Victoria Falls (ZGP25)			Lupata (E-162)		
		Min.	Max.	Calibrated	Min.	Max.	Calibrated
1	SoilWHC	110	250	174	100	120	79.3
2	Soil Depth	100	200	100	97	124	101.2
3	Ks	0.1	1	0.18	0.08	0.19	0.09
4	Interflowlag	16	120	120	84	120	120
5	Hill Slope	0.03	0.75	0.33	0.15	0.37	0.2
6	Baseflow	50	360	180	252	360	180
7	Basin Loss	0.95	0.99	0.99	0.97	0.97	0.97
8	Celerity	0.15	1.2	0.6	0.5	0.75	0.75
9	River width	119	597	597	271	830	702

The calibration results (Figure 6.9) show a good fit between the observed and simulated flows for the Victoria Falls sub-basin. The percent bias between the means of both the observed and simulated streamflows was within the acceptable behavioural range (±10%).

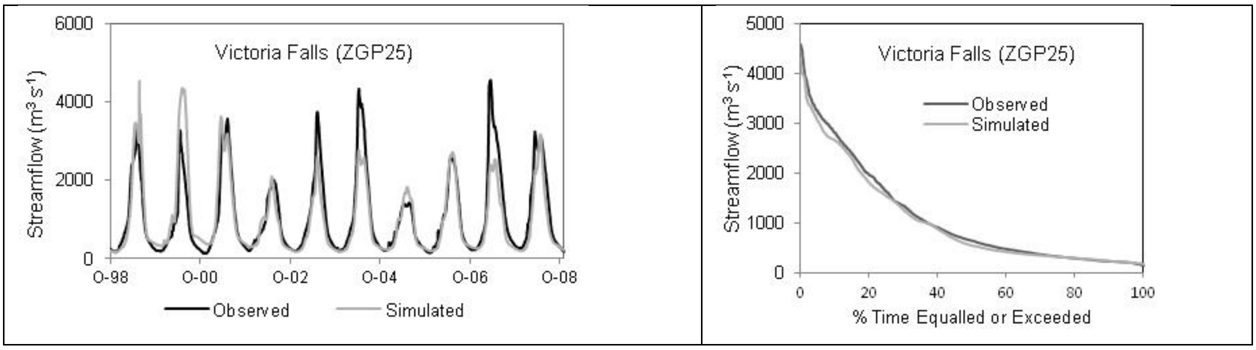

Figure 6.9: Comparison between simulated and observed streamflow time series – Victoria Falls. Streamflow time series (left side) and flow duration curves (right side) at Victoria Falls (ZGP25) after modelling calibration

Kafue

The Kafue Flats, the Lukanga swamps and the Kafue Gorge dam sub-basins were parameterised as impervious areas using the land cover land use classification data (Section 4.3.2.2). The final calibrated parameters for the Kafue basin are presented in Table 6.6. The calibration statistics (Table 6.3) indicated good simulations where both the R^2 and CE values were above 0.7. Figure 6.10 shows that the low streamflows have been reasonably well simulated; the high streamflows were over-simulated, but all fell within the acceptable behavioural range (±10%) of the percentage bias. The flow duration curves (Figure 6.10) illustrate the agreement between the observed and simulated streamflow. The RSR at Kafue-Hook at Bridge (460500) and Kafue-Gorge (470800) was within acceptable range of 0.1 to 0.7.

Table 6.6: Initial parameter ranges and calibrated parameter for example of selected sub--basins at Kafue drainage area

ID	Parameters	Kafue sub-basins					
		Kafue-Hook at Bridge (460500)			Kafue-Gorge (470800)		
		Min.	Max.	Calibrated	Min.	Max.	Calibrated
1	SoilWHC	140	200	170	150	200	172.6
2	Soil Depth	120	200	133.4	120	200	133.4
3	Ks	0.13	1	1	0.13	1	1
4	Interflowlag	3	120	32.84	3	120	32.84
5	Hill Slope	0.01	0.18	0.04	0.01	0.18	0.04
6	Baseflow	8	360	49.3	8	360	49.3
7	Basin Loss	0.95	0.97	0.95	0.95	0.97	0.95
8	Celerity	0.15	0.45	0.3	0.15	0.45	0.45
9	River width	118	478	478	121	385	369

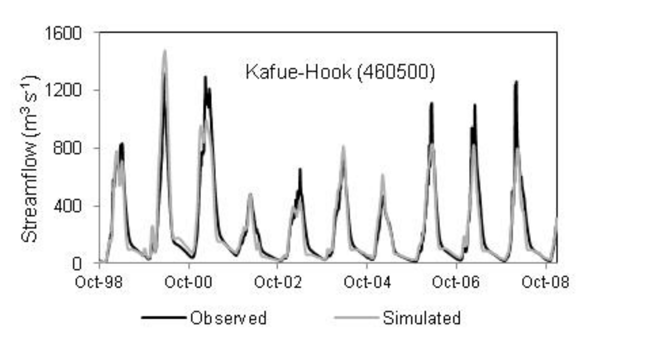

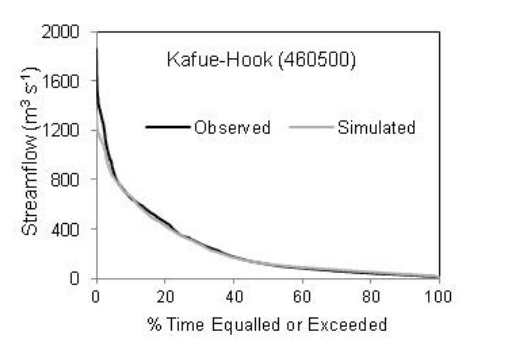

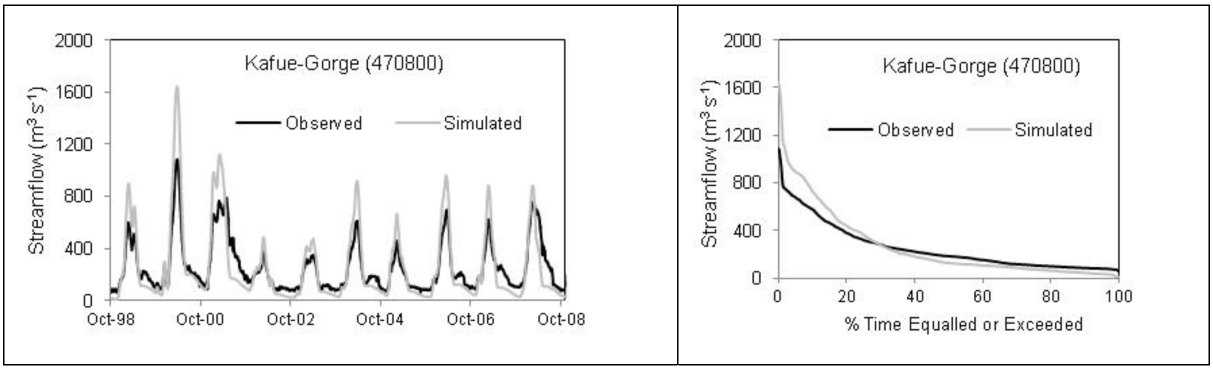

Figure 6.10: Comparison between simulated and observed streamflow time series – Kafue-Hook Bridge and Kafue-Gorge. Streamflow time series (left side) and flow duration curves (right side) at Kafue-Hook Bridge (460500) and Kafue-Gorge (470800) respectively

Lower Zambezi

The Cahora Bassa Lake, Luia, Mazoe, Manyame, Revubue, Caia, Shire and Marromeu sub-basins represent the Lower Zambezi drainage area. The sub-basins are dominated by loam and clay soils, resulting in lower SoilWHC values (Table 6.7). The sub-basins (such as Tete, Manyame and Mazoe) are located in the dry and low rainfall (500 to 700 mm y^{-1}) areas of the basin. The initial SoilWHC values for Tete (E-320) and Caia (E-291) respectively indicated that the soil moisture storage capacity was not as high as in the wet upstream areas (such as the Kabompo and the Kafue). All of the sub-basins located downstream of Cahora Bassa dam (except Revubwe) were modelled as ungauged sub-basins because no observed data was available for model calibration. Sub-basins (such as Tete, Caia and Marromeu), located downstream of the Cahora Bassa dam, were calibrated after modelling integration. Calibration plots of the observed and simulated streamflows were only done for Revubue (E-302) and are presented in Figure 6.11.

Table 6.7: Initial parameter ranges and calibrated parameter for selected sub-basins in the Lower Zambezi drainage area

ID	Parameters	Sub-basins								
		Tete (180)			Caia (205)			Revubue (148)		
		Min.	Max.	Calibrated	Min.	Max.	Calibrated	Min.	Max.	Calibrated
1	SoilWHC	140	200	170	150	200	172.6	140	280	146.5
2	Soil Depth	120	200	133.4	120	200	133.4	130	200	133.4
3	Ks	0.13	1	1	0.13	1	1	0.13	1	1
4	Interflowlag	3	120	32.84	3	120	32.84	3	120	32.84
5	Hill Slope	0.01	0.18	0.04	0.01	0.18	0.04	0.01	0.18	0.04
6	Baseflow	8	360	49.3	8	360	49.3	8	360	49.3
7	Basin Loss	0.95	0.97	0.95	0.95	0.97	0.95	0.95	0.97	0.95
8	Celerity	0.15	0.45	0.3	0.15	0.45	0.45	0.15	0.45	0.45
9	River width	118	478	478	121	385	369	118	478	478

Figure 6.11 shows that the low flows were well simulated; the high flows were over-simulated. The relatively low objective function values (Table 6.3) when compared with the upstream sub-basins, were related to uncertainties in the observed high flow measurements. In general it seems there has been a problem with the modelling of high flows in most parts of the basin. This could be because unquantified anthropogenic activities may be influencing the extent to which the observed data represented the actual natural conditions. The problem with the modelling may also be connected to the rating equations that were used to quantify the flows once the maximum gauge capacity has been exceeded – which may not have resulted in accurate calculations. Poor model performance for the Revubue, among others, also could be due to small area of the sub-basins. Previous studies have shown that combining GeoSFM and satellite- based rainfall data does not work well for relatively small basins (Artan *et al*., 2002; 2007; Asante *et al*., 2007c; 2008; Shrestha *et al*., 2008).

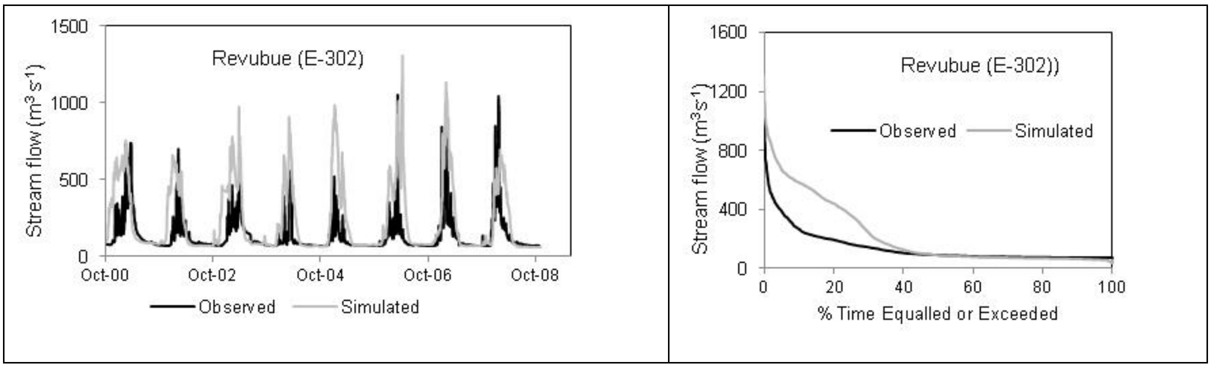

Figure 6.11: Comparison between simulated and observed streamflow time series – Revubue. Streamflow time series (left side) and flow duration curves (right side)

Cuando, Luangwa, Shire and Lake Malawi

The Cuando, Lwangwa, Shire and Lake Malawi sub-basins were modelled as ungauged because of both a lack of gauge measurements on these main tributaries of the Zambezi Basin and the poor quality of tributary streamflow data for model calibration at the daily time step (where data were available – such as for Shire sub-basin). The Cuando drainage area is characterised by an elevation ranging from about 700 to 1 600 m amsl. The mean annual rainfall received in the upper reaches of each sub-basin is above 1 100 mm and below 600 mm in the downstream areas. High values of the soil moisture holding capacity (SoilWHC), that reflect the high storage capacity of the deep sands soils, were assigned and the initial parameters ranged between 150 and 250 mm m^{-1}. These SoilWHC conditions result in the Cuando drainage area generating less runoff when compared with the other large sub-basins (such as Barotse, Lake Kariba and Kafue).

The Luangwa sub-basin is a headwater catchment and is characterised by a high mean annual rainfall of 1 000 mm and by a large surface drainage area (166 210 km^2). The initial soil water holding capacity ranges from 110 to 180 mm m^{-1}. The land cover and land use in Kafue and Luangwa are mainly miombo woodland, dry ever-green forests, and vast floodplains, resulting in sandy and loam soils that require moderately high surface absorption parameters. These conditions result in a substantial amount of runoff being generated by this drainage area, with reduced attenuation effects when compared with other large sub-basins (such as the Barotse and Kariba Lake). From the results presented above, three reasons explain the irregularity of the distribution of high flow within the basin. The first reason is because most of the rainfall occurring within the Zambezi River Basin is associated with the Inter tropical Convergence Zone (ITCZ) activities during the hot summers. The second is the impact of major dam operations (Kariba, Itezhi-Tezhi and Cahora Bassa) in the Zambezi Basin, which alter the natural regime of river flow. The third is the influence of the cyclone activities (Eline-2000 and Jokwe-2008) in the summer from the Indian Ocean (Chapter 3). The patterns of high streamflows are consistent with the findings of INGC (2008) which concluded that, during the overall period 1998 to 2008, high streamflows caused major flooding in the Zambezi (which occurred in the years: 1999; 2000; 2001; 2006 and 2008). However, it is known that the releases from the Kariba dam (done for dam safety considerations) have an effect on the flows downstream of the dam and often cause flooding in the Lower Zambezi Basin.

6.3.2.2. Evaluation of daily streamflow after modelling integration

To evaluate the daily streamflow after the modelling integration, an analysis was done downstream of Kariba and Cahora Bassa dams at three selected flood control streamflow gauging sites (Figure 6.12). A further gauging station analysed was Lupata (E-162), located downstream of Kariba dam. The Kariba and Cahora Bassa dams were modelled using the reservoir component of MIKE BASIN Reservoir simulation model. To model the Kariba dam, the data to allocate the reservoir parameters were adopted from a previous study by Beilfuss (2001). Although the analysis was performed for a period of 11 years, from 1998 to 2008, the results have been presented for only 5 years (1998–2002) for clarity. The designed Rule Curves for Kariba and Cahora Bassa dams were used in the MIKE BASIN model to set the maximum end-of-day water levels for the reservoir, resulting in periodic drawdowns prior to each flood season.

For Kariba, release1 (flows between 3 000 – 5 000 m^3 s^{-1}) was defined to take place if the water level at Kariba reached 477.5 m; release 2 (flow from 5 000 – 7 000 m^3 s^{-1}) is activated when the water level has reached 488.5 m. Release 3 (flows between 7 000 – 9 500 m^3 s^{-1}) only may take place if the inflow from the Victoria Falls and other tributaries is greater than 6 500 m^3 s^{-1} *and* if the water level has reached 489 m. To meet these rules, the initial water level at the start of each rain season should be 487 m.

For Cahora Bassa, release 1 was defined as the top of the flood control level (326 m), and reservoir releases (flows between 4 000 – 6 500 $m^3 s^{-1}$) may take place when the inflow from the Kariba and other tributaries is approximately 5 000 $m^3 s^{-1}$. Release 2 (with flows between 6 500 – 8 500 $m^3 s^{-1}$) is 2 m above the top of the flood control level (328 m). Release 3 has been set for the top of the crest level (329 m) where the maximum dam discharges (16 250 $m^3 s^{-1}$) may take place if the inflow from from Kariba and other tributary is greater than 10 000 $m^3 s^{-1}$. Flows between 4 000 – 6 000 $m^3 s^{-1}$ are the optimal for meeting both power production requirements and to mitigate downstream floods impact without causing a dam failure. The maximum duration of the releases ranging from 4 000 – 16 250 $m^3 s^{-1}$ is approximately seventy two (72) days, depending on the persistence of the high inflow; after this set period the outflow must return to the set minimum required operation flow. In addition the minimum water level of the dam at the start of each rain season is estimated to be 319.5 m.

The rule curve approach was also used to maintain certain defined minimum and maximum flows at some downstream control locations. In this study flood control points were selected as Tete (E-320), Caia (E-291) and Marromeu (E-295) (Section 4.5.1). Table 6.8 summarises the level of statistical agreement between observed and simulated streamflows. The CE values were above 0.5. The relatively low objective performance function values R^2 and CE and high RSR for the Lupata (E-162), could be attributed to the fact that the model applied in this study did not include the operating rules for the Kafue Gorge dam, and that, in reality, the reservoir operating rules are not fixed and could change depending on the amount of available water and the water uses.

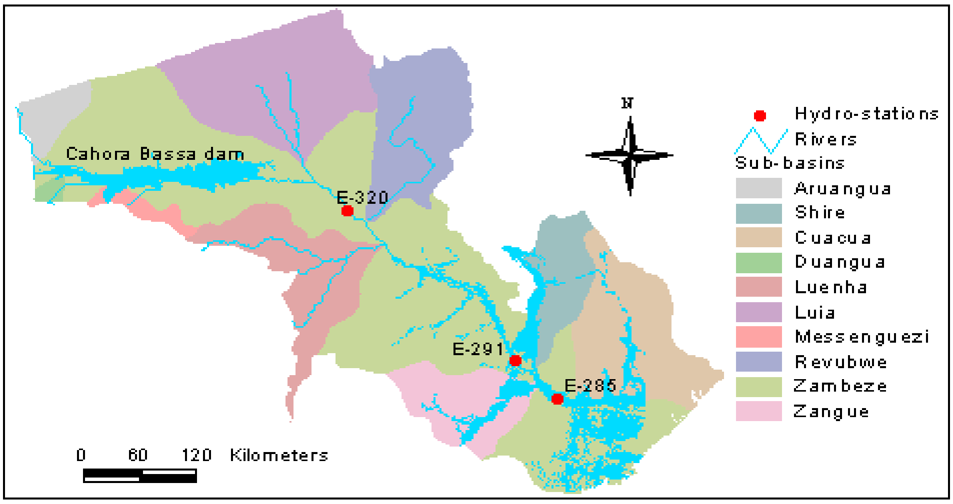

Figure 6.12: Flood control sites downstream of Cahora Bassa dam

Table 6.8: Statistical agreement between observed and simulated results after model integration

Location	Goodness-of-fit indicator			
	R^2	CE	RSR	PBIAS
Lupata (E-162)	0.53	0.5	0.69	-2.1
Tete (E-320)	0.9	0.82	0.48	1.2
Caia (E-291)	0.89	0.8	0.52	3.5
Marromeu (E-285)	0.83	0.77	0.49	4.8

The time series plots and flow duration curves of sample results are presented in Figure 6.13. The low flow was reasonably well simulated; the high streamflows were under-estimated, except at Marromeu (E-285), where the model tended to over-simulate the peak flows in those years when floods occurred. Results obtained from integrated modelling also show that the model performed well in estimating the timing of peak flows for all the selected stream gauges. The flow duration curves (Figure 6.13) indicated that the model had under-estimated the streamflows. One of the reasons was because of the uncertainties related to the observed streamflow data used in this study – the data were obtained without technical information (such as rating curves) to help in the detailed analysis related to measurement errors. Another reason could be related to the operational uncertainties of the large dams (Kariba and Cahora Bassa) – these dams are operated subjectively and without rigorously following the defined Rule Curve (RC) or any model predicting tool. Unfortunately, inconsistencies in dam releases were not properly taken into account in the model setup.

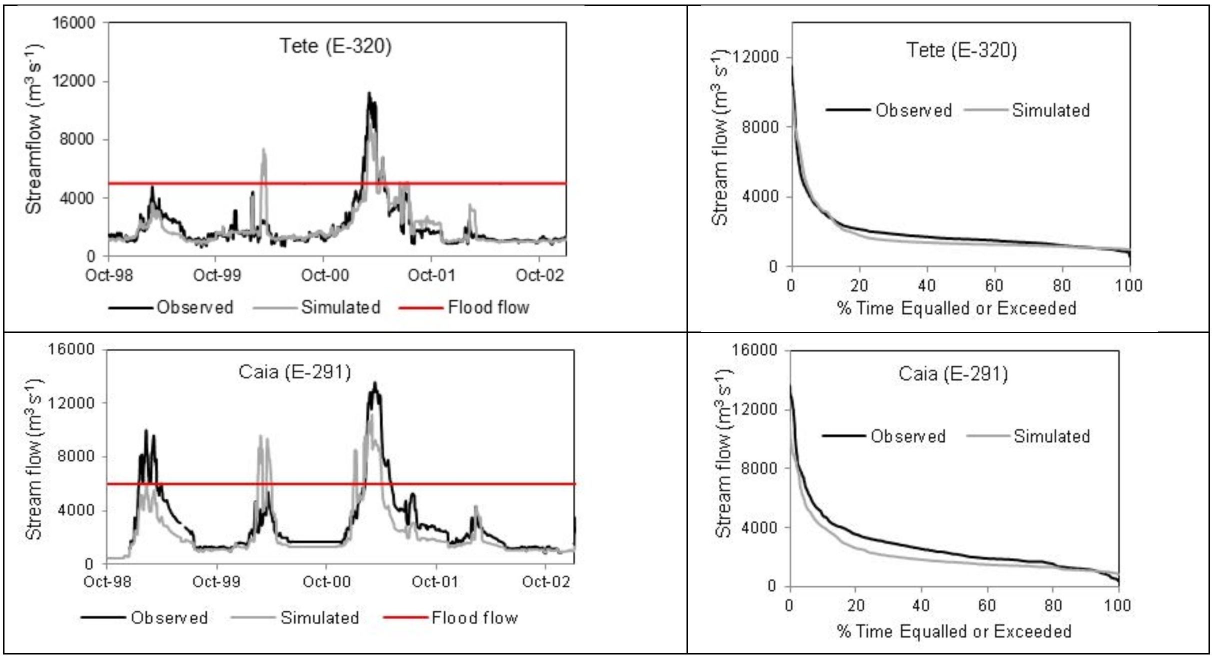

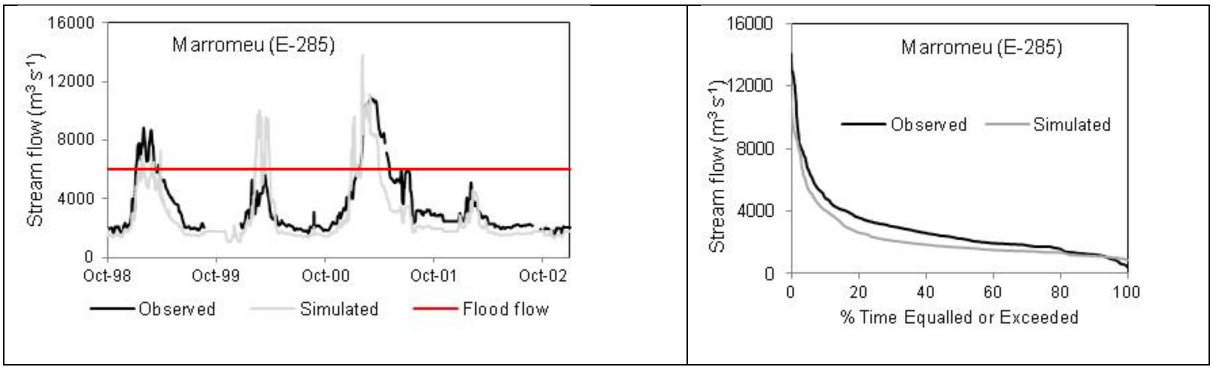

Figure 6.13: Comparison between forecasted and observed streamflow – Tete, Caia, Marromeu. Streamflow (left side) and exceedence frequency curves for observed and simulated streamflow after model calibration (right side) at Tete (E-320), Caia (E-291) and Marromeu (E-285) after modelling integration

6.3.2.3. Evaluation of daily water level at Kariba and Cahora Bassa dams

The performances of both the GeoSFM and MIKE BASIN models after the calibration process for flood control, firstly in terms of dam levels and, secondly, for flood levels downstream of the dam, are discussed in this section. In adapting the GeoSFM and MIKE BASIN approach for flood forecasting – however, there are numerous potential sources of error that must be considered. These include: the reliability of the input data; the reliability of the Kariba and Cahora Bassa Rule Curves (RCs); the measurement of storage change in the reservoirs; and the estimation of discharge from Kariba and Kafue Gorge. Thus errors in the Cahora Bassa inflow series are related to errors in discharge measurements from the Kariba and Kafue Gorge dams. In general, there were limited options available for improving the incremental data series for the upper and middle Zambezi sub-basins. Reliable time series data from the upper and middle Zambezi sub-basins, particularly at Cuando and Luangwa, were needed to improve the estimates of inflows into Cahora Bassa dam through model calibration. Figure 6.14 shows that the water levels simulated by the integrated model provided a reasonable estimation of the long-term trends in the Kariba dam. The simulated water level closely matched the magnitude and the timing of water level rising. Since several of the long-term changes in the daily flow regime may be attributed to cyclical changes in rainfall, this analysis also compared inflows and outflows at Kariba from 1998 to 2008. Both simulated and observed hydrographs of mean daily inflows registered similar trends. The recession limb of the inflow hydrograph is flattened by the delayed releases from the Barotse floodplain during the dry season. Figure 6.14 shows that the high streamflow releases by Kariba dam (between February and March in both 2000 and 2001) forced the Cahora Bassa dam to release artificial floods downstream of the dam (Figure 6.15c). Conversely the artificial floods, which occurred in 2006 and 2008 downstream of Cahora Bassa, were not forced by Kariba releases, but may have been forced by the contributions from the Kafue and Luangwa systems, in conjunction with the management of dam releases of the Cahora Bassa dam.

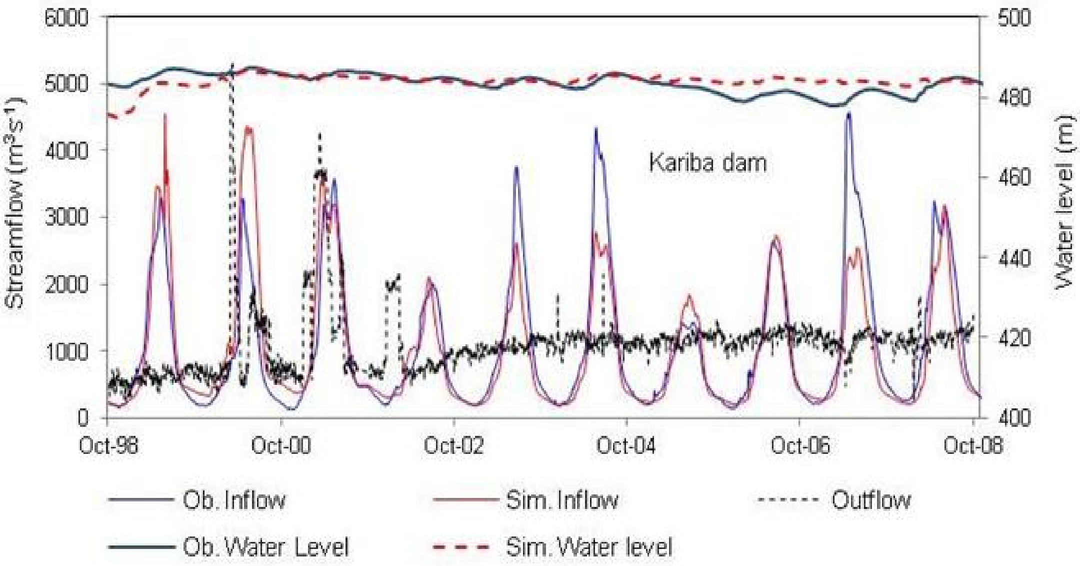

Figure 6.14: Comparison between simulated and observed water levels in Kariba dam. The graph includes inflows into the dam between 1998 and 2008 (after model integration)

The Rule Curve of the Cahora Bassa dam was also used in the MIKE BASIN model to set up several operation rules for flood control at the dam site and downstream of the dam. The main operation objectives (Section 4.5.2) were defined to enable the MIKE BASIN model to simulate the required streamflows to both meet the objective functions and take into account the constraints. Currently the Cahora Bassa Reservoir is operated to regulate the Zambezi flow regime for hydropower production, operating with four turbines, for a total generating capacity of 2 075 MW, and the electricity generated (surplus to Mozambican requirements) is exported to South Africa and Zimbabwe. The lower Zambezi relies – to a large extent – on the water resources generated in the upper Zambezi and stored in the reservoirs in the middle Zambezi. Hence, with man-made reservoirs playing an important role in redistributing (upstream) water in time for (downstream) uses, the management of the upstream reservoirs needs to be coordinated, taking into account various operating constraints (e.g. flood control, environmental flow requirements) and the financial constraints (such as the existing Power Purchase Agreement (PPA) with South Africa's Electricity Supply Commission – Eskom). It is important to note that the minimal required environmental flow was also modelled as one of mandatory boundary conditions. Therefore the relationship between hydropower production and required minimal flow was simulated in MIKE BASIN, according to the effective head difference and turbine efficiencies of Cahora Bassa reservoir (Section 4.5.1). It has been claimed that the simulation shown in Figure 6.15a reasonably replicated the timing of the water level, however Figure 6.15a reveals a consistent lag of approximately 1 month. This is a substantial lag considering that the simulation was calculated using a daily time step. When using the designed rule curve for Cahora Bassa dam and applying the objective function, the results showed that a flow of 4 179 $m^3 s^{-1}$ is the optimal required for generating the actual demanded power 1 375 MW – indicated by the red line (Figure 6.15b) – at 95 percent of engine efficiency. It has been stated that the Cahora Bassa reservoir operation can be improved to meet both actual power demand (MW) and flood control downstream – as shown by the grey line in Figure 6.15. Therefore the application of the modelling tools (designed to enable the operators to predict the discharges) may play an important role in future flood mitigation downstream of the Zambezi Basin.

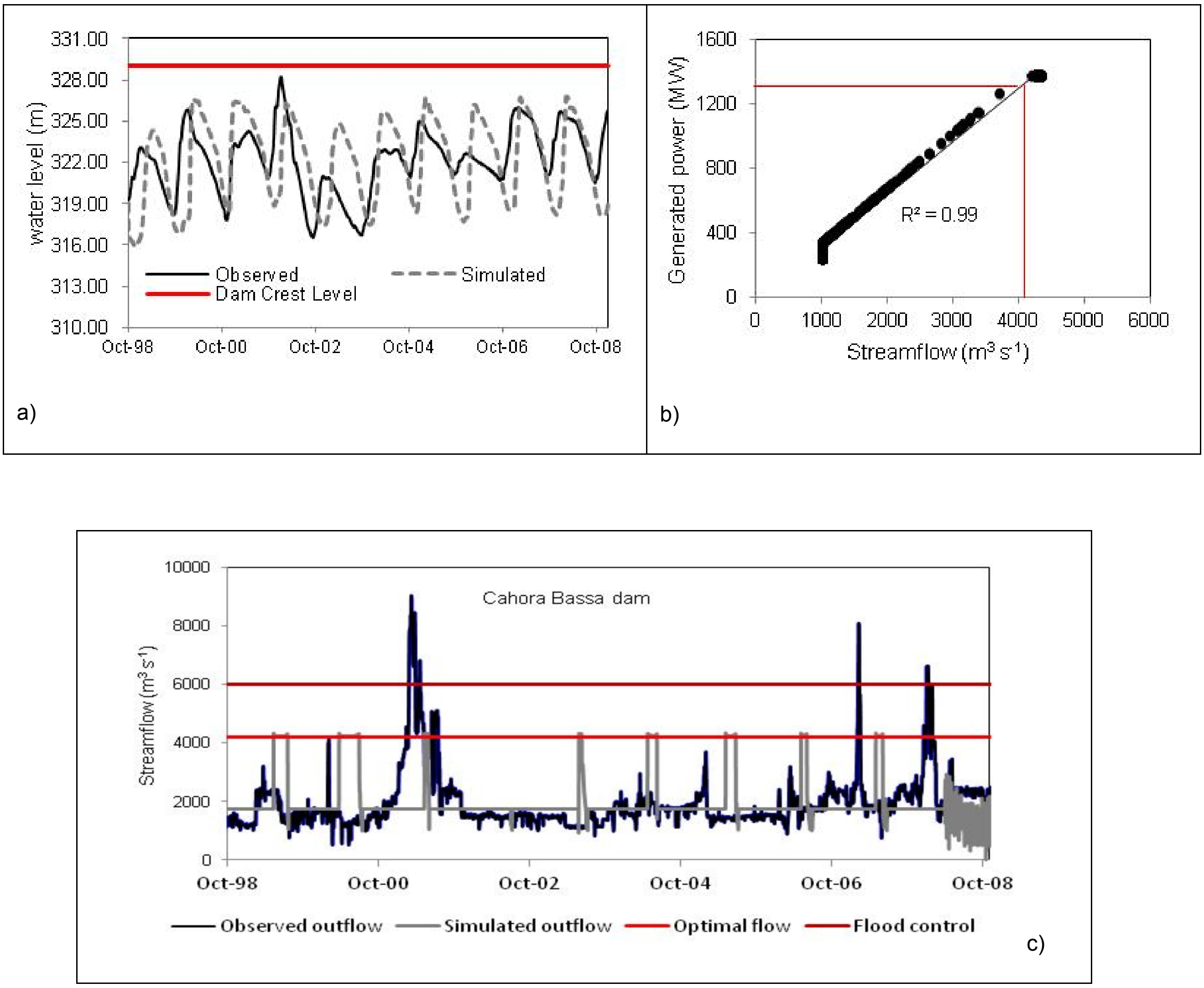

Figure 6.15: Comparison between simulated and observed water levels – Cahora Bassa. Water levels (a) and regression plot (b) between generated power and required flow (right side) in Cahora Bassa dam between 1998 and 2008 after modelling integration and (c) the relationship between observed and simulated dam releases in the context of meeting the actual power demand (MW) and flood control downstream ($m^3 s^{-1}$)

6.3.2.4. Evaluation of daily water level downstream of Cahora Bassa dam

For the evaluation of the daily water level downstream of Cahora Bassa dam, the simulated daily streamflows were converted to estimated water levels using the *(Q-h)* relationship (discussed in Section 4.6.1) and compared with the observed water levels at Tete (E-320), Caia (E-291) and Marromeu (E-285). In general, the model results showed good agreement between the observed and estimated daily water levels, with both R^2 and CE values above 0.65 – there was no significant difference between the maximum simulated and observed water level, with an average of 0.22 m shown by RSR (Table 6.9). Figure 6.16 shows that the flood control levels at Tete (E-320), Caia (E-291) and Marromeu (E-285) were 4.5, 5.0 and 5.0 m. respectively. Although the use of the integrated model slightly under-estimated the water levels, all variations were within the acceptable behavioural range (±5%) of the percentage bias (Table 6.9).

Table 6.9: Modelling performance statistics indicating the agreement between observed and simulated flows obtained (after model integration)

Location	Goodness-of-fit indicator			
	R^2	CE	RSR	PBIAS
Tete (E-320)	0.93	0.65	0.32	3.1
Caia (E-291)	0.91	0.84	0.25	2.6
Marromeu (E-285)	0.89	0.82	0.28	2.9

The following three pairs of graphs outline the performance trends after model integration.

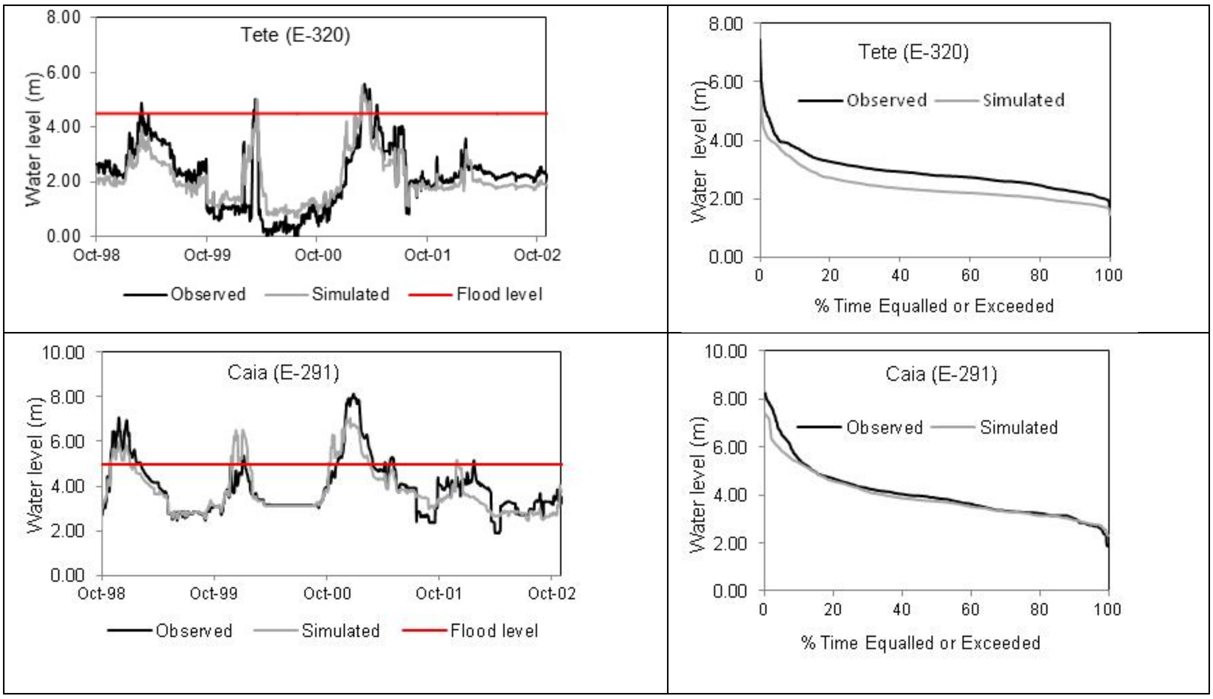

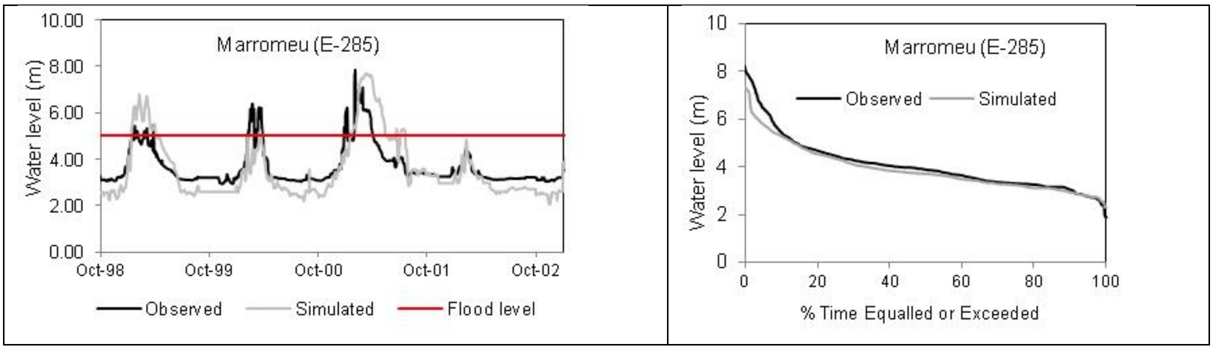

Figure 6.16: Modelling performance trends between simulated and observed water levels and exceedance curves. Water levels (left side) and exceedence frequency curves (right side) after model integration

6.4. Model validation

Since the overall objective of this study is to develop a flood forecasting tool for the Lower Zambezi, it was necessary to test whether the calibrated model would perform well outside the calibration period (2009 – 2011). The validation results are presented in Table 6.10 and Figure 6.17. Although the validation results showed a decrease in the percent bias between the means of the observed and simulated flows compared with the calibration results, R^2 and CE values indicated that the model can be used with confidence for flood prediction downstream of the Cahora Bassa dam.

Table 6.10: The statistical agreement between observed and forecasted flows after model integration

Location	Goodness-of-fit indicator			
	R^2	CE	RSR	PBIAS
Tete (E-320)	0.89	0.76	0.23	-4
Caia (E-291)	0.73	0.68	0.2	-3
Marromeu (E-285)	0.63	0.54	0.28	-11

The following three pairs of graphs outline the performance trends after model integration.

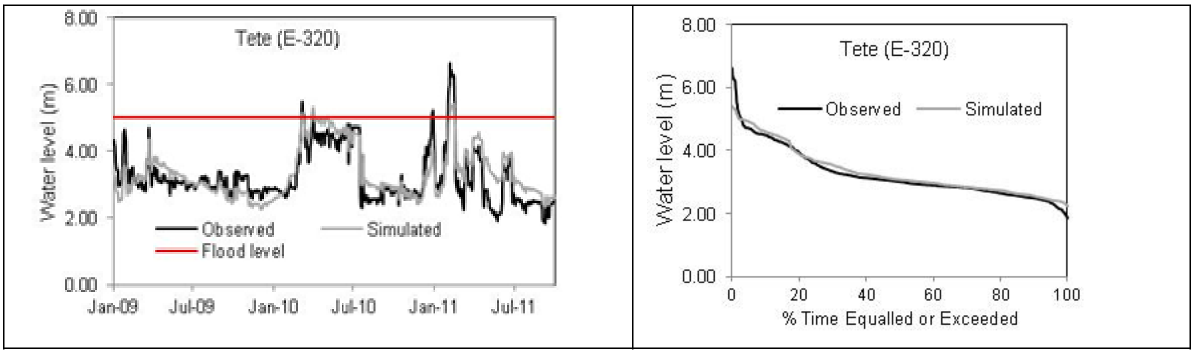

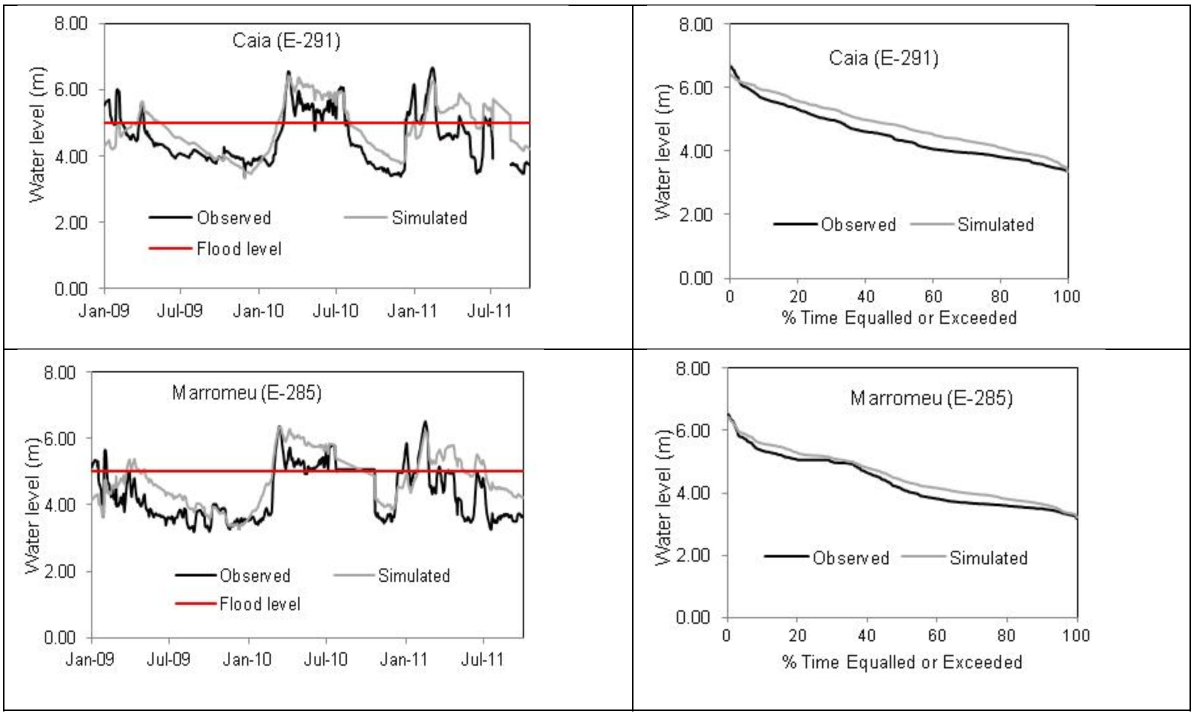

Figure 6.17: Hydrograph comparisons between simulated and observed water level fluctuation and exceedance curves – Tete (E-320), Caia (E-295), Marromeu (E-285). Water levels (left side) and exceedence frequency curves (right side) (after model integration) at Tete (E-320), Caia (E-291) and Marromeu (E-285) for modelling validation from 2009 – 2011

7. Operation of Lower Zambezi integrated reservoir model

This study recognises that the multi-purpose use of the reservoirs presents additional challenges for flood and water-resource management in the basin. Releases from the reservoirs can aggravate flooding in downstream communities, especially when intense rainfalls or tropical cyclone events in the downstream areas coincide with above-normal inflows to the reservoirs upstream (WMO and USAID, 2012). To establish a flood release programme in the Lower Zambezi sub-basin, runoff from the Upper Zambezi sub-basins has been based on the streamflow simulated by the GeoSFM. In the case of the Kariba and Cahora Bassa dams, the structural feasibility of flood releases includes adequate outlet capacity and reservoir storage volume to enable desired flood releases. Ideally, a flood management programme for the Lower Zambezi system would consist of an integrated flood release strategy involving the coordinated management of both the Kariba and Cahora Bassa dams. This section presents the structure of the proposed operational integrated flood management tool for the Lower Zambezi developed in this study (Figure 7.1). The proposed integrated flood management tool (as collated through this research) incorporates guidelines for management alternatives for reducing the impact of flooding downstream of the Cahora Bassa dam – these guidelines are designed for the water resources managers and dam operators to follow. The integrated flood management tool for the Lower Zambezi is a summary of the work carried out and it constitutes one of the main objectives of this study. Operationally the proposed integrated flood management tool is composed of four (Figure 7.1) main components:

i. an integrated modelling system;

ii. a framework for converting the daily streamflows formats from GeoSFM to feed the MIKE BASIN model;

iii. a framework for the hosting and converting of streamflows from integrated GeoSFM-MIKE BASIN into water levels in Lower Zambezi; and

iv. flood risk mapping.

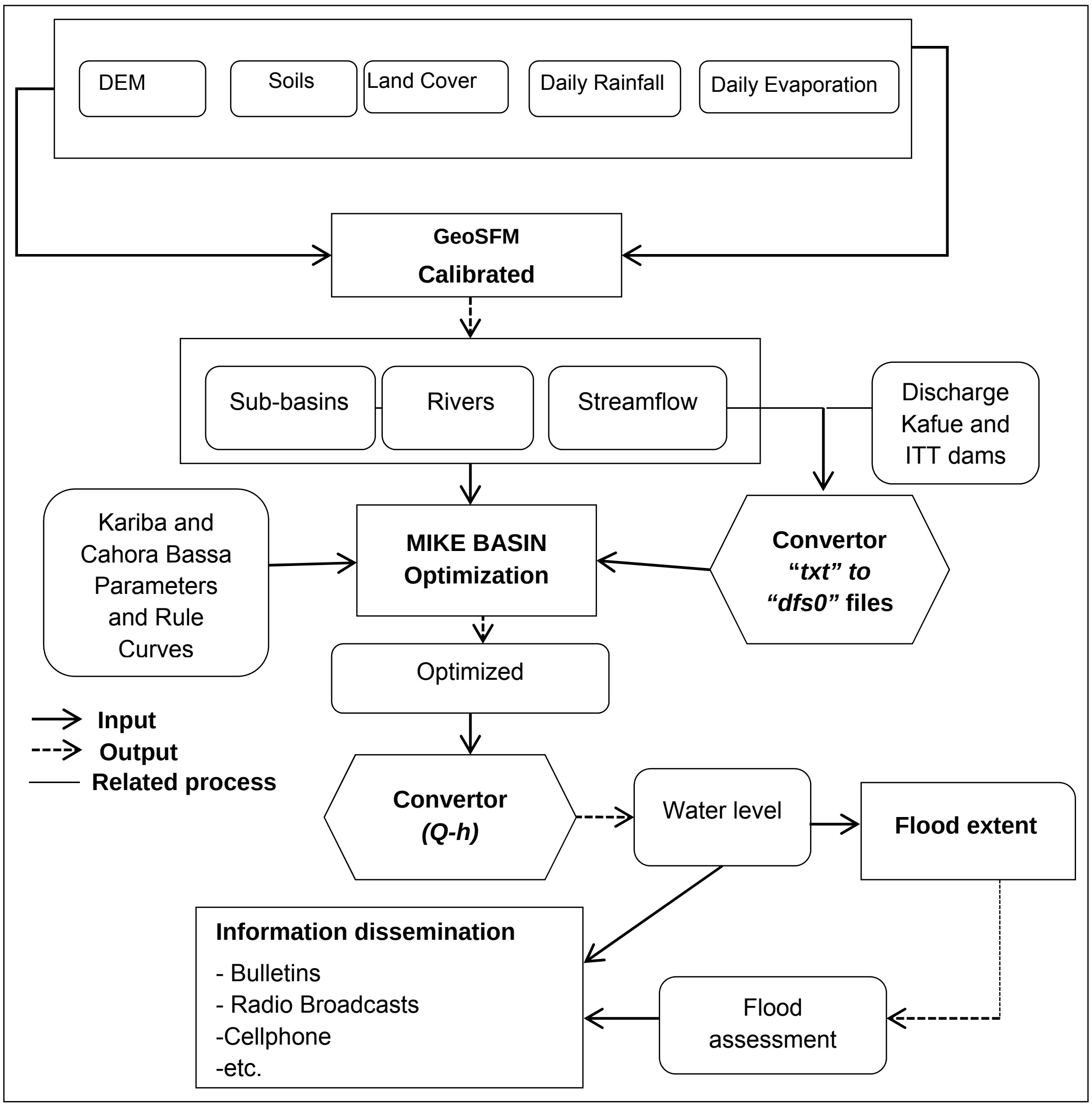

Figure 7.1: Structure of the proposed Zambezi Basin flood forecasting system

7.1. Integrated modelling system

The integrated modelling system consists of the GeoSFM (for daily streamflow forecast) which feeds into the MIKE BASIN Reservoir model to simulate flows and checking whether pre-defined operating objectives have been met (Chapter 4). Operationally the GeoSFM will generate the past (previous) 6 days daily streamflow and continuously forecast for the next three days forced by the daily CPC-RFE 2.0 and PET. The CPC-RFE 2.0 and PET should be downloaded from http://earlywarning.usgs.gov/fews/africa/ and feed the GeoSFM at daily time scale.To examine the availability of water for flood releases from the Kariba and Cahora Bassa dams, the Rule Curve Reservoir (RCR) model in MIKE BASIN was adopted (Section 4.5.1).The RCR model was defined so that flood releases may take place if the Kariba dam is releasing more than 3 000 m^3 s^{-1} and the water level in Cahora Bassa is approximately 326 m. Releases also may take place if the inflow to Cahora Bassa is more than the expected

3 000 m^3 s^{-1} flow generated by either the Kafue or Luangwa sub-basins. Therefore the integrated modelling system assumes that both Kafue and Luangwa are unregulated and the streamflow into Cahora Bassa dam should be generated by the GeoSFM. If the Kafue Gorge or ITT dams release more than the volumes predicted by the GeoSFM, the daily streamflow from Kafue sub-basin may adjusted manually in the MIKE BASIN – if the discharge plans from these two dams are known.

7.2. Framework for converting of streamflows formats from GeoSFM to feed MIKE BASIN

The framework consists of a Microsoft Excel macro, developed in this study to enable the data exchange between GeoSFM and MIKE BASIN. This data exchange process will be achieved by calling the predicted flows from GeoSFM using the Microsoft Excel Macro (Figure 7.2) as daily flow input for the water balance calculations of the Cahora Bassa Reservoir. The Macro changes the “txt”.files from GeoSFM to the “dfs0” file format required by MIKE BASIN.

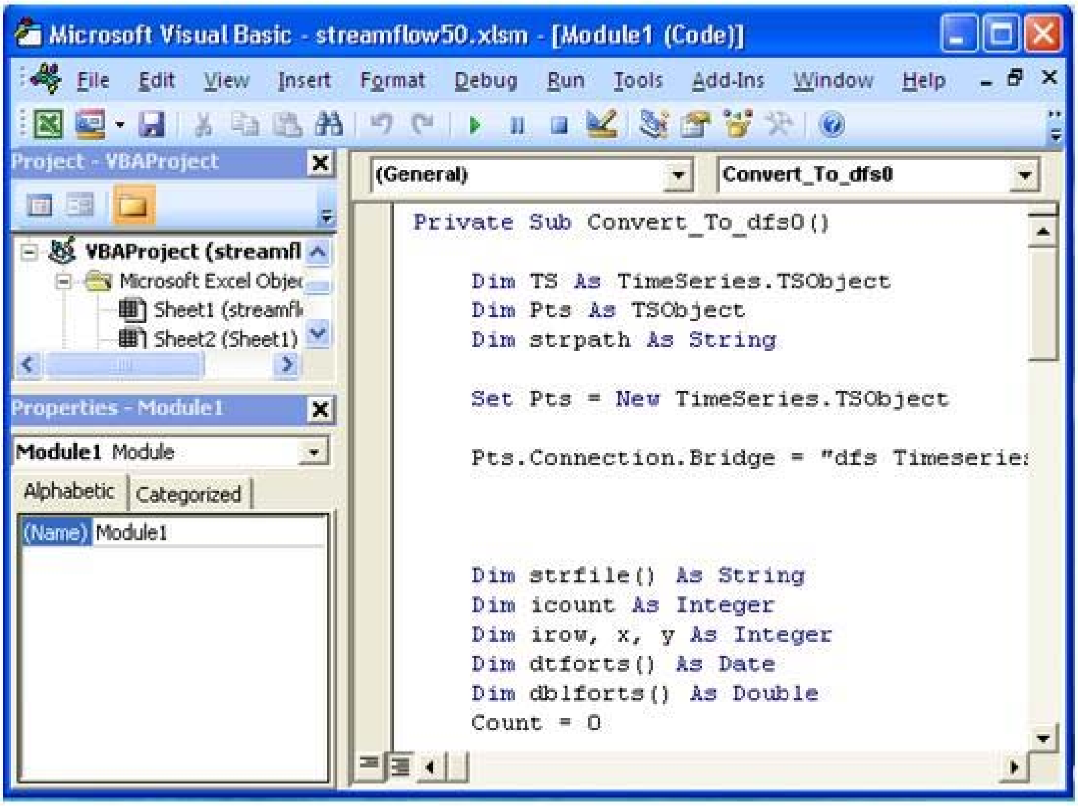

Figure 7.2: A screenshot of the Microsoft Excel macro to allow data exchange between Geospatial Stream Flow Model and MIKE BASIN

7.3. Framework for converting streamflows into water levels

This section discuss the application of the proposed framework taking the 2000 and 2001 floods as an example to evaluate the performance of the system. To test the performance of the framework, various stapes were formulated to derive the daily operating rules for the Cahora Bassa reservoir (Section 4.5.2). These steps include the definition of the storage target levels, four storages allocation zones and definition of three levels of releases namely release 1, release 2 and release 3, ranges of inflow and outflow (Section 4.5.2; Figure 7.4). The framework was tested using peaks of inflow and outflow hydrographs from reservoir during each flood. Downstream sub-basins contribution were simulated by calibrated GeoSFM to evaluate the contribution of downstream Cahora Bassa tributaries on aggravating of floods (measured by water level rising) at Tete (E-302), Caia (E-291) and Marromeu (E-285). The outflow from Cahora Bassa dam is a combination of release for power generation and spill from reservoir. The distances between Cahora Bassa dam and Tete (E-320) is 150 km, between Cahora Bassa dam and Caia (E-21) is 450 km and between Cahora Bassa dam and Marromeu is 520 km. So apart from the measured outflow, there are a considerable number of flows coming from Luia River, contributing to Tete (E-320), and with the Mazoe, Revubue and Shire Rivers, contributing to Caia (E-291) and finally all upstream rivers join the Luenha River and also contribute to the Marromeu flows (Figure 7.3).

Operationally the framework was applied, using simulated streamflow (inflow into the reservoir and sub-basins contribution), generated from the calibrated GeoSFM (Section 6.2) from 1st October 1999 to 31st October 2001 and feed MIKE BASIN. To optimize the outflow from the reservoir the Reservoir Rule Curve of Cahora Bassa dam, was used subsequently evolving in 762 time steps. The results were expressed in term of streamflow and water levels (Section 4.6.1) and comparison with observed records, using graphical plots (Section 7.3.1 and Section 7.3.2). These synthetically generated results are termed as representative in the present study since represent the big floods events observed in the Zambezi basin in the last 15 years (INGC, 2009). Figure 7.4 shows the schematisation of the proposed framework for flood monitoring and forecasting for the Lower Zambezi. Four flood control site were selected one at the dam site, and three at downstream of Cahora Bassa dam namely Tete (E-320), Caia (E-291) and Marromeu (E-285).

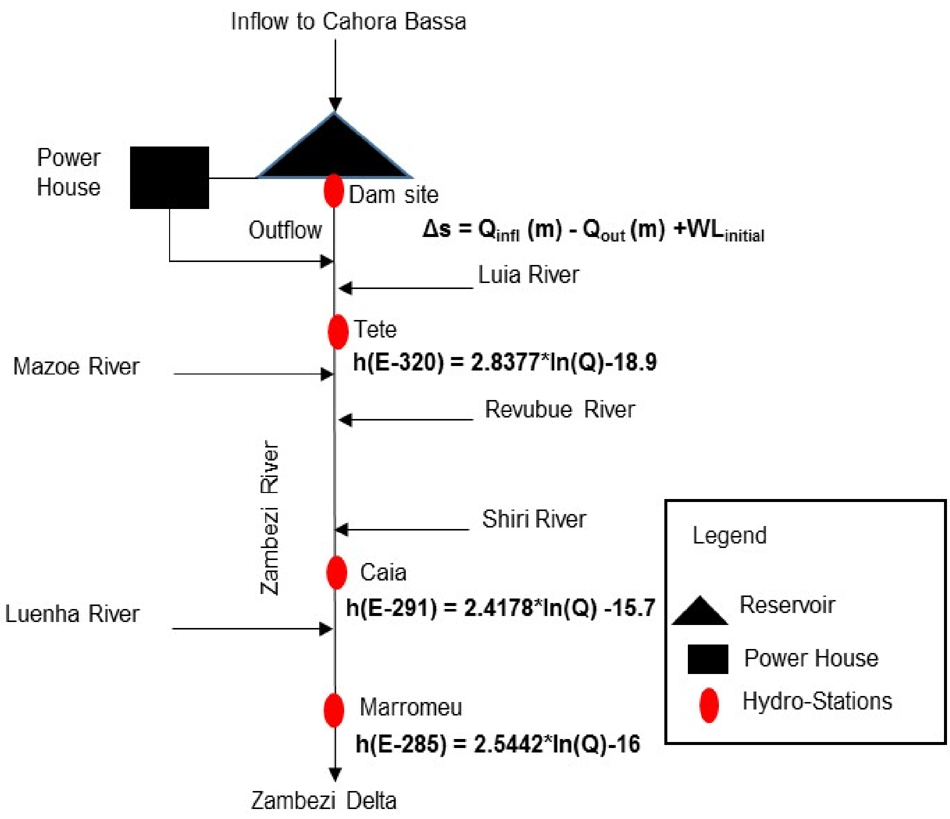

Figure 7.3: Schematic diagram of the proposed framework for converting of streamflows – Tete (E-320), Caia (E-291) and Marromeu (E-285) and downstream Cahora Bassa dam

7.3.1. Simulation of framework to evolve Rule Curve for floods at dam site

As the objectives of the Cahora Bassa dam are power generation and flood control, operating rules were developed for the entire hydrological year, i.e., from 1st October to 30th September. The minimum and maximum possible storages at each time step are dependent on the inflow into the reservoir, maximum release capacity during that time step and the maximum permissible release from reservoir for both power generation and flood control purpose at Cahora Bassa dam, which varies with respect to time. The initial storage state on 1st October is taken as the minimal operation level storage and final desired storage state on 31st March at the end of the rainy season is the normal operation zone or full capacity of reservoir. So, forward pass alone is sufficient to find out the maximum possible storage state, starting from initial time step and uses the Volume- Area- Height- (VAH) relationship as shown in (Equation 7.1, Equation 7.2 and Equation 7.3). The Equation 7.1 and Equation 7.2 were derived by converting the inflow and outflow in $m^3\ s^{-1}$ into inflow and outflow in m.

The Equation 7.3 was adopted for monitoring and predicting the water levels at dam site.

$Q_{out}\ (m) = (Q_{out}\ (m^3\ s^{-1})\ *\ day\ s^{-1}\ *\ Area\ m^2)/1000\ 000$ **Equation 7.1**

$Q_{in}\ (m) = (Q_{in}\ (m^3\ s^{-1})\ *\ day\ s^{-1}\ *\ Area\ m^2)/1000\ 000$ **Equation 7.2**

$\Delta s = Q_{infl}$ (m) - Q_{out} (m) +$WL_{initial}$ **Equation 7.3**

where Δs is changes in storage, Q_{infl} (m) is daily inflow expressed in m; Q_{out} (m) is daily outflow and $WL_{initial}$ is the initial water level.

However, the equations presented above were used to obtain the final values of minimum and maximum storages level for each time step. In case of Cahora Bassa dam , release for power and spill from the reservoir joins to the Luia, Mazoe, Revubue, Shire and Luenha rivers downstream of the dam and ultimately contributes to the flow at Tete (E-320), Caia (E-291) and Marromeu (E-285) respectively. The amount of outflow from Cahora Bassa dam has to be regulated at reservoir during flood to restrict the flow at Tete (E-320), Caia (E-291) and Marromeu (E-285) below non-damaging. This study consider non-damaging flows downstream of Cahora Bassa to the flows ranging from 5000 - 6 000 $m^3 s^{-1}$. So, this factor is to be taken care of while finding minimum and maximum possible storages.

However, a reservoir operation criterion for the Cahora Bassa dam has been defined as a function of an index level for each reservoir storage zone (Equation 7.3). These storage zone were defined in Section 4.5.1. Figure 7.4 shows a sample of the comparison between simulated and observed minimum and maximum possible storages for the 2000 and 2001 floods. From simulated results was observed that the combination between 9 000 $m^3 s^{-1}$ and 13 500 $m^3 s^{-1}$ – grey line, as peak inflow into reservoir during 2000 and 2001 floods can be handled by Cahora Bassa reservoir, releasing flows from 4 000 $m^3 s^{-1}$ to 6 000 $m^3 s^{-1}$ – blue line, in average of 75 days and keeping the water levels at the dam site and at Tete (E-320), Caia (E-291) and Marromeu (E-285) within flood control zone (Figure 7.4). From graphical analysis was observed that outflow ranging from 7 000 $m^3 s^{-1}$ to 9 500 $m^3 s^{-1}$ – black line, released from Cahora Bassa during 2000 and 2001 floods jointly to the downstream sub-basins contribution – green line (Figure 7.5) had high impact on water level rising at Lower Zambezi and consequently aggravated the flood impacts in term of the total population affected (Section 7.5). Figure 7.4 shows that there is chance in minimum and maximum possible storages for the variation of inflow and outflow to minimise impacts of flooding downstream of Cahora Bassa communities. Then, the 2000 and 2001 floods at downstream of Cahora Bassa should be avoided by optimising the discharges from reservoir and keeping the water level within the flood control zone. Therefore the observed peaks outflow was in average 60% high compared with the optimal flow during the floods and releases in shortime of 40 days, what should be in range of 4000 – 6000 $m^3 s^{-1}$- blue line, released in 75 days in 15 days before the maximal inflow.

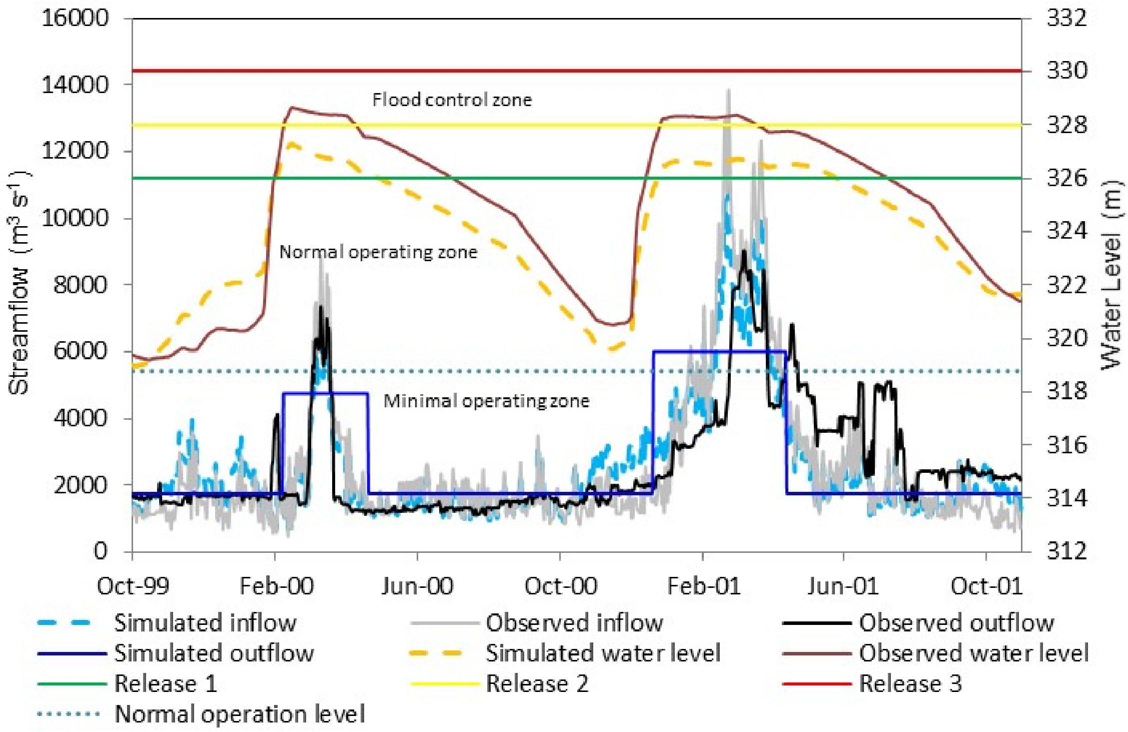

Figure 7.4: An example of the proposed framework showing how the releases should be taken to maintain the water level within the flood control zone at the Cahora Bassa dam site. It illustrates different release zones where the releases decisions should be made, the comparison between simulated optimal release flow and the flow released during 2000 and 2001 floods

7.3.2. Simulation of framework at downstream Cahora Bassa dam flood control sites

The contribution of Cahora Bassa dam during the 2000 and 2001 floods was calculated from the known values of outflow released during the floods. As the downstream sub-basins contribution such as Luia, Mazoe, Revubue, Shire and Luenha Rivers was not measured during 2000 and 2001 floods, however this information was calculated using the calibrated GeoSFM (Chapter 4 and Chapter 6). Figure 7.5 shows the impact of outflow from Cahora Bassa dam on the water levels rising resulting from the combination of release for power generation and spill from reservoir. It also shows the impacts of outflow from Cahora Bassa joins to the contribution of downstream sub-basins contribution on water level rising at Tete (E-320), Caia (E-291) and Marromeu (E-285).

For both 2000 and 2001 floods considered, the initial flow to be the same as the initial value of outflow from the reservoir and statistical procedure was carried out to get the relationship between peak outflow from reservoir and the simulated flow as contribution from downstream Cahora Bassa Rivers at Tete (E-320), Caia (E-291) and Marromeu (E-285). Because of the needs of express the streamflow in term of water level for flood control (discussed in Section

4.6.1) at Tete (E-320), Caia (E-291) and Marromeu (E-285) the (Q-h) relationships was established for converting the outflow and simulated streamflows into water levels as the following:

$$h(E\text{-}320) = 2.8377 * \ln(Q) - 18.9 \quad \textbf{Equation 7.4}$$

$$h(E\text{-}291) = 2.4178 * \ln(Q) - 15.7 \quad \textbf{Equation 7.5}$$

$$h(E\text{-}285) = 2.5442 * \ln(Q) - 16 \quad \textbf{Equation 7.6}$$

where h is predicted water level (m) and Q is simulated streamflow ($m^3\ s^{-1}$).

Figure 7.5 shows that the operation of Cahora Bassa dam had a significant impact on water level rising during 2000 and 2001 floods – black line. Therefore, these floods were characterized by the peaks outflow from reservoir. From data analysis was observed that, the difference between flood control flow and downstream sub-basins contribution is the maximum permissible release, which can be made from the Cahora Bassa to keep the water levels at Tete (E-320), Caia (E-291) and Marromeu (E-285) within flood control level. This study considered that a certain flood control site is within flood control level if the instantaneous water level ≤ 1.0 m above flood level. It was observed that there is a chance to minimise impacts of flood downstream of Cahora Bassa by adjusting the outflow by simultaneously simulating the contribution of downstream contribution. Therefore from graphical analysis shows that the impact of 2000 and 2001 on water level rising was caused because of the peak outflow from Cahora Bassa dam rather than the contribution of downstream rivers. So these impacts should be minimized optimizing the peak outflow. The impacts of 2000 and 2001 floods it also aggravated by the contribution of o downstream Cahora Bassa tributaries-grey line, therefore if the Cahora it was well operated the impact of both outflow and downstream tributaries it would be within flood control Zone Figure 7.5.

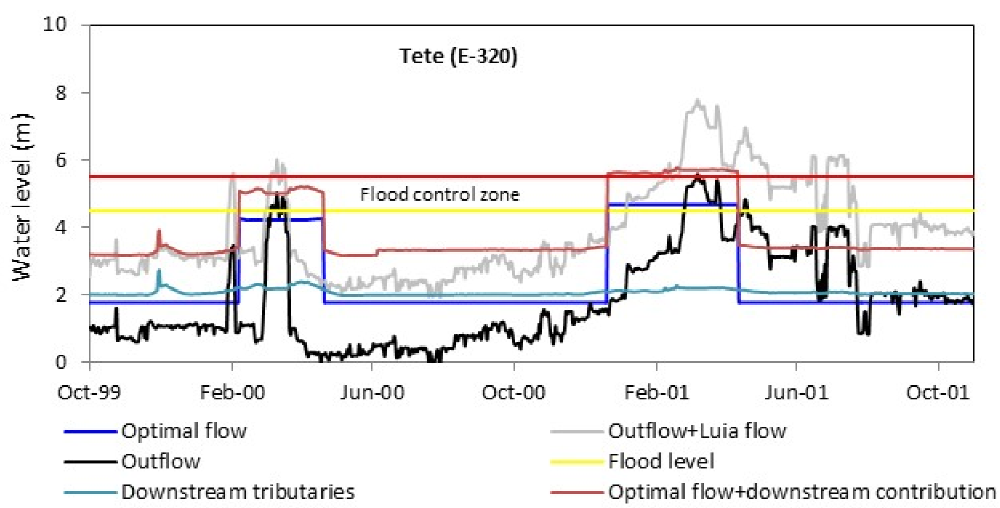

a)

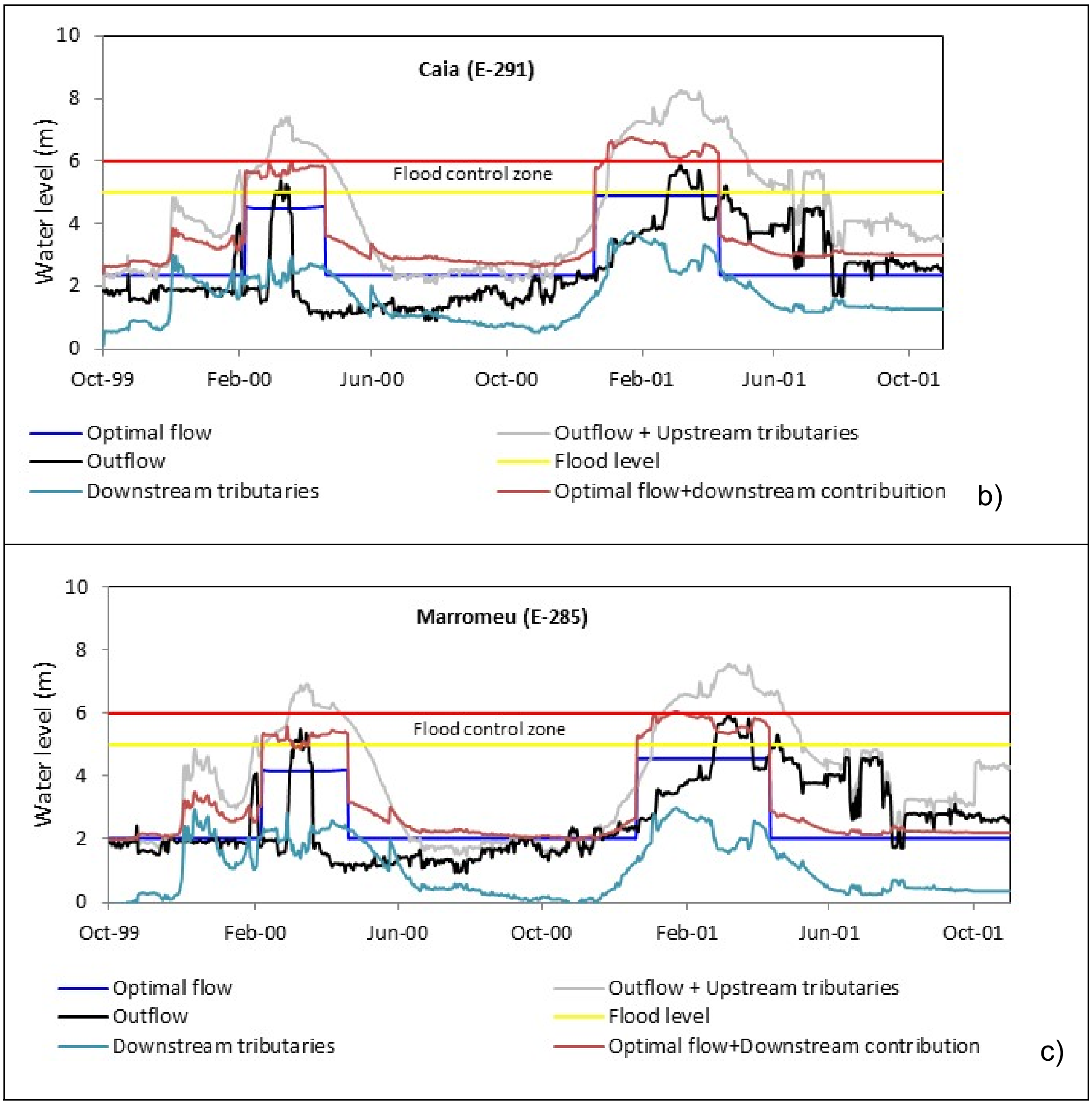

Figure 7.5: Example of the application of the proposed framework showing how the Cahora Bassa should be operated to mitigate 2000 and 2001 floods at Tete (a), Caia (b) and Marromeu (c). It illustrates the impact of the optimal flow, downstream rivers, outflow and the contribution resulting from the combination of outflow during 2000 and 2001 + downstream rivers and simulated optimal flow + downstream rivers and their contribution to the water levels rising.

7.4. Predicted flood flows and travel time

The analysis of hydrograph peak flow from 1998 to 2008 results (Section 4.6.2) show that the peak flows which occurred at Tete (E-320) in 1998, 2000, 2001, 2006 and 2008 were released at the Cahora Bassa dam. This means that dam flows above 4 500 m^3 s^{-1} travel from Cahora Bassa to Tete (E-320) took one day. From Cahora Bassa dam to Caia (E-291), which is further downstream, the peak flow took between two to four days. The flood peak then took between three to five days to travel from Cahora Bassa dam to reach Marromeu (E-285) (Table 7.1).

Table 7.1: Peak flood travel time from Cahora Bassa to Tete (E-320), Cahora Bassa to Caia (E-291) and Cahora Bassa to Marromeu (E-285)

Flood categories		Travelling time			
Streamflow ($m^3\ s^{-1}$)	Water level (m)	Cahora Bassa dam	Tete (E-320)	Caia (E-291)	Marromeu (E-285)
4 500 – 7 000	4.5-6.5	0	1	4	5
7 000 – 10 000	6.5-8.5	0	1	2	4
>10 000	>8.5	0	1	2	3

7.5 Flood risk maps

Rather than acting as mere identifications of severe flood events (drawn from the integrated GeoSFM and MIKE BASIN simulation results), flood risk maps are an important tool for flood prediction and management, because they complement the information predicted from hydrological models and allow the development of relief profiles. Mapping is the method used to present risk information and to decide where to spend money on flood risk management measures (and, additionally, to help the water managers and dam operators to enhance their response to flooding). These flood risk maps can serve as a basis for designing measures to minimize loss of life. Since one of the objectives of this study was to generate a flood hazard map, the geomorphologic approach employing Shuttle Radar Topographic Mission (SRTM) DEM integrated with GIS, was used to delineate flood hazard extent (Section 4.7 and Appendix 1), and the results validated through comparison with the Landsat images of flood extent (Section 3.7). Figure 7.6 shows the three different levels of floods produced in the Lower Zambezi.

i. Flood Level 1 corresponds to water levels between 5 m and 7 m;

ii. Flood Level 2 for water levels between 7 m and 9 m and

iii. Flood Level 3 when the water level is above 9 m.

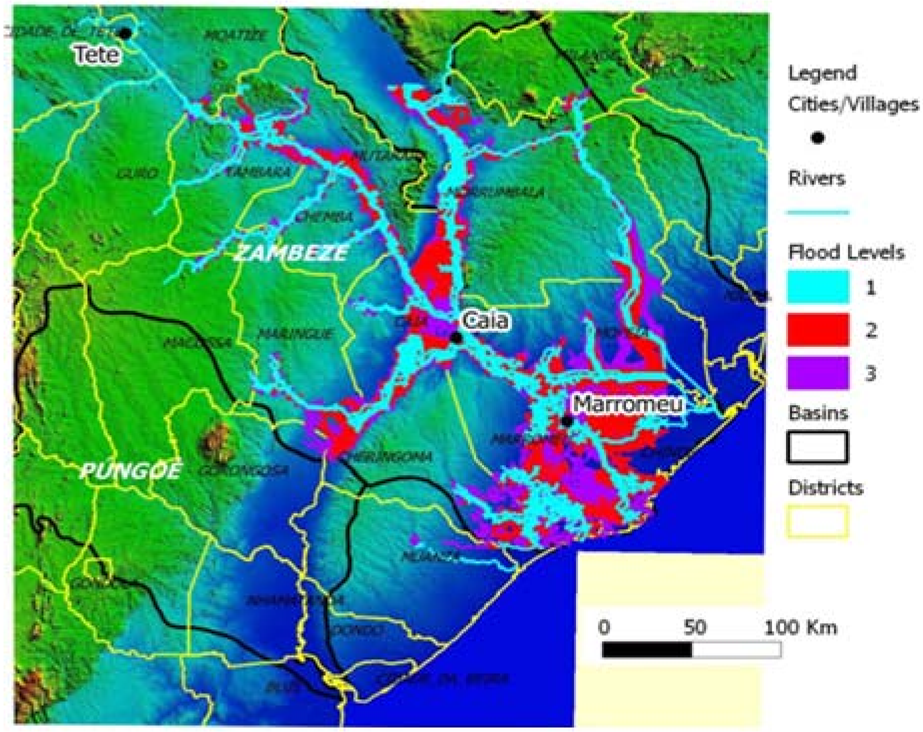

Figure 7.6: Shows the extent of flooded areas for different flood water levels and the location of the nine (9) districts in the Lower Zambezi sub-basin

7The results produced from the DEM are shown in Figure 7.7a, b and c, which are reasonably consistent with Landsat images of 2000/2001 flood extent (Figure 7.7d) with a flow of approximately 12 000 $m^3 s^{-1}$, measured in Caia (E-291), corresponding to Flood Level 2. From overlay analysis between the flood maps and socio-economic infrastructures (villages, school and hospitals) the impact of the Lower Zambezi River floods can best be evaluated relative to the known impacts of the floods in 2000 and 2001. These two flood events were classified as Flood Level 2, where the water level in Caia (E-291) was ≥ 7.0 m and ≤ 9 m (Section 7.3.2).

This study estimated that 281 138 people were affected. The results are in accordance with the SMEC (2004) study which quantified the losses: approximately 217 000 people were temporarily relocated and 115 lives were lost. It may be inferred that at least 50 000 houses, more than 100 schools and hospitals were inundated, during the same flood. One of the major impacts of Zambezi River flooding at the downstream areas is in the lowest reaches of the, Mazoe, Luenha, Revubue and Shire Rivers – sometimes referred to as the Inhamgoma Triangle.

The Inhamgoma Triangle is a fertile area that supports a large rural population, but is very low-lying (Brouwer and Nhassengo, 2006). Table 7.2 shows the total area inundated (by district and the percentage of the total area), the maximal flood levels (both observed and simulated) and the duration in days. The % of the total was estimated using GIS and the maximal flood level and duration estimated from graphical comparison of hydrographs.

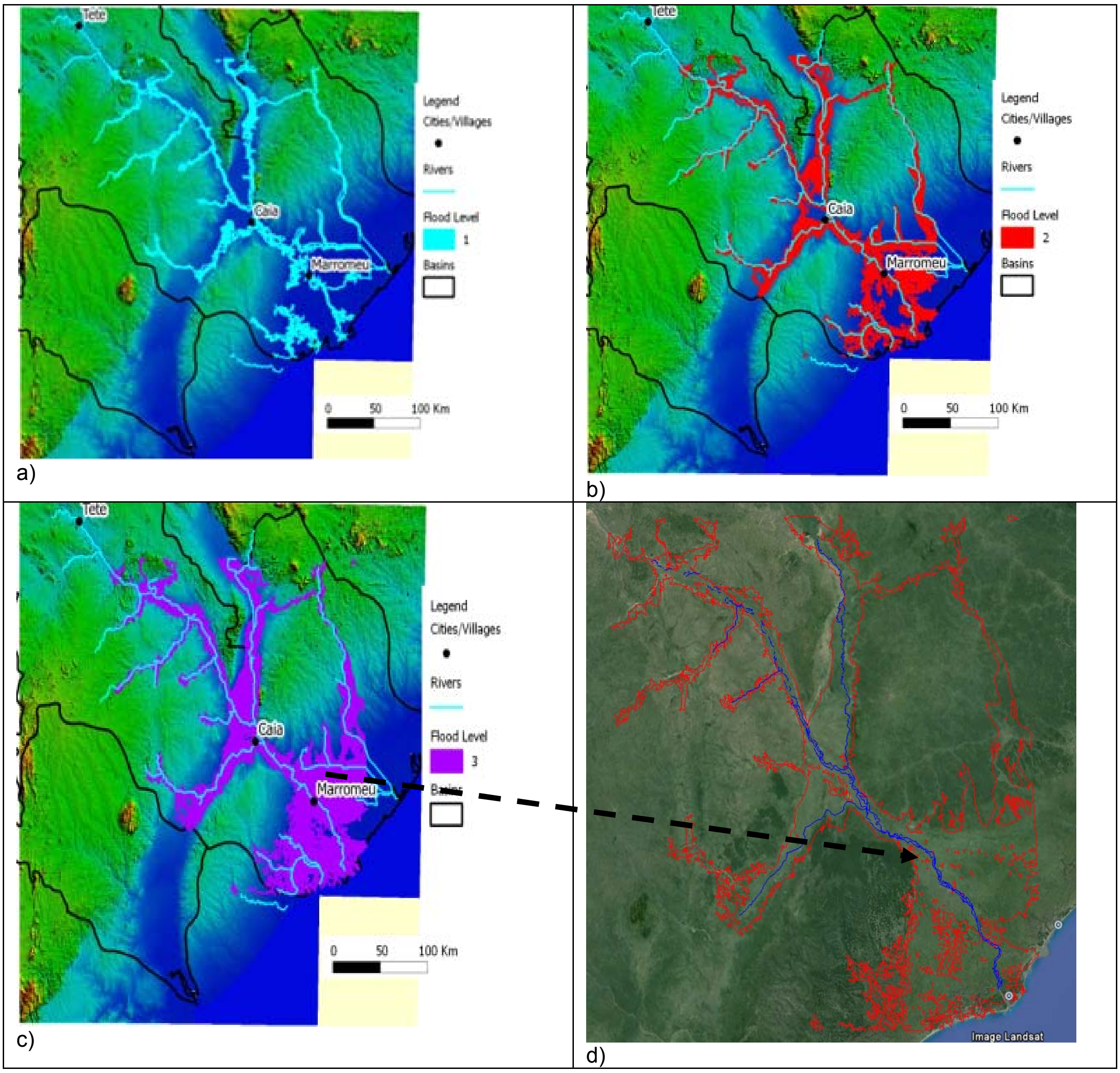

Figure 7.7: Three separate layers of flood areas for comparison between results produced by DEM and Landsat images. Results for different levels (5 –10.5 m) and comparison between results produced by DEM (a, b and c) and the Landsat images downloaded on 3^{trd} May 2001 (d) – the red colour shows the area covered by the year 2000/2001 flood, with a flow of approximately 12 000 m^3 s^{-1}

Table 7.2 shows that, during the 2000/2001 flood, 23.5% of the Lower Zambezi was inundated. The situation was even worst at Marromeu, Caia, Mopeia and Mutarara, where more than 30% of the total area were flooded for average of 40 days. The observed maximal water level was 1.4 m higher and 4 days lower in duration when compared with the simulated water level. The difference between the observed and simulated water level may have been related to the operations at the Cahora Bassa dam (Section 6.3.2.3).

Table 7.2: Percentage of inundated areas, maximal flood level and duration taking an example of 2000/2001 flood event

ID	Districts	Total Area (Km^2)	Maximal inundated area (Km^2)	% of the total Area	Duration in days	
					Observed	Simulated
1	Tambara	4 736.1	348.7	7.4	38	42
2	Mutarara	6 584.0	2228.8	33.9	38	42
3	Chemba	3 888.0	295.1	7.6	38	42
4	Caia	3 542.0	1380.1	41.8	38	42
5	Morrumbala	12 801.2	1671.3	13.1	38	42
6	Chiringoma	7 404.4	1058.7	14.3	39	42
7	Mopeia	7 792.9	2991.3	38.4	39	42
8	Marrínguè	6 411.4	799.7	12.5	48	51
9	Marromeu	5 786.0	3016.8	52.2	48	51
Total	**-**	**58699.5**	**13790.5**	**23.5**	**-**	-

Table 7.3 shows the results of the sensitivity of the number of people affected by flooding to the level of flooding. Sensitivity analysis tables were obtained by calculating the relationship between the flood extent areas and the total number of villages (and the population), which were likely to be affected by flood. The assumption was that the total population affected by floods increases when the water level also increases. Analysing the sensitivity of change in flood level and the impact on the population downstream of the Cahora Bassa dam, five (5) out of nine (9) districts were identified as being highly sensitive (Table 7.3). Through assessment of the flood risk maps (Appendix 2), results illustrated that these districts are also highly populated in areas dominated by the flood plain system of the Zambezi River and its tributaries. At Chemba, Chiringoma and Marromeu the sensitivity was reduced – even though the flooding severity had increased – because of the lower concentration of villages in these areas (Appendix 2.2-B; 2.6-F and 2.7-G). These results are similar to previous studies (Brouwer and Nhassengo, 2006), which concluded that the severity of flood impact in the Lower Zambezi is explained by the fact that over 80% of Lower Zambezi's population depends on small-scale, rain-fed agriculture on the floodplain, where the most fertile soils are located.

Table 7.3: Sensitivity analyses between numbers of affected people at different flood levels

ID	District	Total Population	Province	Area (km^2)	Population (affected)			(%) of the Total
					Level 1	Level 2	Level 3	Level 3
1	Tambara	44 394	Manica	4 736	9 324	13 460	13 826	31
2	Mutarara	148 438	Tete	6 584	35 193	57 519	73 870	50
3	Chemba	56 096	Sofala	3 888	8 478	18 134	22 998	41
4	Caia	89 268	Sofala	3 542	17 427	25 886	27 713	31
5	Morrumbala	211 286	Zambeze	12 801	16 810	32 062	34 773	16
6	Chirringoma	39 972	Sofala	7 404	672	2 731	2 731	7
7	Mopeia	95 855	Zambeze	7 793	9 270	17 086	45 341	47
8	Marrínguè	70 417	Sofala	6 411	9 847	9 847	14 135	20
9	Marromeu	55 425	Sofala	5 786	16 857	44 226	45 751	83
Total	-	**811 151**	-	-	**123 878**	**220 951**	**281 138**	**35**

(green)	Less sensitive
(orange)	Moderately sensitive
(red)	Highly sensitive

7.6. Summary

The main objective of this chapter was to establish a hydrological baseline for the Zambezi River basin, which could then be used for flood prediction and management in the basin. The chapter also reports on the assessment of the use of simulated streamflow as an input for reservoir operation at a daily time step. The major problems experienced during the modelling process were availability and accessibility of data (to force and calibrate the hydrological model), and the quality of the data when available. The un-calibrated GeoSFM model outputs were compared with observed historical data on a daily time step, and the results showed significant differences in magnitudes of peak streamflow, although the timing of the flows matched well in all circumstances. The reliability of the gauging stations' data is also a problem because the time series were often not continuous – this strongly impacted on the parameterisation of the model through the calibration process. Thus, in calibrating the model, the uncertainty parameter bounds were generated using subjective and 'rule based' assessments of available basin physical property data – these were then used as input to the Sensitivity Analysis Routine in GeoSFM to generate a parameter space that could inform the manual calibration process.

The behavioural parameters, based on statistical objective function assessments, were refined using manual calibration to establish regional parameters for the Zambezi Basin. The coefficients of determination (R^2); efficiency (CE) of at least 0.5; and the Bias of ±20% were used to determine acceptable model simulations. The choice was driven by the quality of the available data at the selected streamflow gauges. The results suggest that, in general, the GeoSFM is capable of reproducing most of the main hydrological response characteristics of the various sub-basins of the Zambezi Basin. However, any modelling process is affected by uncertainties from various sources. Since the parameterisation of the GeoSFM relied heavily on an initial interpretation of the physical property data, it is possible that the available data (or the DEM information) were inadequate – based on the scales at which these data were available and compared with the scale of model operation – for sufficiently describing the physical process relationships. It is also possible that subjectivity in the interpretation of the data may have been an important issue, leading to possible misinterpretations.

Data paucity has been identified as one of the major sources of uncertainty in the calibration process for the Zambezi Basin. The problem of simulating peak flows may be attributed to limitations in the rainfall data in individual months (or in wet seasons) and also to the inability of the sparse rain gauge networks to capture the storms accurately (Mazvimavi, 2003) and to measure the extremely high rainfall in the wetter parts of the Zambezi Basin. Apart from rainfall and other physical properties, reservoir management also impacts streamflow (through water storage in the rainy season) and releases (in dry seasons and in extremely wet conditions). To enhance the modelling prediction, the GeoSFM was integrated with MIKE BASIN to simulate the impacted hydrology of the Zambezi River basin. The integrated model results showed a good agreement with selected streamflow gauges. Hydrological modelling in ungauged catchments still remains a challenge. The integrated GeoSFM and MIKE BASIN constitutes an opportunity to develop a robust flood forecasting and early warning system in the Zambezi Basin, mainly for the low-lying floodplain in Mozambique, which is the region most prone to floods. The developed Decision Support Framework was used to monitor the water flow/levels for the past (previous) 6 days and to present a 3 day flood forecast and control procedure, for both the dam site and downstream of the dam. Flood risk maps were also produced to complement the information predicted from the hydrological models and to allow the development of relief profiles.

8. CONCLUSION AND RECOMMENDATIONS

The Zambezi River Basin regularly experiences extreme rainfall and flood events. This study was carried out with the aim of addressing the challenges of hydrological modelling and improving flood forecasting – for the Zambezi Basin – in an operational context. These challenges were considered the main concerns of reservoir managers in the basin. Flood forecasting is still one of the uncertain problems of operational hydrology, given the scarcity of observational data and that rainfall-runoff models are far from perfect. The main research themes covered in this study are:

i. the lack of adequate data for hydrological information;
ii. lack of modelling tools that could be used to adequately represent the hydrology of the basin;
iii. the uncertainties inherent in applying models in the basin;
iv. the uncertainties about the results simulated by the modelling application.

Recent developments and advances in integrated technologies of Geographic Information Systems (GIS), remote sensing and hydrological modelling offer opportunities for improving daily streamflow simulation by assimilation of the remote sensing information into hydrological models to improve reservoir management in a data scarce environment. This chapter summarises the main findings that come from model application in the Zambezi Basin and makes recommendations for further improving the integrated hydrological modelling system of the basin.

8.1. Data issues and decision support tools

One of the main questions is whether there are enough data and analysis tools available and appropriate for solving the problems of flood prediction for large river basins (such as the Zambezi). The Zambezi Basin is limited in climate and hydrological data – the major challenges being the sparseness of observed data, missing values and short hydrological records. This problem exacerbated by deteriorating gauging networks, reduced budgets and the lack of adequate monitoring capacity within the national hydrological agencies – all issues that are partly related to the recent history of civil wars in countries like Angola and Mozambique. The Zambezi Water Information System (ZAMWIS), a web-based and information systems portal for the Zambezi basin and Global Runoff Data Centre (GRDC). are purportedly in place but was difficult to access at the time this study was conducted. The Southern African Development Community Hydrological Cycle Observing System (SADC HYCOS) is another potential source of data for the Zambezi basin but regrettably there are many formalities that have to be addressed – attempts to obtain data from this source were largely unsuccessful. Because of these limitations, and to meet the set objectives, this study was forced to resort to the use of limited observed data and global data sets. Ironically the latter are easier to access when compared with accessing local data (from local water authorities). These global data include climate (temperature, rainfall and, evaporation), topography, land cover and soil types. Global datasets have the advantage of having reasonable or adequate spatial and temporal coverage.

A review of previous studies (Beilfuss and Dos Santos, 2001; Winsemius *et al*., 2006; Asante *et al.*, 2008; Tirivarombo, 2012 – researches that had attempted to model the hydrology of the Zambezi Basin) showed that a lack of data was the major constraint preventing successful model applications in the basin. The development of an appropriate database was, therefore, a prerequisite for undertaking any modelling experiments. In hydrological modelling, data are not only used as input to the model, but also to assess the characteristics of physiographic controls that influence runoff generation processes – and to discover relationships between different physical features of a basin and its hydrological response to climate inputs. Understanding these relationships should contribute to decisions involving conceptual formulations of models and the methods that can be used to establish appropriate model parameter sets. One major aim achieved in this study was the development of a database of climate, physiographic and hydrological characteristics of the basin. Several local, regional and global sources of data were explored (Chapter 3).

8.2. Stream flow prediction

In general terms, the hydrological processes in the Zambezi Basin are complex. This complexity is partly because of the different response characteristics of the sub-basins that compose the Zambezi River system. Assessment of the basin physical characteristics in this study shows that the basin stretches over a large geographic area, consisting of different combinations of physiographic characteristics. The seasonal cycle in the basin has a bimodal pattern of rainfall distribution. The basin also experiences highly variable rainfall, both spatially and temporally, which contributes to risks in the availability of sustainable water resources (World Bank, 2006). The distribution of the land cover over the Zambezi Basin varies from the savannah type (which covers 58% of the area), followed by deciduous broadleaf forests (covering 15%). Other land cover types in the basin include: cropland/woodland mosaic (covering 14%); dry land cropland and pasture (5%); evergreen broadleaf forests (4%); water bodies (3%); barren or sparsely vegetated surfaces; grassland; urban and built-up surfaces; irrigation areas; shrub land and herbaceous wetlands – each of these in this long list cover less than 1% of the total area. Variability in land cover composition for the basin implies variability in surface canopy – which will also affect the variability in rainfall interception storage, infiltration and evapotranspiration losses across the basin. Associated with the types of vegetation cover are litter depths and types, rooting depths and densities – all of which also affect the water balance and runoff generation mechanisms (Loveland *et al.*, 2000).

There are two main rain seasons – both are strongly related to the spatial and temporal distribution of rainfall within the basin. The wet season occurs from November to March, with mean rainfall between 250 and 1 500 mm – the rainfall level generally decreases from north to south. In the central part of the region, dry-season precipitation is rare, and there is usually no measurable rain for six months or more. In the Zambezi Basin, flood producing high rainfalls are a major problem and during these periods, areas of land adjacent to the main rivers are flooded (Katjavivi, 2009). The situation is even worse on the Mozambican side of the Zambezi basin where intense rainfall is associated with the cyclone activities – which cause extensive flooding, destruction of property and the displacement of millions of people (INGC, 2009). In this study the initial task was both to investigate the applicability of using satellite-based rainfall estimates for daily streamflow forecasting in the Zambezi River Basin and to study the improvements brought by an assimilation of this information into hydrological models for improving reservoir management in a data scarce environment.

Therefore CPC-RFE 2.0 rainfall grids were used to address the first research question of this study – *Can satellite rainfall data be successfully used as input into hydrological modelling for flooding forecasting in data scarce environments?* It was concluded that, with the advancement of technology, CPC-RFE 2.0 offered an opportunity (and may be an attractive option) for hydrologists for the forecasting of streamflows in the Zambezi Basin. These data are readily available and have greater coverage (Verdin, 2000; Rahman *et al*., 2002; Asante *et al.*, 2008). The rainfall analyses results of this study are similar to conclusions reached by earlier studies (Shrestha *et al.,* 2008; Roca *et al.,* 2010; Romilly and Gebremichael, 2011; Liechti *et al*., 2011; Gao and Liu, 2013), which concluded that the magnitude of rainfall given by the CPC-RFEs and TRMMs was often lower than the observed rain gauge station rainfall. This resulted in the under-estimation of the simulated streamflows and the need for methods to remove the bias. This study assumed that an adequate conceptual representation of storages (such as soil moisture and groundwater, and wetland, lake and river systems) would represent the hydrological behaviour of the system under study. The GeoSFM model was able to simulate the daily flow variation for all the tested sub-basins of the Zambezi River (between 1998 and 2008) with acceptable levels of agreement given the limited available field observation values from the National Water Agency and the Global River Discharge databases. Following a number of trial automatic and manual calibration runs of the GeoSFM model, it was concluded that this model could be successfully applied for flood forecasting and management of the Zambezi Basin and also has the potential to be used for solving problems of reservoir management by providing inflows for the MIKE BASIN reservoir model, allowing the future release of water from the dam to be done in an optimised manner thereby minimising the impact of floods downstream of the dam.

The calibration process established the model for the whole Zambezi basin, including 150 sub-basins and the model setup was validated using 11 gauging sites. Model calibration was successful in various areas of the Zambezi Basin – which exhibit inherently different hydrological responses – thus proving to be robust enough to represent the complexity of natural processes in the basin. Several parts of the basin include very large wetland, floodplain and lake areas (Barotse, Kafue, and Lake Malawi). Despite the problems with simulating such complex systems, the model results were considered adequate for the designated purposes of flood estimation below the Cahora Bassa dam.

To address the second research question of this study – *How can a rainfall runoff model be integrated with existing reservoir simulations for daily water resources operation systems?* – Geospatial Stream Flow Model (GeoSFM) and MIKE-BASIN models were used. Assessment of the calibration results using the integrated GeoSFM-MIKE BASIN System show that the model works reasonably well and has been able to reproduce the desired characteristics of the hydrological response. Therefore the study concluded that integrated modelling results can be used to support the formulation of management strategies both to inform water resource managers about the water balance in the Zambezi Basin and to serve as a reasoned basis for deciding on daily monitoring and dam operations activities. This investigation serves as a useful example of the application of a simplified distributed model for the assessment of catchment hydrology – and this model can be considered as an alternative option, instead of models that adopt similar surface flow and soil process representations, although in a spatially lumped framework. This research also recognised that it is not sufficient to apply the integrated modelling system for daily stream flow forecasting on selected sites without also connecting the Kafue sub-basin existing dams into the model.

8.3. Prediction of flood impacts

In addressing the third research question – *How can the impact of flood be minimised by the use of integrated hydrological models?* – this study recognised that readily available satellite data products (which capture the spatial distribution of rainfall) are capable of estimating rainfall data for feeding into the integrated GeoSFM and MIKE BASIN modelling system for flood forecasting downstream of the Cahora Bassa dam.

One major aim achieved in this study was the development of additional tools that may enable the hydrologists and the dam operators to convert the daily streamflow predicted by the integrated GeoSFM-MIKE BASIN System into predicted water levels and to generate flood risk maps for 9 (nine) districts located downstream of the Cahora Bassa dam. Moreover, peak flows ranging from 5000 – 10 000 $m^3 s^{-1}$ would take a maximum of five (5) days to travel from the Cahora Bassa dam (downstream) to Marromeu, in the Lower Zambezi.

Flood risk maps, generated through using the models, may be used to predict the impacts of different ranges of releases and for warning the downstream villages of potential impact before the flow releases take place.

Therefore, operationally on the Mozambican side of the Zambezi Basin, the integrated GeoSFM-MIKE BASIN System can be applied by the National Directory of Water, together with ARA-Zambezi for flood forecasting. These institutions have the overall role of flood prediction and warning for the Lower Zambezi. The Revised Protocol on Shared Watercourses in the Southern African Development Community (SADC) and the Permanent Joint Commissions (PJC) are important tools for Mozambique – they provide forums for collaborating and cooperating (for the data exchange process) with the other countries who share the Zambezi basin. In addition, the study concludes that it is important not only to discuss flood impact assessment after it has occurred but also to quantify the impacts of the flood before it happens, through using flood risk maps. Inundation maps, based on forecast outlet discharges, could be useful in providing additional information to the public during forecast warnings in the Lower Zambezi sub-basin area. Therefore flood mapping would help stakeholders to understand floods and thereby to improve thedecision-making process (Hess *et al*., 1995; Nico *et al.,* 2000; Horritt and Bates*,* 2001a, b).

8.4. Recommendations

As far as the author of this study can determine, this is the first time that a model has been established that can adequately predict floods in the Zambezi Basin in an integrated manner – one that includes the natural hydrology and the management of storage within the basin. It is therefore considered important that these research findings are disseminated and further assessed in terms of their value for water resources management in the Basin. Currently the following organisations have been established (to work towards sustainable water resources management but also including flood management issues of the Zambezi Basin):

- the Zambezi River Basin Commission (ZAMCOM);
- Zambezi River Authority (ZRA, Zambia and Zimbabwe) – operator of the Kariba dam;
- *Hidroeletrica de Cahora Bassa* (HCB, Mozambique) – operator of the Cahora Bassa dam;
- Disaster Management and Mitigation Unit Centre (DMMU), Zambia;
- Department of Civil Protection (DCP) in Zimbabwe;

- ARA-Zambezi, Mozambique;
- Water Boards of the Southern African Development Community (SADC).

Therefore, it is intended that these River Basin Organisations (RBOs) should be made aware of the results of the study and encouraged to make use of the research findings and be trained in their practical application. In addition, scientific communication should be boosted through the publication of scientific papers and the presentation of the results at conferences and workshops.

The streamflow data used in this study were obtained without sufficient technical information (such as water heights and rating curves) to help deeper analysis of the measurement errors. This is an aspect should be further researched – particularly for the reliability of the discharge data provided by the various distribution centres. The model calibration in this study has proved to be adequate in simulating the desired hydrological information for flood forecasting in the basin. However, there are outstanding modelling issues, related mainly to the shortage of the observed data. So it is important to explore other sources of the observed historical data that can be used to reduce uncertainties and enhance the confidence in model calibration.

It is also recommended that the model calibration and application for flood forecasting downstream of the Zambezi Basin can be improved through:

- integrating the Kafue sub-basin dams into the modelling system;
- and establishing and improving the existing hydro-climatic (rainfall, evaporation and streamflow) network density.

This would ensure that the application of new satellite data products would be improved by better and more widely obtained observational data.

It is nonetheless important to recognise that, from an operational point of view, creating a dense hydro-climatological network in the Zambezi Basin is a major challenge – especially because of the financial constraints hindering proper maintenance (Asante *et al.,* 2008; WMO and USAID, 2012).

The physically-based parameter estimation procedures have proved to be a valuable tool for process understanding and hydrological predictions in the Zambezi Basin, but remain challenged by the lack of appropriate physical basin property data – in particular data on the subsurface processes. Closing this gap would ideally be achieved by field observations, although this is extremely difficult to undertake in such a large and remote basin. The alternative of using a model, together with earth observation information, appears to be a practical approach. Experiments (undertaken by other researchers – such as the Gravity Recovery and Climate Experiment (GRACE); Light Detecting and Ranging (LIDAR); Shuttle

Radar Topographic Mission (SRTM); Moderate Resolution Imaging Spectroradiometer (MODIS); (Giri and Reed, 2005; Tenenbaum *et al*., 2006; Strabala, 2009; Werth *et al*., 2009) and radar altimetry products are becoming more useful for informing modelling studies and for detecting soil and groundwater moisture fields, the connectivity of hill slope flow paths, patterns of land forms, and generating water height time series. Application of such innovative techniques should have a positive impact on data availability and can almost certainly be used to enhance confidence in parameter estimation procedures for the Zambezi Basin.

8.5. Areas for further study and improvements

This study has generated information that can be used for the development of the Zambezi Basin integrated decision support system. Tools and methods used in this study will form an important part of this development. The flood forecasting system will be a step towards the development of the Zambezi Basin communication strategy. Although these are important aspects, when it comes to the implementation of early warning systems, they were not incorporated into this study because it was beyond the scope of the current work. Therefore, there is a need to develop a user interface, in a suitable programming language, that will incorporate the rating curves developed for Tete (E-320), Caia (E-291) Marromeu (E-285) and the Cahora Bassa dam.

Uncertainty has been part of all modelling studies – mainly because of poor input data but also through issues of scale, model structure, and issues related to equifinality. Therefore, there is need for accurately assessing the uncertainties of any integrated hydrological modelling approach – such assessments should be directed towards model structural improvements and uncertainty reduction for the decision-makers.

REFERENCES

Acreman, M. (2009) Managed Flood Releases from Reservoirs: Issues and Guidance, Center for Ecology and Hydrology, UK.

Adler, R., Wu, H. and Tian, Y. (2012) Estimation using satellite rainfall information and hydrological models: status and future, *Water Resource Research, 6th Workshop of the International Precipitation Working Group (IPWG6).*

Administração Regional de Aguas do Sul (ARA-Sul) and Direcção Nacional de Águas (DNA), (2000) Cheia do ano hidrológico 1999-2000, Final Report, Maputo, Moçambique.

Administração Regional de Aguas do Sul (ARA-Sul), (2005) Mapas de inundação da bacia do Incomati, Final Report, Maputo, Moçambique.

Ahmad, S. and Simonovic, S.P. (2000) System dynamics modelling of reservoir operations for flood management, *Journal of Computing in Civil Engineering,* 14(3), 190-198.

Alam, M. and Rabbani, M.D.G. (2007) Vulnerabilities and responses to climate change for Dhaka, *Environmental Urban Journal,* 19, 81-92.

Alexander, W.J.R. (2002a) The Standard Design Flood: Theory and practice, Department of Civil Engineering, University of Pretoria, SA.

Alexander, W.J.R. (2002b) Statistical Analysis of Extreme Floods, URL, Online Report, http://www.up.ac.za/academic/civil/divisions/water/upflood.html, Accessed: 20th May 2012.

Allen RG, Pereira LS, Raes D & Smith M. (1998) Crop evapotranspiration: Guidelines for computing crop requirements. Irrigation and Drainage Paper 56, FAO, Rome, Italy.

Allen, R. G., Pereira, L.S., Raes, D. and Smith, M. (1998) Crop Evapotranspiration – Guidelines for Computing Crop Water Requirements, *FAO Irrigation and Drainage Paper*, 56, 1-34.

American Meteorological Society (AMS), (2000) A multistep Automatic Calibration Scheme for River Forecasting Models, Online report, http://www.fao.org/docrep/, 22nd July 2010.

Anderson, M.G. and Burt, T.P. (1985) Hydrological forecasting, Wiley & Sons Ltd, Salisbury, Wiltshire, UK.

Andjelkovic, H. (2001) Guidelines on non-structural measures in urban flood management, School of Geography Planning and Environmental Management, University of Queensland, Brisbane, Australia, Online international Hydrological Programme Report, http://unesdoc.unesco.org/, visited 30th Jun, 2012.

Andreassian, V., Perrin, C., Michel, C., Usart-Sanchez, I. and Lavabre, J. (2001) Impact of imperfect rainfall knowledge on the efficiency and the parameters of watershed models, *Journal of Hydro*logy, 250(1–4), 206–223.

Ao, T., Ishidaira, H., Takeuchi, K., Kiem, A.S., Yoshitari, J., Fukami, K. and Magome, J. (2006) Relating BTOPMC model parameters to physical features of MOPEX basins, *Journal of Hydrology*, 320(1-2), 84-102.

Arkin, P. A. and Meisner, B. N. (1987) The Relationship between Large-Scale Convective Rainfall and Cold Cloud over the Western Hemisphere during 1982-84, *Monthly Weather Review,* 115(1), 51–74.

Arnall, A., David, S.G., Chasca, T., and Liverman, D. (2013) Flooding, resettlement, and change in livelihoods: evidence from rural Mozambique, Published by Blackwell Publishing, 9600 Garsington Road, Oxford, OX4 2DQ, UK and 350 Main Street, Malden, MA 02148, USA.

Arnold, J.G., Allen P.M. and Bernhardt, G. (1993) A comprehensive surface–groundwater flow model, *Journal of Hydrology*, 142, 47–69.

Aronica, G., Tucciarelli T. and Nasello, C. (1998) Multilevel model for flood wave propagation in flood-affected areas, *Journal of Water Resources,* 124(4), 210-217.

Arora, V.K. (1999) A river flow routing scheme for general circulation models, *Geophysics Research Journal,* 104, 347-357.

Artan, G., Verdin, J. and Asante, K. (2001) A wide-area flood risk monitoring model, *Proceeding of the fifth International Workshop on application of Remote Sensing in Hydrology, Montpellier*, France.

Artan, G.A., Restrepo, M. and Asante. K. (2002) Flood early warning system for Southern Africa, U.S. Geological Survey Open File Report, Reston, Virginia, USA.

Artan, G.A., Asante, K.O. and Verdin, J.P. (2004) A continental scale flood hazard monitoring system, *Eos Trans. AGU, 85(17), Jt. Assem. Suppl.*

Artan, G.A., Gardai, H., Smith, E., Asante, K.O., Bandaragoda, C.H. and Verdin, J.P. (2007) Adequacy of satellite derived rainfall data for streamflow modelling, *Natural Hazard,* 43, 167–185.

Asante, K.O, Verdin, J.P., Restrepo, M., Artan, G.A., Macuacua, R.D. and Vilanculos, A. (2005) A new algorithm for delineating flood inundation from Digital Elevation Models, ARA-Sul Technical Report, Maputo, Mozambique.

Asante, K.O., Artan, G.A., Pervez, S., Bandaragoda, C. and Verdin, J.P. (2007a) Technical Manual for the for the Geospatial Streamflow Model (GeoSFM), U.S Geological Survey Open-File Report, 2007-1441, Reston, Virginia, USA.

Asante, K.O., Artan, G.A., Pervez, S., Bandaragoda, C. and Verdin, J.P. (2007b) User Manual for the Geospatial Streamflow Model (GeoSFM), U.S Geological Survey Open-File Report, 2007-1441, Reston, Virginia, USA.

Asante, K.O., Macuacua, R.D., Artan, G.A. Lietzow, R.W. and Verdin, J.P. (2007c) Developing a flood monitoring system from remotely sensed data for the Limpopo Basin, *Transition in Geoscience and Remote Sensing,* 45, 1709– 1713.

Asante, K.O., Artan, G.A., Pervez, S., Bandaragoda, C. and Rouland, J. (2008) A linear geospatial streamflow modelling system for data sparse environments, *International Journal of River Basin Management*, 6(3), 233–241.

Asante, K.O., Tadross, M. and Vilanculos, A. (2009) The Impact of Climatic Changes in Water Resources, Open-File Report 2009, INGC, Maputo, Mozambique.

Australian Bureau of Meteorology (2005) Flood Classification, Online Technical Report, http://www.bom.gov.au/, 21st Jun, 2012.

Bahremand, A. and DeSmedt, F. (2008) Distributed hydrological modelling and sensitivity analysis in Torysa Watershed, Slovakia, *Water Resource Management,* 22, 393-408.

Balsamo, G., Albergel, C., Beljaars, A., Boussetta, S., Brun, E., Cloke, H. L., Dee, D., Dutra, E., Pappenberger, F., Munoz Sabater, J., Stockdale, T., and Vitart, F. (2012) A global land-surface reanalysis based on ERA-Interim meteorological forcing, European Centre for Medium-Range Weather Forecasts Report Series, 13, 1–25.

Bambaige, A. (2007) Human development report 2007/2008 – National adaptation strategies to climate change impacts – A case study of Mozambique, *Human Development Occasional Papers (1992-2007)*, United Nations Development Programme (UNDP).

Bandaragoda, Ch. (2007) Distributed hydrologic modelling for streamflow prediction at ungauged basins, PhD Thesis, Utah State University.

Bardsley, W.E A, Jorgense, M.A, Alpert, P. and Ben-Gai, T. (1999) A significance test for empty corners in scatter diagrams, J*ournal of Hydrology*, 66–77.

Barrett, R.C. (2001) Satellite remote sensing precipitation progress and problems, *Association of Scientific Hydrology Publication*, 267.

Barros, A. P., Kim, G., Williams, E. and Nesbitt, S. W. (2004) Probing orographic controls in the Himalayas during the monsoon using satellite imagery, *Natural Hazards and Earth Systems Sci*ence, 4, 29–51.

Bates, P.D. and DerRoo, A.P.J. (2000) A simple raster-based model for floodplain inundation, *Journal of Hydrology*, 236, 54-77.

Baumann, J., Rodriguez, J. and Monterrosas, J. (2010) The effect of rainfall, slope gradient and soil texture on hydrological processes in a tropical watershed, National Water Commission. Online report, http://tucson.ars.ag.gov/isco/isco15/pdf/Baumann, 15th November 15, 2011.

Beasley, D.B., Huggis, L.F. and Monke, E.J. (1980) ANSWERS: A model for watershed planning.*Transactions of the American Society of Agricultural Engineers*, 23, 938-944.

Beilfuss, R. and Dos Santos (2001) Prescribed flooding and restoration potential in the Zambezi delta, Mozambique, *International Crane Found*ation, 17, 1-72.

Beilfuss, R. D. & Davies, B. R. (1998) Prescribed flooding and Wetland Rehabilitation in the Zambezi Delta, Mozambique. In: Streever, W. (ed.), *International Perspectives on Wetland Rehabilitation*, Kluwer Publ., Dordrecht.

Beilfuss, R.D. (1997) Restoring the flood: a vision for the Zambezi Delta, *The ICF Bugle* 23(4), 1-2.

Beilfuss, R.D. (2005) Water quality; Workshop on water management for the Zambezi Delta – Evaluation of Scenarios, Maputo.

Beilfuss, R.D., and Davies, B.R. (1999) Prescribed flooding and wetland rehabilitation in the Zambezi Delta, Mozambique. Pages 143-158. In: An international perspective on wetland rehabilitation (Ed. W. Streever). Amsterdam: Kluwer Academic Publishers.

Beilfuss, R.D., Guale, R.J., Chiburre, J.A., Kamwenesh, D. and Bento, C.M. (2009) Implementing environmental flow releases in the Zambezi River Basin: Experiences and Prospects, *Inland Empire Wrestling Association*, 25(12), 1-16.

Belward, A.S., Estes, J.E., and Kline, K.D. (1999) The IGBP-DIS 1-Km Land-Cover Data Set DISCover: A Project Overview, *Photogrammetric Engineering and Remote Sensing*, 65 (9), 1013-1020.

Beven, K. (2004) Robert E. Horton's perceptual model of infiltration processes, *Hydrological Processes*, 18, 3447-3460.

Beven, K. (2012) Rainfall-Runoff Modelling, Second edition Wiley Blackwell.

Beven, K. and Freer, J. (2001) Equifinality, data assimilation, and uncertainty estimation in mechanistic modelling of complex environmental systems using the GLUE methodology, *Journal of Hydrology*, 249(1-4), 11-29.

Beven, K.J. (1986) Hillslope Runoff Processes and Flood Frequency Characteristics: In A. D. Abrahams (ed.) Hillslope Processes, 187-202, Allen and Unwin, Boston.

Beven, K.J. (1987) Towards the use of catchment geomorphology in flood frequency predictions, *Earth Surface Processes and Land forms*, 12, 69-82.

Beven, K.J. (2006) A manifesto for the equifinality thesis, *Hydrological Process*, 320, 18-36.

Beven, K.J. and Binley, A.M. (1992) The future of distributed models-model calibration and uncertainty prediction, *Hydrological Processes,* 6(3), 279-298.

Beven, K.J., Smith, P.J. and Freer, J.E. (2008) So just why would a modeller choose to be incoherent?, *Journal of Hydrology,* 354, 15–32.

Bilberry, M., Asce, A. C.S. and Pinkard, F. (2011) Case study of rapid levee armouring during 2011 Mississippi River flood and potential future applications, Deutsche Gesellshaft fur Internationale Zusammenarbeit (GIZ) Gmbh, 1-66.

Bílková, D. and Mala, I. (2012) 'Application of the L-moment method when modeling the income distribution in the Czech Republic', *Austrian Journal of Statistics*, 41(2), 125-132.

Birkmann, J. (2006) Indicators and Criteria for Measuring Vulnerability: Theoretical Bases and Requirements. Birkmann, J. (Ed.): Measuring Vulnerability to Hazards of Natural Origin, Tokyo, New York, UNU Press.

Black, R. (1994) Livelihoods under stress: A case study of refugee vulnerability in Greece, *Journal of Refugee Studies*, 7, 360 – 377.

Blasco, F., M., Bellen, F. and. Chaudhury, M. U. (1992) Estimating the Extent of Floods in Bangladesh Using SPOT Data, *Remote Sensing of Environment*, 39, 167–178.

Blasone, R.S., Madsen, H. and Rosbjerg, D. (2006) Parameter estimation in distributed hydrological modelling: comparison of global and local optimisation techniques, *Proceeding 9th DHI Software Conference,* Scanticon Conference Centre, Denmark, June, 2006.

Blazkova, S. and Beven, K. (1997) Flood frequency prediction for data limited catchment in the Czech Republic using a stochastic rainfall model and TOPMODEL, *Journal of Hydrology*, 195, 256-278.

Blöschl, G. (2006) Rainfall-runoff modelling of ungauged catchments. Encyclopaedia of hydrological sciences (ed. M.G. Anderson), John Wiley and Sons, Chichester, UK.

Bobee, B. and Rasmussen, P.F (1995) Recent advances in flood frequency analysis. U.S. National report 1991-1994, *Twenty-first General Assembly International Union of Geodesy and Geophysics Boulder*, Colorado.

Bogaard T.A., Mazvimavi, D., Mkhandi, S., Parida, B.P., and Winsemius, R. H.C. (2010) Water Resources Assessment in Sub-Saharan Africa: Prediction in Ungauged and Data Scarce Basins, Water Resources Assessment, in Sub-Saharan Africa: Prediction in Ungauged and Data Scarce Basins, Cape Town, South Africa.

Bogardi, J. and Birkmann, J. (2004) Vulnerability assessment: the first step towards sustainable risk reduction. In: Malzahn, D., Plapp, T. (Eds.), Disaster and Society – From Hazard Assessment to Risk Reduction, Logos Verlag, Berlin, 75–82.

Bohle, H. (2001) Vulnerability and Criticality-Perspectives from social geography, *IHDP, Update 2*.

Bollin, C., Cardenas, C., Hahn, H. and Vatsa, K.S. (2003) Natural disasters network: comprehensive risk management by communities and local Governments, Inter-American Development Bank, Washington, USA.

Boughton, W and Chiew, F. (2006) Estimating runoff in ungauged catchments from rainfall, PET and the AWBM model, *Environmental Modelling Software*, 22(4), 476-487.

Bowman, K. P. (2005) Comparison of TRMM precipitation retrievals with rain gauge data from ocean buoys, *Journal of Climatology*, 18, 178–190.

Brakenridge, G.R. (1999) River flooding and Global Climate Change: A Multisensor Approach *in Earth Science Enterprise Reference Handbook*, R. Greenstone, 163-165.

Brandon, J. (2011) Planetary-scale tropospheric systems, accessed from www.recreationalflying.net/tutorials 18th May 2012.

Brouwer, R. and Nhassengo, J. (2006) About Bridges and Bonds: Community responses to the 2000 floods in Mabalane District, Mozambique, *Disaster,* 30(2), 234-255.

Brugnach, M., Pahl-Wostl, C., Lindenschmidt, K.E., Janssen, J.A.E.B., Filatova, T. Mouton, A., Holtz, G., Van Der Keur, P. and Gaber, N. (2008) Chapter Four: Complexity and Uncertainty: Rethinking the Modelling Activity Developments, *Integrated Environmental Assessment*, 3, 49-68.

Bulkley, J. and Kirchhoff, C. (2008) Transboundary Water Resources Management and the Potential for Integrated Water Resources Management (IWRM): Rhine River, Mekong River, and Zambezi River Case Studies, Department of Natural Resources and Environment, University of Michigan, Ann Arbor, USA.

Cannon, T. (1993) A Hazard Need not a disaster make: Vulnerability and the causes of natural disaster'. In: Merriman, P. A.; Browitt, C. W. (Eds.): Natural Hazard, London, Thomas Telford.

Chang, F.J., Chen, L. and Chang, L.C. (2005) Optimizing the reservoir operating rule curves by genetic algorithms, *Journal of Hydrology,* 19(11), 2277-2289.

Chatteri, M. (2002) *Conflict Management of Water Resources*. Hampshire, Ashgate Publishing Ltd. p 146.

Chen, F., Mitchell, K., Schaake, J., Xue, Y., Pan, H., Koren, V., Duan, Q. Y. and Betts, A. (1996) Modelling of land surface evaporation by four schemes and comparison with FIFE observations, *Journal of Geophysical Research*, 101, 2896–2916.

Chen, L. (2003) Real time genetic algorithm optimisation of long term reservoir operation, *Journal of American Water Resource Association,* 39(5), 1157-1165.

Cheng, Ch. and Chau, K.W. (2004) Flood control management system for reservoirs, *Environmental Modelling & Software*, 19, 1141-1150.

Chiesa, Ch., Cowhe, P. and Laben, C. (2012) Mapping flood risk and vulnerability in the Lower Mekong Basin, Map Book Gallery Volume 20, online: http://www.esri.com/mapmuseum/mapbook_gallery/volume20/safety2.html, 12th July 2011.

Chiew, F.H.S and Siriwardena, L. (2005) Estimation of SYMHYD parameter values for application in ungauged catchments. In: Zerger A and Argent RM (eds.), *Proceeding MODSIM 2005 International Congress on Modelling and Simulation*, 2(9) 2883-2889.

Chow, V.T., Maidment, D.R. and Mays, L.R. (1988) Applied Hydrology, McGraw-Hill, New York, USA.

Chowdary, V.M., Desai, V.R., Gupta, M., Jeyaram, A. and Murthy, Y.V.N.K. (2012) Runoff simulation using distributed hydrological modelling approach, remote sensing and GIS techniques: A case study from an Indian agricultural watershed, *International Archives of the Photogrammetric Remote Sensing and Spatial Information Science*, XXXIX-B8, 203-207.

Ciach, G. J. and Krajewski, W. F. (1999) On the estimation of radar rainfall error variance, *Advance in Water Resources,* 22, 585–595.

Clarke R.T. (1973) A review of some mathematical models used in hydrology, with observations on their calibration and use, *Journal of Hydrology,* 19, 1–20.

Consultec (2011) Hydrological and Hydraulic Study along the Revubue River Roads, Final Report, Maputo, Mozambique.

Conway, D. (2002) Extreme rainfall events and lake level changes in East Africa: recent events and historical precedents. In: The East African great lakes: limnology, palaeolimnology and biodiversity, *Advance Global Change Research*, 12, 63–92.

Conway, D., Persechino, A., Ardoin-Bardin, S., Hamandawana, H., Deulin, C. and Mahe, G. (2008) Rainfall and water resources variability in sub-Saharan Africa during the 20th century, Working Paper 119, Tyndall Centre for Climate Change Research, University of East Anglia, UK.

Cooper, M.R. and Fernando, D.A. K. (2009) The effect of the raingauge distribution on storm water models, *Proceeding 18th World IMACS / MODSIM Congress*, Cairns, Australia 13-17, July 2009.

Cordery, I. and Pilgrim, D.H. (2000) The state of the art of flood prediction, Vol. II, Routledge, London, UK, 185-197.

Cranston, M., Werner, M., Janssen, F.H., Lardet, P., Oxbrow, J. and Piedra M. (2007) Flood Early Warning System (FEWS) Scotland: An example of real time system and forecasting model development and delivery best practice, Scottish Environment Protection Agency Report.

Danehelka, J. (2007) Uncertainty of hydrological forecasting due to inputting precipitation forecast and possible solution using probabilistic approach in the Czech Republic, Czech Hydrometeorological Institute, NaŠabatce, Jan Danhelka, Czech Republic.

Daren, R. and Smith, P. K. (2007) Consideration of measurement uncertainty in the evaluation of goodness-of-fit in hydrologic and water quality modelling, *Journal of Hydrology*, 337, 326–336.

Davies, B.R. (1986) The Zambezi River system, pp. 225–267 In B.R. Davies and K.F. Walker (eds.) The Ecology of River Systems. Dr. W. Junk Publishers, Dordrecht, The Netherlands.

Davies, B.R. (1998) Sustainable Use of the Cahora Bassa Dam and the Zambezi Valley, Final Report*,* Maputo, Mozambique.

Dee, D. P., Uppala, S. M., Simmons, A. J., Beresford, P., Poli, P., Kobayashi, S., Andrae, U., Balmaseda, M. A., Balsamo, G., Bauer, P., Bechtold, P., Beljaars, A. C. M., van de Berg, L., Bidlot, J., Bormann, N., Delsol, C., Dragani, R., Fuentes, M., Geer, A. J., Haimberger, L., Healy, S. B., Hersbach, H., Hólm, E. V., Isaksen, L., Kållberg, P., Köhler, M., Matricardi, M., McNally, A. P., Monge-Sanz, B. M., Morcrette, J. J., Park, B. K., Peubey, C., de Rosnay, P., Tavolato, C., Thépaut, J. N., and Vitart, F. (2011) The ERA-Interim reanalysis: configuration and performance of the data assimilation system, *Meteorological Society*, 137, 553– 597.

Demirtas, M., Nance, L., Bernardet, L., Lin, Y., Chuang, H. Y., Loughe, A., Mahoney, J., Gall, R. and Koch, S. (2005) The developmental tested center verification system, http://www.mmm._25_ucar.edu/wrf/users/workshops/WS2005/abstracts/Session3/23-DEMIRTAS.pdf, 12th May 2013.

Denmark Danish Hydraulic Institute (DHI), (1998) MIKE 11 GIS, A flood modelling and management tool, Reference and user manual, Danish Hydraulic Institute, Horsholm, Denmark.

Denmark Hydraulic Institute (DHI) and Aurecon (2011) Progressive realization of the IncoMaputo agreement operating objective, PRIMA Final Report, Maputo.

Denmark Hydraulic Institute (DHI), (2000) MIKE BASIN, A tool for river basin planning and management, User Manual for MIKE BASIN 2000, Denmark.

Denmark Hydraulic Institute (DHI), (2005) Modelling the World of Water, http://www.dhisoftware.com/mikefloodwatch, 10th April 2011.

Denmark Hydraulic Institute (DHI), (2006) MIKE 11: Rainfall-Runoff Modelling for flood forecasting in the Lower Zambezi, Basin, Final Report, Tete, Mozambique.

Denmark Hydraulic Institute (DHI), (2006) MIKE BASIN User's Manual, DHI Water and Environment, Inc. Report, Copenhagen, Denmark.

Denmark Hydraulic Institute (DHI), (2010) MIKE BASIN User Manual, Open-File Report, 10 June 2010.

Denmark Hydraulic Institute (DHI), Water & Environment, Inc. and Lane Council of Governments (2008) McKenzie River MIKE BASIN Model, Report for Eugene Water & Electric Board, *DHI Water and Environment, Inc.,* Denmark.

Diak, G. R., Mecikalski, J. R., Anderson, M. C., Norman, J. M., Kustas, W. P., Torn, R. D., and Dewolf, R. L. (2004) Estimating Land Surface Energy Budgets from Space: Review and Current Efforts at the University of Wisconsin-Madison and USDS-ARS, *Bulletin of the American Meteorological Society*, 85, 65–78.

Dillow, J.J.A. (1997) Technique for estimating magnitude and frequency of peak flows in Maryland, *Water Resource Investigation Journal,* 95, 41-54.

Dinku T, Ceccato P., Grover-Kopec, E., Lemma, M., Connor, S.J. and Ropelewski, C.F. (2007) Validation of satellite rainfall products over East Africa's complex topography, *International Journal of Remote Sensing*, 28(7), 1503–1526.

Dinku, T., Chidzambwa, S., Ceccato, P., Connor, S. J. and Ropelewski, C.F. (2008) Validation of high-resolution satellite rainfall products over complex terrain in Africa, *International Journal of Remote Sensing,* 29(14), 4097–4110.

Dirceu, S., Reis, Jr. and Stedinger, R. (2005) Bayesian MCMC flood frequency analysis with historical information, *Journal of Hydrology*, 313, 97–116.

Direção Nacional de Aguas 2014 Avaliação da estacão hidrológica e hidráulica das cheias em Moçambique 1977-2013, Relatório Final, Maputo.

Djokic, D. and Maidment, D. (2004) GIS as Integration tool for Hydrologic Modelling: a Need for Generic Hydrologic Data Exchange Format, Sydney.

Dong, X., Dohmen-Janssen, M. and Booij, M.J. (2005) Appropriate spatial sampling of rainfall for flow simulation, *Hydrology Science Journal*, 50(2), 279-298.

Dooge, J.C.I. (1973) Linear theory of hydrologic systems, Tech. Bull. No. 1468, US Agricultural Research Service, Washington, D.C.

Doran, D. G., and Pilgrim, D. H. (1986) Choice Between Flood Estimates Based on Design Rainfalls and Flood Frequency Analysis, *Civil Engineering Transactions*, CE28, 74-91.

Droegemeier K.K., Smith, J.D., Businger, S., Doswell, C., Doyle, Duffy, C.J., Foufoula-Georgiou, T., Graziano, L.D, L.D., James, V., Krajewski, M., LeMone, D., Lettenmaier, C., Mass, R., Pielke, S., Ray, S., Rutledge, D., Schaake, J. and Zipser, E. (2000) Hydrological aspects of whether prediction and warning, *American Meteorology Society,* 81(11), 2665-2680.

Droogers P & Allen RG, (2002) Estimating reference evapotranspiration under inaccurate data conditions, Irrigation *and Drainage Systems* 16(1), 33-45.

Duan, Q., Sorooshian, S. and Gupta, V. (1992) Effective and efficient global optimisation for conceptual rainfall–runoff models, *Water Resource Research,* 28(4), 1015–1031.

Dubrovin, T., Jolma, A. and Turunen, E. (2002) Fuzzy model for real time reservoir operation, *Journal of Water Resource Planning and Management,* 128(1), 66-73.

Duranyildiz, I., Onoz, B. and Bayazit, M. (1999) A Chance-Constrained LP Model for Short term reservoir operation optimisation, Turkish *Journal of Environmental Engineering,* 23, 181-186.

East-west Center (EWC), Asian Disaster Preparedness Center (ADPC), United Nations development programme (UNDP) and National Oceanic and Atmospheric Administration (NOAA), (2003) Symposium on Climate Extreme Events in Asia Pacific Enhancing Resilience and Improving Decision Making, *Proceeding 20th Pacific Science Congresses,* Bangkok, Thailand.

Ebert, E.E. (2007) Method for verifying satellite precipitation estimates. In Measuring precipitation from Space: EURAINSAT and the future, *Advanced in Global Change Research,* 28, 345-356.

Ebert, E.E., Janowiak, J.E. and Kidd, C. (2007) Comparison of near-real-time precipitation estimates from satellite observations and numerical models, *Bulletin of the American Meteorological Society*, 88, 47–64.

El-Raey, M. and Beoro, G. (2003) Inventory a Mitigation Option and Vulnerability Adoption Assessment, Ministry of Water Resources and Irrigation, Egypt, 1-116.

Emergency Management Australia (EMA), (2002), Disaster loss assessment, Guidelines Australian Emergency Manuals Series III, 1-101.

Entenman, D. (2005) Geo-spatial Streamflow Model (GeoSFM) Training Manual. U.S. Geological Survey, Open-File Report 2005–1327, 1–65.

European Union and Southern African Development Community (EU) and (SADC), (2002) SADC-HYCOS (Hydrological Cycle Observing System), SADC-HYCOS Evaluation Report, May, 2002.

Faber, B. (2010) Current Methods for Flood Frequency Analysis, USACE, Hydrologic Engineering Center, *Proceeding Workshop on Non-Stationarity, Hydrological Frequency Analysis and Water Management*, 13.

Farr, T. G., Coltelli, M.G., Fornaro, G., Franceschetti, R. Lanari, M., Migliaccio, J. R. and Moreira, K. P. (2007) The Shuttle Radar Topography Mission, *Reviews of Geophysics,* 45.

Fenton, J.D. (1992) Reservoir routing, *Hydrological Sciences Journal,* 37(3), 233-246.

Ferraro, R., Grody, N. C., Weng, F. and Basist, A. (1996) An Eight-Year (1987–1994) Time Series of Rainfall, Clouds, Water Vapour, Snow Cover, and Sea Ice Derived from SSM/I Measurements, *Bulletin of the American Meteorological Society,* 77(5), 891–906.

Ferraro, R.R. and Marks, G. F. (1995) The Development of SSM/I Rain Rate Retrieval Algorithms Using Ground-Based Radar Measurements*, Journal of Atmospheric and Oceanic Technology*, 12, 775–780.

FEWS Net Data Portal (2012) Africa Data Dissemination Services http://earlywarning.usgs.gov/fews/ , 12th February 2012.

Fonseca, R.M.S. (2012) Flood warning system for the Lower Pungwe Basin: Buzi, Dondo and Nhamatanda Districts in Mozambique, MSc Thesis, University of Zimbabwe, Harare.

Food and Agriculture Organization of the United Nations (FAO), (1995) Digital soil map of the world and derived soil properties, CD-ROM, version 3.5 November 1995.

Food and Agriculture Organization (FAO), (1998) “Digital Soil Map of the World and Derived Soil Properties,” FAO Land and Water Media Series, Rome, Italy.

Food Agriculture Organization (FAO), (1999) New concepts and approaches to land management in the tropics with emphasis on steep lands. FAO Soils Bulletin No. 75, Food and Agriculture Organization, Rome, Italy.

Food Agriculture Organization (FAO), (2001) FAOCLIM – world-wide agroclimatic data. Version 2. FAO – SDRN Environment and Natural Resources Service, Rome, Italy.

Food Agriculture Organization (FAO), (2003) Drought impact mitigation and prevention in the Limpopo River Basin, Final-Report, Maputo.

Food and Agriculture Organization of the United Nations (FAO), (2003) World Reference Base Map of World Soil Resources, 1:25 000 000, FAO, Rome, Italy.

Food and Agriculture Organization of the United Nations (FAO), United Nations Department of Economic and Social Affairs (UNDES), United Nations Educational, Scientific and Cultural Organization (UNESCO) and the International Association of Hydrogeologists (IAH), (2003) Groundwater management – The search for practical approaches, Water Reports, ISSN 1020-1203.

Ford, D.T. and Killed, J.R. (1995) PC-based decision-support system for Trinity River, Texas, *Journal of Water Resource Planning and Management,* 121(5), 375–381.

Foster, G. R. and Lane, L.J. (1987) User requirements, USDA-Water erosion prediction project (WEPP), NSERL Report No.1, National Soil Erosion Research Laboratory, West Lafayette, IN.

Franchini, F. and Pacciani, M. (1991) Comparative analysis of several conceptual rainfall-runoff models, *Journal of Hydrol*ogy, 122, 161–219.

Francou, J. and Rodier, J. A. (1967) Essai de classification des crues maximales, *Proceeding, Leningrad Symposium on Floods and their Computation*, UNESCO.

Fread, D.L. (1993) Flow Routing in D.R. Maidment, ed. Handbook of Hydrology, Chap.10, McGraw-Hill, New York.

Fread, D.L., Shedd, R.C. Smith, G.F., Farnsworth, R., Hoffeditz, C., Wenzel, L.A., Wiele, S.M., Smith, J.A. and Day, G.N. (1995) Modernization in the National Weather Service River and Flood Program. American Meteorological Society, *Weather and Forecasting*, 10, 1-10.

Frieling, B. (2012) The scale of indirect damage from flooding – A case study: Mississippi River flooding of May 2011, *Journal of Sustainability Development,* 8(1), 12–19.

Funk, C., Michaelsen, J. and Verdin, J. (2003) The collaborative historical African rainfall model: description and evaluation, *International Journal of Climatology,* 23, 47–66.

Funk, C., Michaelsen, J. and Verdin, J. (2004) Comparing Satellite Rainfall Estimates and Reanalysis Precipitation Fields with Station Data for Western Kenya, *Presented at the JRC-FAO International Workshop on Crop Monitoring for Food Security in Africa,* January 2003, Nairobi, Kenya.

Funk, C. (2009) New satellite observations and rainfall forecasts help provide earlier warning of African drought, *Earth Observation*s, 21, 23–27.

Funk, C., Eilerts, G. Davenport, F. and Michaelsen, J. (2010) A climate trend analysis of Kenya, U.S. Geological Survey Open-File Report, 1327(2005).

Gabriele, S., Arnell, N. (1991) A hierarchical approach to regional flood frequency analysis, *Water Resources Research*, 27(6), 1281-1289.

Gao, Y. C. and Liu, M. F. (2012) Evaluation of high-resolution satellite precipitation products using rain gauge observations over the Tibetan Plateau, *Hydrology and Earth System Sciences*, 17, 837–849.

Gardai, H., Smith, E., Asante, K., Bandaragoda, Ch. and Verdin, J. (2007) Adequacy of satellite derived rainfall data for streamflow modelling, *Natural Hazard*, ds(2007), 167–185.

Gingras, D. and Adamowski, K. (1994) Performance of L-moments and nonparametric flood frequency analysis, *Canadian Journal of Civil Engineering*, 21(5), 856–862.

Giri, C., Zhu, Z. and Reed, B. (2005) A comparative analysis of the Global Land Cover 2000 and MODIS land cover data sets," *Remote Sensing and Environment*, 94, 123–132.

Glenn, E. P., Huete, A. R., Nagler, P. L., Hirschboeck, K. K., and Brown, P. (2007) Integrating Remote Sensing and Ground Methods to Estimate Evapotranspiration, Canadian Journal of Plant Science, 26, 139–168.

Global Water Partnership (GWP), (2003) Status of National Integrated Water Resources Management processes in southern Africa, Online Report, www.gwpsatac.org.zw, 21st December 2011.

Görgens, A.H.M. and Boroto, J. (2003) Limpopo River: an overview of alternative methods for estimating transmission losses, hydrology of Mediterranean and semiarid regions, *Association of Scientific Hydrology Publication,* 278.

Görgens, A, Lyons, S., Hayes, L., Markhabane, M. and Maluleke, D. (2007a) Modernised South African Design Flood Practice in the Context of Dam Safety, WRC Report No 1420/2/07, Water Research Commission, Pretoria, South Africa.

Görgens, A.H.M. (2007b) Joint Peak-Volume (JPV) Design Flood Hydrographs for South Africa, WRC Report No 1420/3/07, Water Research Commission, Pretoria, South Africa.

Gosain, A., Mani, A. and, Dwivedi, Ch. (2009) Hydrological Modelling – Literature Review, Report No. 1, October 2009.

Green W. and Ampt, G. (1911) Studies on soil physics – The flow of air and water through soils, *Journal of Agricultural Science,* 4(1), 1-24.

Grigg, N. S. Doesken, F.A., Frick, D.M., Grimm, M., Hilmes, H., McKee, B.T. and Oltjenbruns, K.A. (1999) "Fort Collins flood 1997: Comprehensive view of an extreme event", *Journal of Water Resource Planning and Management,* 125(5), 255–262.

Gupta, H.V., Sorooshian, S. and Yapo, P.O. (1998) Toward improved calibration of hydrologic models: Multiple and non-commensurable measures of information, *Water Resource Research*, 34(4), 751–76.

Gupta, H.V., Beven, K.J. and Wagener, T. (2005) Model calibration and uncertainty estimation. *In: Anderson, M, G. (Ed), Ency. Hydrol. Sci*., Wiley, Chichester.

Gupta, H. and Schaffner, M. (2006) Development of a Site-Specific Flash Flood Forecasting Model for the Western Region, Final Report for COMET proposal entitled.

Gupta, H.V., Kling, H., Yilmaz, K.K., Martinez, G.F. (2009) Decomposition of the mean squared error and NSE performance criteria: implications for improving hydrological modelling, *Journal of Hydrology*, 377, 80–91.

Guttman N. B., Hosking, R.M. and Wallis, J.R. (1993) Regional precipitation quantile values for the continental US computed from L-moments, *Journal of Climatology,* 6, 2326–2340.

Harun, S.M.R. (2009) Flood mapping in Bangladesh – A literature review, Bangladesh Development Research, Final Report, 1–215.

Hendrick, J. M. H., Imam, B., Kuligowski, R., Skahill, B. and Skofronick-Jackson, G. (2011) Advanced concepts on remote sensing of precipitation at multiple scales, *Bulletin of the American Meteorological Society*, 92, 1353–1357.

Hénonin, J., Russo, B., Roqueta, D.S., Sanchez, R., Domingo, D.N., Thomsen, F., and Mark, O. (2010) Urban Flood Real-time Forecasting and Modelling: A State-of-the-Art Review, DHI Denmark, Final Report.

Herman, A., Kumar, V., Arkin, P. and Kousky, J. (1997) Objectively determined 10-day African rainfall estimates created for famine early warning systems, *International Journal of Remote Sensing,* 18(10) 2147–2159.

Hernando, H. T. (2007) General guidelines for setting-up a community-based flood forecasting and warning system, Philippines Atmospheric, Geophysical and Astronomical Services Administration Report.

Hess, L.L., Melack, J.M., Filoso, S. and Young, W. (1995) Delineation of inundated area and vegetation along the Amazon floodplain with the SIR-C Synthetic aperture Radar, *Transactions on Geoscience and Remote Sensing,* 33, 896–904.

Ho, L. T. K.; Umitsu, M. b and Yamaguchi, Y. (2010) Flood hazard mapping by satellite images and SRTM DEM in the vu gia – thu bon alluvial plain, central Vietnam, *International Archive of the Photogrammetry, Remote Sensing and Spatial Information Science*, Part 8, Kyoto Japan 2010.

Horritt, M.S. and Bates, P.D. (2001a) Predicting floodplain inundation: Raster-based modelling versus the finite element approach, *Hydrological Processes*, 15, 825–842.

Horritt, M.S. and Bates, P.D. (2001b) Effects of spatial resolution on raster based model of flood flow, *Journal of Hydrology*, 253, 239–249.

Hosking, J.R.M. and Wallis, J.R. (1995) A comparison of unbiased and plotting-position estimators of L-moments, *Water Resource Research,* 31(8), 2019–2025.

Howard, CH. (2007) Optimal Integrated Scheduling of Reservoirs and Generating Units*,* PhD. Dissertation, University of California, Berkeley, USA.

Hudson, P.F, Middelkoop, H and Stouthamer, E. (2008) Flood management along the Lower Mississippi and Rhine Rivers (The Netherlands) and the continuum of geomorphic adjustment, *Geomorphology,* 101, 209–236.

Hughes, D.A. and Smakhtin, V.Y. (1996) Daily flow time series patching or extension: a spatial interpolation approach based on flow duration curves, *Hydrological Science Journal,* 41(6), 851–871.

Hughes, D.A. (1997) Southern African "FRIEND" – The application of rainfall-runoff models in the SADC region, Water Research Commission Report No. 235/1/97.

Hughes, D.A. (2004) Three decades of hydrological modelling research in South Africa, *South African Journal of Science,* 100, 638–642.

Hughes, D.A. and Forsyth, D.A. (2006) A generic database and spatial interface for the application of hydrological and water resource models, *Computers & Geosciences,* 32 (9), 1389–1402.

Hughes, D.A., Andersson, L., Wilk, J. and Savenije, H.H.G. (2006) Regional calibration of the Pitman model for the Okavango River, *Journal of Hydrology*, 331(1–2), 30–42.

Hughes, D.A., Kapangaziwiri, E. and Sawunyama, T. (2010) Hydrological model uncertainty assessment in southern Africa, *Journal of Hydrology*, 387, 221–232.

Hughes, D.A., Kingston, D.G. and Todd, M.C. (2011) Uncertainty in water resources availability in the Okavango River Basin as a result of climate change, *Hydrology and Earth System Sciences,* 15, 931–941.

Institute of Water Research (IWR), (2012) Implementing Uncertainty Analysis in Water Resources Assessment and planning, *Water Research Commission,* K5/2058, Rhodes University.

Instituto Nacional de Estatísticas (INE), (2007) CENSO Populacional de 2007, INE, Maputo, Moçambique.

Instituto Nacional de Gestão de Calamidades (INGC) and Universidade Eduardo Mondlane (UEM), (2003) Disaster Preparedness and Response in the Limpopo Basin, INGC Disaster Management Atlas, Maputo, Mozambique.

Instituto Nacional de Gestao de Calamidades (INGC), (2009) Study on the Impact of Climate Change on Disaster Risk in Mozambique, INGC Final Report, Maputo, Mozambique.

Intergovernmental Panel on Climate Change (IPCC), (2007) Climate Change (2007) – The Physical Science Basis, Contribution of Working Group I to the Fourth Assessment Report of the IPCC, Cambridge, University, Press, New York, NJ.

International Association of Hydrological Sciences (IAHS), (2012) Prediction in Ungauged Basins, *Association of Scientific Hydrology Publication,* Online: www.iahs-pub.org.

International Centre for Integrated Mountain (ICIMOD) and United States Agency for International Development (USAID), (2008) Satellite Rainfall Estimation in the Hindu Kush-Himalayan Region, ICIMOD, Nepal, ISBN 978 92 9115 107 3.

International Commission on Large Dams (ICOLD), (1992) Selection of design flood – Current methods, International Commission on Large Dams (ICOLD), Meeting of the International Commission of Large Dams, Paris, France, June, 1992.

International Commission on Large Dams (ICOLD), (1999) Benefits and concerns about dams, International Commission on Large Dams, Paris, France, June, 1999.

International Water Research Institute (IWRI), (2000) Climatic data, CD-ROM.

Islam and Sado (2002) Flood Hazard Assessment for the Construction of Flood Hazard Map and Land Development Priority Map Using NOAA/AVHRR Data and GIS – A Case Study in Bangladesh, *Journal of Hydrologic Engineering*, 7(5), 346–355.

James, L.D. and Korom, S.F. (2001) Lessons from grand forks: planning non-structural flood control measures, *Natural Hazard,* 183–192.

Jasper, A., Vrugt, C., Diks; G., Hoshin, Gupta, V., Bouten, W. and Verstraten, M. (2005) Improved treatment of uncertainty in hydrologic modelling: Combining the strengths of global optimisation and data assimilation, *Water Resources Research*, 41, 30–57.

Jensen, R., Butts, M. and Madsen, J. (1999) Flood forecasting for the Yangtze River, *World Water Environment Engineering*, 14, 78–98.

Jiménez, C., Prigent, C., Mueller, B., Seneviratne, S. I., Mc-Cabe, M. F., Wood, E. F., Rosso, W. B., Balsamo, G., Betts, A. K., Dirmeyer, P. A., Fisher, J. B., Jung, M., Kanamitsu, M., Reichle, R. H., Reichstein, M., Rodell, M., Sheffield, J., Tu, K., and Wang, K. (2011) Global intercomparison of 12 land surface heat flux estimates, *Journal of Geophysical Research*, 116, 145–155.

Jinchi H. (2005) Lessons learned from operation of flood detention basins in China, United Nations Development Programme Report.

Jobard, I., Chopin, F., Berges, J. C. and Roca, R. (2011) An inter-comparison of 10-day satellite precipitation products during West African monsoon, *International Journal of Remote Sensing*, 32, 2353–2376.

John, L. (2004) Optimal operation of multireservoir system: State-of-the-Art review. *Water Resources Planning and Management,* 130 (2), 93-111.

Jones, J.L., Halusk, T., Williamson, A.K. and Erwin, M.L. (1998) Updating flood inundation maps efficiently: building on existing hydraulic information and modern elevation data with a GIS, U.S. Geological Survey, Open-File Report, 98–200.

Joyce, R. J., Janowiak, J. E., Arkin, P. A. and Xie, P. (2004) CMORPH: A method that produces global precipitation estimates from passive microwave and infrared data at high spatial and temporal resolution, *Journal of Hydrometeorology*, 5, 487–503.

Jury, M.R. and Gwanzantini, M.E. (2002) Climate Variability in Lake Malawi, Part 2: Sensitivity and Prediction of Lake Levels, *International Journal of Climatology,* 22, 1303–1312.

Kanamitsu, M. (1989) Description of the NMC global data assimilation and forecast system, *Weather Forecast,* 4, 335–342.

Kannan, N., White, S. M., Worrall, F. and Whelan, M. J. (2007) Sensitivity analysis and identification of the best evapotranspiration and runoff options for hydrological modelling in SWAT-2000, *Journal of Hydrology*, 332, 456–466.

Kapangaziwiri, E. (2008) Revised parameter estimation methods for the Pitman monthly model, MSc Thesis, Rhodes University, Grahamstown, South Africa.

Kapangaziwiri, E. and Hughes, D.A. (2008) Towards a physically-based parameter estimation method for the Pitman monthly rainfall-runoff model, *Water SA*, 32(2), 183–191.

Karim, A. and Chowdhury J. (1995) A comparison of four distributions used in flood frequency analysis in Bangladesh, *Hydrological Science Journal*, 40 (1) 55–66.

Kasetsart, J. and Taesombat, W. (2011) Estimation of the IHACRES model parameters for flood estimation of ungauged catchments in the Upper Ping River Basin, *Natural Sciences,* 45, 917–931.

Katjavivi, P.H. (2009) Post-disaster needs assessment, Namibia flood 2009, Government of the Republic of Namibia, National Planning Commission Report, 1–154.

Kovács, Z. (1988) Regional maximum flood peaks in Southern Africa, Technical Report TR 137, Department of Water Affairs, Pretoria, South Africa.

Keith, H. and Spe, C. (1982) Reservoir simulations: State of the art*, Journal of Petroleum Technology, SPE* 10 020, 1634–17.

Kelman, J., Stedinger, J., Cooper, L. and Hsu, E. (1990) Sampling stochastic dynamic programming applied to reservoir operation, *Water Resource Research*, 26(3), 447–454.

Kennie T. and Petrie, G. (1990) Terrain Modelling in Surveying and Civil Engineering, Publication, London: Whittles Publishing, 1990.

Keys, C. (1999) Upgrading Practices in the Field of Flood Warning, paper presented at the 32nd annual conference of the Flood Mitigation Authorities of New South Wales, Bankstown.

Khalequzzaman, M.D. (1994) Recent Floods in Bangladesh: Possible causes and solutions, *Natural Hazards,* 9, 65–80.

Kidd, C. (2001) Satellite rainfall climatology: A review, *International Journal of Climatology*, 21, 1041–1066.

Klemes, V. (1982) Operational testing of hydrological simulation models, *Hydrological Sciences Journal,* 31, 13–23.

Kling, H., Fuchs, M. and Paulin, M. (2012) Runoff conditions in the upper Danube basin under an ensemble of climate change scenarios, *Journal of Hydrology,* 424(425), 264–277.

Knutti, R. (2011) Should we believe model predictions of future climate change?, *Journal of Hydrology*, 366, 4647–4664.

Koenker, R. and Bassett, G. (1978) Regression quantiles, Econometrica 46, 33–50.

Kokkonen, T., Koivusalo, H. and Croke, B. (2004) Exploring stream response to effective rainfall across event magnitude scale, *Hydrological Processes*, 18, 1467–1486.

Kolva, J. (1993) Effects of the Great Midwest Flood of 1993 on Wetlands, *U.S Geological Survey Water Supply Paper*, 2425, 109–363.

Krajewski, W.F., Lakshmi, V., Georgakakos, K.P. and Jain, S.C. (1991) A Monte Carlo study of rainfall sampling effect on a distributed catchment model, *Water Resource Research,* 27(1), 119–128.

Krajewski, W.F. and Smith, J.A. (2002) Radar hydrology: rainfall estimation, *Advance in Water Resources*, 25(2002), 1387–1394.

Krzysztofowicz, R. (2001) “The case for probabilistic forecasting in hydrology”, *Journal of Hydrology*, 249(2001), 2–9.

Kubal, C., Haase, D., Meyer, V. and Scheuer, S. (2009) Integrated urban flood risk assessment – adapting a multicriteria approach to a city, *Natural Hazard and Earth Systems Science*, 1881–1895.

Kuczera, G. and Mroczkowski, L. (1998) Assessment of hydrologic parameter uncertainty and the worth of data, *Water Resource Research*, 34(6), 1481–1489.

Kugler, Z., Groevea, T.D., Brakenridge, G. R. and Anderson, E. (2007) Towards a near-real time global flood detection system, *Joint Research Centre*, Ispra Site, European Commission, Ispra 21020, Via Fermi 1, Italy.

Kummerow, C., Barnes, W., Kozu, T. and Simpson, J. (1998) The Tropical Rainfall Measuring Mission (TRMM) Sensor Package, *Journal of Atmospheric and Oceanic Technology*, 15(3), 809–817.

Kundzewicz, Z. and Takeuch, K. (1999) Flood protection and management: quo vadimus? *Hydrological Science Journal,* 44(3), 417–432.

Kundzewicz, Z.W. and Robson, A.J. (2004) Change detection in hydrological records – review of the methodology, *Hydrological Science Journal*, 49(1), 7–19.

Kundzewicz, Z. W. (2007) Predictions in ungauged basins – a systemic perspective, *Association of Scientific Hydrology Publication,* 309, 79–89.

Kunkel, K., Stanley, A., Changnon, S.A. and Angel, J.R. (1994) Climatic Aspects of the 1993 Upper Mississippi River Basin Flood, *Bulletin of the American Meteorological Society,* 103–116.

Kwak, Y., Takeuch, K., Fukami, K. and Magome, J. (2012) A new approach to flood risk assessment in Asia-Pacific region based on MRI-AGCM outputs., 1 of International Centre for Water Hazard and Risk Management (ICHARM) under the auspices of UNESCO.

Labadie, J.W. (1987) Reservoir System Optimisation Models, Colorado State University, USA. .http://www.ucowr.org/updates/pdf/V108_A7.pdf, 14th April, 2010.

Labadie, L.W. (2004) Optimal operation of multireservoir system: State-of-the-Art review, *Water Resource Planning and Management,* 130(2), 93–111.

Laurenson, E. M. (1987) Back to Basics on Flood Frequency Analysis, Civil Engineering Transactions, CE29, 47–53.

Lawrence, D., Haddeland, I. and Langsholt, E. (2009) Calibration of HBV hydrological models using PEST parameter estimation Norwegian, Water Resources and Energy Directorate Report, 2009.

Layberry, R., Knivn, D. R., Todd, M. C., Kidd, C. and Bellerby, T. J. (2006) Daily precipitation over Southern Africa A new resource for climate studies, *Journal of Hydrometeorology,* 7, 149–159.

Le Ngo, L. (2006) Optimising reservoir operation – A case study of HoaBinh reservoir, Vietnam, PhD Thesis, Institute of Environment & Resource, Technical University of Denmark.

Leenaer, H. (1990) Estimating the Impact of Land Use Change on Soil Erosion Hazard in the Zambezi River Basin, JVP-90 – JVP-90-024.

Legates, D.R. and McCabe, G. J. (1999) Evaluating the use of "goodness-of-fit" measures in hydrologic and hydro climatic model validation, *Water Resources Research,* 35(1), 233-241.

Legates, D.R. and Willmott, C. J. (2011) Mean seasonal and spatial variability in gauge-corrected, 30 global precipitation, *International Journal of Climatology,* 10, 111–127.

Levine, J.G. (2017) Pumped Hydroelectric Energy Storage and Spatial Diversity of Wind Resources as Methods of Improving Utilization of Renewable Energy, MSc Thesis, University of Colorado.

Liechti, T.C., Matos, J. P., Boillat, J.L. and Schleiss, A.J. (2011) Comparison and evaluation of satellite derived precipitation products for hydrological modelling of the Zambezi River Basin, *Hydrology and Earth System Sciences Discussion*, 8, 8173–8201.

Linsley, R.K., Kohler, M.A. and Paulhus, J.L.H. (1982) Hydrology for Engineers. McGraw-Hill, New York, N.Y., 3rd ed., 508pp.

Littlewood, I.G., Down, K., Parker, J.R. and Post, D.A. (1997) The PC Version of IHACRES for catchment-scale rainfall-streamflow modelling version 1.0 User Guide-April 1997, Institute of Hydrology, Centre for Ecology and Hydrology, Wallingford, Oxon, UK.

Liu, Y. and Gupta, H.V. (2007) Uncertainty in hydrological modelling: Towards an integrated data assimilation framework, *Water Resource Research*, 43. W07401, doi: 10.1029/2006 WR 005756.

Loague, K.M and Freeze, R. A. (1985) A comparison of rainfall-runoff modelling techniques on small upland catchments, *Water Resource Research,* 21(2), 229-248.

Lobbrecht A.H. and Solomatine D.P. (2002) "Intelligent Real-Time Control of Urban Water Systems", *Urban Water Journal*, 4(3), 283 – 289.

Local Flood Early Warning System (LFEWS) (2012) Local Flood Early Warning System (2012), Deutsche Gesellschaft für Internationale Zusammenarbeit (GIZ) GmbH, Germany.

Loumagne, S., Weisse, L. and Le Hégarat-Mascle, C. (2001) Assimilation of soil moisture into hydrological models for flood forecasting: a variation approach, Canadian Journal of Remote Sensing, 29(6), 679–686.

Loveland, T.R., Reed, B.C., Brown, J.F., Ohlen, D.O., Zhu, J., Yang, L. and Merchant, J.W. (2000) Development of a Global Land Cover Characteristics Database and IGBP DISCover from 1-km AVHRR Data, *International Journal of Remote Sensing*, 21(6), 1303–1330.

Lund J.R. and Guzman, J. (1999) Some Derived Operating Rules for Reservoirs in Series or in Parallel, Department of Civil and Environmental Engineering, *Journal of Water Resource Planning and Management,* 125(3), 143–153.

Macuacua, E. (2012) Impact of Land Use Change and Increased Agricultural Water Use on the Incomati River Flow Regime, MSc Thesis University of Zimbabwe.

Madsen, H. (2003), Parameter estimation in distributed hydrological catchment modelling using automatic calibration with multiple objectives, *Advance in Water Resource,* 26 (2), 205-216.

Madsen, H., Rasbejerg, D., Damgard, J. and Hansen, F. (2003) Data assimilation in the MIKE 11 flood forecasting system using Kalman filtering, *International Association of Scientific Hydrology Publication,* 281, 75–81.

Madsen, H., Host-Madsen, J. and Rosbjerg, D. (2007) Combined flow prediction and reservoir control system optimizes production at Hoa-Binh, *International Journal of Hydrology*, 1, 80-93.

Maidment, D. (1993) Developing a Spatial Distributed Unit Hydrograph by Using in Application of GIS in Hydrology and Water Resource Management, *International Association of Scientific Hydrology Publication,* 201, 181–192.

Maidment, D. (2002) GIS for Water Resources, User Manual, McGraw-Hill, New York, USA.

Maidment, D. and James, D. (1996) What does GIS Bring to Hydrologic Modelling, http://geosun.sjsu.edu/paula/285/285/cfsem.htm, 24th July 2012.

Malilay, J. (1997) Floods – The public health consequences of disasters, Oxford University Press, New York, USA

Mark, B., Bain, J., Finn, and Booke, E. (1988) Streamflow Regulation and Fish Community Structure, *Ecology*, 69, 382–392.

Marshall, M., Tu, K., Funk, C., Michaelsen, J. P., Williams, C., Williams, J. Cappelaere, C. (2013) Improving operational land surface model canopy evapotranspiration in Africa using a direct remote sensing approach, *Hydrology and Earth System Science* , 17, 1079–1091.

Mays, L.W. (1996) Water Resources, ed. Handbook, Cap. 24–25, McGraw-Hill, New York.

Mays, L.W. and Tung, Y.K. (2002) Hydrosystems Engineering and Management, *Water Resource Publications*, 1–320.

Mays, W. L. and Tung, Y.K. (1992) Hydro systems engineering and management, McGraw-Hill, New York.

Mazvimavi, D. (2003) Estimation of flow characteristics of ungauged catchments, PhD Thesis, Wageningen University and International Institute for Geo-Information and Earth Observation, ITC, Enschede, The Netherlands.

Mazvimavi, D. and Wolski P. (2006) Long–term variations of annual flows of the Okavango and Zambezi Rivers, *Physic and Chemistry of Earth*, 31, 944–951.

McCuen, R.H. (1998) Hydrologic Analysis and Design, Prentice Hall, Upper Saddle River, NJ.

Meier, P, Omelt, F. and Kinzelbach, W. (2011) Hydrological real-time modelling in the Zambezi river basin using satellite-based soil moisture and rainfall data, *Hydrology and Earth System Sciences,* 120-136.

Meigh, J. (1995) The impacts of small farm reservoirs on urban water supplies in Botswana, *Natural Resource Forum*, 1, 71-83.

Mein R.G. and Larson, C.L. (1973) Modelling infiltration during a steady rain, *Water Resource Research*, 9(2), 384-394.

Mekong River Commission (MRC), (2011) Integrated Water Resources Management-based on Basin Development Strategy Cambodia, Lao PDR Final Report, Thailand and Viet Nam, 13–56.

Merkel, W. (2002) Muskingum-Cunge flood routing procedure in NRCS Hydrologic Models, *Presented at the Second Federal Interagency Hydrologic Modelling Conference,* USA, July 2002.

Midgley D.C, Pitman, W.V and Middleton, B.J. (1994) Surface Water Resources of South Africa 1990, Water Research Commission, Pretoria, South Africa.

Ministério para a Cordrenacção de Acção Ambiental (MICOA), (2006) Avaliação das experiências de Moçambique na gestão de desastres climáticos (1999 a 2005), Final Report, MICOA, Maputo, Mocambique.

Miralles, D.G., De Jeu, R. A. M., Gash, J. H., Holmes, T. R. H., and Dolman, A. J. (2011a) Magnitude and variability of land evaporation and its components at the global scale, *Hydrology and Earth System Science*, 15, 967–981.

Miralles, D.G., Holmes, T. R. H., De Jeu, R. A. M., Gash, J. H. Meesters, A. G. C. A., and Dolman, A. J. (2011b) Global land-surface evaporation estimated from satellite-based observations, *Hydrology and Earth System Science*, 15, 453–469.

Moel, H., Van Alphen, J. and Aerts, J. (2009) Flood maps in Europe – methods, availability and use Institute for Environmental Studies, Vrije University, Amsterdam, the Netherlands.

Moges, S.A. (2007) Flood Forecasting and Early Warning System (FFEWS) an Alternative Technology for Flood Management System and Damage Reduction in Ethiopia: A Concept Note, Technical Report, Arba Minch University.

Moore, C. and Doherty, J. (2005) The role of the calibration process in reducing model predictive error, *Water Resource Research*, 41(5), 127–153.

Moriasi, D.N., Arnold, J.G., Van Liew, M.W., Binger, R.L., Harmel, R.D. and Veith, T.L. (2007) Model evaluation guidelines for systematic quantification of accuracy in watershed simulations, *Transition of the ASABE*, 50(3), 885–900.

Morris, E. M. (1980) Forecasting Flood Flows in Grassy and Forested Basins Using a Deterministic Distributed Mathematical Model, *International Association of Scientific Hydrology Publication, 129*, 247–255.

Morris, M.D. (1991) Factorial sampling plans for preliminary computational experiments. *Technimetrics,* 33(2), 161–174.

Morrissey, M. L., Maliekal, J. A., Greene, J. S. and Wang, J. (1995) The uncertainty of simple spatial averages using rain gauge networks, *Water Resource Research*, 31, 2011–2017.

Mu, Q., Heinsch, F. A., Zhao, M., and Running, S.W. (2007) Development of a global evapotranspiration algorithm based on MODIS and global meteorology data, *Remote Sensing of Environment*, 111, 519–536.

Mu, Q., Zhao, M., and Running, S. W. (2011) Improvements to a MODIS global terrestrial evapotranspiration algorithm, *Remote Sensing of Environment*, 115, 1781–1800.

Mujumdar, P.P. and Ramesh, T.S.V. (1997) Real-time reservoir operation for irrigation, *Water Resource Research,* 33(5), 1157–1164.

Mujumdar, P.P. and Teegavarapu, R. (1998) A short-term reservoir operation model for multicrop irrigation, *Hydrological Sciences Journal,* 43(3), 479–494.

Mul, M.L., Savenije, H.H.G. and Uhlenbrook, S. (2009) Spatial rainfall variability and runoff response during an extreme event in a semi-arid catchment in the South Pare Mountains-Tanzania, *Hydrology and Earth System*, 13, 1659–1670.

Munasinghe, M. (2004) Evaluation of the UNEP project on dams and development, UNEP Report No. K070951.

Murwira, A. (2006) Regional training course on flood forecasting and early warning, proceeding, *training on floods forecasting and early warning,* Boskop, South Africa, 11–15 September 2006.

Muzik, I. (1993) Derived, physics based distribution of flood probabilities, *Proceedings of the Yokohama Symposium, July 1993.*

Mwelwa, E.M. (2004) The application of a monthly time step Pitman rainfall-runoff model to the Kafue river basin of Zambia, MSc Thesis, Rhodes University, Grahamstown, South Africa.

Myšiak, J. (2010) The adaptive water resource management handbook, Earthscan, UK.

Nash, J.E. and Sutcliffe, J.V. (1970) River flow forecasting through conceptual models part I – A discussion of principles, *Journal of Hydrology,* 10(3), 282–290.

Nasira, D.G, Lecturei, K., and Erode, N. (2008) A comparative study of fuzzy logic with artificial neural networks algorithms in clustering, *Journal of Computer Applications*, 1(4), 111-117.

National Institute of Meteorology (INAM), (2002) Manual for seasonal forecasting interpretation, INAM Technical Report, Beira, Mozambique.

Ndiritu, J. (2009) A comparison of automatic and manual calibration using the Pitman model, *Physics and Chemistry of Earth*, 34, 729–740.

New Roods Construction Concepts (NR2C), (2008) Towards reliable, green, safe & smart and human infrastructure in Europe. Final Report, European Union.

Nico, G., Pappalepore, M., Pasquariello, G., Refice, A., and Samarelli, S. (2000) Comparison of SAR amplitude vs. coherence flood detection methods – a GIS application, *International Journal of Remote Sensing*, 21(8), 1619–1631.

Nyambe, I.A. and Feilber, M. (2007) Energy and water development, Technical Report, Ministry of Energy, Republic of Zambia.

Nyatsanza, F.F. and Van der Zaag, P. (2011) Reservoir operating policies for environmental flows of large dams in the Zambezi River Basin, UNESCO-IHE, Institute of Water Management, The Netherlands.

Oliveira, R. and Loucks, D.P. (1997) Operating rules for multireservoir systems, *Water Resource Research,* 33(4), 839–852.

Opere, A.O, A.O., Mkhandi, S., Willems, P. (2012) At site flood frequency analysis for the Nile Equatorial Basins, University of Nairobi, Kenya.

Oudin, L., Hervieu, F., Michel, C., Perrin, C., and Andréassian, V. (2005) Which potential evapotranspiration input for a lumped rainfall–runoff model?: Part 2—Towards a simple and efficient potential evapotranspiration model for rainfall–runoff modelling, *Journal of Hydrology* 1(4), 290–306.

Palmeira, F.L.B., Morales, C. A., Franca, G.B. and Landau, L. (2003) Rainfall estimation using Satellite Data for Paraiba do Sul Basin, Rio de Janeiro, Federal University of Rio de Janeiro, Rio de Janeiro, Brazil, 1–6.

Panigrahi, D.P. and Mujumdar, P.P. (2000) Reservoir Operation Modelling with Fuzzy Logic, *Water Resource Research,* 14, 89–109.

Pechlivanidis, I., Jackson, B., McIntyre, N. and Wheater, H. (2011) Basin scale hydrological modelling: A review of model types, calibration approaches and uncertainty analysis methods in the context of recent developments, *Global NEST Journal,* 13(3), 193–214.

Pegram, G.G.S. and Parak, M. (2006) A review of the Regional Maximum Flood and Rational Formula using geomorphologic information and observed floods, *Water SA*, 30(3), 377-392.

Pelling, M. and Dill, K. (2010) Disaster politics: tipping points for change in the adaptation of sociopolitical regimes, *Progress in Human Geography,* 34(1), 21–37.

Penna, D., Tromp-van, H., Meerveld, J., Gobbi, A., Borga, M, M. and Dallaand, F. G. (2002) The influence of soil moisture on threshold runoff generation processes in an alpine headwater catchment, *Hydrology and Earth System Sciences*, 7, 8091–8124.

Perrin, C., Michel, C. and Andréassian, V. (2003) Improvement of a parsimonious model for streamflow simulation, *Journal of Hydrology,* 279(1–4), 275–289.

Pilgrim, D.H. and Cordery, I. (1993) Chapter 9: Flood Runoff. In: Maidment, D.R. (Ed.), Handbook of Hydrology, McGraw-Hill, New York, USA.

Pilon, P.J. and Adamowski, K. (1992) The value of regional information to flood frequency analysis using the method of L-moments, *Canadian Journal of Civil Engineering*, 9(1) 137–147.

Pitman, W.V. (1978) Flow generation by catchment models of differing complexity – a comparison of performance, *Journal of Hydrology*, 38, 59–70.

Queensland Flood Commission of Inquiry (QFCI), (2011) Brisbane River 2011 flood event – Flood frequency Analysis, QFCI Final Report No. 111024.

Rahman A, Weinmann P.E., Hoang, T.M.T. and Laurenson, E.M. (2002) Monte Carlo simulation of flood frequency curves from rainfall, *Journal of Hydrology,* 256, 196–210.

Ramírez, J.A. (2000) Prediction and modelling of flood hydrology and hydraulics, Water Resources, Hydrologic and Environmental Sciences, Civil Engineering Department, Colorado State University, USA.

Ramírez, J.A. and Hobbins, M.T. (2005) Observational evidence of the complementary relationship in regional evaporation lends strong support for Bouchet's hypothesis, *Geophysical Research Letters*, I(32), 1029–1053.

Ramlal, B., Serwan, J. and Baban, J. (2008) Developing a GIS based integrated approach to flood management in Trinidad, *Journal of Environment Management,* 88, 1131–1140.

Refsgaard, J.C, Van Der Sluijs, J.P, Hojberg, A.L, Vanrolleghem, P.A. (2007) Uncertainty in the environmental modelling process A framework and guidance, *Environmental Modelling and Software,* 22,1543–1556.

Renard, B., Kavetski, D., Kuczera, G., Thyer, M. and Franks, W. S. (2009) Understanding predictive uncertainty in hydrologic modelling: the challenge of identifying input and structural errors, *Water Resource Res*earch, 46, W05521, doi: 1029/2009WR008328.

Republic of Mozambique (RM) and United Nations Development Programme (UNDP), (2000) Flood in Mozambique, *International Reconstruction Conference*, March, 2000, Rome, Italy.

Reza, G.M. (2007) Evaluation of flood mitigation alternatives using hydrological modelling, *Journal of Applied Sciences and Environmental Management,* 11(4), 113–117.

Roca, R., Chambon, P., Jobard, I., Kirstetter, P., Gosset, M., Gosset, M. and Bergès, J. (2010) Comparing Satellite and Surface Rainfall Products over West Africa at Meteorologically Relevant Scales during the AMMA Campaign Using Error Estimates, *American Meteorological Society*, 4(49), 778–785.

Rodell, M., Houser, P. R., Jambor, U., Gottschalk, J., Mitchell, K., Meng, C.J., Arsenault, K., Cosgrove, B., Radakovich, J., Bosilovich, M., Entin, J. K., Walker, J. P., Lohmann, D., and Toll, D. (2004) The Global Land Data Assimilation System, *Bulletin of the American Meteorological Society*, 85, 381–394.

Romilly, T. G. and Gebremichael, M. (2011) Evaluation of satellite rainfall estimates over Ethiopian river basins, *Hydrology and Earth System Sciences* 15, 1505–1514.

Samarasinghe, S.M.J.S., Nandalal, H.K., Weliwitiya, D.P., Fowze, J.S.M., Hazarika, M.K., and Samarakoon, L. (2010) Application of remote sensing and GIS for flood risk analysis: A case study at Kalu-Ganga River, Sri Lanka, *International Archives of the Photogrammetry, Remote Sensing and Spatial Information Science*, XXXVIII.

Samuels, P and Gouldby, B. (2009) Integrated Flood Risk Analysis and Management Methodologies, Report Number T32-04-01, 2009.

Santhi, C.J.G., Arnold, J.R., Williams, W. A., Dugas, R. and Hauck, L.M. (2001) Validation of the SWAT model on a large river basin with point and nonpoint sources, *Journal of the American Water Resources Association,* 37(5), 1169–1188.

Sawunyama, T. (2008) Evaluating uncertainty in water resources estimation in southern Africa: A case study of South Africa, PhD Thesis, Rhodes University, Grahamstown, South Africa.

Sawunyama, T. and Hughes, D. (2009) Application of satellite derived rainfall estimates to extend water resource simulation modelling in South Africa, *Water SA,* 34(1), 379-386.

Sawunyama, T. and Hughes, D.A. (2010) Using satellite based rainfall data to support the implementation of Environmental water requirements in South Africa, Institute for Water Research, Rhodes University, Grahamstown, South Africa.

Scepan, J. (1999) Thematic Validation of High-Resolution Global Land-Cover Data Sets: *Photogrammetric Engineering and Remote Sensing,* 65, 9, 1051–1060.

Schäfer, N.W. (1991) Modelling the areal distribution of daily rainfall, MSc Thesis, University of Natal, Pietermaritzburg, South Africa.

Schneider, U., Fuchs, T., Meyer-Christoffer, A. and Rudolf, B. (2008) Global precipitation analysis products of the GPCC, *Global Precipitation Climatology Centre*, Germany, 2008.

Schoups, G., Addams C. L. and Gorelick, S. M. (2005) Multi-objective calibration of a surface water-groundwater flow model in an irrigated agricultural region: Yaqui Valley, Sonora, Mexico, Hydrological *Earth System Sciences*, 9, 549-568.

Schultz, C.B. (1985) The Sensitivity of output from a distributed hydrological model to rainfall input, MSC edn, University of Natal, Pietermaritzburg.

Schulze, R.E. (2005) Setting the scene: the current hydroclimatic landscape in Southern Africa. In Schulze R.E. (ed.). Climate change and water resources in Southern Africa: studies on scenarios, impacts, vulnerabilities and adaptation, Water Research Commission (WRC) Report 1430/1/05, 6, 84–94.

Schulze, R.E. (2006) Rainfall: Background In: Schulze, R.E. (Ed) South African Atlas of Climatology and Agrohydrology, Water Research Commission, Pretoria, RSA.

Schulze, R.E. (2007) Soils: Agrohydrological Information Needs, Information Sources and Decision Support. In: Schulze, R.E. (Ed). 2007. South African Atlas of Climatology and Agrohydrology. Water Research Commission, Report 1489/1/06, Section 4.1, Pretoria, South Africa.

Schuurmans, J.M., Bierkens, M.F.P. and Pebesma, E.J. (2007) Automatic Prediction of High-Resolution Daily Rainfall Fields for Multiple Extents: The Potential of Operational Radar, *Journal of Hydrometeorology,* 8, 1204–1224.

Searcy, J.K. (1959) Flow-Duration Curves, *Geological Survey Water-Supply Paper, 1542-A,* 33-45.

Segond, M.L. (2006) Stochastic Modelling of space-Time Rainfall and the Significance of Spatial Data for Flood Runoff Generation, PhD Thesis, Department of Civil and Environmental Engineering, Imperial College, London.

Senay, G.B., Budde, M., Verdin, J.P. and Melesse, M. (2007) A coupled Remote Sensing and simplified surface energy balance approach to estimate actual evapotranspiration from irrigated fields A Coupled Remote Sensing and Simplified Surface Energy Balance Approach to Estimate Actual Evapotranspiration from irrigated Fields, *Sensors*, 17, 979-1000.

Senay, G.B., Budde, M.E and Verdin, J.P. (2010) Enhancing the simplified surface energy balance approach for estimating landscape ET: validation with the metric model, *Agricultural Water Management*, 98(2011) 606–618.

Sheila, O. (2000) Management of shared basins: The case of the Zambezi River, *Journal of Hydrology*, 2, 65–81.

Sherman L.K. (1932), Streamflow from rainfall by the unit-graph method, Engineering News Record, 108, 501–505.

Shim, K.C., Fontane, D.G. and Labadie, J.W. (2002) Spatial decision support system for integrated river basin flood control, *Journal of Water Resources Planning and Management,* 128(3), 190–201.

Showstack, R. (2001) Scientists and planners look for ways to stem future flood disaster in Mozambique, *Eos Trans. AGU*, 81(13).

Shrestha, M.S., Artan, G.A., Bajracharya, S.R. and Sharma, R.R. (2008) Using satellite-based rainfall estimates for stream flow modelling: Bagmati Basin, *Flood Risk Management*, 1, 89–99.

Simonovic, S.P. (1999) Decision support systems for flood control management in the Red River Basin, *Canadian Water Resource Journal,* 24(3), 203–223.

Simonovic, S.P. (2002).Two new non-structural measures for sustainable management of floods, *Water International,* 27(1), 38–46.

Singh, J. H., Knapp, V., Arnold, J. G., and Demissie. M. (2005) Hydrologic modeling of the Iroquois River watershed using HSPF and SWAT, *Journal of American Water Resources Association,* 41(2), 361–375.

Singh, R.D. (2012) Real time flood forecasting – Indian experiences, National Institute of Hydrology, National Institute of Hydrology Report, India.

Sivapalan, M, Beven, K.J. and Wood, E.F. (1987) On Hydrological similarity: 2 A scaled model of storm runoff production, Water *Resource Research,* 23(12), 2266–2278.

Sivapalan, M., K., Takeuchi, S. W., Franks, V. K., Gupta, H., Karambiri, V., Lakshmi, X., Liang, J.J., McDonnell, E. M., Mendiondo, P. E., O'Connell, T., Oki, J. W., Pomeroy, D., Schertzer, S. and Zehe, E. (2003) IAHS Decade on Predictions in Ungauged Basins (PUB), 2003–2012: Shaping an exciting future for the hydrological sciences, *Hydrological Sciences Journal,* 48(6), 857–880.

Skotner, C., Klinting, A. and Ammentorp, H.C. (2002) Mike Flood Watch – Managing real time Forecasting, DHI & Environment, Denmark.

Smithers, J., Schulze, R. and Kienzle, S. (1997) Design flood estimation using a modelling approach: a case study using the ACRU model, *International Association of Scientific Hydrology Publication*, 240, 365–397.

Smithers, J.C. (2012) Methods for design flood estimation in South Africa, School of Engineering and University of KwaZulu-Natal, South Africa, *Water SA*, 38(4), 633-646.

Snowy Mountains Engineering Corporation (SEMEC), (2004) Zambezi, River Basin, Mozambique Flood Risk Analysis Project, Final Report, Maputo, Mozambique.

Snyder, F.F. (1938) Synthetic Unit Graphs, *Transition American Geophysics Union,* 19, 447-454.

Society of Engineering and Development (SEED), (2001) Hydrological Characteristics, Flood February and March 2001, the Zambezi River Basin, Final Report, Maputo, Mozambique.

Socolow, R.S., Leighton, C. R., Zanca, J.L. and Ramsey, L.R. (1997) Water Resources Data, Massachusetts and Rhode Island: Water Year 1997, Water-Data Report MA-RI-97-1, U.S.G.S Water Resources Division, Marlborough, MA.

Soil Conservation Service (1972) Sec. 4 of National Engineering Handbook, Soil Conservation Service, U.S. Department of Agriculture, Washington, D.C.

Solomatine, D.P. and Avila Torres, L.A. (1996) Neural Network Approximation of a Hydrodynamic Model in Optimising Reservoir Operation, *Proceeding International conference on Hydroinformatics*, Zurich, Switzerland, September 1996.

Sorooshian, S. Duan, Q. and Gupta, V.K. (1993) Calibration of rainfall–runoff models: Application of global optimisation to the Sacramento Soil Moisture Accounting Model, *Water Resource Research,* 29, 1185–1194.

Sorooshian, S., Hsu, K.L., Gao, X., Gupta, H.V., Imam, B. and Braithwaite, D. (2000) Evaluation of PERSIANN system satellite-based estimates of tropical rainfall, *Bulletin of American Meteorology Society*, 81(9), 2035-2046.

Southern African Development Community (SADC), (2002) Environmental sustainability in water resources management in Southern Africa, Report A44O, Maseru, Lesotho.

Southern African Development Community (SADC), (2006) Regional water strategy, Final Report.

Southern African Research and Documentation Centre (SARDC) and India Musokotwane Environmental Resource Centre for Southern Africa (IMMERCSA), (2007) Action on climate change to advance sustainable development in the Zambezi Basin, *The Zambezi*, 7(3), 771–1152.

Spachinger, K.K., Dorner, W., Metzka, R., Serrhini, K. and Fuchs, S. (2008) Flood risk and flood hazard maps – Visualisation of hydrological risks*, Earth and Environmental Sciences,* 4, 1755–1307.

Sparks, R.E., Bayley, P.B., Kohler, S.L. and Osborne, L.L. (1990) Disturbance and recovery of large floodplain rivers, *Environmental Management,* 14, 699–709.

Stanski, H. R., Wilson, L.J. and Burrows, W. R. (1989) Survey of common verification methods in 20 meteorology, World weather watches, Technical Report, 8, WMO/TD, No. 358, Geneva, Switzerland.

Stenseth, N., Myterud, A., Ottersen, G., Hurrell, J., Chan, K., Lima, M. (2002) Ecological Effects of Climate Fluctuations, Science; Department of Biology, Division of Zoology, University of Oslo, Norway.

Stokstad, E. (1999) "Scarcity of Rain, Stream Gauges Threatens Forecasts," *Science*, 285, 1199.

Strabala, K. (2009) MODIS Applications MODIS direct broadcast data for enhanced forecasting and real-time environmental decision making, Cooperative Institute for Meteorological Satellite Studies University of Wisconsin, Madison, USA.

Stuebe, M.M. and Johnston, D.M. (1990) Runoff volume estimation using GIS techniques, *Water Resource Bulletin,* 26(4) 611–620.

Tallaksen, L.M. and Van Lanen, H.A.J. (2006) Developments in Water Science: Hydrological Drought-processes and Estimation Methods for Streamflow and Groundwater, *Elsevier, 579pp.*

Tanavud, C., Yongchalermchai, C., Bennui, A. and Densreesereku, O. (2004) Assessment of flood risk in Hat Yai Municipality, Southern Thailand, using GIS, *Journal of Natural Disaster Science,* 26(1),1–14.

Tang, Y., Reed, P., Wagener, T. and Werkhoven, K. (2006) Comparing sensitivity analysis methods to advance lumped watershed model identification and evaluation, *Hydrology & Earth System Sciences,* 11, 793–817.

Tarboton, G.D. (2003) Rainfall-Runoff processes. A workbook to accompany the Rainfall-Runoff Processes Web module, http://www.engineering.usu.edu/dtarb/rrp.html, 4th November 2012.

Taylor, D. (2007) Methods of calibration a comparative approach, *ISPOR 12th Annual International meeting*, Boston, USA.

Tenenbaum, D.E, Band, L.E, Kenworthy, S.T, Tague, C.L. (2006) Analysis of soil moisture patterns in forested and suburban catchments in Baltimore, Maryland, using high resolution photogrammetric and LIDAR digital elevation datasets, *Hydrological Process*, 20, 219–240.

Thiemig, V., Rojas, R., Levizzani, V. and Deroo, A. (2012) Validation of high resolution satellite-based precipitation products over different, African river basins, *Journal of Hydrometeorology*, 13, 1760–1783.

Tilmant, A., Beevers, L., Muyunda, B. and Juizo, D. (2010) Restoring a flow regime through the coordinated operation of a multireservoir system: The case of the Zambezi River basin, *Water Resource Research,* 46, 1–8.

Tirivarombo, S. (2012) Climate variability and climate change in water resources management of the Zambezi River Basin, PhD Thesis, Rhodes University.

Todd, M.C., Taylor, R. G., Osborn, T. J., Kingston, D. G., Arnell, N. W. and Gosling, S. N. (2011) Uncertainty in climate change impacts on basin-scale freshwater resources, preface to the special issue: the QUEST-GSI methodology and synthesis of results, *Hydrology & Earth System Sciences*, 15, 1035–1046.

Trambauer, P., Dutra, E., Maskey, S., Werner, M., Pappenberger, F., van Beek, L. P. H. and Uhlenbrook, S. (2013) Comparison of different evaporation estimates over the African continent, *Hydrology and Earth System Science*, 18, 193–212.

Tshimanga, R.M. (2012) Hydrological uncertainty analysis and scenario-based streamflow modelling for the Congo River basin, PhD Thesis, Rhodes University, South Africa.

Tumbare, M.J. (2004) The Zambezi River, its threats and opportunities, Zambezi River Authority.

Uddin, K., Gurung, D. R., Giriraj, A. and Shrestha, B. (2013) Application of remote sensing and GIS for flood hazard management: A Case study from Sindh Province, Pakistan, *American Journal of Geographic Information System*, 2(1), 1–5.

United States Agency for International Development (USAID), (2002) Disaster risk reduction in Mozambique: Better Information for better outcomes (2004–2010), United States Agency for International Development (USAID), Maputo, Mozambique.

United States of Geological Survey (USGS) and ARA-Sul (Administração Regional de Águas do Sul), (2002) Mapas de Inundação da Bacia do Limpopo, Final Report, Maputo, Mozambique.

United States of Geological Survey (USGS), (2000a) Use and Description of the Famine Early Warning System Flood Model, USGS, USA.

United States of Geological Survey (USGS), (2000b) Global Land Cover Characteristics (GLCC) database, World Reference Base Global Land Caver Characteristics at 1km of spatial resolution, (http://edcdaac.usgs.gov/data).

United States of Geological Survey (USGS), (2002) Training Manual for the Geo-Spatial Stream Flow Model. USGS, USA.

Unver, O.I. and Mays, L.W. (1990) Model for real-time optimal flood control operation of a reservoir system, *Water Resource Management,* 4(1), 21–46.

US Army Corps of Engineers (2003) HEC-ResSim Reservoir System Simulation, Online User's Manual, http://www.hec.usace.army.mil/software/hec-ressim/features.html, 16th November 2012.

Van Beek, L. P. H. and Bierkens, M. F. P. (2009) The Global Hydrological Model PCR-GLOBWB: Conceptualization, Parameterisation and Verification, Utrecht University, Faculty of Earth Sciences, Department of Physical Geography, Utrecht, The Netherlands.

Van Beek, L. P. H., Wada, Y., and Bierkens, M. F. P. (2011) Global monthly water stress: 1. Water balance and water availability, *Water Resource Research*, 47, 75–87.

Van Dijk, A.I.J.M. (2011) Model-data fusion: using observations to understand and reduce uncertainty in hydrological models, *19th International Congress on Modelling and Simulation*, Perth, Australia, 12–16 December 2011.

Van Liew, M. W., Veith, T. L., Bosch, D. D. and Arnold, J. G. (2007) Suitability of SWAT for the conservation effects assessment project: A comparison on USDA-ARS experimental watersheds, *Journal of Hydrological Engineering,* 12(2), 173–189.

Varas, E. (1995) Expert System for Selection of Methods to Calculate Design Flood Flows, *Hydrological Sciences Journal*, 40, 739–749.

Vasan, A. and Raju, K. (2006) Optimal reservoir operation using differential evolution, Birla Institute of Technology and Science, Pilani, Rajasthan.

Vaz, A.C. (2000) Coping with floods – The experience of Mozambique, *1st WARFSA/WaterNet Symposium, Sustainable Use of Water Resources*, Maputo, Mozambique.

Verdin, K.L. and Greenlee, S.K. (1996) Development of Continental Scale Digital Elevation Models and Extraction of Hydrographic Features, *Proceedings 3rd International Conference on Integrating GIS and Environmental Modelling, Santa Fe, New Mexico*.

Verdin, J. (2000) Data and applications for study of the water cycle in Africa, *Earth Resource Observation Systems*, 1–12.

Verdin, J.P. and Klaver, R.W. (2002) Grid Cell Based Crop Water Accounting for the Famine Early Warning System, *Hydrological Processes,* 16, 1617–1630.

Vilanculos, A. (2006) Towards improving flood forecasting and early warning systems through integrated technology in the Limpopo Basin, MSc Thesis, University of Zimbabwe, Harare, Zimbabwe.

Viljoen, M and Plassis, L. (1999) Determining the Benefits of Flood Mitigation Measures in the Lower Orange River – A GIS application, Department of Agricultural Economics.

Vrugt, J. and Bouten, W. (2002) Toward improved identifiability of hydrologic model parameters, *Water Resource Research*, 38, 1312–1325.

Vrugt, J.A., Gupta, H.V., Bastidas, L.A., Bouten, W. and Sorooshian, S. (2003a) Effective and efficient algorithm for multiobjective optimisation of hydrologic models, *Water Resource Res*earch, 39(8), 5.1-5.19.

Vrugt, J.A., Gupta, H.V., Bouten, W. and Sorooshian, S. (2003b) A shuffled complex evolution metropolis algorithm for optimisation and uncertainty assessment of hydrologic model parameters, *Water Resource Res*earch, 39(8), 1.1-1.18.

Vrugt, J.A., Diks, C.G.H., Gupta, H.V., Bouten, E. and Verstraten, J.M. (2005) "Towards a complete treatment of uncertainty in hydrologic modelling" Combining the strengths of global optimisation and data assimilation, *Water Resource Research,* 41, 30–59.

Wagener, T., McIntyre, N., Lees, H.S. and Gupta, H.V. (2003) Towards reduced uncertainty in conceptual rainfall-runoff modelling: Dynamic identifiability analysis, *Hydrological Processes*, 17(2), 455–476.

Wagener, T.T. (2007) Can we model the hydrological impacts of environmental change? *Hydrological Processes*, 21, 3233–3236.

Walford, N. (1994) Geographical Data Analysis, University of Leeds, Leeds, LS2 9JT. UK.

Walker, J.P. and Willgoose, G.R. (1999) On the effect of digital elevation model accuracy on hydrology and geomorphology, *Water Resource Research*, 35(7), 2259–2268.

Walker, W. E., Harremoes, P., Rotmans, J., Van der Sluijs, J.P., Van Asselt, M.B.A., Janssen, P. and Krayer, M.P. (2003) Defining uncertainty a conceptual basis for uncertainty management in model-based decision support, *International Journal of Technology Assessment*, 4(1), 5–17.

Walter, I.A., Allen, R.G. and Elliott, R. (2000) ASCE Standardized Reference Evapotranspiration Equation. In: Evans RG, Benham BL, Trooien TP (eds.) *Proceeding of the National Irrigation Symposium*, ASAE, Nov. 14–16, Phoenix, AZ, 209 – 215.

Wang, J., Yuan X. and Zhang, Y. (2004) Short-term scheduling of large-scale hydropower systems for energy maximization, *Journal of Water Resource Planning and Management,* 130(3), 198–205.

Ward, J.V. and Stanford, J.A. (1995) The serial discontinuity concept: extending the model to floodplain rivers, *Regulated Rivers Research and Management,* 10,159–168.

Webb, R.S., Rosenzweig, C.E. and Levine, E.R. (1993) Specifying land surface characteristics in general circulation models: soil profile data set and derived water-holding capacities, *Global Biogeochemical Cycles*, 7, 97–108.

Werth, S., Güntner, A., Petrovic, S. and Schmidt, R. (2009) Integration of GRACE mass variations into a global hydrological model, *Earth and Planetary Science Letters*, 277, 1–2, 166–173.

Wheater, H.S., Jakeman, A.J. and Beven, K.J. (1993) Progress and directions in rainfall runoff modelling, *Modelling change in environmental systems,* ed. Jakeman A.J *et al*. editors, John Wiley and Sons, 101–132.

Wheater, H.S. (2002) Progress in and prospects for fluvial flood modelling, Transactions of the Royal Society of London, 360(1796), 1409–1431.

Wilk, J., Knivpetn, D., Anderson, L.; Layberry, R. and Todd, M. (2006) Estimating rainfall and water balance over the Okavango River Basin for hydrological applications, *Journal of Hydrology,* 331, 18–29.

Williams, M.S. (1997) A regression technique accounting for heteroscedatic and asymmetric errors, *Journal of Agricultural, Biological, and Environmental Statistics*, 2, 108–129.

Winsemius, H. C., Savenije, H. H. G., Gerrits, A. M. J., Zapreeva, E. A. and Klees, R. (2006) Comparison of two model approaches in the Zambezi river basin with regard to model reliability and identifiability, *Hydrology and Earth System Sciences*, 10, 339–352.

Wolski, P., Todd, M.C., Murray-Hudson, M.A. and Tadross, M. (2011) Multidecadal variability in hydroclimate of Okavango river system, southwest Africa, in the past and under changing climate, *Journal of Hydrology*, 12, 1203–1216.

World Bank (WB), (2006) Zambezi River Basin – Sustainable Water Resources Development for Irrigated Agriculture. TFESSD Africa Poverty and Environment Programme, World Bank, Washington, DC.

World Commission on Dam (WCD), (2000) Kariba Dam Zambia and Zimbabwe, Final Report: November 2000.

World Meteorological Organization (WMO) and United States Agency for International Development (USAID), (2012) Mozambique National Consultations on the development of the flood forecasting and early warning strategy for the Zambezi river basin, Country Report, 2012.

World Meteorological Organization (WMO), (1986) Manual for estimation of probable maximum precipitation, Operational Hydrology Report 1, WMO No. 332, 2nd ed., Secretariat of the World Meteorological Organization, Geneva, Switzerland.

World Meteorological Organization (WMO), (2006) Guidelines on the Role, Operation and Management of National Hydrological Services, Operational Hydrology Report No. 49, WMO-No. 1003, WMO, Geneva.

World Meteorological Organization (WMO), (2011) Manual on flood forecasting and warning, WMO No. 1072, Geneva, Switzerland, ISBN 978-92-63-11072-5.

Xie, P. and Arkin, P.A. (1996) Analysis of Global Monthly Precipitation Using Gauge Observations, Satellite Estimates, and Numerical Model Prediction, *Journal of Climat*ology, 9, 840–858.

Xie, P., Yarosh, Y., Love, T., Janowiak, J. and Arkin, P.A. (2002) A real-time daily precipitation analysis over South Asia 16th conference on hydrology, Orlando, *FL, American Meteorological Society,* 9, 840−858.

Xie, P., Chen, M., Yang, S., Yatagai, A., Hayasaka, T., Fukushima, Y. and Liu, C. (2007) A Gauge-Based Analysis of Daily Precipitation over East Asia, *Journal of Hydrometeorology*, 8, 607–626.

Xu, C.Y. and Singh, V.P. (1998) A Review on Monthly Water Balance Models for Water Resources Investigations, *Water Resource Management,* 12, 31–50.

Yates, D. and Strzepe*,* K. (1994) Potential Evapotranspiration Methods and their Impact on the Assessment of River Basin Runoff under Climate Change, International Institute for Applied Systems Analysis, 14–2361, Laxenburg Austria.

Yates, D.N., Warner, T.T. and Leavesly, G.H. (2000) Prediction of a flash flood in complex terrain. Part II: A comparison of flood discharge simulations using rainfall input from radar, a dynamic model and an automated algorithm system, *Journal of Applied Meteorology*, 39, 815–825.

Yeh, W. (1985) Reservoir management and operations models: A state-of-the-art review, *Water Resource Research*, 21(12), 1797–1818.

Young, C.B., Bradley, A.A., Krajewski, W.F., Kruger, A. and Morrissey, M.L. (2000) Evaluating NEXRAD Multisensor Precipitation Estimates for Operational Hydrologic Forecasting, *Journal of Hydrometeorology*, 1, 241–254.

Zambezi Action Program (ZACPRO), (2010) Water Resources and Hydrological Modelling, Water Policy 2 (2000), *Elsevier Science Ltd*.

Zambezi Society and Biodiversity Foundation for Africa (2004) Reviews of Existing Biodiversity Information, *Biodiversity,* 5, 1–31.

Zambezi Watercourse Commission (Zamcom), (2011) Interim agreement, http://www.icp-confluence-sadc.org/rbo/66, 21st December 2011.

Zeeuw, J.W. (1973) Hydrograph analysis for areas with mainly groundwater runoff In: Drainage Principle and Applications, *International Institute for Land Reclamation and Improvement (ILRI)*, 2, 321–358.

Zentner, M. (2012) Design and impact of water treaties: Managing climate change, Intergovernmental Panel on Climate Change Report.

Zhao, L., Ferraro, R. and Moore, D. (2000) Validation of NO AA-15 AMSU-A Rain Rate Algorithm, *10th Conference on Satellite Meters*, 192–195.

Zhou, C.H., Luo, J.C., Yang, J., Li, B.L. and Wang, S. (2000) Flood monitoring using multi–temporal AVHRR and RADARSAT imagery, *Photogrammetric Engineering and Remote Sensing*, 66(5), 633–638.

Zobler, L. (1986) A World Soil File for Global Climate Modelling, NASA Tech. Memo. 87802, NASA Goddard Institute for Space Studies, New York, NY.

APPENDICES

LIST OF APPENDIX FIGURES

LIST OF APPENDIX TABLES

Appendix 1: FLOOD RISK MAPPING

The calculation of flood risk extent was first computed by using the Digital Elevation Model (DEM) and Spatial Analysis in GIS. The original DEM was obtained from The SRTM digital topographic database of the Earth at 90 m x 90 m spatial resolution scale. The sinks contained in the DEM were filled. Assuming that *FL1* is Flood Level 1, Zamdem the original DEM and *Filled Map Calculation1* the filled DEM, which results from the correction of the sinks of the original DEM, the estimation of Flood Level 1 was done by subtracting the original DEM from the filled modified DEM, using the *BufferByRise* tool in ArcView 3.2a. The logical expression applied in computation of *FL1* is given in Appendix Equation 1 and the logical process of flood mapping extent is shown in Appendix Figure 1.

FL1 = ([Filled Map Calculation 1] – [Zamdem] **Appendix Equation 1**

where *Filled Map Calculation 1* is the filled modified DEM and *Zamdem* is the original DEM.

Appendix Figure 1 illustrates a hypothetical example of the approach above, if Appendix Figure 1-a is the original DEM and Appendix Figure 1-b is the filled DEM then using equation 1.1 will result in Appendix Figure 1-c, showing the flow accumulation grid which results in a flooded area extent of Flood Level 1

151	150	150	149	151
154	148	147	148	150
152	149	147	148	150
152	151	148	146	149
154	151	151	150	145

a)

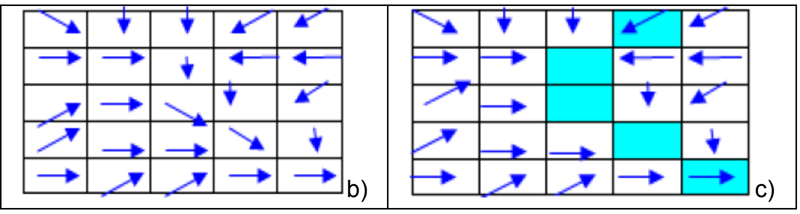

Appendix Figure 1: An illustration of the processing step for flood mapping methodology

Flood mapping using GIS analysis functions; elevation grid (a), flow directions (b) and flow accumulation based on topography (c). The flow accumulations in (c) represent Flood Level 1

The second step is the computation of Flood Level 2 (FL2) using a similar approach. To compute the FL2, the *Filled Map Calculation 1* was refilled first to get *Filled Map Calculation 2.*

Filled Map Calculation 2 is then the 'new' refilled DEM and *Zamdem* is the original DEM. The flood extent of Flood Level 2 is then estimated by subtracting *Zamdem* from *Filled Map Calculation 2* using the *BufferByRise* tool in ArcView 3.2a.

The logical process of flood mapping extent is shown by Appendix Figure 2 and the logical expression given in Appendix Equation 2.

FL2 = ([Filled Map Calculation 2] – [Zamdem]) **Appendix Equation 2**

where *Filled Map Calculation 2* is the Filled modified DEM resulting from flood extent level 1 and *Zamdem* is filled original DEM.

Appendix Figure 2 illustrates the approach above, where Appendix Figure 2-a is exemplification of the refilled DEM and Appendix Figure 2-b the raising of the cells along the flow path and the filling of sink cells, re-establishing hydraulic connectivity and consequently creating a new flood area as shown in Appendix Figure 2-c.

151	150	150	149	151
154	148	147	148	150
152	149	147	148	150
152	151	148	146	149
154	151	151	150	145

a)

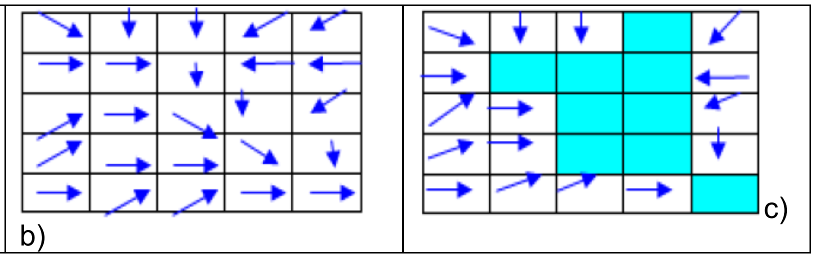

Appendix Figure 2: An example of processing step for flood mapping methodology using GIS

GIS Analysis functions detailing the elevation grid a); flow directorate b); and flow accumulation c), which constitute a flood at level 2 when the water level increases

To estimate the other flood area extents the process is similar to the first two stages used to generate flood extent of Flood Level 1 and Flood Level 2 as presented in Asante *et al.* (2005).

Appendix 2: FLOOD IMPACT ASSESSMENT

Quantifying the effects of streamflow on the socio-economic infra-structures and other hydrological indicators is crucial for flood management, as water managers need to be well prepared to deal with such effects in the future. Streamflow represents an integrated catchment response and it is therefore the best hydrological indicator of the flood impacts. Identification of severe flood events (identified through using GeoSFM simulation results) allows for the development of hazard profiles, particularly in areas where data availability, accessibility, or communication problems limit access to hazard warning information. These hazard profiles can serve as a basis for designing measures to minimize loss of life and damage to property. Appendix Figures 3-A, (thereafter appropriately numbered through to Appendix Figure 11-I (i.e. for A, B, C, D, E, F, G, H and I)) show the detailed results obtained from a relationship between streamflow and extended flood areas that are likely to be inundated at different magnitudes of streamflow. Appendix Tables 1-A, (thereafter appropriately numbered through to Appendix Table 9-I (i.e. for A, B, C, D, E, F, G, H and I)) quantify the impacts of different levels of floods on the social infra-structures.

Appendix 2–A: Flood impacts assessment at Tambara district

Tambara district is located in Manica province, covers an area of 4 736 km^2 and contains three administrative posts: Nhacafula, Nhocolo and Bozua city. Almost 44 394 inhabitants were counted in the 2007 district census; approximately 54% were female and 46% male. The North and the Central region of the district are dominated by the flood plain system of the Zambezi River and two of its tributaries namely: Muira and Chidje Rivers. In Flood Level 1 (which corresponds to water levels between 5 m and 7 m at Tete – the control gauging point), four (4) villages and two (2) primary schools are affected. In total 9 324 people can be affected, which corresponds to 20% of the total population. At this level of flood no cities and hospitals are prone to flood.

Flood Level 2 (which corresponds to the water level 7-8 m at Tete) thee scenario tends to increase – affecting a total of seven (7) villages, and seven (7) primary schools (where five (5) are impacted by level 1 and two (2) by level 2) are inundated. In total 13 460 people can be affected.

For Flood Level 3 (which corresponds to the water level between 8 and 10 m at Tete) the floods would now impact eight (8) villages and three (3) hospitals would be inundated. In total 13 866 people can be affected by flood – corresponding to 31% of the total population. Nine (9) schools can also be affected. Where six (6) would be primary schools at level 1 and three (3) primary schools at level 2.

Appendix Table 1-A summarises the impact of floods at different levels of flood and the spatial location of affected infra-structures is presented in Appendix Figure 3.

Appendix Table 1-A: Summary of impact of floods at different levels on Tambara's infrastructure

Infrastructure	Level 1	Total	Level 2	Total	Level 3	Total
1. Cities:	-	**-**	-	**-**	-	**-**
2. Villages:	Casado, Ngondonga, Nhaunama, Thope	**4**	Capamba, Mafunda, Casado, Ngondonga, Ntsangazasue, Nhaunama, Thope	**7**	Capamba, Nhamichengezi, Mafunda, Casado, Ngondonga, Ntsangazasue, Nhaunama, Thope	**8**
3. Hospitals:	-	**-**	-	**-**	Buzua, Nhacafula, Sabeta	**3**
4. Schools:	**EP1** (Chigoza, Sandozue)	**2**	**EP1** (Chigoza, Sandozue, casado, Sadzassue,Ngondonga) **EP2** (Nhacafula, Chiramba)	**7**	**EP1** (Chigoza, Sandozue, casado, Sadzassue,Ngondonga, Nhacatoe) **EP2** (Nhacafula, Chiramba, Sabeta)	**9**

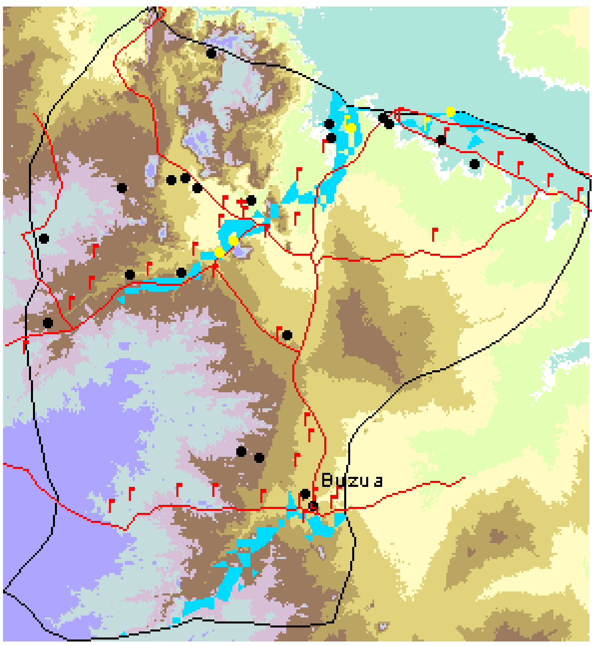

a)

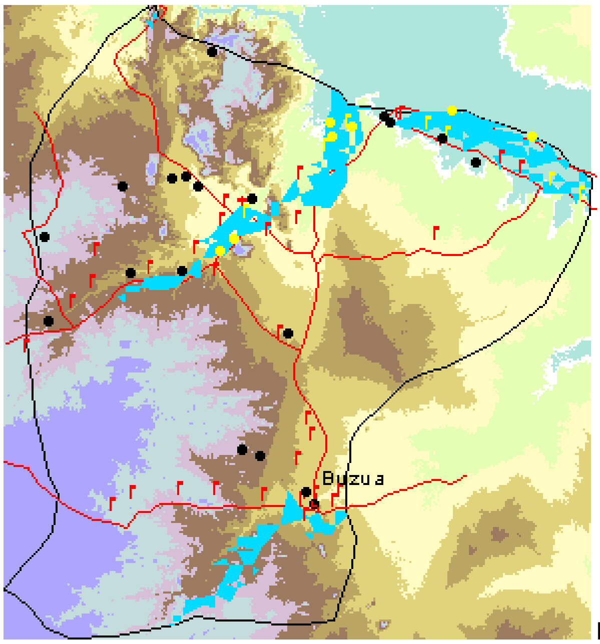

b)

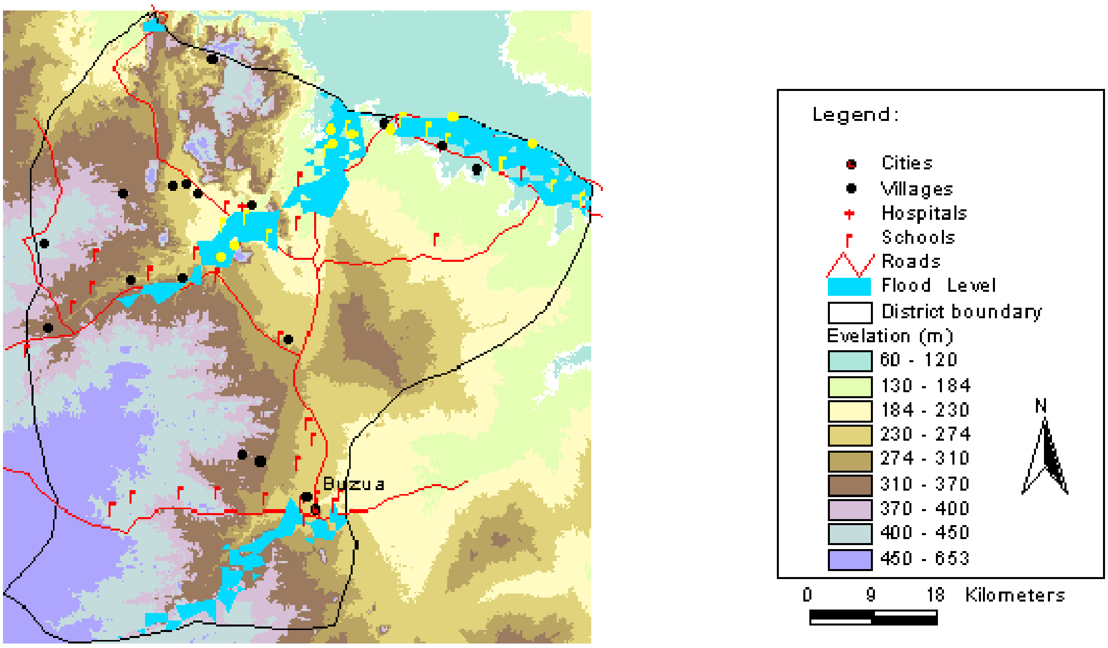

c)

Appendix Figure 3-A: Flood area map at Tambara

Flood level 1 (5-7 m) (a); level 2 (7-8 m) (b) and level 3 (8-10 m) (c) at Tambara

Appendix 2.2–B: Flood impacts assessment at Chemba district

Chemba district is located in Sofala province, covers an area of 3 888 km^2, and contains three administrative posts: Chiramba, Chemba and Mulima city. Almost 56 096 inhabitants were counted in the 2007 district census, where 54% were female and 46% male. The eastern and central region of the district is dominated by the flood plain system of the Zambezi River and three of its tributaries namely: Pampue, Nhazimba and Sangadeze Rivers.

At Flood Level 1 (which corresponds to water levels between 5 m and 7 m at Tete), three (3) villages and one (1) city would be inundated and affecting a total of 8 478 people. There two (2) hospitals and one (1) primary school would be inundated at level 1.

At Flood Level 2 (which correspond to the water level between 7 and 8 m at Tete) six (6) villages and two (2) cities, with a total of 18 134 people would be affected. There are also two (2) hospitals and two (2) primary schools that would be affected at level 1.

For Flood Level 3 (which corresponds to the water level between 8 and 10 m at Tete) of six (6) villages and two (2) cities would be inundated. In total 22 998 people would be affected by floods, corresponding to 41% of the total population. Two (2) hospitals and five (5) primary schools would be affected at level 1.

Appendix Table 2-B summarises the impact of floods at different levels of flood and the spatial location of affected infra-structures is presented in Appendix Figure 4-B.

Appendix Table 2-B. Summary of impact of floods at different levels on Mutarara's infrastructure

Infrastructure	Level 1	Total	Level 2	Total	Level 3	Total
1. Cities:	Chiramba	**1**	Chiramba, Chemba	**2**	Chiramba, Chemba	**2**
2. Villages:	Tchaca, Regulo Chimbwe	**3**	Tchaca, Regulo Nsusso, Nhanduza, Regulo Chimbwe and Regulo Sanhabuzi	**6**	Tchaca, Regulo Chaves, Regulo Nsusso, Nhanduza, Regulo Chimbwe and Regulo Sanhabuzi	**6**
3. Hospitals:	Mulina and Chiramba	**2**	Mulina and Chiramba	**2**	Mulina and Chiramba	**2**
4. Schools:	Ep1 Pauserere	**1**	Ep1 (Pauserere and Lambane)	**2**	Ep1 (Pauserere, Lambane, Tchola 1, Tchola 2 and Janue)	**5**

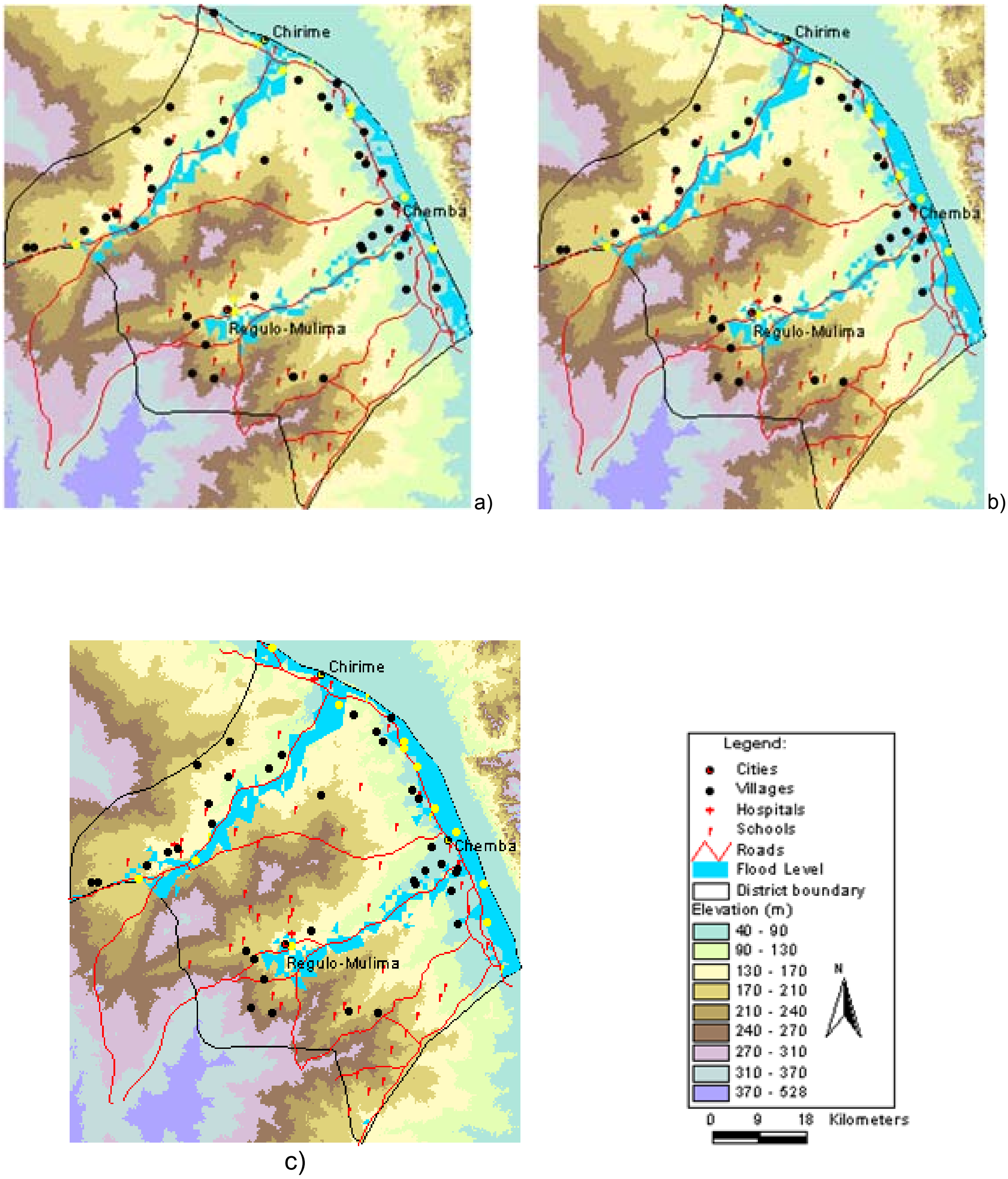

Appendix Figure 4-B: Flood area map forChemba

Flood level 1 (5-7 m) (a); level 2 (7-8 m) (b) and level 3 (8-10 m) (c) at Chemba

Appendix 2.3–C: Flood impacts assessment at Mutarara district

Mutarara district is located in Tete province, covers an area of 6 584 km^2, and contains two administrative posts: Doe and Nhamayabue cities. Almost 148 438 inhabitants were counted in the 2007 district census; 52% were female and 48% male. The Central region of the district is dominated by the flood plain system of the Zambezi River and its tributaries namely: Minjova, Sarodeze, Muati, Nhavudezi, Muira, Nhancali, Goma, Handime, Pompue, Chidje, Goma, Pougue, Nhazimba, Sangadeze, Mangole and Messeca Rivers.

At Flood Level 1 (which corresponds to water level between 5 and 7 m at Tete), twenty (20) villages and three (3) cities would be inundated, affecting a total of 35 193 people. One (1) hospital and sixteen (16) primary schools (fourteen (14) at level 1 and one (1) at level 2) and the one (1) secondary school would be inundated.

At Flood Level 2 (which corresponds to the water level between 7-8 m at Tete), thirty-nine (39) villages, three (3) cities would be inundated, with a total of 57 519 people being affected. There are also three (3) hospitals and thirty-eight (38) schools (twenty-eight (28) primary schools at level 1, six (6) at level 2, and one (1) secondary school and three (3) colleges (adults education, professional and boarding house) would be affected.

For Flood Level 3 (which corresponds to the water level between 8 and 10 m at Tete) forty-eight (48) villages and three (3) cities would be inundated. In total of 73 870 people would affected by the flood – corresponding to 50% of the total population. Forty-four (44) schools would also be also affected. Of these thirty-two (32) are primary schools would be affected at level 1, seven (7) primary schools at level 2, one (1) secondary school and four (4) colleges (adults education, professional, boarding house and distance training) would also be affected.

Appendix Table 3-C summarizes the impact of floods at different flood levels on infra-structures and the spatial location of these infra-structures is presented in Appendix Figure 5-C.

Appendix Table 3–C. Summary impact of floods at different levels on Mutarara's infra-structures

Infrastructure	Level 1	Total	Level 2	Total	Level 3	Total
1. Cities:	Megaza, Nhacolo, Nhamayábuè	**3**	Megaza, Nhacolo, Nhamayábuè	**3**	Megaza, Nhacolo, Nhamayábuè	**3**
2. Villages:	Masso, Megaza, Chitunguane, Panducane, Simbi, Thoera, Gimo, Chirembue, Nhandandanda, Jon Buss, Mbuia Muiapha, Nhansanha, Nkonga, Ducuta Mkumbua, Mafunga, Maphute, Campange, Nhamitanda and Magamba	**20**	Matamia, Ingomua, Bone, Reio, Tengane, Malemia, Muange, Magamba, Chipaia, Candiero, Zogo, Chautengo, Chipupo, N'toa, Changata, Chazuca, Joao, Mosse, Impido, Abissene, Gimo, Calula, Alface, Nhanda, Namagila, Inchiza, Derre,Nofre, Passura, Sanhiua, Manuel, Mussito, Massenda, Angurete,Chatengo, Ungule, Gera, Chipaluo, Sampinda	**39**	Masso, Megaza, Chitunguane, Muanda, Panducane, Sacamago,Incali, Semente, Simbi, Thoera, Chirembue, Nhandandanda, Fortuna, Jumaqui, Khembo, Gimo, Khokote, Correia, Chicote, Jon Busa, Cebola, Mortal, Diogo, Mbuia Muiapha, Nhansanha, Jolinda, Khambanka, Nkongo, Nkhonga, Mkumbua, Mafunga, Maphute,Chombe, Chirembe, Cafuluca, Mapulango, Viagem, Catsamo, Sanjala, Robeca, Joao, Alfazema, Moluissa, Chibure, Campange, Nhamitanda, Magamba	**48**
3. Hospitals:	Tambara	**1**	Tambara, Inhagoma, Mutarara	**3**	Tambara, Inhagoma, Mutarara	**3**

Infrastructure	Level 1	Total	Level 2	Total	Level 3	Total
4. Schools:	EP1 (Cherembe, Ntchatcha, Nango, Panducane, Sancomango, Ponga1, Ponga2, Nhumbiya, Coutinho, Moni, Foguete, Micaula, Ndambuenda) EP2 (Canhungue, Anexo) ESG. (Dona Ana)	**16**	EP1 (Cherembe, Ntchatcha, Nango, Panducane, Sancomango, Ponga1, Ponga2, Nhumbiya, Coutinho, Moni, Foguete, Micaula, Ndambuenda, Mapulanga, cachago, Chapita, Cali, Mbobo, Canxixe, Acuazi, Jardim, Cadjazira, Americano, 1 de Maio, Sompaha, Dzingue, Chavudira, Valeta) EP2 (Canhungue, Anexo, Inhagoma1, Inhagoma2, Capage,Missussua) ESG. (Dona Ana) Centro (Afabetizacao, habilitados, Internato)	**38**	EP1 (Cherembe, Ntchatcha, Nango, Panducane, Sancomango, Ponga1, Ponga2, Nhumbiya, Coutinho, Moni, Foguete, Micaula, Ndambuenda, Mapulanga, cachago, Chapita, Cali, Mbobo, Canxixe, Acuazi, Jardim, Cadjazira, Americano, 1 de Maio, Sompaha, Dzingue, Chavudira, Valeta,Ncali, chamarucha, Cassamo, chindia) EP2 (Canhungue, Anexo, Inhagoma1, Inhagoma2,Inhagama Capage,Missussua) ESG. (Dona Ana) Centro (Afabetizacao, habilitados, Internato, ens. Distancia)	**44**

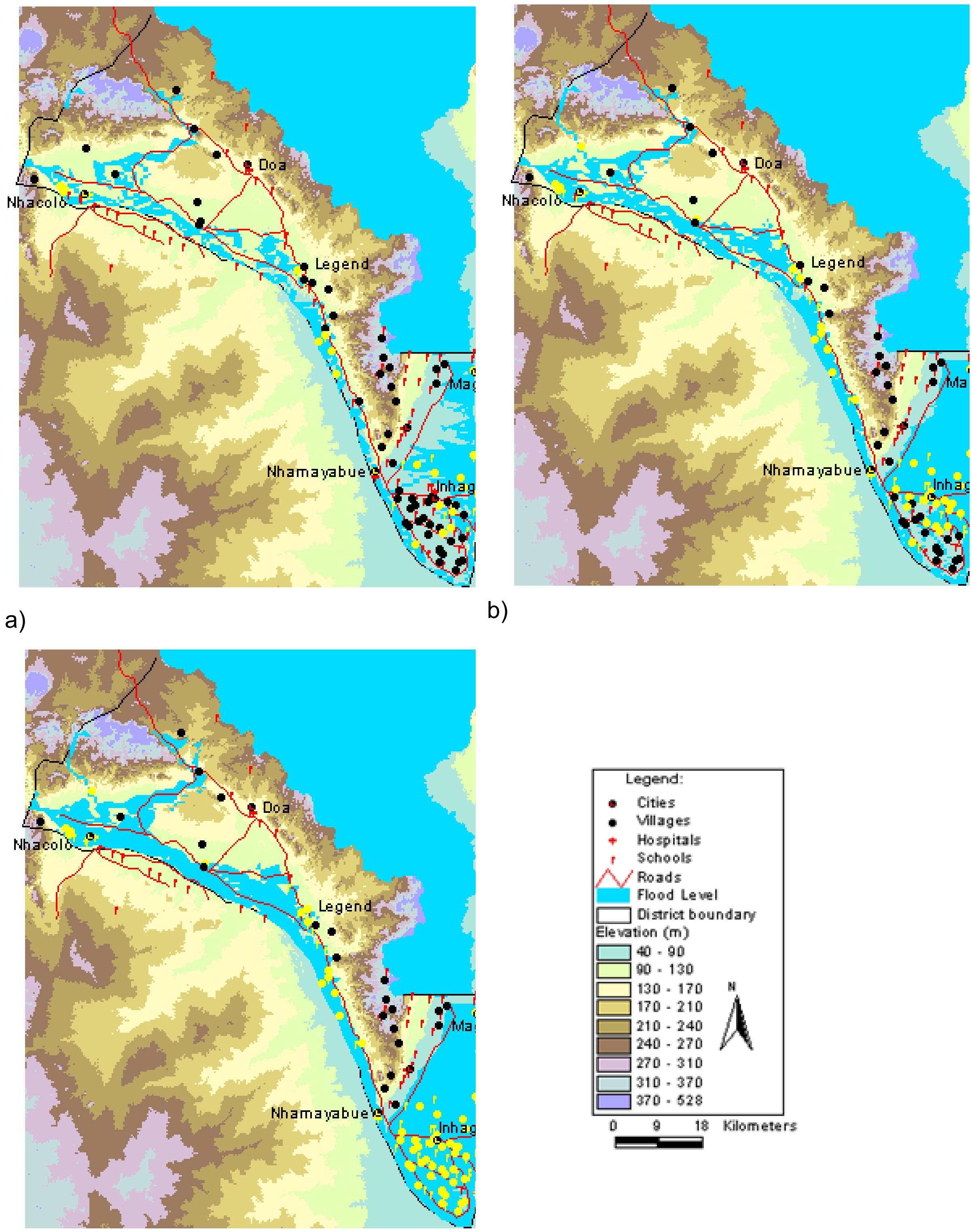

Appendix Figure 5-C: Flood area map for Mutarara

Flood level 1 (5-7 m) (a); level 2 (7-8 m) (b) and level 3 (8-10 m) (c) at Mutarara

Appendix 2.4–D: Flood impacts assessment at Marrínguè district

Marríngue district is located in Sofala province, covers an area of 6 411 km^2, and contains three administrative posts: Canxixe, Marríngue and Subui city. Almost 70 417 inhabitants were counted in the 2007 district census; 54% were female and 46% male. The southern region of the district is dominated by the flood plain system of the Zambezi River and Nhamapasa River one of its tributaries.

At Flood Level 1 (which corresponds to water level between 5 and 7 m at Tete), one (1) village and one (1) city would be inundated, affecting a total of 9 847 people. One (1) hospital and four (4) primary schools would be inundated.

At Flood Level 2 (which corresponds to the water level between 7-8 m at Tete), one (1) village and one (1) city, with a total of 9 847 people would be affected. Five (5) schools, four (4) at level 1 and one (1) primary school at level 2, would be inundated.

For Flood Level 3 (which corresponds to the water level between 8 and 10 m at Tete) two (2) villages and one (1) city would be inundated affecting a total of 14 135 people – corresponding to 20% of the total population. One (1) hospital and five (5) schools, (four (4) at level 1 and one (1) primary school at level 2) would be inundated.

Appendix Table 1-D below summarises the impact of floods at different flood levels on the infra–structures. The spatial location of these infra-structures is presented in Appendix Figure 6-D: Flood area map for level 1 (5-7 m) (a); level 2 (7-8 m) (b) and level 3 (8-10 m) (c) at Marríngue.

Appendix Table 4-D: Summary impact of floods at different levels on Marríngué's infra-structures

Infra-Structure	Level 1	Total	Level 2	Total	Level 3	Total
1. Cities:	Marringuè	**1**	Marríngue	**1**	Marríngue	**1**
2. Villages:	Regulo Nhamacolomo	**1**	Regulo Nhamacolomo	**1**	Regulo Nhachiri, Regulo Nhamacolomo	**2**
3. Hospitals:	Marríngue	**1**	Maringue	**1**	Marríngue	**1**
4. Schools:	EP1 Anexo Traquila; EP2 (Marríngue, 1 and Marríngue 2)	**4**	EP1 Anexo Traquila; EP2 (Marríngue1,2,3 and 4)	**5**	EP1 Anexo Traquila; EP2 (Marríngue 1,2,3 and 4)	**5**

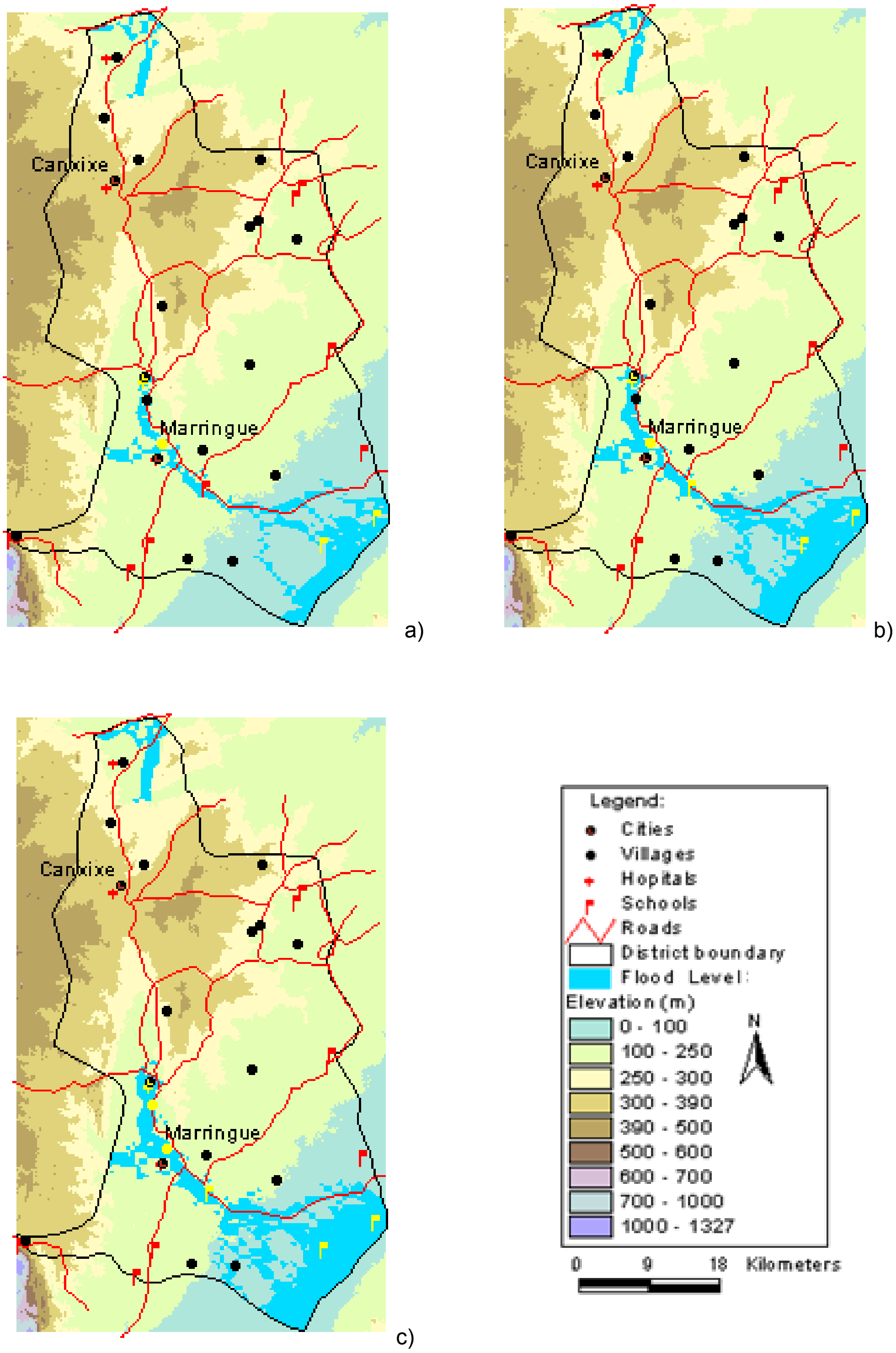

Appendix Figure 6-D: Flood area map for Marríngué

Flood level 1 (5-7 m) (a); level 2 (7-8 m) (b) and level 3 (8-10 m) (c) at Marríngué

Appendix 2.5–E: Flood impacts assessment at Caia district

Caia District is located downstream of Cahora Bassa dam, in Sofala province, covers an area of 3 542 km^2, and contains three administrative posts: Murraça, Sena and Caia cities. Almost 90 000 inhabitants were counted in the 2007 district census; 53% were female and 47% male. The eastern region of the district is dominated by the flood plain system of the Zambezi River and its tributaries namely: Nhamgue, Mepuce, Shire, Zoogue Mwana and Zangue Rivers.

At Caia district, at 1 (which corresponds to water level between 5 and 7 m at Caia), seven (7) villages, one (1) city and eleven (11) primary schools at level 1 and 1 Primary school at level 2, would be are inundated. In total 17 427 people can be affected – which corresponds to 10% of the total population. At this level of flood, no hospitals are prone to flood.

At Flood Level 2 (which corresponds to the water level between 7-8 m at Caia), the scenario tends to increase the number of villages: a total of eleven (11) villages, one (1) city and one (1) hospital can be inundated. At this flood level there are twenty six (26) schools of which, twenty-one (21) are primary schools at level 1, one (1) primary school at level 2, two (2) for adult education and two (2) agriculture schools would be inundated. In total 25 886 people can be affected.

For Flood Level 3 (which corresponds to the water level between 8 and 10 m at Caia) twelve (12) villages, one (1) city and one (1) hospital would be affected. In total 27 713 would be affected – corresponding to 31% of the total population. Forty-one (41) schools would also be affected (of which thirty-one (31) are primary schools at level 1, one (1) primary school at level 2, two (2) are for adult education and two (2) agriculture schools).

Appendix Table 5-E summarizes the impact of floods on infra-structures. The spatial location of these infra-structures is presented in Appendix Figure 7-E.

Appendix Table 5-E. Summary impact of floods at different levels on Caia's infra-structures

Infra-Structure	Level 1	Total	Level 2	Total	Level 3	Total
1. Cities:	Murraça	**1**	Murraça	**1**	Murraça	**1**
2. Villages:	Sombe, R.Camba,Phaza, Chipuaza, R.Njerera, Nhacuecha, Nharugue	**7**	Sombe, R.Chipende, R.Camba, Phaza, Sombreiro, Chandimba, Chipuaza, R. Njerera, Nhacuecha, Nharugue, Chibongoloua	**11**	Sombe, R.Chipende, R.Camba, R. Goncande, Phaza, Sombreiro Chandimba, Chipuaza, R.Njerera, Nhacuecha, Nharugue Chibongoloua	**12**
3. Hospitals:	0	**0**	Murraça	**1**	Murraça	**1**
4. Schools:	EP1 (Gambadeve1, Marra1, Marra2, Marra3, 7 de Abril1, Tubwe1,, Zangua, Matondo, Tubwe2, 7 de Abril2 and Gamadeve2); EP2, Nangue	**12**	EP1 (Nhachirane1, Gambadeve1, Marra1, Marra2, Marra3, Viano1, Viano2, Mangani1, Tubwe1,Nhacuecha, Nhachirane2 ,Gambadeve2, Mangani1, Mangane2,, 7 de Abril1, 7 de Abril2, Tubwe2, Zangua and Matondo, Hnassengo1 and Nhanssego2) ; Ep2 (Nangue); Albatizacao1, Albatizacao2, Prof. Agrario1 and Prof.Agrario2.	**26**	EP1 (Ntopa1, Nhachirane1, Gambadeve1, Marra1, Marra2, Chineta1, Nhavu1, Sacatucua1,Canto, Nhampunga, Anexo, 4 de Outubro, Gesera, Marra3, Ntopa2,Chineta2, Nhavu2, Sacatucua2, Viano1, Viano2, Mangani1, Nhassengo1, Murrema1, Tubwe1,Nhacuecha, Nhachirane2 ,Gambadeve2, Mangani2, Nhassengo2, 7 de Abril1, 7 de Abril2, Murema2, Tubwe2, Mapagade, Zangua andMatondo) ; Ep2 (Amilcar Cabral and Nangue); Albatizacao1, Albatizacao 2, Prof. Agrario1 and Prof.Agrario2.	**41**

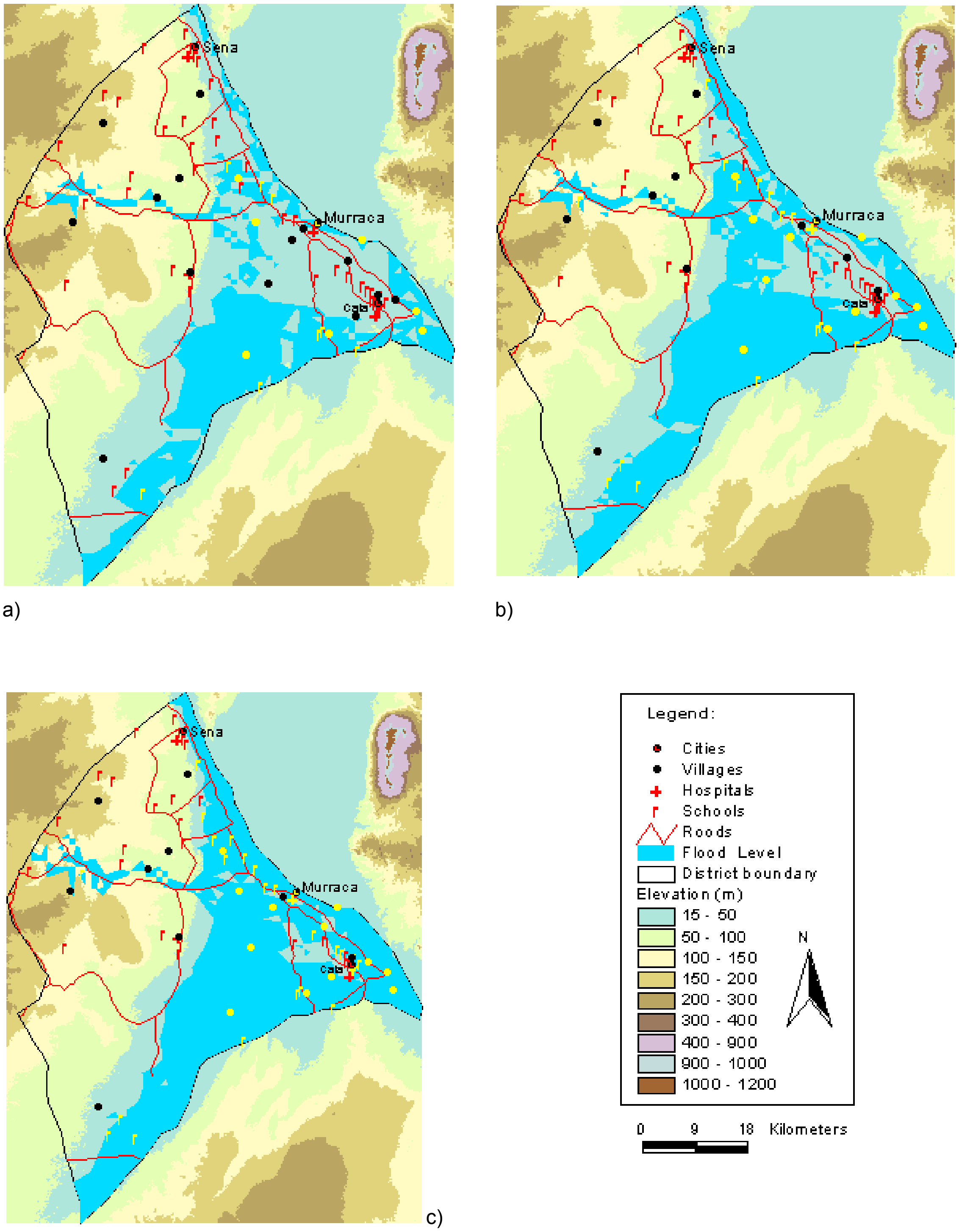

Appendix Figure 7-E: Flood area map for Caia

Flood level 1 (5-7 m) (a); level 2 (7-8 m) (b) and level 3 (8-10 m) (c) at Caia

Appendix 2.6–F: Flood impacts assessment at Morrumbala district

Morrumbala district is located in Zambeze province, covers an area of 12 801 km^2, and contains four administrative posts: Chire, Darre, Morrumbala and Megaza cities. Almost 211 286 inhabitants were counted in the 2007 district census; approximately 51% were female and 49% male. The western region of the district is dominated by the flood plain system of the Shire River, Lua-Lua and Luambo Rivers.

At Flood Level 1 (which corresponds to water level between 5 and 7 m at Caia) twenty-four (24) villages and one (1) city would be inundated, affecting a total of 16 810 people. There are ten (10) primary schools inundated at level 1. At this level there are no hospitals inundated.

At Flood Level 2 (which correspond to the water level between 7-8 m at Caia) thirty -six (36) villages and one (1) city, with a total of 32 062 of people would be affected. Twelve (12) schools, where eleven (11) are at level 1 and one (1) higher education institute would be inundated. No hospitals would be inundated.

For Flood Level 3 (which corresponds to the water level between 8 and 10 m at Caia) thirty-six (36) villages and one (1) city would be inundated, 34 773 people would be affected – corresponding to 16% of the total population. One (1) hospital and fourteen (14) schools, (thirteen (13) at level 1 and one (1) higher education institute) would be inundated.

The Appendix Table 6-F summarizes the impact of floods at on infra-structures in Mutarara district. The spatial location of these infra-structures is presented in Appendix Figure 8.

Appendix Table 6-F: Summary impact of floods at different levels on Morrumbala's infra-structures

Infra-Structure	Level 1	Total	Level 2	Total	Level 3	Total
1.Cities:	Derre	**1**	Derre	**1**	Derre	**1**
2. Villages:	Matamia, Bone, Tengane, Muange, Magamba, Chipaia, Zogo,Chautengo, Chipupo, Changata, Chazuca, Joao, Mosse, Impido, Abissene, Calula, Alface, Derre, Passura, Sanhiua, Manuel, Mussito, Ungule/Ngule, Sampinda	**24**	Masso, Megaza, Chitunguane, Muanda, Panducane, Incali, Semente, Simbi, Thoera,Chirembue, Nhandandanda, Fortuna, Jumaqui, Khembo, Gimo, Khokote, Correia, Chicote, Jon Busa, Mortal, Diogo, Mbuia Muiapha, Nhansanha, Nkhonga, Mkumbua, Mafunga, Maphute, Cafuluca, Mapulango, Catsamo, Procura, Ducuta, Campange, Nhamitanda, Magamba	**36**	Masso, Megaza, Chitunguane, Muanda, Panducane, Incali, Semente, Simbi, Thoera,Chirembue, Nhandandanda, Fortuna, Jumaqui, Khembo, Gimo, Khokote, Correia, Chicote, Jon Busa, Mortal, Diogo, Mbuia Muiapha, Nhansanha, Nkhonga, Mkumbua, Mafunga, Maphute, Cafuluca, Mapulango, Catsamo, Procura, Ducuta, Campange, Nhamitanda, Magamba	**36**
3. Hospitals:	-		-		Murrine	**1**
4. Schools:	EP1 (Sabe, Gomua, Mponha, Medubua, Namarrema1, Camanga, Gaute, Maco, Chirriparuo) Inst.Superior (Pinda)	**10**	EP1 (Sabe, Gomua, Medubua, Namarrema1, Camanga, Gaute, Maco, Chirriparuo, Mponha, Namarrema2, Namalinde); Inst.Superior (Pinda)	**12**	EP1 (Sabe, Gomua, Medubua, Namarrema1, Camanga, Gaute, Maco, Chirriparuo, Mponha, Namarrema2, Namalinde, Gera, Macena); Inst.Superior (Pinda)	**14**

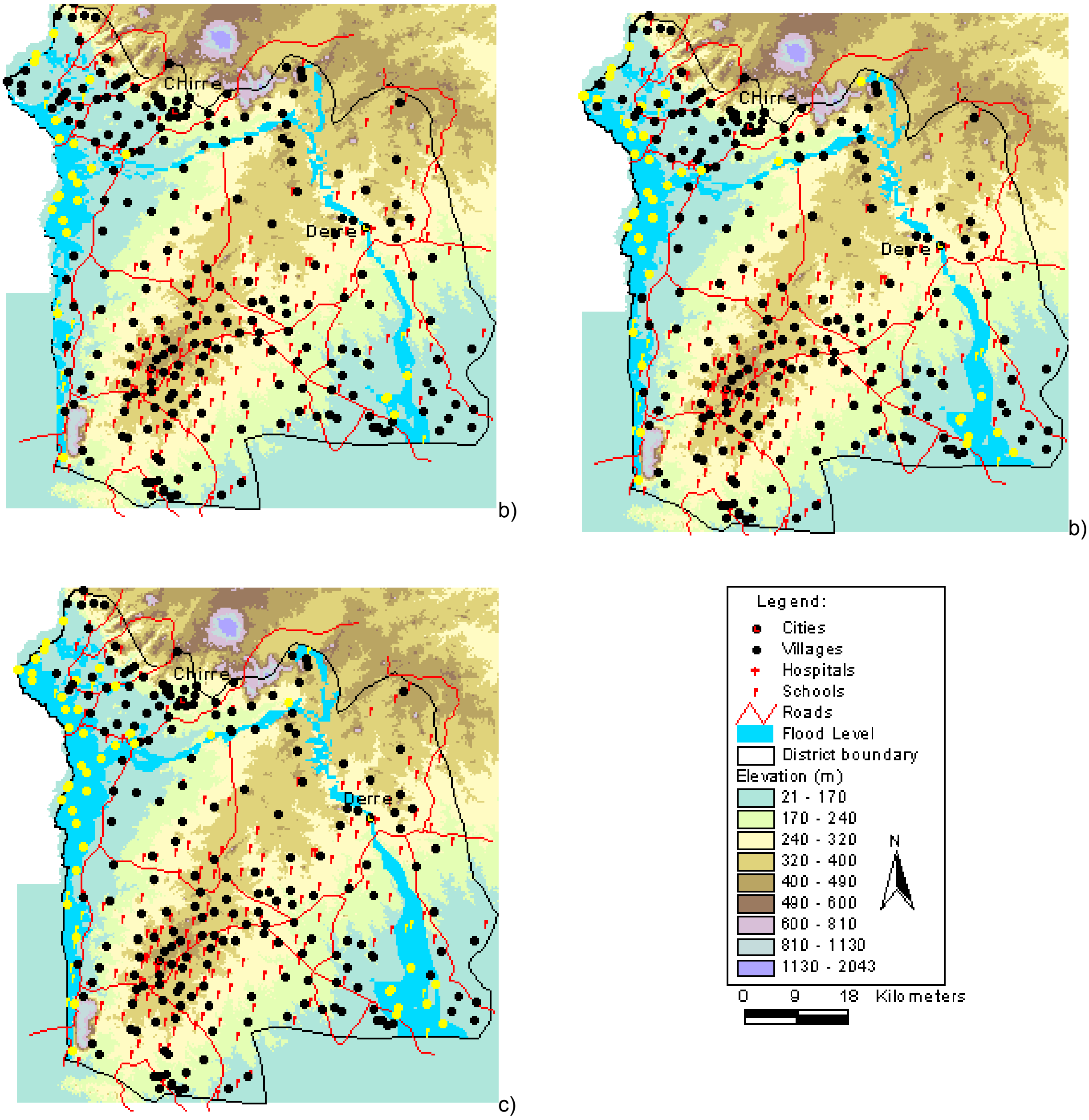

Appendix Figure 8-F: Flood area map for Morrumbala

Flood level 1 (5-7 m) (a); level 2 (7-8 m) (b) and level 3 (8-10 m) (c) at Morrumbala.

Appendix 2.7–G: Flood impacts assessment at Chirringoma district

Chirringoma district is located in Sofala province, covers an area of 7 404 km^2, and contains two administrative posts: Inhatanga and Inhaminga city. Almost 39 972 inhabitants were counted in the 2007 district census; approximately 51% were female and 49% male. The western region of the district is dominated by the flood plain system of the Zambezi River system.

At Flood Level 1 (which corresponds to water level between 5 and 7 m at Caia) one (1) village would be inundated, affecting a total of 672 people. Five (5) schools (4 (four) at level 1 and one (1) primary school at level 2) would be inundated. No hospitals or cities would be inundated.

At Flood Level 2 (which corresponds to the water level between 7-8 m at Caia), two (2) villages with a total of 2 731 of people would be affected. Six (6) schools, (five (5) at level 1 and one (1) primary school at level 2)would be are inundated.

For Flood Level 3 (which corresponds to the water level between 8 and 10 m at Caia) two (2) villages with a total of 2 731 of people would be affected. Six (6) schools, where five (5) of level 1 and one (1) primary school of level 2 are inundated. In total 2 731 people are affected by flood corresponding to 7% of the total population. Eight (8) schools, where seven (7) of level 1 and one (1) primary school of level 2 are inundated.

Appendix Table 7-G summarizes the impact of floods at different levels on infra-structures in Chirringoma district. The spatial location of these infra-structures is presented in Appendix Figure 9-G.

Appendix Table 7-G: Summary impact of floods at different levels on Chirringoma's infra-structures

Infra-Structure	Level 1	Total	Level 2	Total	Level 3	Total
Cities:	-	-	-	-	-	-
Villages:	Regulo Chirimazi	1	Regulo Chirimazi, Regulo Matondo	**2**	Regulo Chirimazi, Regulo Matondo	**2**
Hospitals:	-	-	-	-	-	-
Schools:	EP1 (Nhataca, Chituco, Chirimadzi and Santove); EP2 Thip-Thip	5	EP1 (Nhataca, Chituco, Chirimadzi, Santove and Pungue); EP2 Thip-Thip	6	EP1 (Nhataca, Chituco, Chirimadzi, Santove, Nhandegua, Chimua and Pungue); EP2 Thip-Thip	8

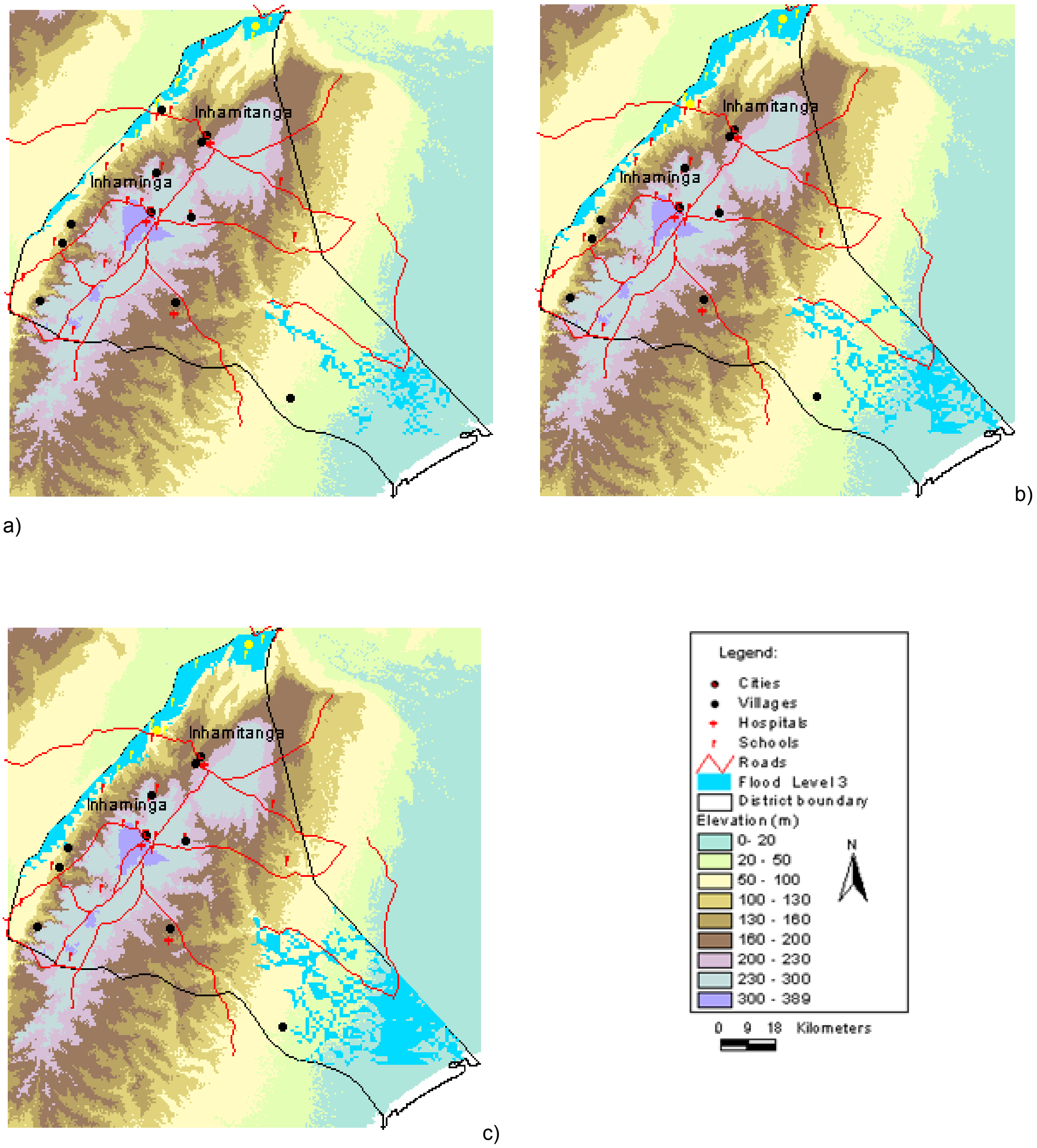

Appendix Figure 9-G: Flood area map for Chirringoma

Flood level 1 (5-7 m) (a); level 2 (7-8 m) (b) and level 3 (8-10 m) (c) at Chirringoma

Appendix 2.8–H: Flood impacts assessment at Mopeia district

Mopeia district is located in Zambeze province, covers an area of 7 793 km^2, and contains two administrative posts: Mopeia and Campo city. Almost 39 972 inhabitants were counted in the 2007 district census; approximately 51% were female and 49% male. The southern and central regions of the district are dominated by the flood plain system of the Zambezi River and its downstream major tributaries namely: Inhamora, Inhaombe; Lua-Lua, Sassue, Longozo, Mutiade, Nhambine, Mecumbire, Mecombeze, Shire and Sacone.

At Flood Level 1 (which corresponds to a water level between 5 and 7 m at Caia), thirteen (13) villages would be inundated, affecting a total of 9 270 people. Eighteen (18) primary schools would also be inundated. No hospitals or cities would be inundated at this level.

At Flood Level 2 (which corresponds to the water level between 7-8 m at Caia), 20 (twenty) villages, with a total of 17 086 people would be affected. One (1) hospital and thirty-two (32) schools would be inundated (thirty (30) are primary schools at level 1, and two (2) at level 2 are affected.

For Flood Level 3 (which corresponds to the water level between 8 and 10 m at Caia) twenty-eight (28) villages and one (1) city would be inundated. In total 45 341 people would be affected – corresponding to 47% of the total population. Forty-seven (47) schools, (forty five (45) primary schools at level 1 and two (2) at level 2) would also be affected.

Appendix Table 8-H: summarizes the impact of floods at different levels on infra-structure in Mopeia district. The spatial location of these infra-structures is presented in Appendix Figure 10-H.

Appendix Table 8-H: Summary impact of floods at different levels on Mopeias's infra-structures

Infra-Structure	Level 1	Total	Level 2	Total	Level 3	Total
1. Cities:	-	**-**	-	**-**	Vila Sede	**1**
2. Villages:	R.Zimbao, Cocorico, Murriua, Dombe, Rosso Capesse, Nofre,3 De Fevereiro, Maone, Chiwirine, B. 2 5 de Junho, Sacuane, Gundine, Cadongo	**13**	R.Zimbao, Cocorico, Murriua, Zamgalaze, Dombe, Rosso Capesse,Mussongue, 3 De Fevereiro, Bairro 25 De Junho, Gundine 'B', Sacuane, Gundine, Cadongo, Sitone, Nofre, Chiwirine, Luala, Maone	**20**	R.Zimbao, Cocorico, Mocha, Vila-Sede, Murriua, Chamanga, Zamgalaze, Dombe, Rosso Capesse, Mussongue, Mungane, Mucurrumba, 3 de Fevereiro, B. 25 de Junho, Gundine 'B', Sacuane, Gundine, Banjone, 25 de Stembro, Milange, Candongo, Sitone, Luala, maone, Nofre, Chiwirine, Simogo, Samolonge	**28**
3. Hospitals:	-	**-**	Lua-Lua	**1**	Lua-Lua	**1**
4. Schools:	EP1 (CudineA, Samurenge1, Mugurumba,1, Chiurime, Sacuane, CudineB, Samurenge2, Sacuane2, Mugumba2, Migoa, Mulamba, Massancar, Namissundo, Cocorico1, Cocorico2, Raso, Vumbi and Mujombe)	**18**	EP1 (CudineA, Samurenge1, Mugurumba1, Chiurime, Sacuane, CudineB, Samurenge2, Sacuane2, Mugumba2, Migoa, Mulamba, Massancar, Namissundo, Cocorico1, Cocorico2, Raso, Vumbi, Mujombe, Amoro, geral1, Geral2, Cunhenhaca, Nhanza, Pedereira, Geral2, Gale, Benjoaque, PSC, Dowe Norte, Moriua Vicente and Muto); EP2 (Chibonzo1 and Chibonzo 2)	**32**	EP1 (CudineA, Samurenge1, Mugurumba1, Chiurime, Sacuane, CudineB, Samurenge2, Sacuane2, Mugurumba2, Migoa, Mulamba, Massancar, Namissundo, Cocorico1, Cocorico2, Raso, Vumbi, Mujombe, Amoro, geral1, Geral2, Cunhenhaca, Nhanza, Pedereira, Geral2, Gale, Benjoaque, PSC, Dowe Norte, Moriua Vicente and Muto, Zue-zue, Trepano, Badjone, Mecumbeze1, Badjone Anexo1, Badjone Anexo2, Mecumbeze2, 8 de Marco1, 8 de Marco2, Cadongo, Diane, Mirrongolne, 3 de Marco1, 3 de Marco2); EP2 (Chibonzo1 and Chibonzo 2)	**47**

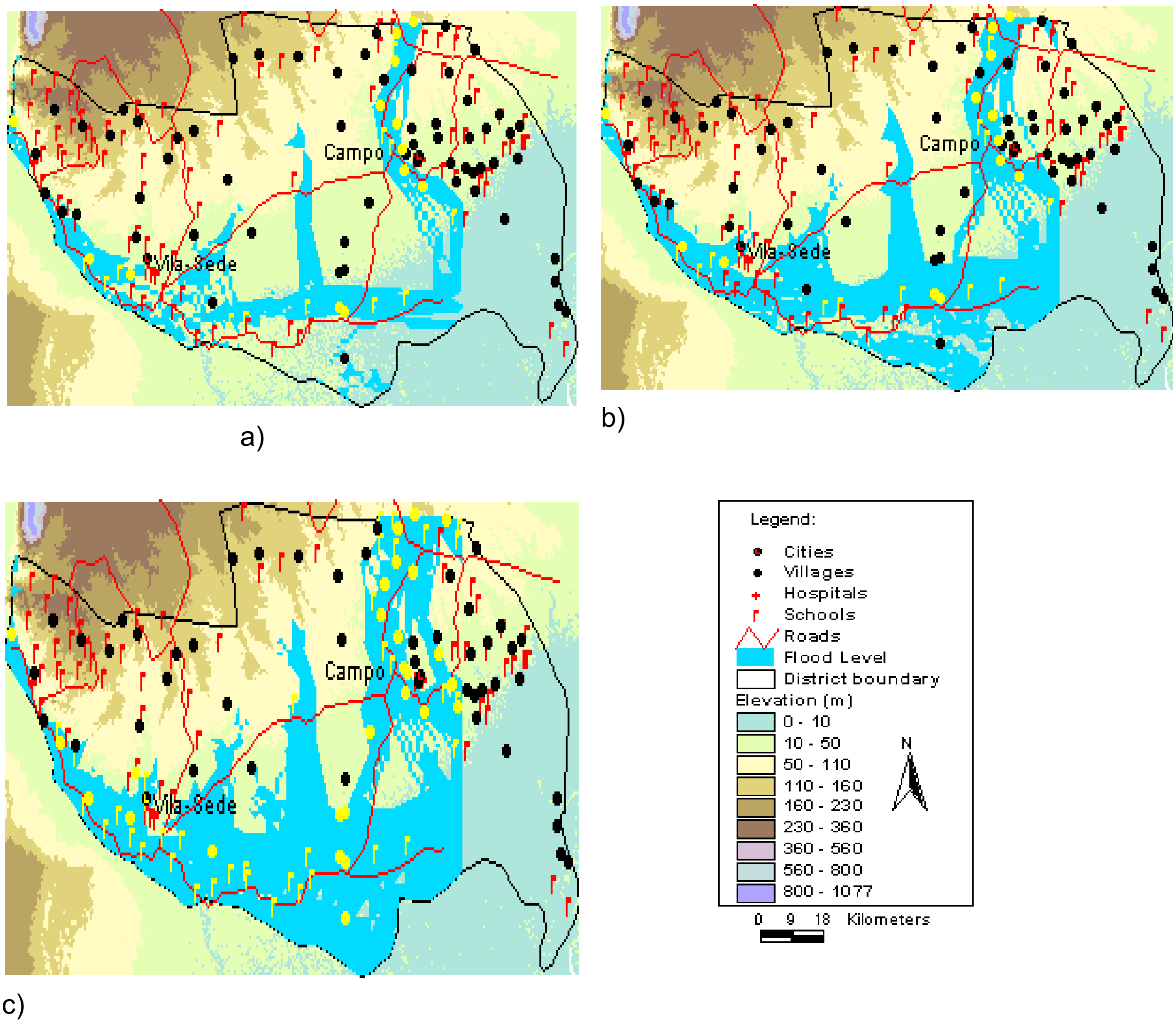

Appendix Figure 10-H: Flood area map for Mopeia

Flood level 1 (5-7 m) (a); level 2 (7-8 m) (b) and level 3 (8-10 m) (c) at Mopeia

Appendix 2.9–I: Flood impacts assessment at Marromeu district

Marromeu district is located in Sofala province, covers an area of 5 786 km^2, and contains three administrative posts: Chupanga, Marromeu and Chinde-sede cities. Almost 55 425 inhabitants were counted in the 2007 district census; approximately 54% were female and 46% male. Most of the eastern and central regions of the district are dominated by the flood plain system of the Zambezi River and its tributaries. It is the district most vulnerable to flood events because of its most downstream location.

At Flood Level 1 (which corresponds water level between 5 and 7 m at Caia), six (6) villages and one (1) city would be inundated, affecting a total of 16 857 people. Two (2) hospitals and 25 (twenty five) schools would be inundated. Of these schools twenty-three (23)) are primary schools at Level 1 and two (2) at Level 2.

At Flood Level 2 (which corresponds to the water level between 7-8 m at Caia), 11 (eleven) villages and one (1) city, with a total of 44 226 people, would be affected. Four (4) hospitals and thirty-eight (38) schools, (thirty four (34) are primary schools at Level 1, three (3) at Level 2, and one (1) secondary school) would be inundated.

For Flood Level 3 (which corresponds to the water level between 8 and 10 m at Caia) twelve (12) villages and one (1) city (with a total of 45 751 people) would be affected – corresponding to 83% of the total population. Four (4) hospitals and forty six (46) schools, (forty two (42) primary schools at Level 1 and three (3) at Level 2, and one (1) secondary school) would be inundated.

Appendix Table 9-I: summarises the impact of floods at different levels on infra-structure in Marromeu district. The spatial location of these infra-structures is presented in Appendix Figure 11-I.

Appendix Table 9-I. Summary impact of floods at different levels on Mutarara's infra-structures

Infra-Structure	Level 1	Total	Level 2	Total	Level 3	Total
1. Cities:	Chupanga	**1**	Chupanga	**1**	Chupanga	**1**
2. Villages:	Marala, Regulo Candue, Regulp Banze	**6**	Marala, Regulo Nhane, Regulo Chueza, Vunganha, Macuerere, Regulo Candue, Regulo Banze	**11**	Marala, Regulo Nhane, Regulo Chueza, Nzero Mbawire, Vunganha, Macuerere, Regulo Candue, Regulo Banze, Thozo	**12**
3. Hospitals:	Chupanga and Cundue	**2**	Chupanga, Cundue, Chueza and Macuere	**4**	Chupanga, Cundue, Chueza and Macuere	**4**
4. Schools:	EP1 (Milha12, Nhandue, Matoro1, Matoro2, Nhapilundo, Central, Salone1, Salone2, Chiverano, Sao Jose, Ermoc, Namaeca, 25 de Setembro, Bongue, Caramanhando, Nhamijale, Pentecosta, 4 de Outubro, Luabo1, Luabo2, Coninarares1 Contenerares 2 and Massengueza); EP2 (Cundue and Chupanga	**25**	EP1 (Milha12, Nhandue, Matoro1, Matoro2, Nhapilundo, Central, Salone1, Salone2, Chiverano, Sao Jose, Ermoc, Namaeca, 25 de Setembro, Bongue, Caramanhando, Nhamijale, Pentecosta, 4 de Outubro, Luabo1, Luabo2, Coninarares1 Contenerares 2, Massengueza, Mazuegue, Nhamirasse, Nhamiambe, Sauze, Chueze, Moma, Socorro1,Socorro 2,Nenguo, Samora Machel, Geral,); EP2 (Cundue, Chupanga and Luabo Sede); ESG Luabo	**38**	EP1 (Milha12, Nhandue, Matoro1, Matoro2, Nhapilundo, Central, Salone1, Salone2, Chiverano, Sao Jose, Ermoc, Namaeca, 25 de Setembro, Bongue, Caramanhando, Nhamijale, Pentecosta, 4 de Outubro, Luabo1, Luabo2, Coninarares1 Contenerares 2, Massengueza, Mazuegue, Nhamirasse, Nhamiambe, Sauze, Chueze, Moma, Socorro1,Socorro 2,Nenguo, Samora Machel, Geral,Epichilolo, Nguninguini, Nhangazi, Bauze Sede and Bavazi); EP2 (Cundue, Chupanga and Luabo Sede); ESG Luabo	**43**

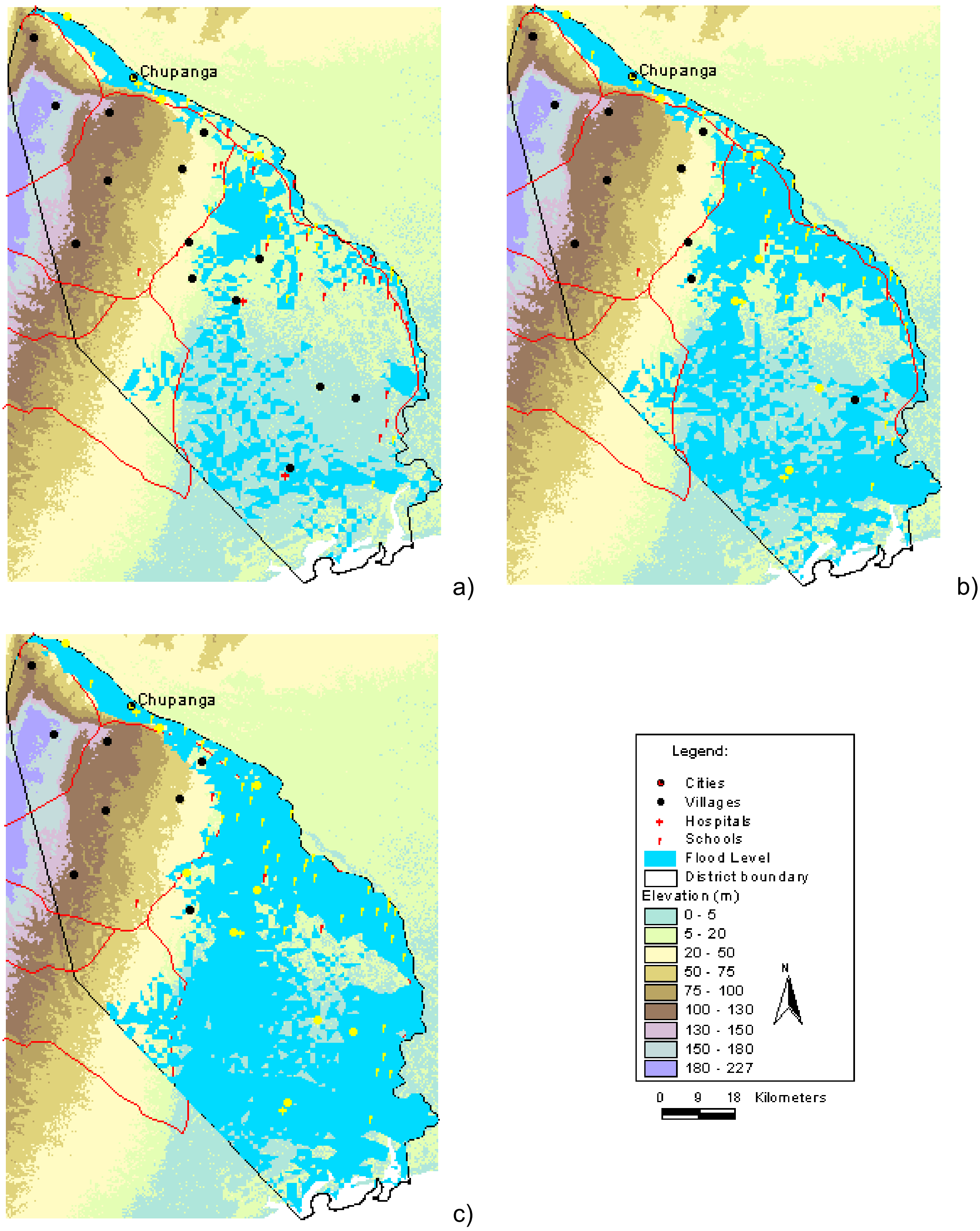

Appendix Figure 11-I: Flood area map for Marromeu

Flood level 1 (5-7 m) (a); level 2 (7-8 m) (b) and level 3 (8-10 m) (c) at Marromeu